



RETURN TO 396-SS  
 Department of Energy  
 Washington, DC 20545

February 26, 1988

FILE COPY



71-9152

Mr. Charles E. MacDonald, Chief  
 Transportation Branch  
 Division of Safeguards and Transportation, M455  
 U.S. Nuclear Regulatory Commission  
 Washington, D.C. 20555

Dear Mr. MacDonald:

The Department of Energy (DOE) requests renewal of the HRC Certificate of Compliance (CoC) Number 9152 having an expiration date of March 31, 1988. DOE programs have a continuing need for the packaging. The operating history and a brief status of the package are given below:

- o Package Identification Number -- USA/9152/G( )
- o Model Number -- CNS 1-BC II
- o Number of Shipments in Last Five Years -- 23 Shipments
- o Operating Incidents -- None
- o Maintenance of packaging has been carried out in accordance with Section 8.2 of the SARP (EGG-TMI-8008)

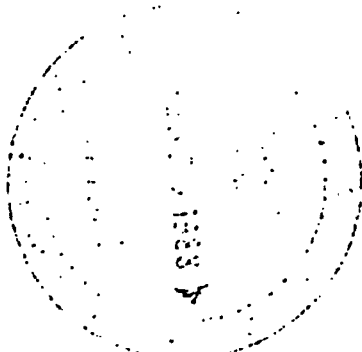
There have been no changes in the packaging, design, hardware or contents during the current period of certification. The Safety Analysis Report for Packaging (SARP) (EGG-TMI-8008) for the CNS 1-13C II has been consolidated to include all amendments made to the SARP when previously held by Chem Nuclear Systems, Inc. The CNS-1-13 II packaging was purchased by DOE in April 1982.

Should you require any further information on this package or enclosures, please call me (353-5394), or Erich Opperman (353-3954) of my staff.

Sincerely,

*Charles J. Mauck*

Charles J. Mauck  
 Chief of Packaging Certification  
 Office of Security Evaluations  
 Defense Programs



6 Enclosures

8803030081 880226  
 PDR ADOCK 07109152  
 C PDR

29085

11/11/38  
11/11/38  
11/11/38  
11/11/38  
11/11/38

FCTC 11/11/38  
DATE 11/11/38 OTHER 11/11/38  
INITIAL 11/11/38

SAFETY ANALYSIS REPORT  
FOR  
MODEL 1-13C II PACKAGING  
TO  
10 CFR 71 TYPE "B" PACKAGING REQUIREMENTS

DECEMBER 1987

Submitted By:

EG&G IDAHO, INC.  
1955 FREMONT AVE.  
IDAHO FALLS, IDAHO 83415

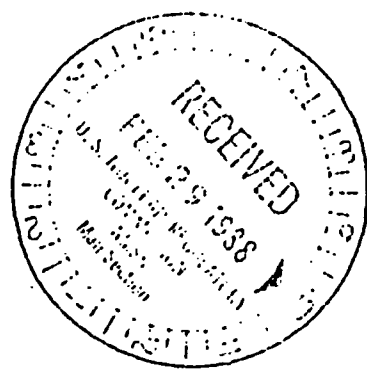
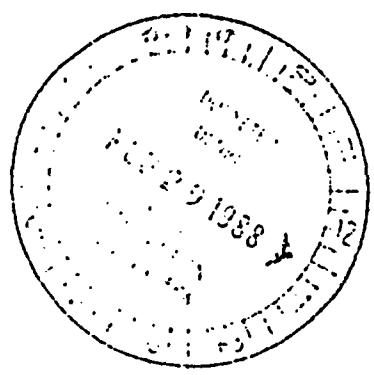
8803030090 880226  
PDR ADDCK 07107152  
C PDR

71-913.4

REGULATORY OPERATIONS  
FILE COPY

EGG-TMI-8008

RETURN TO 396-55



SAFETY ANALYSIS REPORT  
FOR  
MODEL 1-13C II PACKAGING  
TO  
10 CFR 71 TYPE "B" PACKAGING REQUIREMENTS

DECEMBER 1987

Submitted By:

EG&G IDAHO, INC.  
1955 FREMONT AVE.  
IDAHO FALLS, IDAHO 83415

1988

TABLE OF CONTENTS

	Page
1. GENERAL INFORMATION . . . . .	1-1
1.1 Introduction . . . . .	1-1
1.2 Package Description . . . . .	1-3
1.2.1 Packaging . . . . .	1-3
1.2.2 Operational Features . . . . .	1-8
1.2.3 Contents of Packaging . . . . .	1-8
1.3 Appendix . . . . .	1-10
2. STRUCTURAL EVALUATION . . . . .	2-1
2.1 Structural Design . . . . .	2-1
2.1.1 Discussion . . . . .	2-1
2.1.2 Design Criteria . . . . .	2-4
2.2 Weights and Centers of Gravity . . . . .	2-6
2.3 Mechanical Properties of Materials . . . . .	2-7
2.4 General Standards for all Packages . . . . .	2-11
2.4.1 Minimum Package Size . . . . .	2-11
2.4.2 Tamperproof Feature . . . . .	2-11
2.4.3 Positive Closure . . . . .	2-11
2.4.4 Chemical and Galvanic Reactions . . . . .	2-11
2.5 Lifting and Tiedown Standards for All Packages . . . . .	2-11
2.5.1 Lifting Devices . . . . .	2-11
2.5.2 Tiedown Devices . . . . .	2-51
2.6 Normal Conditions of Transport . . . . .	2-66
2.6.1 Heat . . . . .	2-66
2.6.2 Cold . . . . .	2-77
2.6.3 Reduced External Pressure . . . . .	2-79
2.6.4 Increased External Pressure . . . . .	2-79
2.6.5 Vibration . . . . .	2-81
2.6.6 Water Spray . . . . .	2-81
2.6.7 Free Drop . . . . .	2-81
2.6.8 Corner Drop . . . . .	2-91
2.6.9 Compression . . . . .	2-91
2.6.10 Penetration . . . . .	2-91
2.6.11 Conclusions . . . . .	2-91

TABLE OF CONTENTS (CONT'D)

2.7	Hypothetical Accident Conditions . . . . .	2-92
2.7.1	Free Drop . . . . .	2-92
2.7.2	Puncture . . . . .	2-110
2.7.3	Thermal . . . . .	2-112
2.7.4	Immersion - Fissile Material . . . . .	2-116
2.7.5	Immersion - All Packages . . . . .	2-116
2.7.6	Summary of Damage . . . . .	2-116
2.8	Special Form . . . . .	2-117
2.9	Fuel Rods . . . . .	2-117
2.10	Structural Evaluation Appendices . . . . .	2-117
2.10.1	Analytic Methods . . . . .	2-118
2.10.2	Finite Element Stress Summary . . . . .	2-152
2.10.3	Lift Lug Analysis . . . . .	2-154
2.11	Appendix - Engineering Drop Test for 1-13C II Shipping Package . . . . .	2-169
2.11.1	Scope . . . . .	2-169
2.11.2	References . . . . .	2-169
2.11.3	Detailed Procedure: Conduct of Drop Test . . . . .	2-171
2.11.4	Test Results/Data . . . . .	2-189
2.11.5	Interpretation, Correlation, and Conclusions . . . . .	2-204
2.12	Attachment . . . . .	2-213
3.	THERMAL EVALUATION . . . . .	3-1
3.1	Discussion . . . . .	3-1
3.2	Summary of Thermal Properties of Materials . . . . .	3-5
3.3	Technical Specifications of Components . . . . .	3-8
3.4	Thermal Evaluation for Normal Conditions of Transport . . . . .	3-8
3.4.1	Thermal Model . . . . .	3-8
3.4.2	Maximum Temperatures . . . . .	3-20
3.4.3	Minimum Temperatures . . . . .	3-31
3.4.4	Maximum Internal Pressures . . . . .	3-31
3.4.5	Maximum Thermal Stresses . . . . .	3-36
3.4.6	Evaluation of Package Performance for Normal Conditions of Transport . . . . .	3-36
3.5	Hypothetical Accident Thermal Evaluation . . . . .	3-37
3.5.1	Thermal Model . . . . .	3-37
3.5.2	Package Conditions and Environment . . . . .	3-37
3.5.3	Package Temperatures . . . . .	3-38
3.5.4	Maximum Internal Pressures . . . . .	3-56
3.5.5	Maximum Thermal Stresses . . . . .	3-56
3.5.6	Evaluation of Package Performance for Hypothetical Accident Thermal Conditions . . . . .	3-66

TABLE OF CONTENTS (CONT'D)

3.6	Appendix . . . . .	3-67
4.	CONTAINMENT . . . . .	4-1
4.1	Containment Boundary . . . . .	4-1
4.1.1	Containment Vessel . . . . .	4-1
4.1.2	Containment Penetration . . . . .	4-1
4.1.3	Welds and Seals . . . . .	4-2
4.1.4	Closure . . . . .	4-2
4.2	Requirements for Normal Conditions of Transport . . . . .	4-3
4.2.1	Containment of Radioactive Material . . . . .	4-3
4.2.2	Pressurization of Containment Vessel . . . . .	4-3
4.2.3	Containment Criterion . . . . .	4-5
4.3	Containment Requirements for Hypothetical Accident Conditions . . . . .	4-5
4.3.1	Fission Gas Products . . . . .	4-5
4.3.2	Containment of Radioactive Material . . . . .	4-5
4.3.3	Containment Criterion . . . . .	4-8
4.4	Appendix A - Normal and Accident Radioactive Material Limits for the 1-13C II Cask . . . . .	4-15
4.5	Appendix B - Parker Stat-O-Seal Information . . . . .	4-30
5.	SHIELDING EVALUATION . . . . .	5-1
5.1	Discussion and Results . . . . .	5-1
5.2	Source Specification . . . . .	5-1
5.3	Model Specification . . . . .	5-3
5.3.1	Damage Predictions - Corner . . . . .	5-3
5.3.2	Damage Prediction - Side . . . . .	5-8
5.3.3	Damage Prediction - Ends . . . . .	5-10
5.4	Shielding Evaluation . . . . .	5-13
5.5	References . . . . .	5-18
6.	CRITICALITY EVALUATION . . . . .	6-1
6.1	Discussion and Results . . . . .	6-1
6.2	Package Fuel Loading . . . . .	6-1
6.3	Model Specification . . . . .	6-1
6.4	Criticality Calculation . . . . .	6-1
6.5	Critical Benchmark Experiments . . . . .	6-2
6.6	Appendix . . . . .	6-6

TABLE OF CONTENTS (CONT'D)

7.	OPERATING PROCEDURES . . . . .	7-1
7.1	Procedures for Loading Package . . . . .	7-1
7.2	Procedures for Unloading Package . . . . .	7-6
7.3	Preparation of Empty Package for Transport . . . . .	7-6
7.4	Procedures for Shipment of Packages Which Generate Combustible Gases . . . . .	7-6
8.	ACCEPTANCE TESTS AND MAINTENANCE PROGRAM . . . . .	8-1
8.1	Acceptance Tests . . . . .	8-1
8.1.1	Visual Inspection . . . . .	8-1
8.1.2	Structural and Pressure Tests . . . . .	8-1
8.1.3	Leak Tests . . . . .	8-1
8.1.4	Component Tests . . . . .	8-2
8.1.5	Tests for Shielding Integrity . . . . .	8-2
8.1.6	Thermal Acceptance Tests . . . . .	8-2
8.2	Maintenance Program . . . . .	8-2
8.2.1	Structural and Pressure Tests . . . . .	8-2
8.2.2	Leak Tests . . . . .	8-2
8.2.3	Subsystem Maintenance . . . . .	8-2
8.2.4	Valves and Gaskets on containment Vessel . . . . .	8-3
8.2.5	Shielding . . . . .	8-3
8.2.6	Thermal . . . . .	8-3
8.2.7	Appendix - Leak Test Procedures . . . . .	8-3
8.3	Appendix . . . . .	8-4



## 1.0 GENERAL INFORMATION

### 1.1 Introduction

This Safety Analysis Report describes a reusable insulated and shock absorbing shipping package designed to protect radioactive material from both normal conditions of transport and hypothetical accident conditions. The package is designated as the Model 1-13C II Package. It is intended to deliver fissile Class III material, irradiated reactor hardware, and other solid materials including process solids, in excess of Type A quantities.

The package is an improved lineal descendant of the CNS 1-13C, Package Identification Number USA/9081/B ( )F, and the General Electric Model 1600 Shipping Cask, Package Identification Number USA/9044/B ( )F.

The improvements contained in the Model 10-3C II Package include the following:

- A pair of circular shock or impact absorbing limiters, placed peripherally around both top and bottom of the circular cask body. They provide capability to protect the package from damage under hypothetical accident conditions.
- A fire shield surrounding the cylindrical cask body. The fire shield is designed to protect the package from damage during the hypothetical fire events.
- Numerous improvements to closure and sealing details providing greater containment integrity and improved decontamination features.

- Shipment of fissile material within the cask is accomplished through the use of various container configurations. The fissile material is radioactive fuel bearing debris samples with a maximum enrichment of 3% in U-235. Dependent upon the container utilized, size, geometry or mass of the sample will be controlled to preclude criticality.

A. General Debris Container Configuration

Shipment of up to 15.4 kg  $UO_2$  (400 grams of U-235) can be placed in closed debris containers with a defined geometry. The debris containers are placed in DOT approved 2R containers. A shoring cage within the cavity of the cask segregates each of the three 2R containers and ensures a close fit within the cask cavity. The 2R containers provide the supplementary containment of the debris samples. The debris containers define the size and geometry configuration of the debris within the cask cavity which, in turn, limits the mass of fissile material.

## 1.2 Package Description

### 1.2.1 Packaging

#### A. Cask and Impact Limiters (See CNS Drawing No. E-1-436-111)

The packaging system consists of a pair of circular impact limiters (or overpacks) placed peripherally around each end of a cylindrical cask. The cylindrical cask is 39.12 inches in diameter and 68.06 inches high. The cylindrical cask body is comprised of a 1/2 inch stainless steel shell, Type 304, overlaid with 1/4" stainless steel fire shield. Between these two materials is a .065 (16 gauge) stainless steel wire wrap, thus providing an air gap for additional thermal protection. The inner cylindrical shell of the cask, or cavity, is fabricated of 1/2 inch stainless steel, Type 304. The annular space between these inner and outer shells is filled with lead, having a thickness of approximately 5 inches. The base of the cask consists of inner and outer circular plates, fabricated of 1/2 inch stainless steel, Type 304, separated with a lead shield of approximately 6 inches thickness.

The cask lid is comprised of a conical sector attached top and bottom to inner and outer circular flat plates. The conical segment of lid is fitted within a step recess approximately 6 inches depth in the cask body. Conical surfaces and inner surfaces of the lid are fabricated of 1/2 inch stainless steel, Type 304. The outer circular flat plate segment of lid is fabricated from a 1 inch plate, machined to approximately 0.8 inches thickness. A load bearing step of approximately 0.2 inches thickness, surrounds the periphery of this outer lid plate, reacting containment bolt preload forces and confining the flat gasket. A solid silicone O-ring exists near the edge of bottom of the lid. The space between inner and outer flat lid plates is filled with lead, having a thickness of approximately 5.78 inches.

The removable lifting lugs are attached to lifting pads integral with the cylindrical cask body. Tiedown lugs are integral to the top energy absorbing overpack assembly.

Each limiter has an external shell, fabricated from ductile low carbon steel, which allows it to undergo large deformations without fracturing. Each is secured to the cask body by six (6) one inch ratchet binders, connecting top and bottom overpacks. The volume between the inner and outer shell of the overpack is filled with a shock and thermal insulating material consisting of rigid polyurethane foam, having a density of approximately 16.5 lbs/ft<sup>3</sup>. The insulating material is poured into the cavity between the two shells and allowed to expand, completely filling the void. It bonds to the shells, creating a unitized construction of the packaging. Properties of these materials are further described in Section 2.3.

- Containment Vessel

The containment boundary of the package is defined as the inner stainless steel shell of the cask body together with closure features comprised of: the lower surface of the cask lid, 12 equally spaced 1-1/4 inch closure bolts, a solid silicone flat gasket, and a silicone O-ring.

Refer to Section 4.0 for a complete description of the containment boundary for the 1-13C II Package.

- Neutron Absorbers

There are no materials used as neutron absorbers or moderators in the Model 1-13C II Package.

- Package Weight

Gross weight for the package is approximately 27,000 pounds. This includes a payload weight of 3,000 pounds.

- Receptacles

There are no internal or external structures supporting or protecting receptacles.

- Drain/Vent Ports

The cask is provided with two 1/2" O.D. lines. These are used for the draining, venting and removal of entrapped liquids. Refer to Section 4.1.2 for drain/vent system descriptions.

- Tiedowns

Tiedowns are a structural part of the package. From the General Arrangement Drawings shown in Appendix 1.3, it can be seen that four tiedown lugs are provided as an integral part of the top energy absorbing overpack assembly. Refer to Section 2.5 for a detailed analysis of their structural integrity.

- Lifting Devices

Lifting devices are a structural part of the package. From the General Arrangement Drawing shown in Appendix 1.3, it can be seen that two removable lifting lugs attached to the cylindrical cask body are provided. A single lifting lug is also provided for removal and handling of the lid. Refer to Section 2.5 for a detailed analysis of their structural integrity.

- Pressure Relief System

The drain port is provided with a plug, permitting venting of internal pressure within the containment cavity generated by decay heat, prior to lid removal. The top vent port is provided with the same plug for venting any pressure between the O-ring and flat lid gasket prior to lid removal.

Refer to Section 4.1.2 for a description of this pressure relief feature.

- Heat Dissipation

There are no special devices used for the transfer or dissipation of heat. The package maximum design capacity is 800 watts. Refer to Section 3.0 for the thermal evaluation of the 1-13C II Package.

- Coolants

There are no coolants involved.

- Protrusions

There are no outer or inner protrusions. Tiedown lugs are removed prior to transport.

- Shielding

Cask walls provide a shield thickness of 5 inches lead and 1-1/4 inch steel. Cask ends provide a minimum of 6 inches lead and 1 inch steel.

The contents will be limited such that the shielding provided will assure compliance with dose rate limits as specified in 10CFR71.

3. Fissile Material Containers

1. General Debris Container

The general debris container configuration, as described in Part A of Section 1.1 consists of a general debris container (loaded with either a fuel pin sample cell or debris container) loaded into a 2R container in a shoring cage. A shipping configuration is shown in EG & G drawing TMI 1113 in Section 1.3.

The following is a description of these components.

- General Debris Container

This component is a handling insert which consists of a 300 series stainless steel vessel, with welded concentric shells and encapsulated lead shielding. The external dimensions are nominally 8.0 in diameter by 12.75 in height. The cavity size is 2.75 in diameter by 7.79 in height. The nominal cavity volume is 2300-2600 cubic centimeters. The cask exterior walls are smooth. A steel lid closes the upper portion of the cavity. The lid is held in place by a jam-nut arrangement. A 1/4 in drain line located in the lower portion of the container permits dewatering of the contents. A fine steel mesh screen covers the drain tube orifice.

The container permits debris loading into either of two small baskets; (1) The fuel pin sample cell, or (2) the debris basket (see Drawing 2E-3200-1040 in Section 1.3).

Eye bolts on the shielded container body are used for in-plant handling and are removed prior to shipping. The lead shielding in the container is solely required for in-plant handling, (it is not required to augment the cask shielding).

- 2R Container

The 2R container meets the DOT requirements of 49CFR 178.34. It is fabricated from steel pipe and has external dimensions of 10 3/4 inches O.D by 14 1/4 inches high. The bottom end is welded to the container walls. The container cover is one inch thick and is threaded to the container wall to provide closure. Per DOT requirements, a non-hardening thread lubricant is used and the lid closure is adequately torqued. The debris container is placed within the 2R container or it may remain empty. Radial movement of the debris container within the container is accommodated by pine strip shoring (1"x2" x 10").

- Cask Cavity Shoring Cage

The wooden (pine) shoring is constructed in a cylindrical shape, and includes inner and outer 2 x 1/8 in. thick rings of carbon steel as strapping.

1.2.2 Operational Features

Refer to the General Arrangement Drawing of the packaging in Appendix 1.3. There are no complex operational requirements associated with the Model 1-13C II package, and none have any transport significance.

1.2.3 Contents of Packaging

(1) Type and form of material

- (1) Greater than Type A quantity of nonfissile radioactive material as solidified or dewatered process solids (resins) within a sealed secondary container; or
- (11) Greater than Type A quantity of irradiated solid reactor components within a sealed secondary container.
- (111) Greater than Type A quantity of irradiated fuel debris (dewatered) within secondary containers.

(2) Maximum quantity of material per package

For the contents described in (1)(1), (11), and (111):

Not to exceed a decay heat generation of 800 watts and 3,000 pounds including weight of the contents and secondary container; and

For the contents described in (1)(1):



Residual water in the secondary container not to exceed the activity stated in Table 4.3.2-1.

For the contents described in (1)(iii):

The maximum U-235 enrichment of the uranium oxide fuel material must not exceed 3 weight %. The average burnup of the fuel material must not exceed 3,165 MWD/MTU and must be cooled for a least six years.

- General Debris Container Configuration  
Fissile contents not to exceed 15.4 kg  $UO_2$  (400 grams U-235 prior to irradiation).

1.3 APPENDIX

1.3.1 Drawings

1.3.1.1 CNS Drawing No. E-1436 - 111, Rev. D., "CNS  
1-13C II Shipping Cask"

1.3.1.2 GPU Nuclear Drawing No. 2E-3200-1040, Rev. 0,  
"General Debris Shielded Container - 1 Assy & Fuel  
Pin Sample Shielded Container - 2 Assy"

1.3.2 Sketches

1.3.2.1 Model 1-13C II Package

FIGURE 1.3.2.1  
MODEL 1-13C II PACKAGE

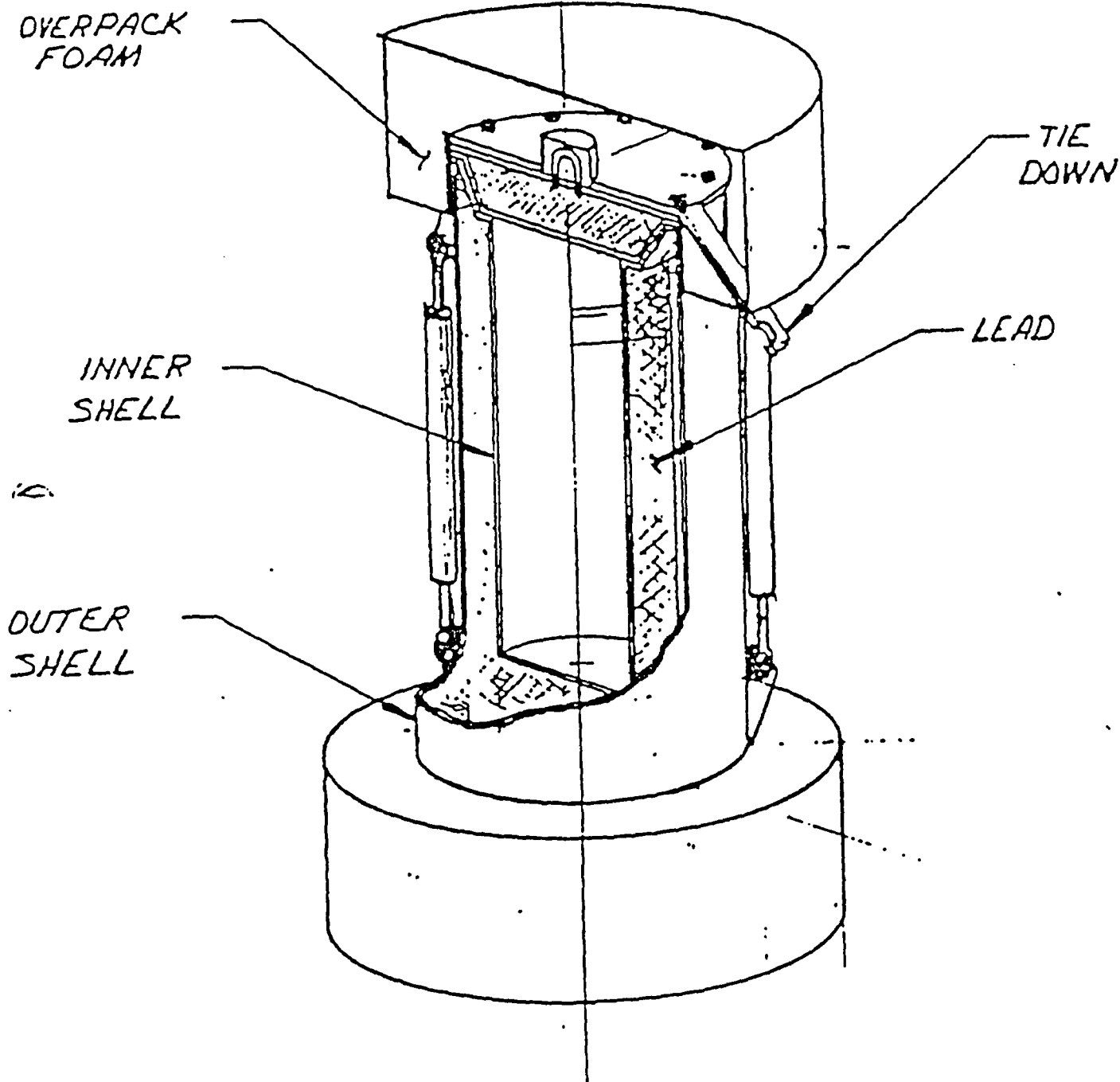


**FIGURE WITHHELD UNDER 10 CFR 2.390**



**FIGURE WITHHELD UNDER 10 CFR 2.390**



**FIGURE WITHHELD UNDER 10 CFR 2.390**





**FIGURE WITHHELD UNDER 10 CFR 2.390**



**FIGURE WITHHELD UNDER 10 CFR 2.390**



**FIGURE WITHHELD UNDER 10 CFR 2.390**



## 2.0 STRUCTURAL EVALUATION

This Chapter identifies and describes the principal structural engineering design of the packaging, components, and systems, important to safety and to compliance with performance requirements of 10 CFR 71.

### 2.1 Structural Design

#### 2.1.1 Discussion

The purpose of the 1-13C II Package is to provide a safe means of transport for radioactive materials in excess of Type A quantities. The package has been designed to provide a shielded containment vessel that can withstand the Normal Conditions of Transport as well as those associated with the Hypothetical Accident Condition.

Principal structural elements of the system consist of:

- A. Containment Vessel
- B. Biological Shield
- C. Fire Shield
- D. Impact Limiters

Components A-D design and function in meeting the requirements of 10 CFR 71 are discussed below.

The 1-13C II assembly is designed to protect the payload from normal transport and hypothetical accident conditions. These include: transport environment, 30 foot drop test, 40 inch puncture test, 1475<sup>0</sup>F thermal exposure and transfer or dissipation of any internally generated heat.



These requirements are satisfied by a straight-forward and strong design of the 1-13C II package. The conservative capabilities of this package design have been conclusively demonstrated by two successive, or cumulative full scale hypothetical accident drop tests, see Section 2.11. Each of the four structural elements are summarized below.

#### 2.1.1.1 Containment Vessel

The cask is comprised of inner and outer stainless steel shells Type 304, one-half inches in thickness, enveloping the lead biological shield. The inner shell serves as the package containment boundary. A removable tapered lid is attached to the cask body with twelve (12) equally spaced 1-1/4 - 7 UNC bolts. All welds are subjected to non destructive examination.

The lid to cask body interface employs a high temperature, solid silicone O-ring and a flat, high temperature, silicone seal. The flat silicone seal is captured in a machined circumferential lid step. This step is designed to preclude overcompression of the flat gasket and O-ring materials under bolt preloads and impact forces. All transport environments as well as accident conditions, i.e., 30 foot drop, 40 inch puncture test requirements etc., are met by the external shell with impact limiters installed as discussed in Section 2.1.1.4 below. All thermal loading and dissipation requirements are met as discussed in Sections 2.1.1.3 and 2.1.1.4 below.

#### 2.1.1.2 Biological Shield

The area between the two shells discussed in Section 2.1.1.1 is filled with lead. The lead fill is subjected to Gamma Scan inspection to assure lead integrity. The designed thickness assures that no biological hazard is presented by the 1-13C II and all shielding requirements of 10 CFR 71 are met. Lead bonding is not assumed to take place between the inner and outer shells.

### 2.1.1.3 Fire Shield

The maximum thermal loading of 800 watts is dissipated via conduction through the cask structure and normal convection to the atmosphere.

The fire shield consisting of .065 diameter stainless wire spiral wound on the outside surface of the cask and covered with 1/4" stainless steel cladding provides thermal protection during the 1475°F thermal exposure test. The impact limiters provide thermal protection for the ends of the package. During hypothetical fire accidents, seal temperature is maintained below 360°F and lead temperature is maintained below 509°F. These temperatures are well below the design limit for the seal material and well below lead melt temperature.

### 2.1.1.4 Impact Limiters

The impact limiters (overpacks) are designed to protect the package from deformation during the 30 foot drop and provide thermal protection as discussed in Section 2.1.1.3. Their construction consists of full welded steel shells filled with foamed in place rigid structural polyurethane foam of a 16.5 lb/ft<sup>3</sup> density. The foam provides controlled deformation rates during impact. The foam degrades at 400°F and forms an air space within the impact limiter shell which provides an effective thermal barrier during the 1475°F thermal exposure test.

### 2.1.1.5 Summary

Detailed discussions of all components and material utilized in the CNS 1-13C II Package including stress, thermal, and pressure calculations are contained in the applicable sections of the SAR.

### 2.1.2 Design Criteria

The 1-13C II has been designed to be a simple strong package that will provide maximum flexibility for multiple usage as well as minimize potential exposure to operating personnel. Its size and shielding capacity will allow a variety of existing and future payloads to be safely transported. The containment vessel is fully sealed and is fully isolated from the cask exterior by lead and a heavy steel jacket. Since the package ends represent the most critical portion of the cask, they are further protected by impact limiters. Impact limiters of this type have been successfully used on many Type "B" packages. They not only reduce impact loads but also provide efficient thermal insulation for the ends of the package.

The dominant loads imposed upon any Type "B" package are due to the hypothetical accident drop events. Successive full scale drop tests have demonstrated the capabilities of the 1-13C II Package to survive these dominant load without incurring stresses or strains measurably in excess of yield values.

Where appropriate, the evaluations of package structural integrity are based upon demonstrated test results. Where not appropriate, analytic methods are used to augment test data. In all cases, the package has been designed to provide well defined load paths which lend themselves to simple, highly reliable structural analysis methods. No new state-of-the-art approaches have been used for energy absorption, thermal insulation or analytic evaluation. All analytic techniques used throughout the SAR are proven methods that have been used in past submittals. Details of these methods have been used in past submittals. Details of these methods appear in Section 2.10.

### 2.1.2.2 Stress Categories

Regulatory Guide 7.6 "Design Criteria for the Structural Analysis of Shipping Cask Containment Vessels" was used in conjunction with Regulatory Guide 7.8 "Load Combinations for the Structural Analysis of Shipping Casks" to evaluate the 1-13C II Package. Material properties used in the analysis can be found on Table 2.3-1.

#### 2.1.2.2.1 Containment Vessel

The containment vessel is interpreted to be the inside stainless steel shell and its closures. Regulatory Guide 7.6 was used for the evaluation of the containment vessel for both the Normal Conditions of Transport and the Hypothetical Accident Conditions. Material properties used in the evaluation correspond to the design stress values  $S_m$ ,  $S_y$  &  $S_u$  given in the ASME Code, Section III, Class I, 1977 Edition as amended.

#### 2.1.2.2.2 Cask and Overpack

Structural evaluation of non-containment vessel items such as the external skins, closures, overpacks, lifting and tiedown fitting were evaluated against yield and ultimate material properties as presented in the ASME Code, Section III, Class I. For Normal Conditions of Transport, yield strength was used as a maximum stress for the cask. The overpack is allowed to exceed yield stress for normal conditions; hence, ultimate evaluating Accident Conditions, ultimate stress or ultimate strains were used as the acceptance criteria.

#### 2.1.2.3 Other Structural Failure Modes

#### 2.1.2.3.1 Brittle Fracture

The primary material used in the cask is 304 stainless steel. This material does not experience a ductile to brittle transition in the temperature ranges of interest (down to  $-40^{\circ}\text{F}$ ); hence is safe from brittle fracture.

#### 2.1.2.3.2 Buckling

Buckling per Regulatory Guide 7.6 is an unacceptable failure mode for the containment vessel. The intent of this provision is to preclude large deformations which would compromise the validity of linear analysis assumptions and quasi-linear stress allowable as given in Paragraph C.6. of NRC Regulatory Guide 7.6.

Successive drop tests at the most critical orientations of the package failed to induce any measurable distortion of the containment vessel, or exterior shell. Under service conditions, internal pressures would induce membrane biaxial tensile stress components in the containment vessel. These tensile stresses would tend to reduce compressive stresses due to hypothetical accident impact induced internal forces. Thus, under these conditions, the package would be less susceptible to buckling failures than under the conditions tested. Since no incipient buckling was experienced during the test, it may be safely concluded that buckling is not a probable failure mechanism for the 1-13C II Package. No further consideration of buckling is therefore provided in this report.

## 2.2 Weights and Center of Gravity

The center of gravity of the 1-13C II package is located at the geometric center of gravity and is shown in the sketch found as Figure 2.5.2-1 on page 2-54.

Weight breakdown is as follows:

Cask Body	17,955
Lid	2,115
Top Overpack	1,550
Bottom Overpack	1,255
Overpack Binders	480
Contingency (2.8%)	<u>645</u>
Net Package	24,000 lbs.
Payload	<u>1,000</u>
TOTAL GROSS PACKAGE WEIGHT:	27,000 lbs.

### 2.3 Mechanical Properties of Materials

The Model 1-13C II package is fabricated from stainless steel, low carbon steel, and structural foam. Drawing E-1-436-111; Section 1.3, defines the specific material used for each item of the package. Table 2.3.1 presents material properties used through the analysis and references the sources of these data.

The energy absorbing overpacks are constructed of rigid polyurethane foam with a density of 16.5 lb/ft<sup>3</sup>, foamed in place, self-extinguishing. Figure 2.3-1 represents the stress-strain curve for the foam used for this package. The curve provides both minimum and maximum compressive properties and was derived from eight samples of varying density and grain direction. A 95% probability factor was applied to the standard deviation to establish the spread shown. CNSI Foam Specification No. 1-436-112 defines the detail foaming testing procedure. It specifies that foam samples will be taken during the actual foaming process and tested to verify that they are within  $\pm 10\%$  of the mean curve at 10%, 30% and 60% strains.

TABLE 2.3-1  
Mechanical Properties of Materials

Material	Grade or Type	Temperature F <sup>o</sup>	Strength (ksi)			Elastic Modulus (4) (x10 <sup>6</sup> psi)	Thermal Expansion Coefficient (5) (x10 <sup>-6</sup> in/in.)
			Yield (1)	Ultimate (2)	Allowable (3)		
ASTM-A240 Plate (Shells)	304	70			-	28.3	9.11
		100	30.0	75.0	20.0	-	9.16
		200	25.0	71.0	20.0	27.7	9.34
		300	22.5	66.0	20.0	27.1	9.47
		400	20.7	64.4	18.7	26.6	9.59
		500	19.1	63.5	17.5	26.1	9.70
ASTM-A479 Bar, Round (Bosses & Lid Lug)	304	70			-	28.3	9.11
		100	30.0	75.0	20.0	-	9.21
		200	25.0	71.0	20.0	27.7	9.50
		300	22.5	66.0	20.0	27.1	9.73
		400	20.7	64.4	18.7	26.6	9.96
ASTM-A514 Plate (Tiedown Frame)	B	70	100 <sup>(8)</sup>	110 <sup>(8)</sup>	-	29.9	6.07
ASTM-A516 Plate (Overpack Inner Shell)	70	70			-	27.9	6.07
		100	38.0	70.0	23.3	-	6.20
		200	34.6	70.0	23.1	27.7	6.67
		300	33.7	70.0	22.5	27.4	7.10
		400	32.6	70.0	21.7	27.0	7.54
ASTM-A414 Sheet (Overpack Ext. Shell) or ASTM-A 285 Plate	C	70			-	29.9	6.07
		100	30.0	55.0	13.7 (min)		
		200					
	300	(8)	(8)				
	C	300	(8)	(8)			
400							
ASTM-A354 Bolts (Closure Bolts) [SAE J429]	BD [R]	70	125 (9)	150 (9)	-	29.9	6.07

Table 1 (Continued)  
Mechanical Properties of Materials

Material	Grade or Type	Temperature F <sup>o</sup>	Yield (1)	Strength (ksi)		Elastic Modulus (4) (x10 <sup>6</sup> psi)	Thermal Expansion Coefficient (5) (x10 <sup>-6</sup> in/in.)
				Ultimate (2)	Allowable (Sm) (3)		
ASTM-A449 Bolts (Ratchet Binder Bolts) [SAE J429]	A & B [5]	70	92 (8)	120 (8)	-	29.9	6.07
QQ-L-171e or ASTM B-29-55 (Lead Shielding)	A or C Chemical	70	5.0 Dynamic Compression Min (6)	10.0	2.3 (yield)  (6)	2.0	16.4 (50 <sup>o</sup> -212 <sup>o</sup> F)  (7)
ASTM-A193 Bolts	Class 1 Grade B8 or Class 1A, Grade B8A	70 or 100	30 @ 100 <sup>o</sup> (8)	75 @ 100 (8)		28.3 @ 70	6.07 @ 70 <sup>o</sup>

2-9

Reference:

- (1) ASME Code, Section III, Appendices, Table I-2.1 for ferritic material; Table I-2.2 for austenitic materials.
- (2) ASME Code, Section III, Appendices, Table I-3.1 for ferritic material; Table I-3.2 for austenitic materials.
- (3) ASME Code, Section III, Appendices, Table I-1.1 for ferritic material; Table I-1.2 for austenitic materials.
- (4) ASME Code, Section III, Appendices, Table I-6.0, Page 69.
- (5) ASME Code, Section III, Appendices, Table I-5.0, Page 68, coefficient B.
- (6) Cask Designers Guide, ORNL-NSIC-68.
- (7) Sandia lab report No. SAND 77-1872 (NUREG/CR-0481)
- (8) ASTM Axxx Standard Specification for . . . . (xxx = Alloy designation).
- (9) ASME Code, Section III, Table I-1.3, Page 98.

Revision 0



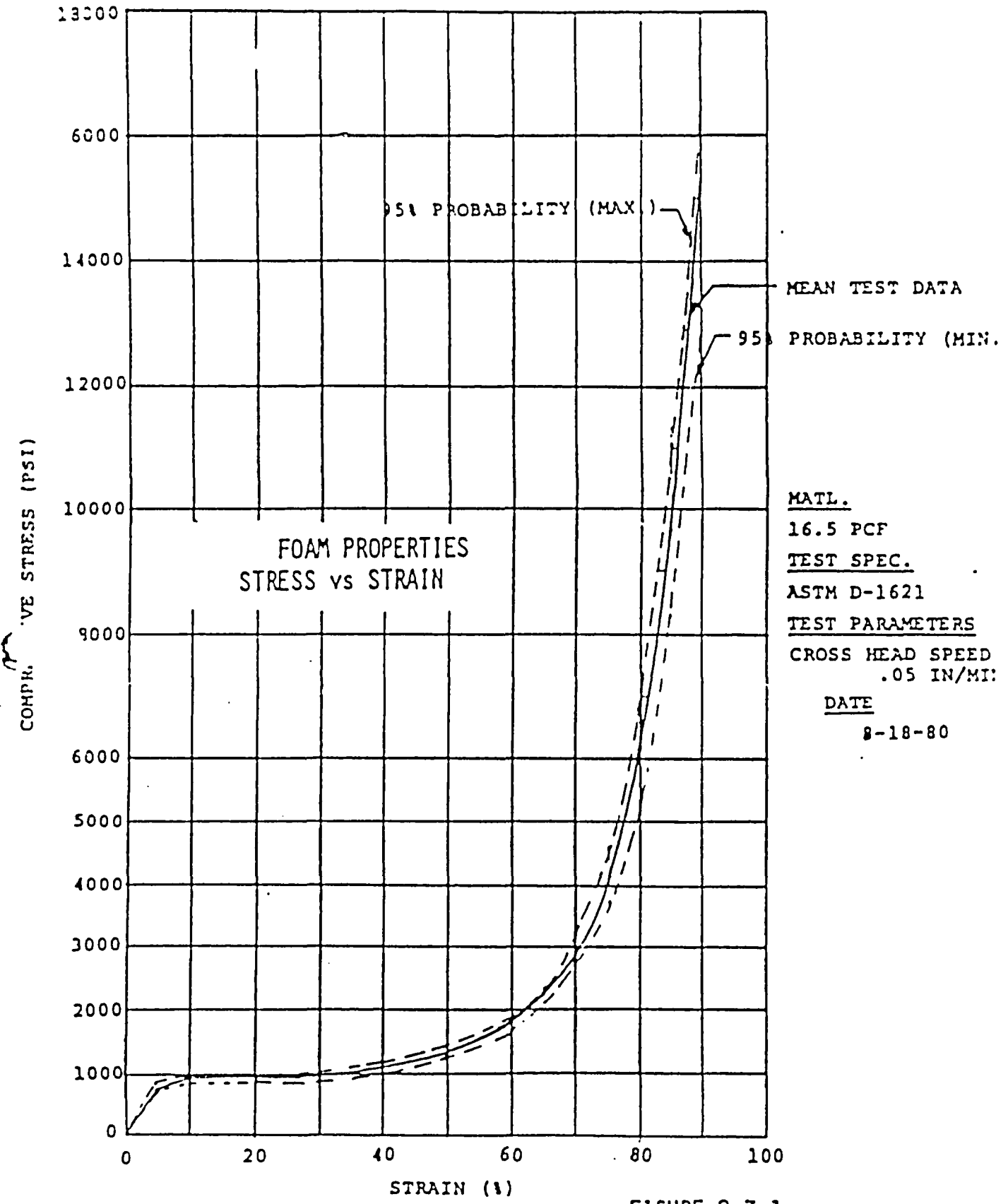


FIGURE 2.3-1

## 2.4 General Standards for All Packages

### 2.4.1 Minimum Package Size

The cylindrical cask is 39.12 inches in diameter and 68.06 inches high.

### 2.4.2 Tamperproof Feature

Seal wires are attached to the designated ratchet binder top and bottom pins.

### 2.4.3 Positive Closure

The positive closure system has been previously described in Section 1.2.1.

### 2.4.4 Chemical and Galvanic Reactions

The materials from which the packaging is fabricated (steel, lead, and polyurethane foam) along with the contents of the package will not cause significant chemical, galvanic, or other reaction in air, nitrogen, or water atmospheres.

## 2.5 Lifting and Tiedown Standards for All Packages

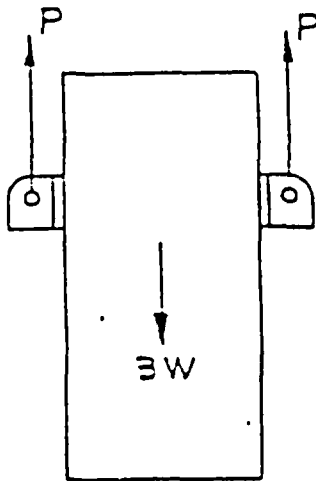
### 2.5.1 Lifting Devices

The 1-13C II Cask is provided with two lifting lugs attached to the side of the cask by which the cask and load can be lifted. The lid is provided with a lifting ring by which the lid may be removed from the cask. Neither the cask lifting lug nor the lid lift ring will be used for tiedown and each will be provided with a cap or locking device to prevent such use.

The load requirements for lifting devices are defined in 10 CFR 71, Subpart E, Para 71.45 as being capable of supporting three times the weight without generating stresses in excess of its (the containers) yield strength.

## 2.5.1.1 Lifting Lugs &amp; Bolts

The load condition imposed on the lift lugs is as follows:



The lugs can be used only with overpacks removed. Therefore, the total lifted weight is:

$$W = 27000 - 3280 = 23720 \text{ lbs.}$$

The lug load is:

$$P = (23720 \text{ lb})(3g)/2 \text{ lugs} = 35,580 \text{ lb/lug}$$

- a. Shear in Bolts - each lifting lug is attached to the container with 4 1-8 UNC-2A x 2-3/4, ASTM-A449 Hex Head cap screws.

For each bolt: Tensile Stress Area =  $0.606 \text{ in}^2$

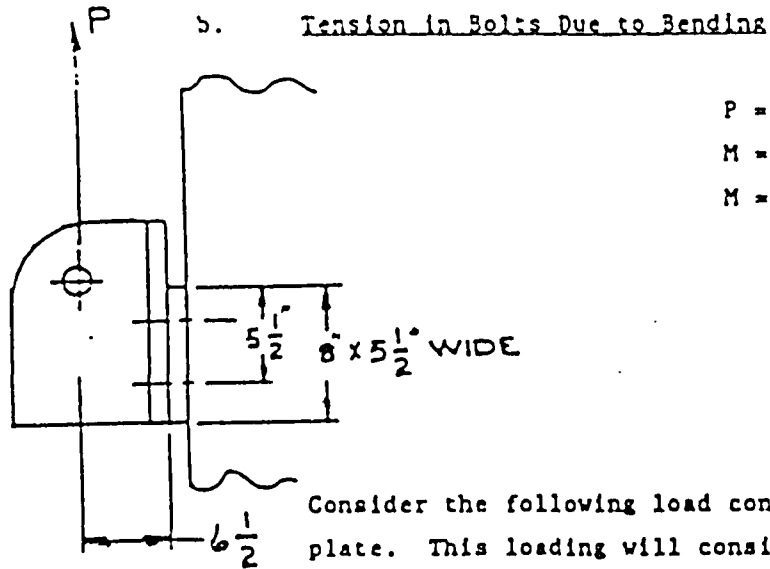
$$\text{Nominal Shear Stress} = \frac{(35,580) \text{ lb}}{4(0.606) \text{ in}^2} = 14678 \text{ psi}$$

The maximum Shear Stress is found at the center of the bolt cross section and is  $4/3$  x the nominal stress.

Therefore

$$\sigma_s = 4/3(14678) = 19570 \text{ psi.}$$

The effects of this stress are evaluated when combined with the Tensile Bolt Stress computed in the next section.

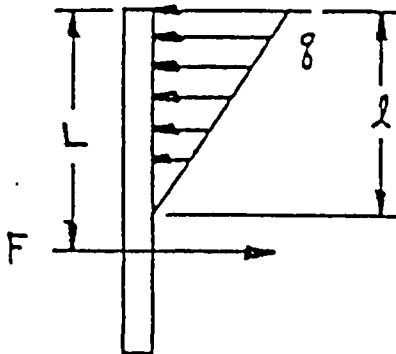


$$P = 35,580 \text{ lbs.}$$

$$M = (35,580) \text{ lbs (6.5) inch}$$

$$M = 231270 \text{ in-lbs.}$$

Consider the following load condition between the bolts and plate. This loading will consist of tension in the lower bolts and a "bearing pressure" between the plate and the lifting car.



(1) Summation of Forces

$$\frac{1}{2} q b l = F$$

(2) Summation of Moments

$$M = F(L - \frac{1}{3})$$

$$L = 5 \text{ inch}$$

$$b = 5.5 \text{ inch}$$

$$A_{\text{bolt}} = 0.606 \text{ in}^2$$

$$E_{\text{stainless steel}} = 28.3 \times 10^6 \text{ psi}$$

$$E_{\text{Bolt}} = 29.9 \times 10^6 \text{ psi}$$

## (3) Condition of Compatibility - Deflection Analysis

$$\frac{\delta \text{ bolt}}{\delta \text{ plate}} = \frac{\sigma \text{ bolt}}{\frac{q}{t_{s.s.}}}$$

$$\frac{\delta \text{ bolt}}{\delta \text{ plate}} = \frac{\sigma \text{ bolt}}{1.06 q} = \frac{2A \text{ bolt}}{1.06 q}$$

Also:

$$\frac{\delta \text{ bolt}}{\delta \text{ plate}} = \frac{L - l}{l}$$

$$\frac{L - l}{l} = \frac{F}{\frac{2A}{1.06 q}}$$

$$F l = 2A q (L - l) (1.06)$$

The above three equations contain three unknowns:

F, q, and l. Substituting the appropriate values produces the following set of equations.

By substituting equation (1) into equation (2), we obtain

$$M = q b l / 2 (L - l / 3)$$

$$\text{or: } q = 2M / b l (L - l / 3) \quad (4)$$

Similarly, substituting equation (1) in equation (3) gives:

$$\frac{1}{2} q b l^2 = 2A q (L - l) (1.06)$$

$$b l^2 + 4.24 A l - 4.24 A L = 0$$

$$l = \frac{-4.24 A \pm \sqrt{(4.24 A)^2 + (4)(b)(4.24 A L)}}{2b}$$

$$l = \frac{-2.12 A}{b} \pm \frac{1}{2b} \left[ (4.24 A)^2 + (16.96 A L b) \right]^{1/2} \quad (5)$$

$$l = 1.39 \text{ inches}$$

Now, using equation (4), the contact pressure is found:

$$q = \frac{(2)(231270)}{(5.5)(1.39)(5.5-1.39/3)} = 12012 \text{ lbs/in}^2$$

Using equation (1), the bolt load is found as:

$$F = 1/2 ab1 = \frac{(12012)(5.5)(1.39)}{2} = 45915 \text{ lbs}$$

Bolt tensile stress is found as:

$$\sigma_b = \frac{45915}{(2)(.606)} = 37884 \text{ psi}$$

Maximum Normal Stress Theory will be used for evaluating the effects of the combined stresses (Tension and Shear) on the bolts. From Mohr's Circle the Maximum Principle Tensile Stress is computed as:

$$\begin{aligned} \sigma_p &= \frac{\sigma_t}{2} + \sqrt{\left(\frac{\sigma_t}{2}\right)^2 + \sigma_v^2} \\ \sigma_p &= \frac{37884}{2} + \sqrt{\left(\frac{37884}{2}\right)^2 + 19750^2} \\ &= 46178 \text{ psi} \end{aligned}$$

Therefore the factor of safety for the bolts is

$$\text{F.S.} = \frac{92000}{46178} = +1.99$$

Bearing safety factor versus yield is found as:

$$\text{F.S.} = \frac{30000}{12012} = +2.50$$

c. Lug Stresses

Figure 2.5.1-1 depicts the lug configuration. The outstanding lug plate is attached to the flush plate with a vertical double vee weld. Net section is equal to the 1" plate thickness of the outstanding lug plate. Shear stress is:

$$f_v = \frac{35580}{(13)(1)} = 2737 \text{ psi}$$

Factor of Safety is:

$$F.S._v = \frac{30000/\sqrt{3}}{2737} = +6.33$$

Using a conventional  $40^\circ$  tearout relation, the capability of the lug at yield stresses is estimated as:

$$P_A = 2 F_{sy} t (E_m - d/2 \cos 40^\circ) = 127,689 \text{ lbs.}$$

Where:

$$F_{sy} = \frac{30000}{\sqrt{3}} = 17,320 \text{ psi; ASTM-A240, Type 304}$$

$$t = 1"$$

$$E_m = 4-1/2"$$

$$d = 2-1/8"$$

The factor of safety versus tearout is therefore:

$$F.S. = \frac{127689}{35580} = +3.59$$

**FIGURE WITHHELD UNDER 10 CFR 2.390**



Bending stress in the lug is found from:

$$f_b = Mc/I$$

$$M = (P) l$$

$$I = bh^3/12$$

For the lug and weld:

$$b = 1 \text{ inch}$$

$$h = 13 \text{ inches}$$

$$l = 5\text{-}1/2 \text{ inch}$$

$$c = h/2$$

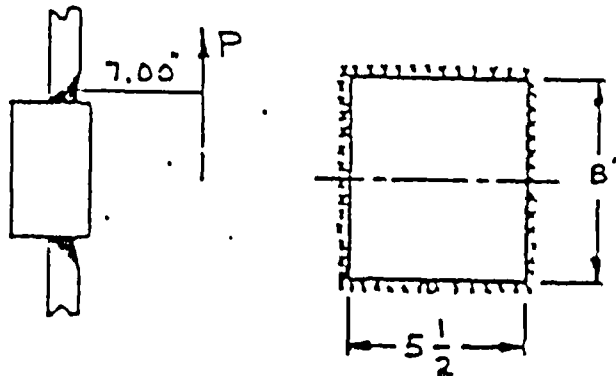
$$f_b = \frac{Plh/2}{bh^3/12} = \frac{6Pl}{bh^2} = \frac{(6)(35580)(5.5)}{(1)(13)^2} = 6948 \text{ psi}$$

The associated factor of safety is:

$$F.S. = \frac{30000}{6948} = +4.32$$

#### 2.5.1.2 Reinforced Lug Plate

The removable lug discussed in the foregoing section bolts to a flat reinforced lug plate of 2 inch thickness. This lug plate is attached to the cask outer shell and integral ring with a 1" circumferential bevel weld.



i. Shear Stress -  $f_s = P/A$

$$A = (\text{Perimeter}) (\text{Effective Weld Thickness})$$

$$= ((2) (8) + 2(5.5))(1)$$

$$= 27 \text{ in}^2$$

$$f_s = \frac{(35580) \text{ lbs}}{27 \text{ in}^2} = 1318 \text{ psi}$$

$$\text{Safety Factor} = \frac{10000/\sqrt{3}}{1318} = +13.1$$

ii. Bending Stress -  $f_b = Mc/I$

$$M = (Px1)$$

Revision 0

$$I = I_{\text{outer}} - I_{\text{inner}} = \left( \frac{bh^3}{12} \right)_o - \left( \frac{bh^3}{12} \right)_i$$

$$b_o = 7.50 \text{ in.}$$

$$b_i = 5.50 \text{ in.}$$

$$h_o = 10.00 \text{ in.}$$

$$h_i = 8.00 \text{ in.}$$

$$l = 7.0 \text{ in.}$$

$$c = h_o/2 = 5.0 \text{ in.}$$

$$I = 1/12 \left( (7.50)(10)^3 - (5.5)(8)^3 \right) = 390 \text{ in}^4$$

$$f_b = \frac{(35580) \text{ lbs } (7.00) \text{ in } (5.00) \text{ in.}}{390 \text{ in.}}$$

$$f_b = 3193 \text{ psi}$$

$$\text{Safety Factor} = 30000/3190 = 9.4$$

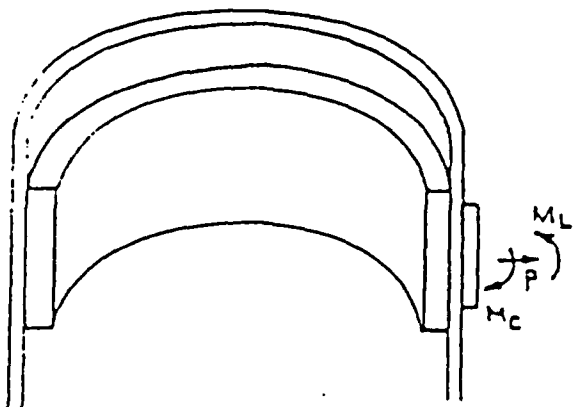
#### 2.5.1.3 Outer Shell and Integral Ring

The 1-13C II cask is designed with a reinforcing ring 8 inches high, 1 inch thick, located directly opposite the lifting lugs on the inside surface of the outer shell.

$P$  = Radial Force

$M_L$  = Moment in Longitudinal  
Direction to Shell

$M_C$  = Moment in Circumferential  
Direction to Shell



It will be necessary to determine the stress generated in the shell due to the loading transmitted by the lifting lug. The presence of the inner reinforcing ring will be accounted for using STARDYNE, see Section 2.10.2.5, finite element idealization of the shell and ring as shown in Figure 2.5.1-2. The model represents a single quadrant of the outer shell, ring and reinforcing plate, or pad. The contributions of inner shell and lead shield are conservatively ignored.

Symmetric boundary conditions are imposed upon the planes of symmetry which slice through the model at the center line of the lifting pad and  $90^\circ$  away from this location.

Loads are introduced by a set of downward load applied at the lower edge of the outer shell. These loads are reacted by vertical restraints at the center line of the lifting eye.

Figures 2.5.1-3, -4, -5, and -6 define the model geometry completely. Figure 2.5.1-3 presents the developed surface of the cask outer shell quadrant shown in Figure 2.5.1-2. Figure 2.5.1-4 presents a detail of the reinforced pad installed in the cask outer shell. Nodes 66-69 represent the points where the lift lug forces are transmitted to the outer shell-ring node. Figure 2.5.1-5 presents the idealized (symmetric half) lift lug, with node 74 corresponding to the center of the lug eye. Figure 2.5.1-6 presents the developed surface of the reinforcing ring. Figures 2.5.1-7, -8, -9, -10, -11, and -12 present computer generated plots of the model visually verifying the example.

Figures 2.5.1-13, -14, -15, and -16 summarize states of stress of all finite elements surrounding the reinforcing plate or pad. Computer stress output for the entire model can be found in Section 2.10.4.

Figures 2.5.1-13, -14, -15, and -16 illustrate a predicted state of stress consistent with expected outer shell and ring behavior. The offset lift lug load induces torsion in the ring. This torsion causes the top edge of the ring to deflect inward with a corresponding outward deformation of the lower edge of the ring. These deformations induce a concave deformation of shell elements above the ring and a convex deformation below the ring. As expected, the concave deformation pattern induces compressive bending stresses on the shell outer surface above the ring. Similarly, convex deformations induce tensile bending stresses on the shell outer surface below the ring. The specific states of stress in the shell elements immediately above and below the lug pad are found from Figures 2.5.1-13 and -14 as follows:

	Above (El. 68)	Below (El. 69)
<u>Membrane</u> (1)		
$S_x$ (Hoop)	-2137	+ 903
$S_y$ (Meridian)	-2018	+7103
$S_{xy}$	+ 536	-1313
<u>Bending</u> (2)		
$S_x$	-8374	+5805
$S_y$	-3970	-2040
$S_{xy}$	- 958	- 802

- NOTES: (1)  $S_M = (S_o + S_i)/2$   
 (2)  $S_B = (S_o - S_i)/2$   
 (3)  $S_o =$  Outside Stress  
 $S_i =$  Inside Stress

FIGURE 2.5.1-2

RING STIFFENER OUTER SHELL

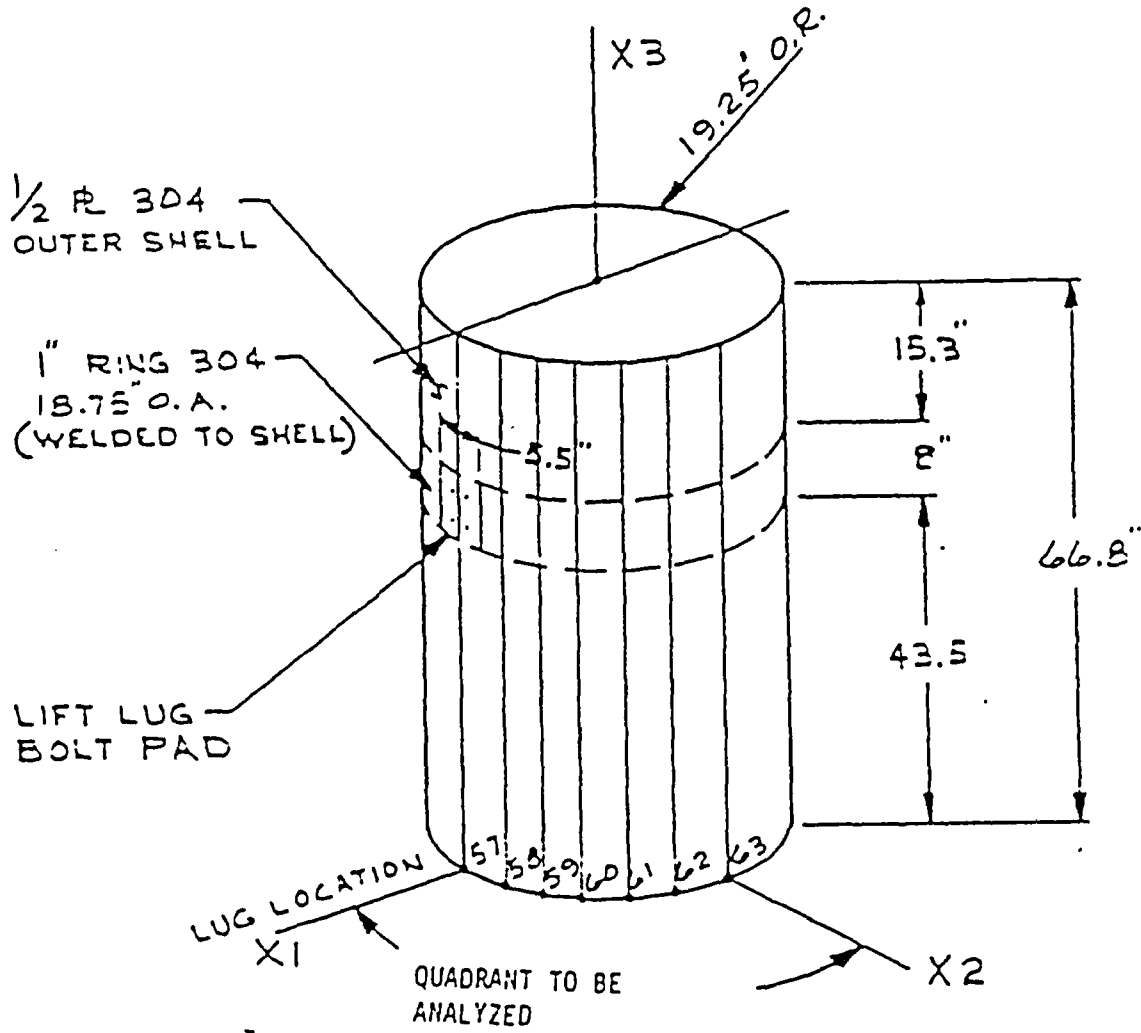


FIGURE 2.5.1-3

DEVELOPED SURFACE - MODELED QUADRANT

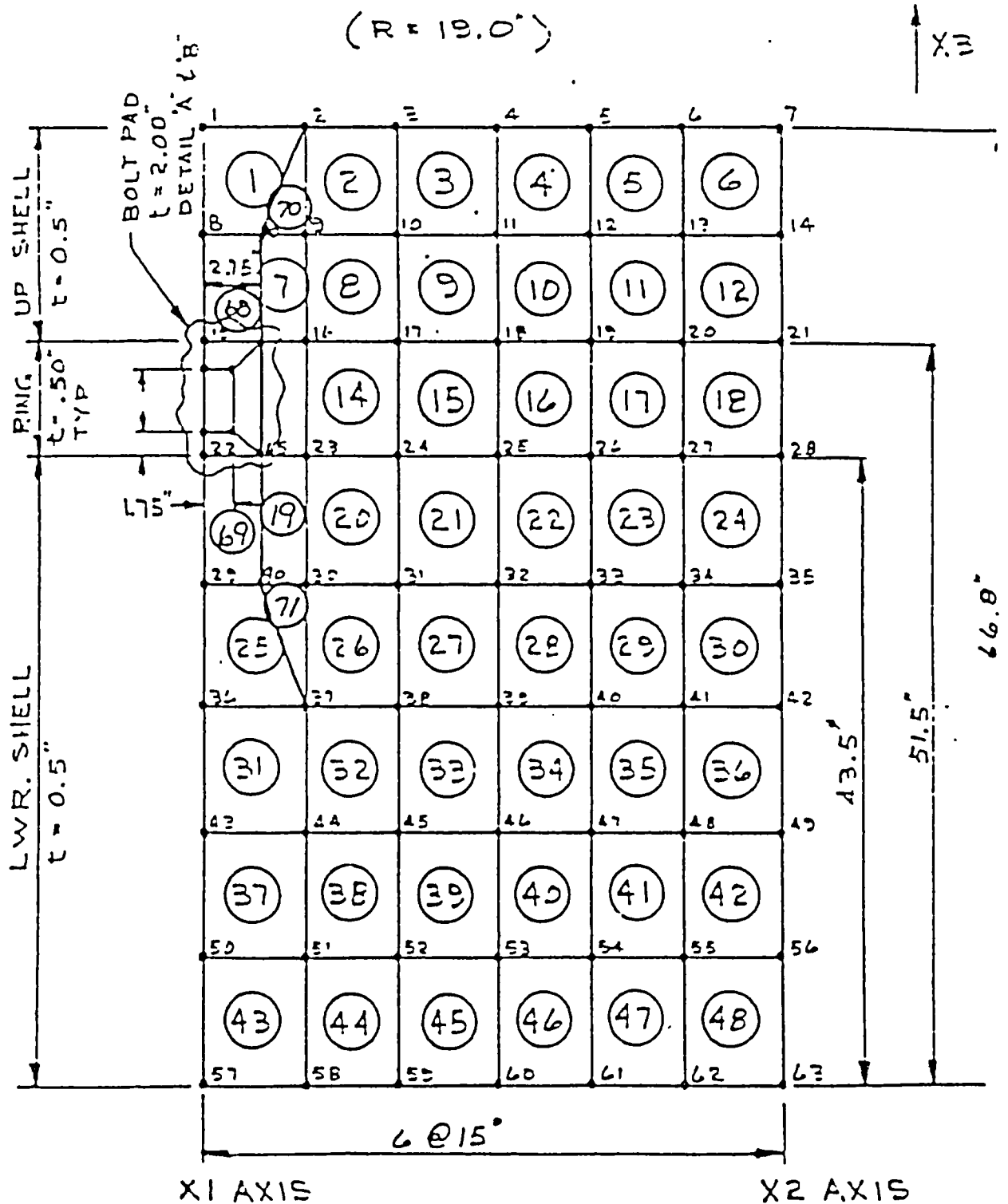


FIGURE 2.5.1-4

DETAIL 'A' BOLT PAD R = 19"

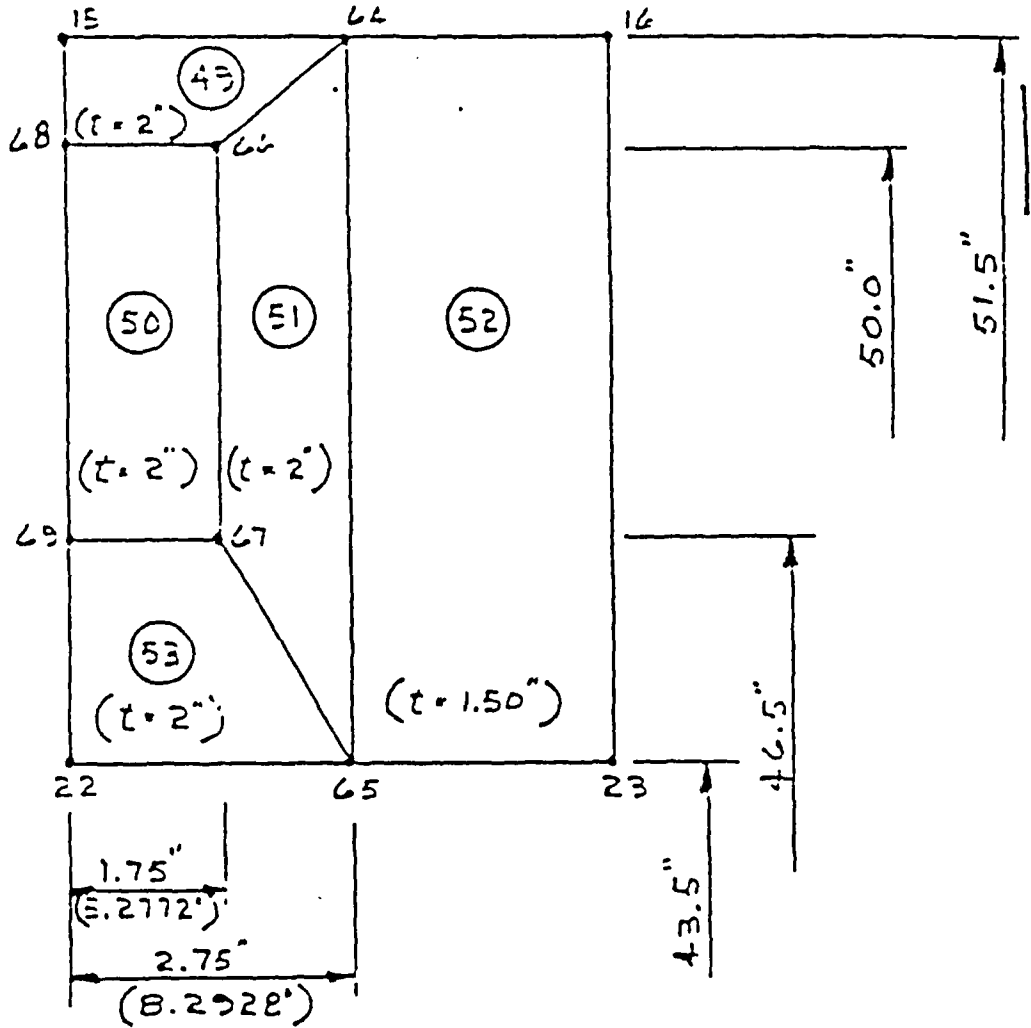
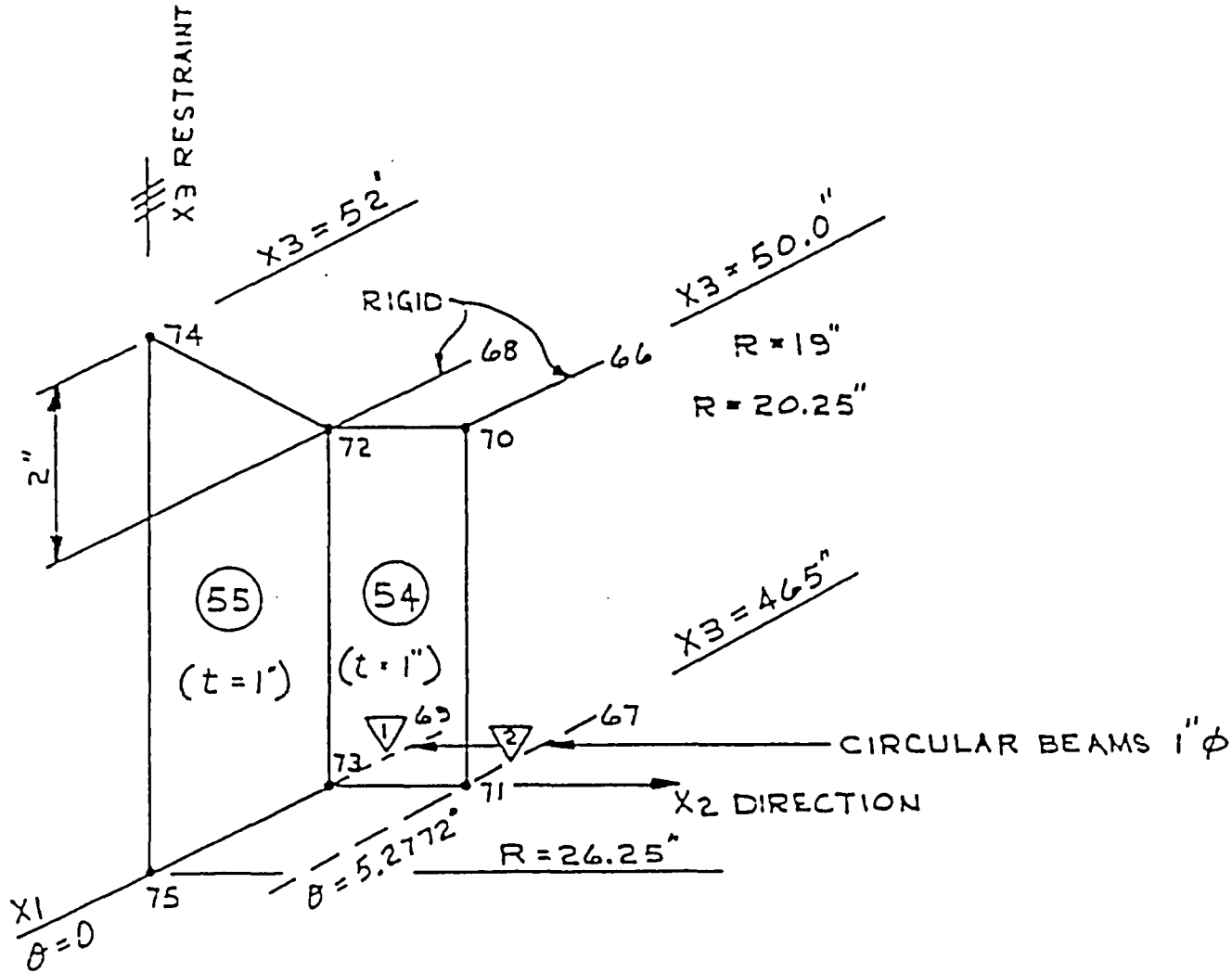




FIGURE 2.5.1-5

DETAIL "B" LIFT LUG (IDEALIZED)



NODE 74 IS THE CENTER OF LUG EYE

FIGURE 2.5.1-6

DEVELOPED SURFACE - REINFORCING RING

(R = 18.25")

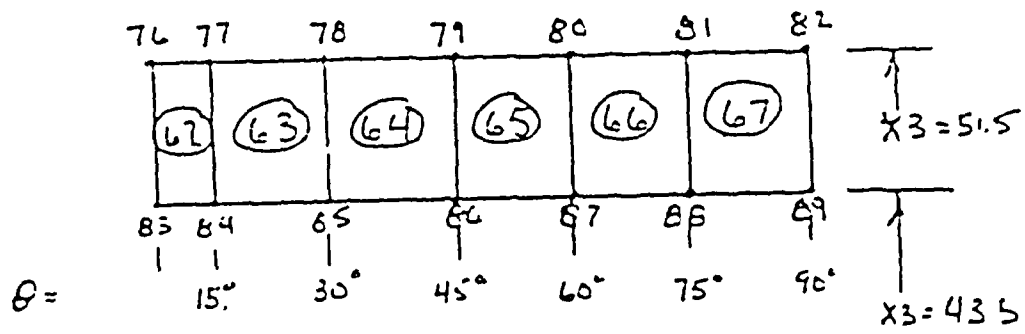
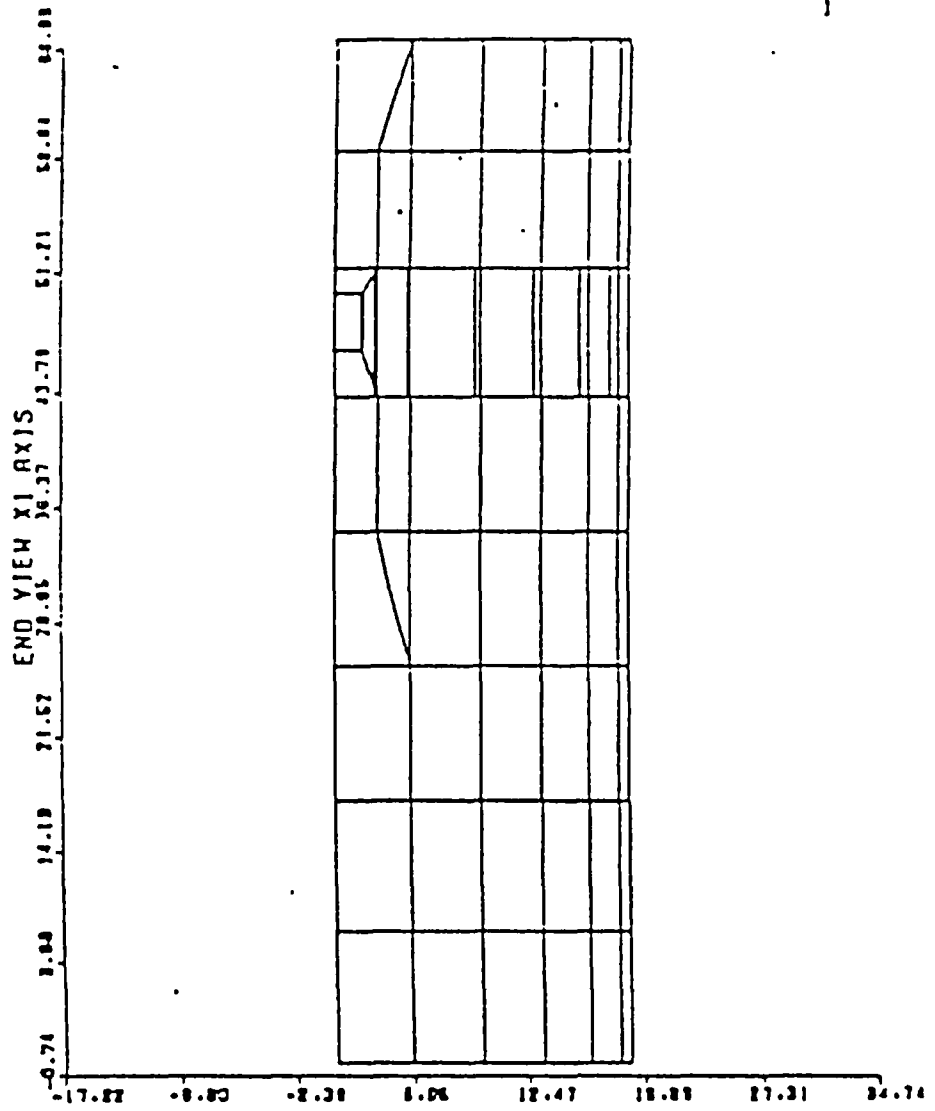


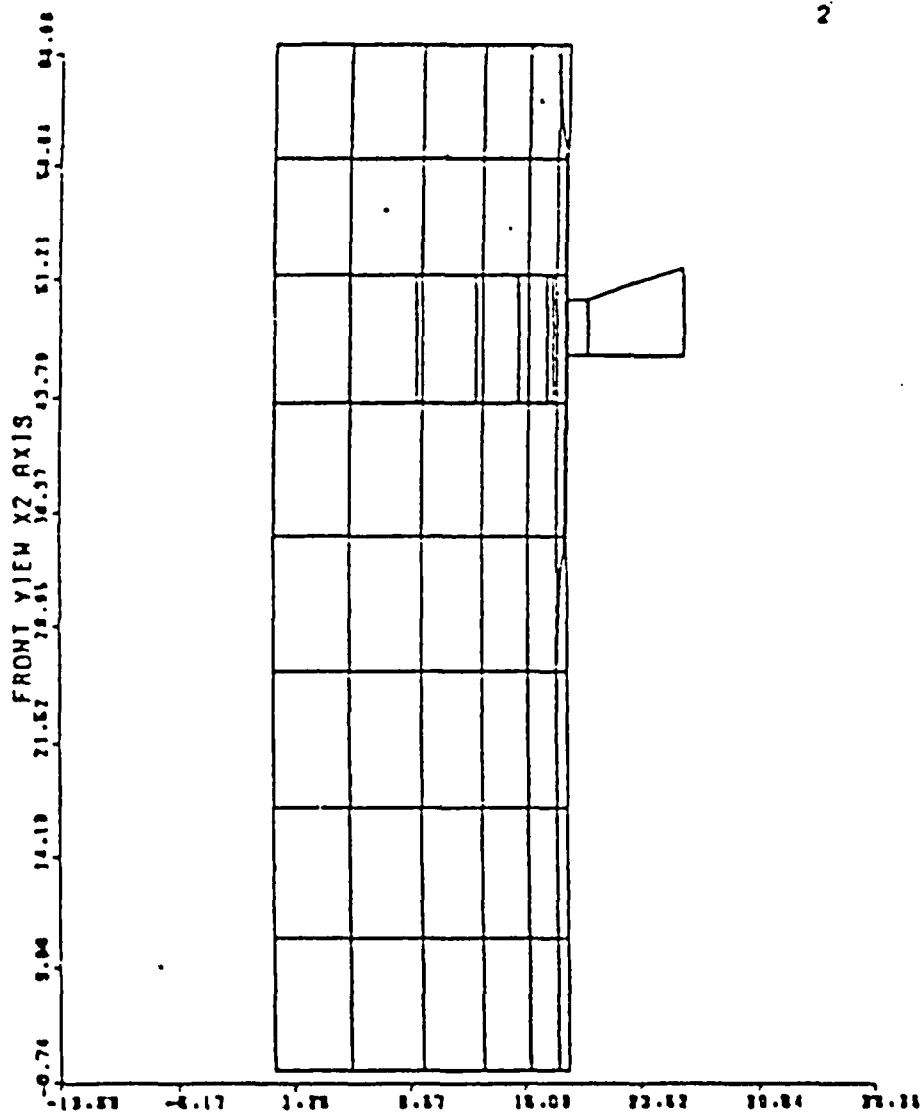
FIGURE 2.5.1-7



COMPUTER GENERATED MODEL PLOT

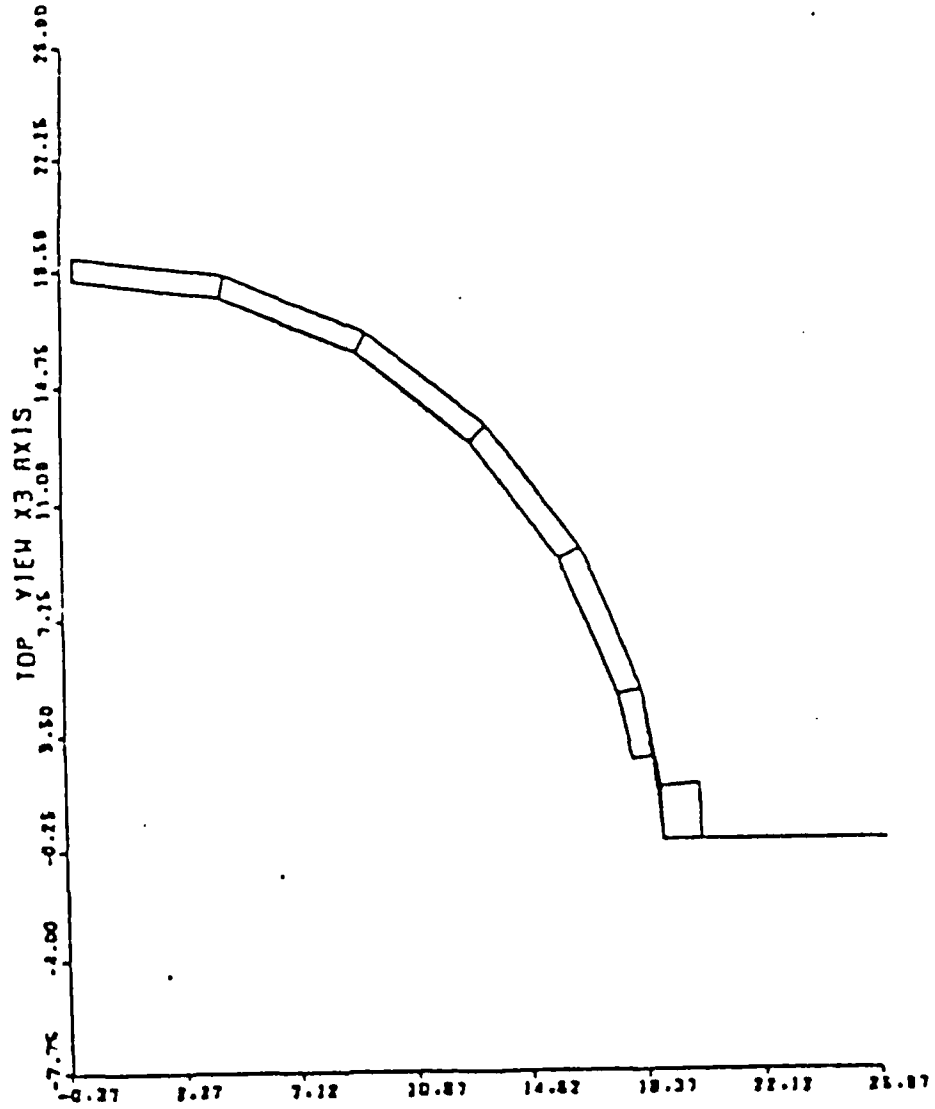
FIGURE 2.5.1-8

2



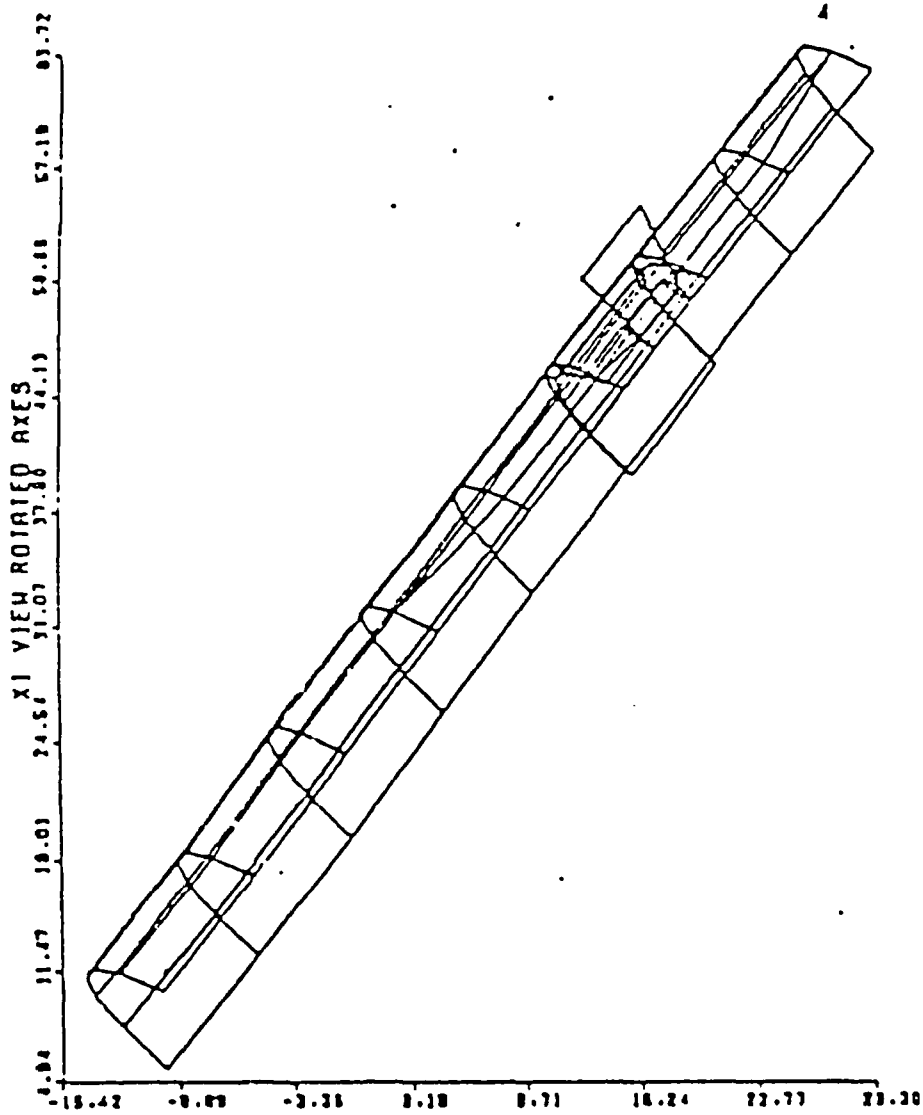
COMPUTER GENERATED MODEL PLOT

FIGURE 2.5.4-9



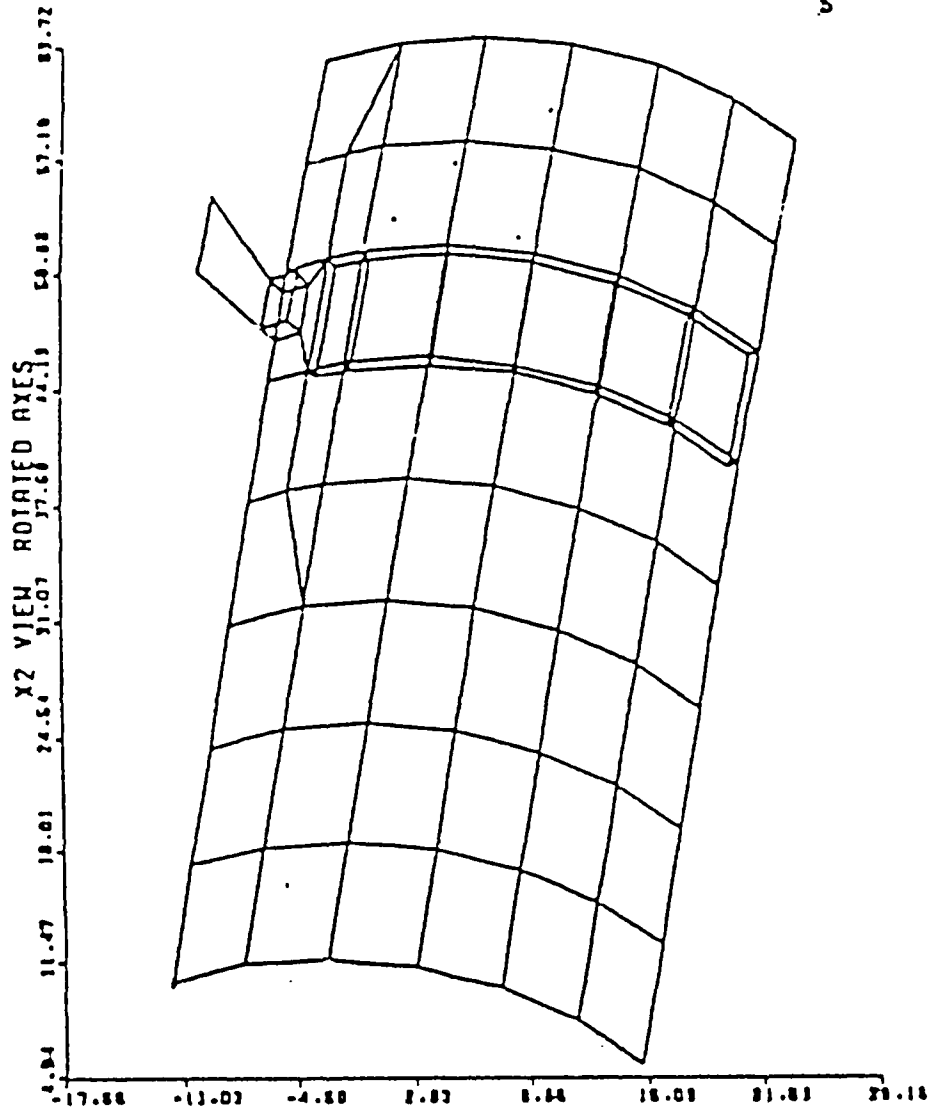
COMPUTER GENERATED MODEL PLOT

FIGURE 2.5.4-10



COMPUTER GENERATED MODEL PLOT

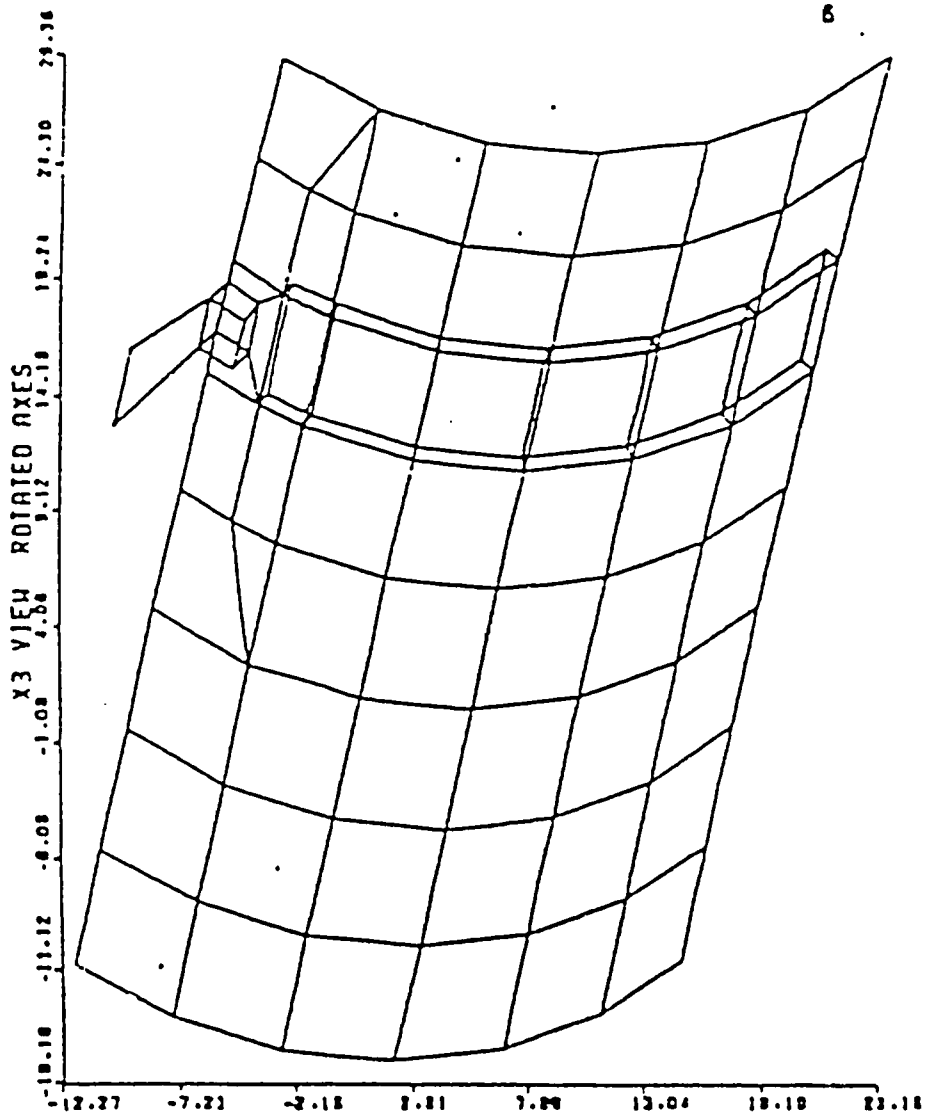
FIGURE 2.5.4-11



S

COMPUTER GENERATED MODEL PLOT

FIGURE 2.5.A-12



COMPUTER GENERATED MODEL PLOT



The predicted stresses all assume a package weight of 23,720 lbs. This weight does not include 3280 lbs. of energy absorbing overpacks. The package is never lifted with overpacks installed; this is geometrically impossible. Thus, the maximum package weight, when lifted, cannot exceed 23,720 lbs.

The maximum stress in the cask outer shell in the region of the reinforcing ring is:

$$f_{\max} = 14,930 \text{ psi} \quad (\text{Quad 15})$$

The maximum stress in the reinforcing ring is:

$$f_{\max} = 18,670 \text{ psi} \quad (\text{Quad 63})$$

The maximum stress in the cask away from the reinforcing ring is:

$$f_{\max} = 21,870 \text{ psi} \quad (\text{Quad 43})$$

Quadrilateral element 43 is at the base of the model where point loads representing the total cask weight is applied. The model neglects cask endplate reinforcement existing at this location. All stresses in this region of the model are considered to be fictitious, although acceptable, and are not utilized in subsequent margin of safety calculations.

Under normal conditions of transport, the maximum temperature of the outer shell is 188.7°F. Therefore, the interpolated yield allowable in 304 available (ASTM A-240) is:

$$f_{\text{allowable}} = 25,565 \text{ psi}$$

Revision 0

The resultant minimum factor of safety versus yield in the outer shell and integral ring is:

$$F.S._y = \frac{25,565}{18,670} = +1.37$$

FIGURE 2.5.1-13

STATE OF STRESS - OUTER SHELL OUTER FACE (+Z)

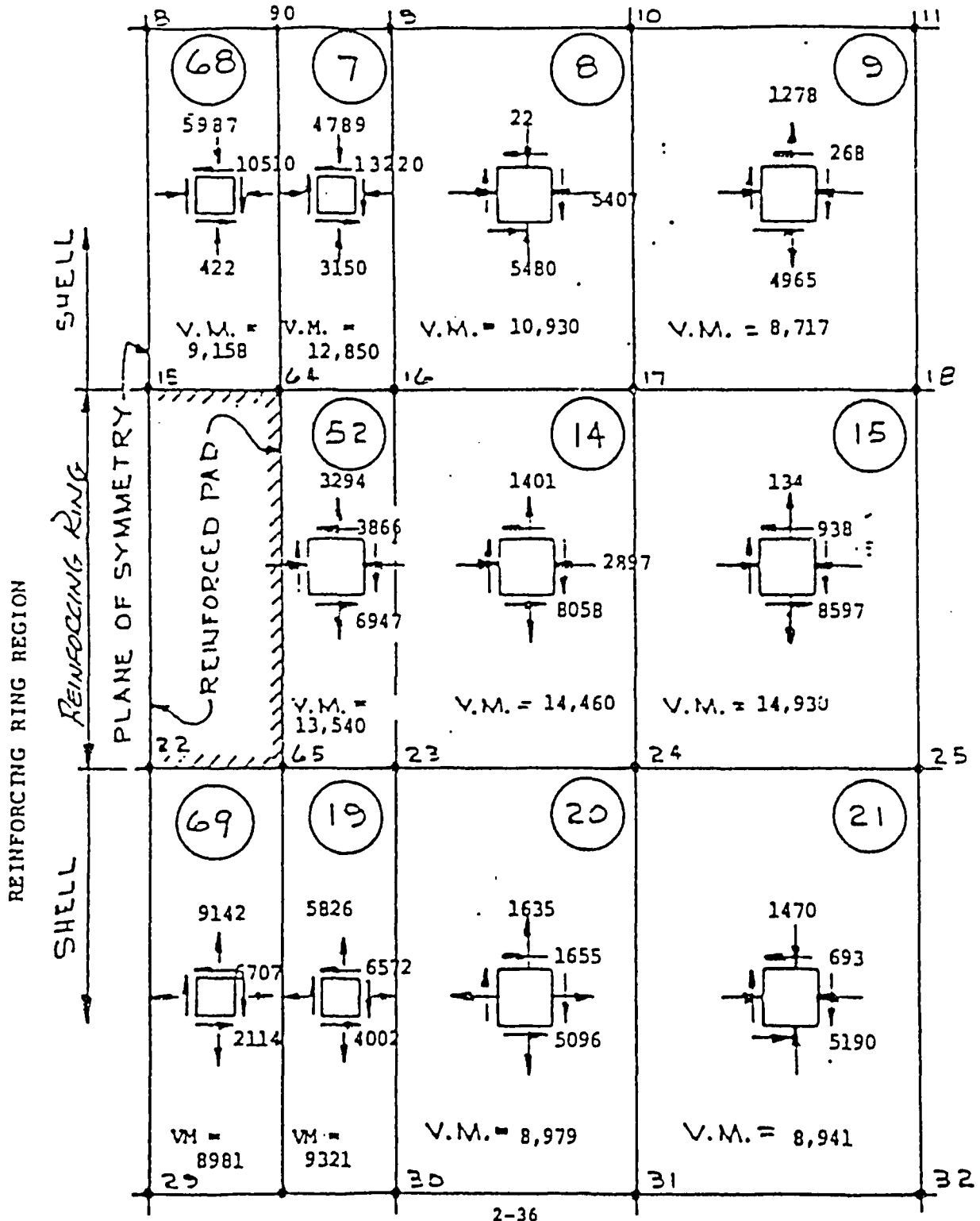


FIGURE 2.5.1-14

STATE OF STRESS - INNER SHELL INNER FACE (-Z)

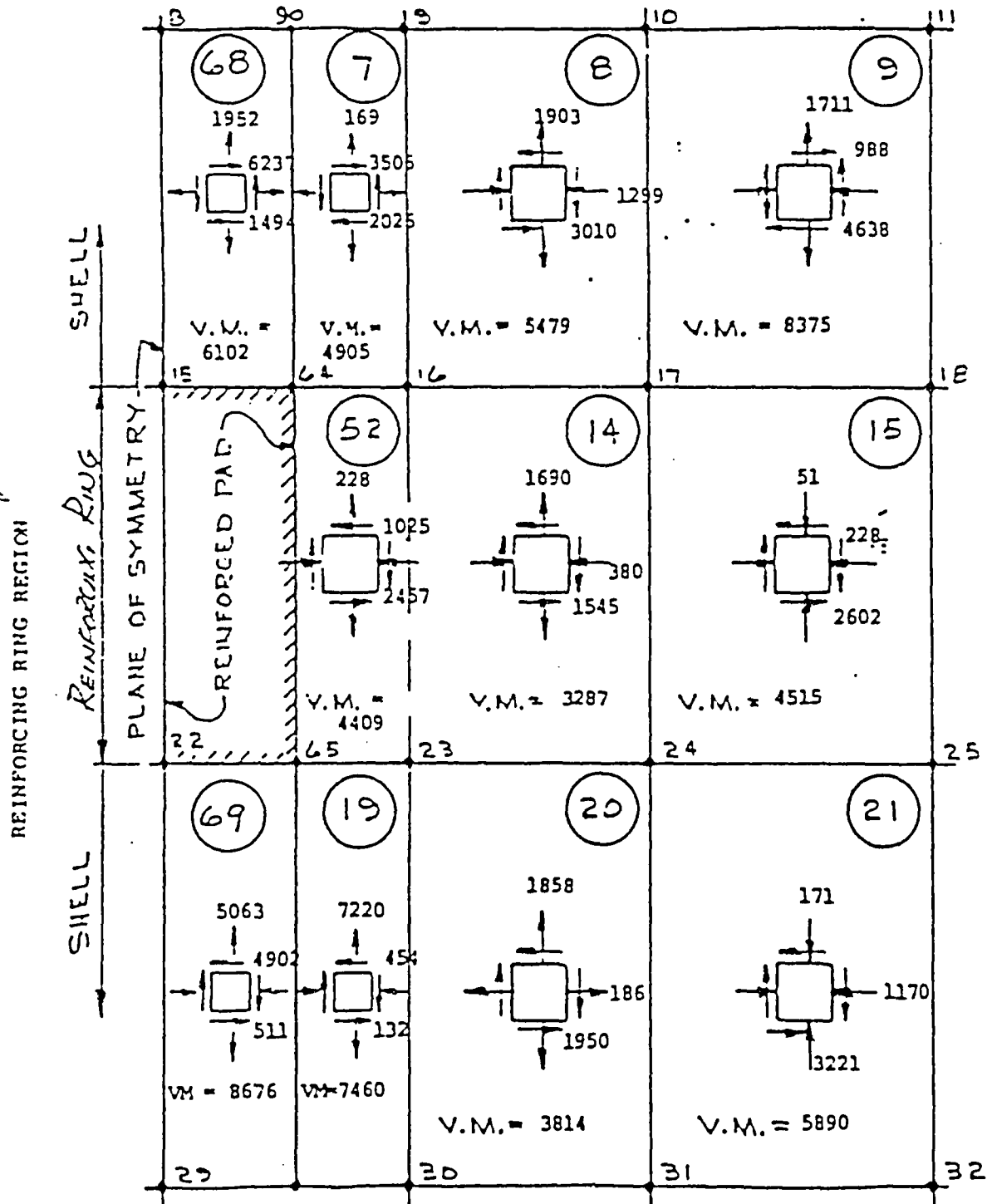


FIGURE 2.5.1-15

STATE OF STRESS - REINFORCING RING OUTER FACE (+ Z)

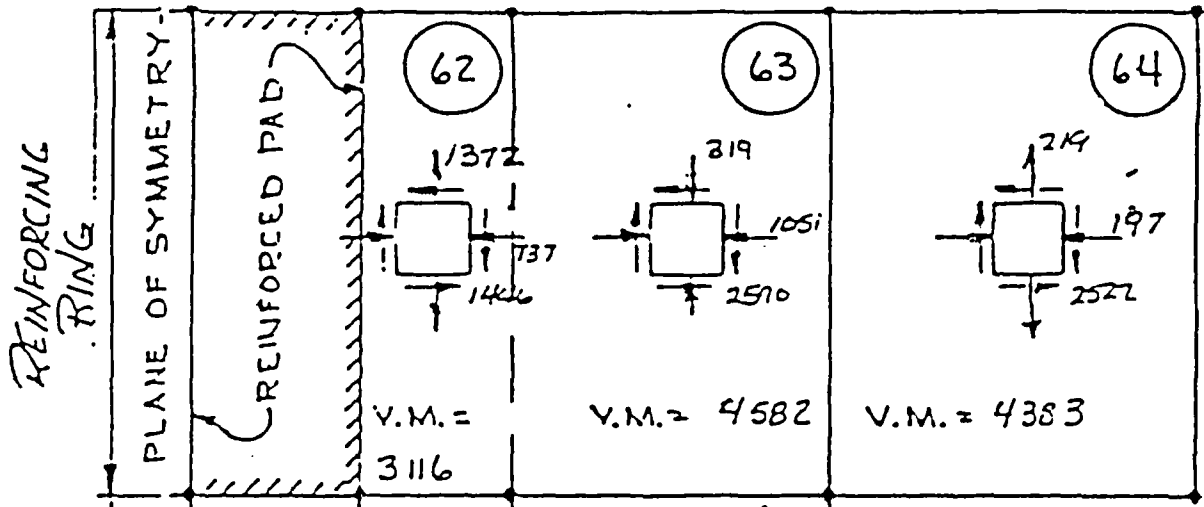
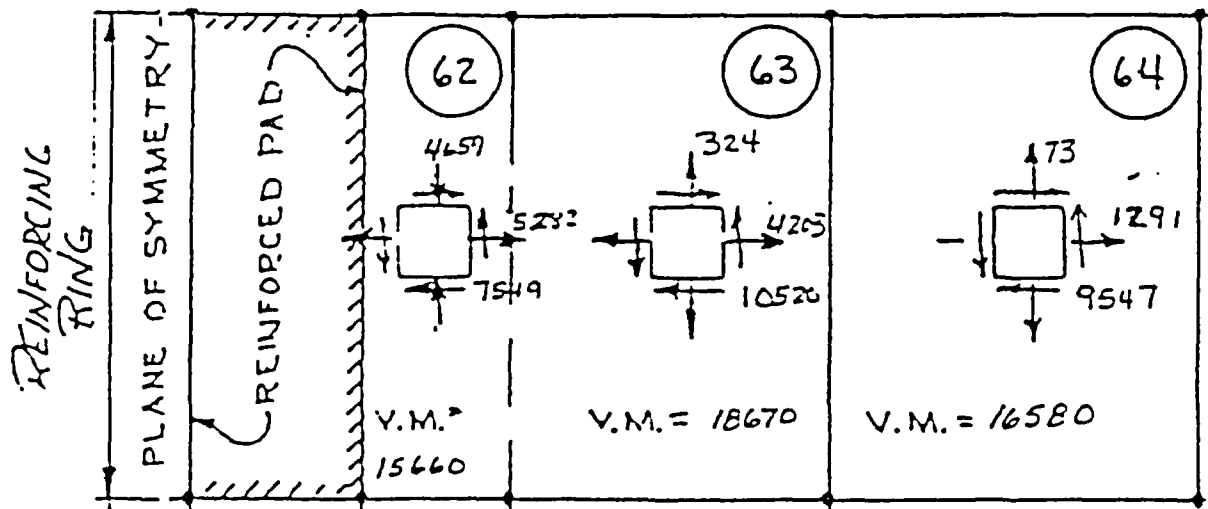


FIGURE 2.5.1-16

STATE OF STRESS - REINFORCING RING INNER FACE (- Z)



Section 2.5.1.2 provided a nominal evaluation of lug plate attachment weld stresses. The finite element analysis discussed in this section provides a basis for detail evaluation of ring attachment weld stresses. Referring to Figure 2.5.1-6, a 1/2" vee-groove weld joins the ring to shell along node lines 76-82 and 83-89. A 1" vee-groove weld attaching the ring to boss extends from nodes 76 to 83. Corner forces applied to the ring at the node points by the welds are as follows:

Joint Node	$\theta$ (See Fig. 2.5.1-6)	Corner Force (Global Coord)		
		FX1 (Lbs)	FX2 (Lbs)	FX3 (Lbs)
76	8.2928°	-8075	-7437	-14449
83	8.2928°	11033	-11516	-9969
77	15°	-3670	18618	-5320
84	15°	4277	-12832	-1995
78	30°	-8509	-17526	-2602
85	30°	6318	-9818	1028

Running weld forces may be computed by transforming the global coordinate values to local coordinate values using the polar angle  $\theta$ . The transformation is as follows:

$$\begin{Bmatrix} F \\ \end{Bmatrix}_L = \begin{bmatrix} \cos\theta & \sin\theta & 0 \\ -\sin\theta & \cos\theta & 0 \\ 0 & 0 & 1 \end{bmatrix} \cdot \begin{Bmatrix} F_X \\ \end{Bmatrix}_G$$

Shear and tension load per unit weld length are found by considering total in-plane and out-of-plane forces:

$$F_S = (F_{L_2}^2 + F_{L_3}^2)^{1/2} / l, \text{ lbs/in.}$$

$$F_T = F_{L_1} / l$$

Where:  $l$  = effective weld length per node  
as listed below.

Node		$l$ (in)
76/83	$4" + 18.25 (15^\circ - 8.2928^\circ) \left(\frac{\pi}{180}\right) (h)$	5.068
77/84	$18.25 \left(\frac{\pi}{180}\right) (22.5^\circ - 11.646^\circ)$	3.457
78-85	$18.25 \left(\frac{\pi}{180}\right) (15)$	4.778

The corresponding weld forces are found as:

Joint (Node)	WELD FORCES (lbs/in)		
	Tension ( $F_T$ )	Shear ( $F_S$ )	Effective Shear ( $F_V$ )*
76	-1788.	+3102	3228
83	1826	3230	3357
77	368	5689	5692
84	234	3948	3950
78	292	4103	4106
85	118	2450	2451

$$*F_V = \left[ F_S^2 + (F_T/2)^2 \right]^{1/2}$$



The most highly stressed weld location occurs at node 77, just beyond the lug pad location. The weld consists of a 1/2" full penetration vee-groove weld with a shear capacity of:

$$F_{vA} = \frac{25565}{3} (1/2) = 7380 \text{ lbs/in}$$

The factor of safety in the weld is:

$$F.S. = \frac{7380}{5692} = + 1.30$$

Computer generated corner forces and plate stresses is provided in Section 2.10.3.

30 BASE WIDE LOAD

MEMBER	NODES	ELEMENT FORCES			ELEMENT STRESSES			PRINCIPAL STRESSES		VECTOR ANGLE	
		FX	FY	FRY	SX	SY	SXY	MAX	MIN		
12	1	FX = 4.2561E+02	FY = -1.1671E+02	FRY = -1.0028E+02	+ZFACE SX = -1.378E+04	SY = -1.615E+03	SXY = -1.676E+03	-ZFACE -1.388E+03	-1.401E+04	6.311E+01	-82.249
		MX = -6.0481E+02	MY = -5.755E+01	MXY = -6.149E+01	-ZFACE SX = 1.549E+04	SY = 1.144E+03	SXY = -1.275E+03	-ZFACE 1.560E+04	1.035E+03	7.282E+03	5.043
									VM	1.511E+04	
12	2	FX = 2.524E+02	FY = 5.107E+00	FRY = -1.616E+02	+ZFACE SX = -7.045E+03	SY = -6.524E+02	SXY = -5.147E+03	-ZFACE 1.387E+03	-4.085E+03	5.236E+03	-63.811
		MX = -3.138E+02	MY = -2.764E+01	MXY = -1.393E+02	-ZFACE SX = 8.017E+03	SY = 6.741E+02	SXY = 3.501E+03	-ZFACE -4.419E+03	-7.275E+02	5.073E+03	-21.818
									VM	9.803E+03	
12	3	FX = -4.192E+01	FY = 4.955E+01	FRY = -1.044E+02	+ZFACE SX = 7.305E+02	SY = 4.048E+02	SXY = -5.431E+03	-ZFACE 5.602E+03	-4.061E+01	4.833E+03	-45.235
		MX = -3.344E+01	MY = 2.624E+01	MXY = -1.922E+02	-ZFACE SX = -8.482E+02	SY = -4.518E+02	SXY = 4.394E+03	-ZFACE 3.725E+03	-5.074E+03	4.399E+03	46.455
									VM	7.650E+03	
12	4	FX = -6.812E+01	FY = 4.487E+01	FRY = -4.414E+01	+ZFACE SX = 5.643E+03	SY = 1.621E+03	SXY = -3.734E+03	-ZFACE 7.873E+03	-6.090E+02	4.241E+03	-30.846
		MX = 2.404E+02	MY = 4.044E+01	MXY = -1.447E+02	-ZFACE SX = -5.907E+03	SY = -1.281E+03	SXY = 3.930E+03	-ZFACE 9.661E+02	-8.155E+03	4.560E+03	60.239
									VM	6.678E+03	
12	5	FX = 1.342E+00	FY = -2.543E+01	FRY = 7.101E+01	+ZFACE SX = 8.002E+03	SY = 1.876E+03	SXY = -2.161E+03	-ZFACE 8.689E+03	1.144E+03	3.745E+03	-17.625
		MX = 3.333E+02	MY = 4.071E+01	MXY = -9.597E+01	-ZFACE SX = -7.947E+03	SY = -1.488E+03	SXY = 2.445E+03	-ZFACE -1.110E+03	-4.266E+03	3.874E+03	70.429
									VM	8.364E+03	
12	6	FX = 4.847E+01	FY = -3.780E+01	FRY = 2.433E+01	+ZFACE SX = 8.429E+03	SY = 2.131E+03	SXY = -6.978E+02	-ZFACE 8.999E+03	2.080E+03	3.470E+03	-5.801
		MX = 3.674E+02	MY = 4.140E+01	MXY = -3.110E+01	-ZFACE SX = -8.733E+03	SY = -2.241E+03	SXY = 7.451E+02	-ZFACE -2.144E+03	-8.824E+03	3.322E+03	83.077
									VM	7.965E+03	
12	8	FX = -6.447E+02	FY = -6.841E+02	FRY = -2.884E+02	+ZFACE SX = -1.178E+04	SY = -7.340E+03	SXY = -1.995E+03	-ZFACE -6.835E+03	-1.248E+04	2.923E+03	-64.670
		MX = -4.237E+02	MY = -2.544E+02	MXY = -6.246E+01	-ZFACE SX = 9.938E+03	SY = 4.421E+03	SXY = 1.103E+03	-ZFACE 1.023E+04	5.647E+03	2.744E+03	11.742
									VM	6.867E+03	
12	9	FX = -7.657E+02	FY = 2.240E+01	FRY = -1.232E+02	+ZFACE SX = -2.274E+03	SY = -2.144E+03	SXY = -1.232E+02	-ZFACE 1.378E+03	-4.345E+03	4.741E+03	-55.047

2-43

Revision 0

2-44

16.-----11	MY	-1.616E+02		SXY	2.704E+01		VM	5.152E+01	
12. 10	FY	-5.074E+02	+ZFACL	SX	-4.734E+02				
10/10/11	FY	5.833E+02		SY	1.700E+03	+ZFACL	5.108E+03	-4.382E+03	4.745E+03
10/10/11	FXY	-8.911E+01		SXY	-4.671E+03				0.227E+01
10/10/11	MX	2.257E+01	-ZFACL	SX	-1.527E+03				
10/10/11	FY	-1.196E+00		SY	1.133E+03	-ZFACL	4.100E+03	-4.732E+03	4.520E+03
17.-----11	MY	-1.872E+02		SXY	4.315E+03		VM	7.431E+01	51.659
12. 11	FY	-5.343E+02	+ZFACL	SX	1.430E+03				
10/10/12	FY	1.633E+02		SY	9.443E+02	+ZFACL	5.001E+03	-2.205E+03	1.643E+03
10/10/12	FXY	6.730E+01		SXY	-3.610E+03				6.472E+03
10/10/12	MX	-1.253E+02	-ZFACL	SX	-4.086E+03				
10/10/12	FY	2.583E+01		SY	-2.933E+02	-ZFACL	2.178E+03	-6.507E+03	4.718E+03
18.-----11	MY	-1.560E+02		SXY	3.879E+03		VM	7.793E+01	52.025
12. 12	FY	-7.157E+02	+ZFACL	SX	3.166E+03				
10/10/13	FY	-8.076E+01		SY	2.485E+02	+ZFACL	4.589E+03	-5.750E+02	2.542E+03
10/10/13	FXY	-4.018E+01		SXY	-2.308E+03				4.402E+03
10/10/13	MX	1.911E+02	-ZFACL	SX	-6.029E+03				
10/10/13	FY	4.208E+01		SY	-1.172E+03	-ZFACL	-1.374E+02	-7.063E+03	3.463E+03
19.-----11	MY	-9.450E+01		SXY	2.468E+03		VM	6.945E+01	67.264
12. 13	FY	-8.505E+02	+ZFACL	SX	3.764E+03				
10/10/14	FY	-9.843E+01		SY	1.122E+03	+ZFACL	3.986E+03	0.944E+02	1.543E+03
10/10/14	FXY	4.044E+00		SXY	-7.980E+02				3.421E+03
10/10/14	MX	2.277E+02	-ZFACL	SX	-7.166E+03				
10/10/14	FY	5.494E+01		SY	-1.515E+03	-ZFACL	-1.398E+03	-7.245E+03	2.945E+03
20.-----11	MY	-3.342E+01		SXY	4.302E+02		VM	6.647E+01	61.812
12. 16	FY	1.654E+02	+ZFACL	SX	-4.729E+03				
10/10/17	FY	1.111E+03		SY	7.300E+02	+ZFACL	1.151E+04	-1.550E+04	1.150E+04
10/10/17	FXY	1.266E+03		SXY	-1.322E+04				2.347E+04
10/10/17	MX	-1.820E+03	-ZFACL	SX	4.977E+03				
10/10/17	FY	-1.494E+00		SY	7.448E+02	-ZFACL	1.792E+04	-1.220E+04	1.506E+04
23.-----11	MY	-5.275E+03		SXY	1.491E+04		VM	7.624E+04	40.461
12. 17	FY	2.240E+01	+ZFACL	SX	-1.684E+03				
10/10/18	FY	1.717E+01		SY	-8.704E+01	+ZFACL	1.141E+04	-1.119E+04	1.230E+04
10/10/18	FXY	7.690E+02		SXY	-1.227E+04				7.132E+04
10/10/18	MX	-2.371E+02	-ZFACL	SX	1.714E+03				
10/10/18	FY	-3.643E+01		SY	1.049E+02	-ZFACL	1.424E+04	-1.241E+04	1.132E+04
24.-----11	MY	-4.705E+03		SXY	1.330E+04		VM	2.310E+04	43.275
12. 18	FY	-1.544E+02	+ZFACL	SX	1.500E+03				
10/10/19	FY	-2.328E+02		SY	-1.471E+02	+ZFACL	1.076E+04	-9.447E+03	1.010E+04
10/10/19	FXY	3.253E+01		SXY	-1.007E+04				1.751E+04
10/10/19	MX	6.023E+02	-ZFACL	SX	-1.712E+03				
10/10/19	FY	-1.196E+01		SY	-1.233E+02	-ZFACL	9.182E+03	-1.102E+04	1.010E+04
25.-----11	MY	-3.776E+03		SXY	1.007E+04		VM	1.752E+04	47.256
12. 19	FY	-3.219E+02	+ZFACL	SX	7.477E+03				
10/10/20	FY	-1.392E+02		SY	-3.440E+01	+ZFACL	4.002E+04	-5.059E+03	7.710E+03
10/10/20	FXY	-2.575E+02		SXY	-2.738E+03				1.234E+04
10/10/20	MX	1.577E+03	-ZFACL	SX	-4.406E+03				
10/10/20	FY	2.114E+01		SY	-1.111E+02	-ZFACL	4.444E+03	-4.011E+03	6.740E+03
26.-----11	MY	-2.477E+01		SXY	2.311E+03		VM	1.149E+04	54.201

Revision 0

27	187	2A	FX = 2.091E+03	-ZFACE	SX = -5.852E+01	SY = -6.927E+01	-ZFACE	6.790E+02	-6.600E+03	3.639E+03	71.249
			FY = 4.571E+01							6.964E+03	
			FX = -8.611E+02								
			FY = 8.208E+02	+ZFACE	SX = 8.120E+03	SY = 9.445E+01	+ZFACE	1.125E+04	6.311E+03	2.472E+03	-52.773
			FY = 3.261E+03							9.771E+03	
			FX = -5.339E+02								
			FY = 2.899E+02	-ZFACE	SX = -4.437E+03	SY = 3.606E+03	-ZFACE	3.613E+03	-4.644E+03	4.229E+03	88.333
			FX = 1.217E+02							7.750E+03	
			FY = -5.473E+01								
			FX = 9.300E+02	+ZFACE	SX = 2.769E+03	SY = 3.260E+03	+ZFACE	-8.160E+03	-2.139E+03	5.153E+03	-46.365
			FY = -1.401E+03							9.421E+03	
			FX = -9.199E+02								
			FY = 3.781E+01	-ZFACE	SX = 9.309E+02	SY = 2.343E+03	-ZFACE	3.271E+03	2.256E+01	1.624E+03	57.686
			FX = 1.910E+01							3.260E+03	
			FY = -1.378E+02								
			FX = -5.144E+02	+ZFACE	SX = -5.045E+02	SY = -1.510E+03	+ZFACE	4.158E+03	-6.173E+03	3.165E+03	-42.206
			FY = -2.401E+02							9.003E+03	
			FX = -4.934E+02								
			FY = -8.384E+01	-ZFACE	SX = 2.562E+03	SY = 3.898E+02	-ZFACE	4.824E+03	-1.872E+03	3.340E+03	35.525
			FX = -3.954E+01							5.484E+03	
			FY = -1.731E+02								
			FX = 4.184E+02	+ZFACE	SX = -8.999E+02	SY = -1.576E+03	+ZFACE	2.413E+03	-5.349E+03	4.131E+03	-42.743
			FY = -5.273E+02							7.258E+03	
			FX = -1.905E+02								
			FY = -7.236E+01	-ZFACE	SX = 2.573E+03	SY = -5.735E+02	-ZFACE	4.706E+03	-2.706E+03	3.766E+03	32.439
			FX = -2.005E+01							6.447E+03	
			FY = -1.557E+02								
			FX = 5.576E+02	+ZFACE	SX = -5.138E+02	SY = 7.540E+01	+ZFACE	2.497E+03	-2.491E+03	2.710E+03	-48.113
			FY = -8.917E+01							4.710E+03	
			FX = -7.892E+01								
			FY = -6.787E+01	-ZFACE	SX = 2.744E+03	SY = -4.321E+02	-ZFACE	4.021E+03	-1.709E+03	2.865E+03	28.164
			FX = -1.057E+01							5.095E+03	
			FY = -1.059E+02								
			FX = -6.938E+02	+ZFACE	SX = -2.390E+02	SY = 1.305E+03	+ZFACE	1.753E+03	-6.872E+02	1.220E+03	-64.624
			FY = 3.128E+02							2.180E+03	
			FX = -7.256E+01								
			FY = -6.777E+01	-ZFACE	SX = 3.014E+03	SY = -4.192E+01	-ZFACE	3.237E+03	-2.647E+02	1.751E+03	14.610
			FX = 2.808E+01							3.377E+03	
			FY = -3.749E+01								
			FX = -4.327E+02	+ZFACE	SX = 1.011E+04	SY = 7.163E+03	+ZFACE	1.074E+04	6.532E+03	2.103E+03	-22.742
			FY = 2.025E+03							4.372E+03	
			FX = -7.690E+02								
			FY = 4.572E+02	-ZFACE	SX = -1.124E+04	SY = 9.378E+02	-ZFACE	9.520E+02	-1.105E+04	6.402E+03	88.040
			FX = 1.297E+02							1.216E+04	
			FY = -4.018E+01								
			FX = -2.440E+02	+ZFACE	SX = 5.142E+03	SY = 4.208E+03	+ZFACE	8.754E+03	5.946E+02	4.061E+03	-43.715
			FY = 1.340E+03							8.474E+03	
			FX = -1.478E+02								
			FY = 2.348E+02	-ZFACE	SX = -8.118E+03	SY = 1.152E+03	-ZFACE	1.435E+03	-4.402E+03	3.918E+03	14.034
			FX = 8.388E+01								
			FY = -1.148E+02								

2-45

Revision 0

37.-----11	FX = 3.8871+02 FY = -5.8731+02 FXY = -1.0191+01 PX = -1.6191+01 PY = -1.1191+02	-ZFACE	SX = 3.8081+02 SY = -3.1781+03 SZ = 2.1521+02 SX = 1.1591+03 SY = 2.8241+03	+ZFACE	5.2471+03 -3.1151+03 VM 8.4871+03	3.1881+03 VM 8.4871+03	-46.604
38.-----11	FX = -1.4491+01 FY = -4.7471+01 FXY = -2.5731+02 PX = -1.6491+02 PY = -6.9311+01 PXY = -1.6411+02	+ZFACE	SX = -3.4971+03 SY = -1.4581+03 SZ = -6.5491+03 SX = 3.9171+03 SY = 1.4491+03 SZ = 3.5701+03	+ZFACE	1.7441+03 -7.4011+03 VM 8.6071+03	4.6731+03 VM 8.6071+03	-51.612
39.-----11	FX = -7.8801+01 FY = 7.1581+01 FXY = -5.1001+01 PX = -2.5071+02 PY = -9.3771+01 PXY = -1.1941+02	+ZFACE	SX = -1.1901+03 SY = -2.1071+03 SZ = -7.7881+03 SX = 5.8651+03 SY = 2.1441+03 SZ = 2.7641+03	+ZFACE	-5.4441+02 -7.7431+03 VM 7.4861+03	3.5441+03 VM 7.4861+03	-62.277
40.-----11	FX = -1.1001+02 FY = 3.5871+02 FXY = 2.4221+01 PX = -2.9761+02 PY = -1.0341+02 PXY = -4.2601+01	+ZFACE	SX = -7.2421+03 SY = -1.7651+03 SZ = -1.0221+03 SX = 6.8021+03 SY = 3.2001+03 SZ = 1.0231+03	+ZFACE	-1.5811+03 -7.4271+03 VM 6.7761+03	2.9231+03 VM 6.7761+03	-74.768
41.-----11	FX = -9.4031+01 FY = 1.3041+03 FXY = -1.4401+02 PX = 6.4941+02 PY = 1.9821+02 PXY = -3.8811+01	+ZFACE	SX = 1.5411+04 SY = 7.3651+03 SZ = -1.2591+03 SX = -1.5741+04 SY = -2.1441+03 SZ = 6.0331+02	+ZFACE	1.5801+04 7.1721+03 VM 1.7531+04	4.2151+03 VM 1.7531+04	-8.691
42.-----11	FX = -2.1981+01 FY = 1.0551+03 FXY = -4.0511+02 PX = 4.1871+02 PY = 1.2531+02 PXY = -1.1061+02	+ZFACE	SX = 1.0001+04 SY = 5.2131+03 SZ = -3.4641+03 SX = -1.0091+04 SY = -9.9141+02 SZ = 1.8441+03	+ZFACE	1.1821+04 3.3471+03 VM 1.0541+04	4.2121+03 VM 1.0541+04	-27.667
43.-----11	FX = 5.1591+01 FY = 6.5871+02 FXY = -4.2061+02 PX = 8.2391+01 PY = 2.6791+01 PXY = -1.4041+02	+ZFACE	SX = 2.0911+03 SY = 3.9541+03 SZ = -4.7611+03 SX = -1.8641+03 SY = 6.7331+02 SZ = 2.4541+03	+ZFACE	-6.7871+03 -2.7371+03 VM 8.4411+03	4.7621+03 VM 8.4411+03	-44.605
44.-----11	FX = 9.4751+01 FY = 3.4631+02 FXY = -3.0781+02 PX = -2.1771+02 PY = -1.2441+03 PXY = -1.1871+02	+ZFACE	SX = -5.0151+03 SY = -8.1401+02 SZ = -4.6441+03 SX = 5.4121+03 SY = 2.2031+03 SZ = 3.4331+03	+ZFACE	2.1401+03 -8.0111+03 VM 9.1271+03	5.1151+03 VM 9.1271+03	-57.112
45.-----11	FX = 7.8271+01 FY = 3.0521+02 FXY = -1.2811+02	+ZFACE	SX = -4.7471+03 SY = -2.1411+03 SZ = -3.7711+03	+ZFACE	-9.8011+02 -1.1011+04 VM 1.4511+04	5.3141+03 VM 1.4511+04	-69.667

2-47

22.	51	FX = 4.9721+01	FFACE	SX = -	1.464				
		FY = 4.1391+02		SY = -2.1111+03	FFACE	-7.3641+03	-1.2241+04	4.4301+03	-03.21
		FZY = -2.7331+01		SZY = -1.1571+03			VM	1.1251+04	
		FX = -2.0141+02	-FFACE	SX = 1.2301+04					
		FY = -1.3171+02		SY = 4.1571+03	-FFACE	1.2541+04	4.6191+03	4.2101+03	7.357
		FZY = -4.6161+01		SZY = 1.0601+03			VM	1.1001+04	
22.	53	FX = -3.0101+02	FFACE	SX = 1.4741+04					
		FY = 0.6321+02		SY = 0.4371+03	FFACE	1.4051+04	0.3271+03	5.7641+03	-5.600
		FZY = -4.7871+01		SZY = -1.1211+03			VM	1.7271+04	
		FX = 0.4701+02	-FFACE	SX = -2.0451+04					
		FY = 2.7461+02		SY = -4.4821+03	-FFACE	-4.4441+03	-2.6481+04	0.0101+03	07.304
		FZY = -3.8031+01		SZY = 7.2921+02			VM	1.4001+04	
22.	54	FX = -1.9401+02	FFACE	SX = 1.3731+04					
		FY = 0.1311+02		SY = 4.1131+03	FFACE	1.4401+04	5.1641+03	4.8441+03	-20.147
		FZY = -2.5441+02		SZY = -3.1341+03			VM	1.3081+04	
		FX = 5.8721+02	-FFACE	SX = -1.4401+04					
		FY = 1.9521+02		SY = -3.0541+03	-FFACE	-2.6031+03	-1.4851+04	6.0041+03	74.473
		FZY = -1.0401+02		SZY = 2.0471+03			VM	1.3711+04	
22.	55	FX = -3.0571+01	FFACE	SX = 4.0001+03					
		FY = 7.0481+02		SY = 2.8041+03	FFACE	7.0591+03	-1.0551+03	4.5571+03	-41.144
		FZY = -3.2361+02		SZY = -4.4171+03			VM	0.4361+03	
		FX = 1.6421+02	-FFACE	SX = -4.1221+03					
		FY = 5.7671+01		SY = 3.5381+03	-FFACE	1.7081+03	-5.7441+03	3.7511+03	21.027
		FZY = -1.5711+02		SZY = 3.1221+03			VM	6.9111+03	
22.	57	FX = 1.6461+02	FFACE	SX = -6.5461+03					
		FY = 5.9041+02		SY = -6.9811+02	FFACE	1.7341+03	-8.6741+03	5.2021+03	-54.016
		FZY = -2.7371+02		SZY = -4.5251+03			VM	9.6631+03	
		FX = -2.4111+02	-FFACE	SX = 6.4451+03					
		FY = -0.7281+01		SY = 3.2921+03	-FFACE	6.6721+03	1.1041+03	3.7441+03	32.522
		FZY = -1.6581+02		SZY = 3.4311+03			VM	0.1761+03	
22.	57	FX = 1.8811+02	FFACE	SX = -1.3741+04					
		FY = 5.4651+02		SY = -3.6891+03	FFACE	-2.6761+03	-1.4761+04	6.0411+03	-71.164
		FZY = -1.5911+02		SZY = -3.3491+03			VM	1.3621+04	
		FX = -5.8831+02	-FFACE	SX = 1.4501+04					
		FY = -1.4431+02		SY = 5.8751+03	-FFACE	1.5281+04	5.0411+03	5.0411+03	12.1401
		FZY = -1.2631+02		SZY = 2.7131+03			VM	1.3471+04	
22.	58	FX = 2.1101+02	FFACE	SX = -1.7781+04					
		FY = 5.5071+02		SY = -5.0791+03	FFACE	-4.4021+03	-1.7841+04	6.4681+03	-84.532
		FZY = -4.7341+01		SZY = -1.2271+03			VM	1.6001+04	
		FX = -7.5431+02	-FFACE	SX = 1.8621+04					
		FY = -2.5711+02		SY = 7.2821+03	-FFACE	1.8721+04	7.1811+03	5.7641+03	5.105
		FZY = -4.7171+01		SZY = 1.0771+03			VM	1.6351+04	
22.	50	FX = -2.4441+02	FFACE	SX = 2.3221+04					
		FY = 4.8831+02		SY = 5.6681+03	FFACE	2.3281+04	5.6081+03	0.8381+03	-1.351
		FZY = -5.0701+00		SZY = -1.0311+03			VM	2.1051+04	
		FX = 4.8841+02	-FFACE	SX = -2.4221+04					
		FY = 1.7801+02		SY = -2.9151+03	-FFACE	-2.8671+03	-2.4271+04	1.0701+04	07.204
		FZY = -4.2551+01		SZY = 1.0111+03			VM	2.2421+04	
22.	51	FX = -1.4131+02	FFACE	SX = 1.6621+04					
		FY = 6.4361+02		SY = 4.4521+03	FFACE	1.7281+04	3.7441+03	6.7381+03	-12.718
		FZY = -1.8731+01		SZY = -2.8441+03			VM	1.5721+04	
		FX = 7.0771+02	-FFACE	SX = -1.7751+04					

REVISION 0

58.-----	59	MY = 1.2771E+02 MXY = -1.1401E+02	SY = -1.6000E+01 SXY = 2.0191E+01	-ZFAC	-1.1866E+03	-1.7841E+04	8.1271E+03 VM 1.1241E+04	40.105
59.-----	57	FY = -6.2481E+01 FY = 6.2751E+02 FXY = -2.5451E+01 MY = 7.1641E+02 MXY = 4.2241E+01	FZ = -6.2481E+01 FZ = 6.2751E+02 FZY = -2.5451E+01 MY = 7.1641E+02 MXY = 4.2241E+01	-ZFAC	8.3411E+03	-4.4541E+02	4.4181E+03 VM 0.6721E+03	-34.565
59.-----	55	MY = -1.6911E+02	SY = 3.7111E+02 SXY = 3.9471E+03	-ZFAC	2.3271E+03	-7.7551E+03	5.0411E+03 VM 4.1411E+03	63.067
60.-----	54	FY = 7.1441E+01 FY = 1.4051E+02 FXY = -4.2461E+01 MY = -2.4231E+02 MXY = -5.0431E+01	FZ = 7.1441E+01 FZ = 1.4051E+02 FZY = -4.2461E+01 MY = -2.4231E+02 MXY = -5.0431E+01	-ZFAC	9.4261E+03	7.4111E+01	4.4771E+03 VM 4.3421E+03	31.173
61.-----	53	MY = -1.7631E+02	SY = 2.5431E+03 SXY = 4.1441E+03	-ZFAC	9.4261E+03	7.4111E+01	4.4771E+03 VM 4.3421E+03	31.173
62.-----	52	FY = 1.8101E+02 FY = 6.6721E+02 FXY = -3.3641E+01 MY = -7.0741E+02 MXY = -1.2641E+02	FZ = 1.8101E+02 FZ = 6.6721E+02 FZY = -3.3641E+01 MY = -7.0741E+02 MXY = -1.2641E+02	-ZFAC	1.8061E+04	3.6511E+03	7.2031E+03 VM 1.6541E+04	12.901
63.-----	51	MY = -1.3341E+02	SY = 3.1351E+03	-ZFAC	1.8061E+04	3.6511E+03	7.2031E+03 VM 1.6541E+04	12.901
64.-----	50	FY = -2.4011E+02 FY = 6.8041E+02 FXY = -1.2481E+01 MY = -9.4171E+02 MXY = -1.6771E+02	FZ = -2.4011E+02 FZ = 6.8041E+02 FZY = -1.2481E+01 MY = -9.4171E+02 MXY = -1.6771E+02	-ZFAC	2.3161E+04	5.2641E+03	8.7431E+03 VM 2.1071E+04	3.755
65.-----	49	MY = -4.9751E+01	SY = 1.1841E+03	-ZFAC	2.3161E+04	5.2641E+03	8.7431E+03 VM 2.1071E+04	3.755
66.-----	48	FY = -3.3011E+03 FY = -7.1301E+03 FXY = -4.3181E+01 MY = -1.2171E+04 MXY = -1.2411E+03	FZ = -3.3011E+03 FZ = -7.1301E+03 FZY = -4.3181E+01 MY = -1.2171E+04 MXY = -1.2411E+03	-ZFAC	1.7511E+04	-1.4071E+03	4.6571E+03 VM 1.4541E+04	5.126
67.-----	47	MY = -2.5441E+03	SY = 1.7191E+03	-ZFAC	1.7511E+04	-1.4071E+03	4.6571E+03 VM 1.4541E+04	5.126
68.-----	46	FY = 3.3191E+03 FY = 3.7541E+03 FXY = 3.0701E+02 MY = -2.1441E+03 MXY = 4.3261E+03	FZ = 3.3191E+03 FZ = 3.7541E+03 FZY = 3.0701E+02 MY = -2.1441E+03 MXY = 4.3261E+03	-ZFAC	6.6641E+03	-6.2771E+03	6.4441E+03 VM 1.1211E+04	14.304
69.-----	45	MY = -2.5441E+03	SY = 4.0361E+03	-ZFAC	6.6641E+03	-6.2771E+03	6.4441E+03 VM 1.1211E+04	14.304
70.-----	44	FY = 1.7741E+01 FY = 2.3271E+03 FXY = -1.4361E+01 MY = 6.4191E+03 MXY = -4.3071E+03	FZ = 1.7741E+01 FZ = 2.3271E+03 FZY = -1.4361E+01 MY = 6.4191E+03 MXY = -4.3071E+03	-ZFAC	1.1421E+04	-4.5411E+01	1.0001E+04 VM 1.7341E+04	6.460
71.-----	43	MY = 2.7161E+03	SY = -4.2471E+03	-ZFAC	1.1421E+04	-1.0201E+04	1.0441E+04 VM 1.4741E+04	-70.446
72.-----	42	FY = 2.4741E+02 FY = 1.7011E+03 FXY = -7.6441E+02 MY = -2.4571E+03 MXY = 1.1111E+03	FZ = 2.4741E+02 FZ = 1.7011E+03 FZY = -7.6441E+02 MY = -2.4571E+03 MXY = 1.1111E+03	-ZFAC	1.1421E+04	-1.0201E+04	1.0441E+04 VM 1.4741E+04	-70.446
73.-----	41	MY = -4.4771E+03	SY = 1.0111E+04	-ZFAC	1.1421E+04	-1.0201E+04	1.0441E+04 VM 1.4741E+04	-70.446
74.-----	40	FY = 2.4741E+02 FY = 1.7011E+03 FXY = -7.6441E+02 MY = -2.4571E+03 MXY = 1.1111E+03	FZ = 2.4741E+02 FZ = 1.7011E+03 FZY = -7.6441E+02 MY = -2.4571E+03 MXY = 1.1111E+03	-ZFAC	1.1421E+04	-1.0201E+04	1.0441E+04 VM 1.4741E+04	-70.446
75.-----	39	MY = -4.4771E+03	SY = 1.0111E+04	-ZFAC	1.1421E+04	-1.0201E+04	1.0441E+04 VM 1.4741E+04	-70.446

02. /QUAD / 67	FXY = 1.339E+03	-----	SXY = -5.402E+03			VM	1.785E+04	
02. / / 68	FY = 8.793E+03	-ZFACE	SX = -1.145E+04					
02. / / 69	FY = 7.622E+03		SY = -8.305E+03	-ZFACE	-2.586E+03	-1.719E+04	7.113E+03	51.216
02. / / 70	FXY = -4.314E+03		SXY = 7.141E+03			VM	1.606E+04	
02. / / 71	FY = -5.157E+03	+ZFACE	SX = -5.070E+03					
02. / / 72	FY = -4.059E+03	-----	SY = -5.174E+03	+ZFACE	-2.315E+03	-1.256E+04	7.437E+03	-44.601
02. /QUAD / 70	FXY = -4.186E+03		SXY = -7.436E+03			VM	1.386E+04	
02. / / 71	FXY = 1.449E+01	-ZFACE	SX = -5.244E+03					
02. / / 72	FY = -1.439E+02		SY = -2.943E+03	-ZFACE	-2.612E+03	-5.376E+03	1.442E+03	-70.453
02. / / 73	FXY = -3.418E+02		SXY = -9.347E+02			VM	4.432E+03	
02. / / 74	FY = -1.477E-08	+ZFACE	SX = -1.477E-08					
02. / / 75	FY = 3.285E+03		SY = 3.285E+03	+ZFACE	6.433E+03	-3.148E+03	4.740E+03	-55.026
02. /QUAD / 77	FXY = -4.500E+03		SXY = -4.500E+03			VM	8.458E+03	
02. / / 78	FY = 0.	-ZFACE	SX = -1.477E-08					
02. / / 79	FY = 0.		SY = 3.285E+03	-ZFACE	6.433E+03	-3.148E+03	4.740E+03	-55.026
02. / / 80	FXY = 0.		SXY = -4.500E+03			VM	8.458E+03	

QUADRILATERAL STRESSES AND FORCES FOR OUTPUT VECTOR CONT'D



## 2.5.1.4 Lid Lifting Eye

The maximum lifting load exerted on the lifting eye of the cask lid is based on:

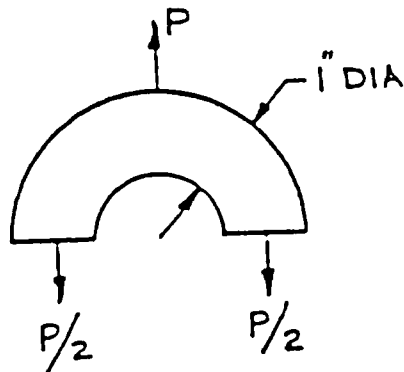
$$W_L = 2115 \text{ lbs.}$$

$$P = 3 W_L$$

$$P = (3) (2115) \text{ lbs.}$$

$$= 6345 \text{ lbs.}$$

## 1. Tension in the lifting eye.



$$\sigma_t = \frac{P}{2A}$$

$$A = \frac{\pi (1.0)^2}{4} = 0.785 \text{ in}^2$$

$$\sigma_t = \frac{(6345) \text{ lbs}}{2(0.785) \text{ in}^2}$$

$$= 4040 \text{ psi}$$

$$\text{Safety Factor} = \frac{35000}{4040} = 8.66$$

## 2. Welding Around Lifting Eye

$$A_{\text{eff}} = \pi D t_{\text{eff}} = \pi (1.0) \left(\frac{3}{8}\right) \left(\frac{\sqrt{2}}{2}\right) = 0.833 \text{ in}^2$$

$$\sigma_s = \frac{P}{2A_{\text{eff}}} = \frac{6345}{2(0.833)} = 3810 \text{ psi}$$

$$\text{Safety Factor} = \frac{20200}{3810} = 5.30$$

### 2.5.2 Tie-Down Devices

The tie-down system for transporting the package is designed to load conditions defined in 10 CFR 71, Paragraph 71-45 (b)(1). This load condition is defined as follows ". . . The system shall be capable of withstanding, without generating stress in any material of the package in excess of its yield strength, a static force applied to the center of gravity of the package having vertical component of two times the weight of the package and its contents, a horizontal component along the direction in which the vehicle travels of 10 times the weight of the package with its contents and a horizontal component in the transverse direction of 5 times the weight of the package with its contents."

The 13C II Cask has been provided with a tie-down frame which is integral with the top mounted overpack assembly. The overpacks surround the cask and are attached together with six (6) 1" diameter ratchet binders. These ratchet binders primarily carry inertial loads only since both end impact loads and tie-down loads are reacted by direct compression of the overpack and the integral tie-down frame upon the cask body.

The tie-down frame is designed for the loading conditions previously described. For purposes of this analysis, the package is assumed to weigh 27,000 lbs. Since a minimum factor of safety of 1.16 is calculated, the tie-down system is considered to satisfy the requirements of 10 CFR 71 for package weights up to 31,300 lbs. The analysis is subdivided into individual sections dealing with: loads, lug stresses, stresses included in the cask and tie-down frame stresses.

#### 2.5.2.1 Tie-Down Forces

Stress in the frame is determined for the forces transmitted by the tiedown cables, in resisting the "G" loading, to the frame. Since the cask will be blocked at the base on the

transporter to prevent sliding, the cable resisting forces will be those resisting tipping.

The individual cable loads are determined from principals of static equilibrium as outlined below. The direction cosines for the cables are found as: (Refer to the Tie-Down Geometry Figure 2.5.2-1 on page 2-54 for notation.)

$$\beta_x = \left[ a - \frac{d_c}{2} \sin \alpha \right] / l$$

$$\beta_y = \left[ \frac{w}{2} - \frac{d_c}{2} \cos \alpha \right] / l$$

$$\beta_z = h/l$$

Where:

$$l = \left[ \left( a - \frac{d_c}{2} \sin \alpha \right)^2 + \left( \frac{w}{2} - \frac{d_c}{2} \cos \alpha \right)^2 + h^2 \right]^{1/2}$$

$$\alpha = \tan^{-1}(2a/w)$$

The 10g longitudinal load is resisted by two cables, in tension. The individual cable force is obtained by taking moments about point "O":

$$-10Wc + 2F_{cx}h + F_{cz}(d_o + d_c) = 0$$

$$\text{But: } F_{cx} = \beta_x \cdot F_{c1}$$

$$F_{cz} = \beta_z \cdot F_{c1}$$

Thus, the cable force due to a 10 g longitudinal load is:

$$F_{c1} = \frac{10 Wc}{2 \beta_x h + \beta_z (d_o + d_c)}$$

The 5g lateral load is resisted by two cables, in tension. The individual cable force is found from the equilibrium expression:

But: 
$$-5 Wc + 2F_{cy}h + F_{cz}(d_o + d_c) = 0$$

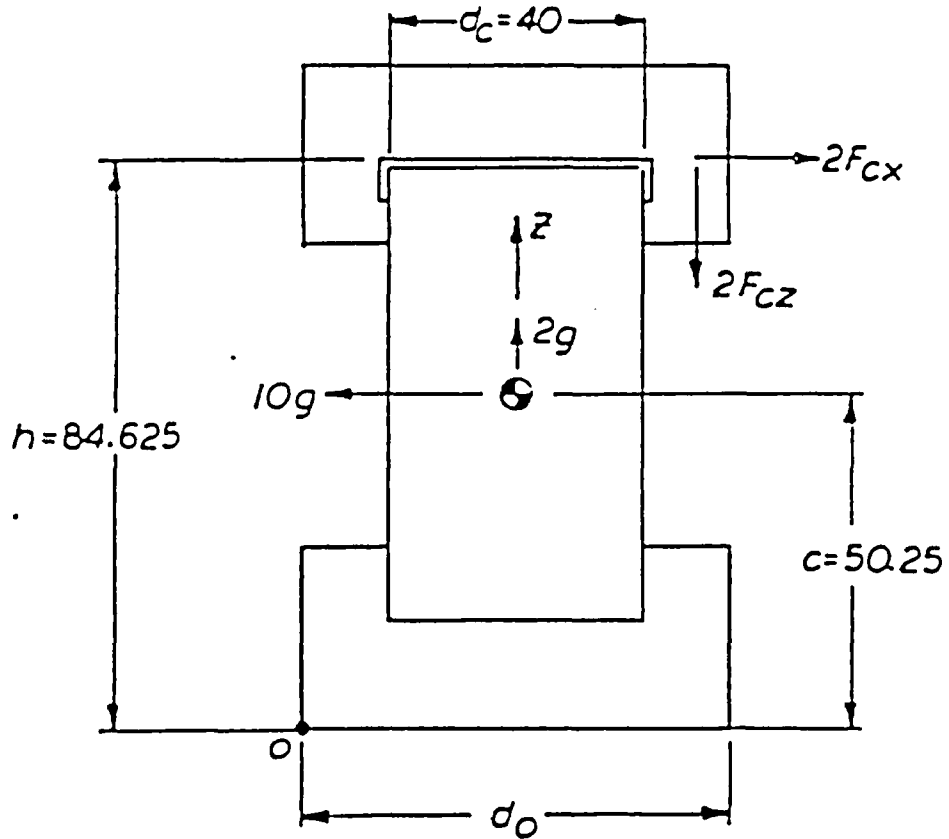
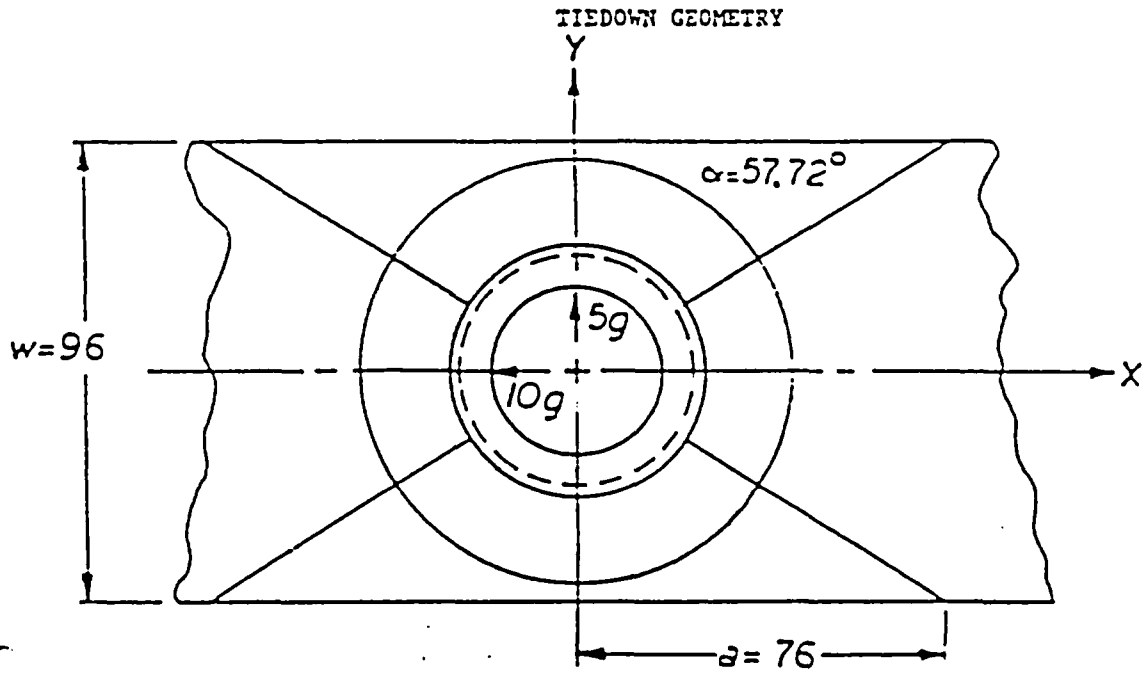
$$F_{cy} = \beta_y \cdot F_{c2}$$

$$F_{cz} = \beta_z \cdot F_{c2}$$

Thus, the cable force due to a 5 g lateral load is:

$$F_{c2} = \frac{5Wc}{2\beta_y h + \beta_z (d_o + d_c)}$$

FIGURE 2.5.2-1



The 2g vertical load is resisted by all four cables, in tension. The individual cable force is found from the equilibrium expression:

$$-2H + 4F_{CZ} = 0$$

$$\text{But: } F_{CZ} = B_z \cdot f_{c3}$$

Thus, the cable force due to a 2 g vertical load is:

$$F_{c3} = 2H/4B_z$$

Assuming the three loadings occur simultaneously, the most severely loaded cable experiences a load of:

$$F_c = H \left[ \frac{10c}{2 B_x h + B_z (d_o + d_c)} + \frac{5c}{2 B_y h + B_z (d_o + d_c)} \right] + \frac{2}{4B_z}$$

This expression is evaluated with the following 1-13C II properties and geometry:

$$H = 27000 \text{ lbs.}$$

$$d = 40.00 \text{ inches}$$

$$a = 76 \text{ inches}$$

$$h = 99 - 5/8 - 15 = 84.625 \text{ in.}$$

$$c = 68.75/2 + 15 - 7/8 = 50.25 \text{ in.}$$

$$w = 96 \text{ inches}$$

The direction cosines of the cable are:

$$B_x = .53829$$

$$B_y = .34004$$

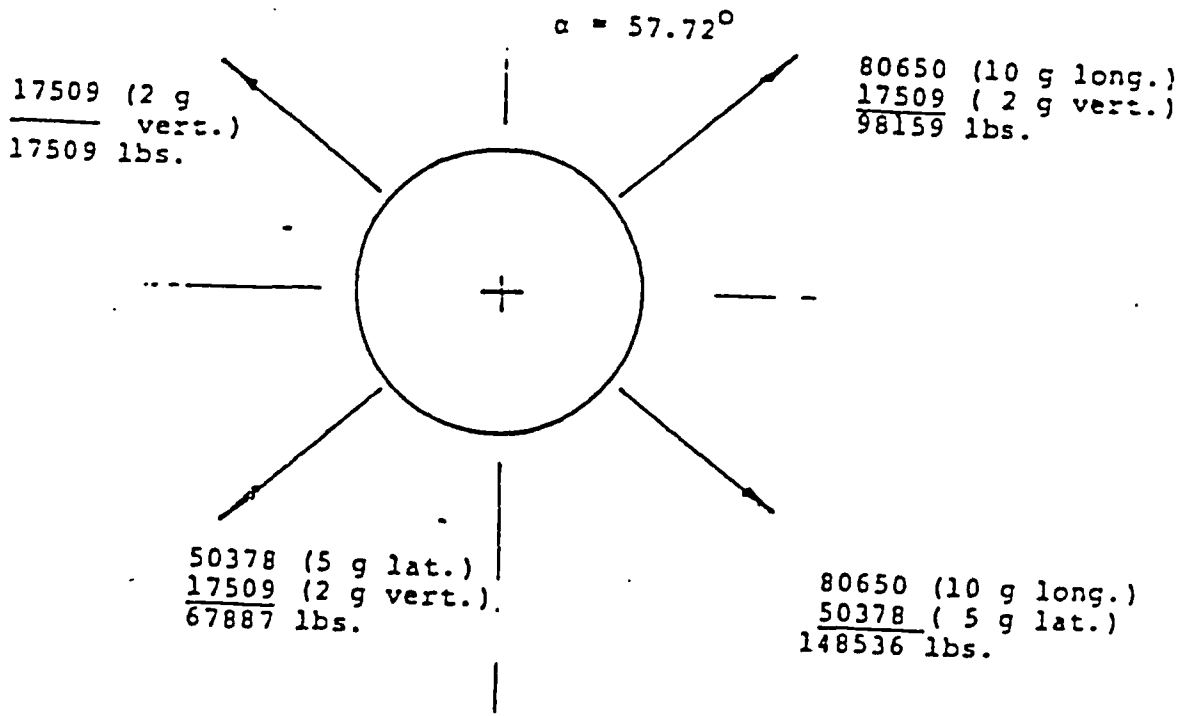
$$B_z = .77105$$

Cable length,  $l = 109.75$  inches

The cable loads are:

<u>Load Case</u>	<u>Magnitude (lbs)</u>
10 g longitudinal	80650
5 g lateral	50378
2 g vertical	<u>17509</u>
Combined	148536

For stress evaluation of components, the corresponding load set based upon simultaneous application of the 10g, 5g, and 2g load cases to the circular tie-down frame imposes consistent cable forces (out of the plane of the sketch) as follows:

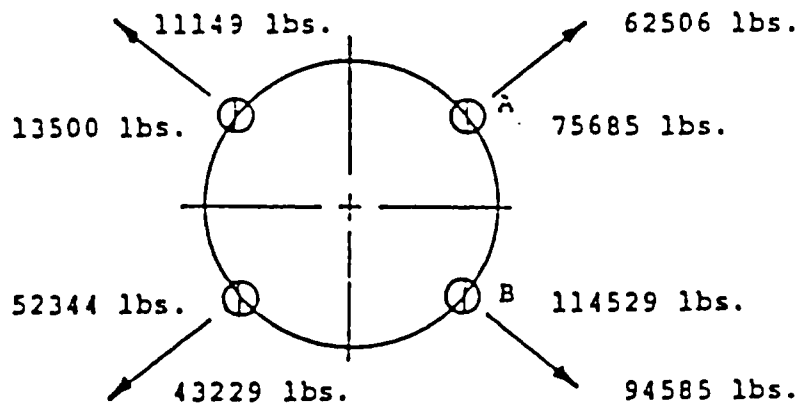


These forces may be resolved into components parallel and perpendicular to the plane of the frame with the following expressions:

$$F_p = (\bar{s}_x^2 + \bar{s}_y^2)^{1/2} \cdot F_c \quad (\text{Parallel})$$

$$F_n = \bar{s}_z \cdot F_c \quad (\text{Normal})$$

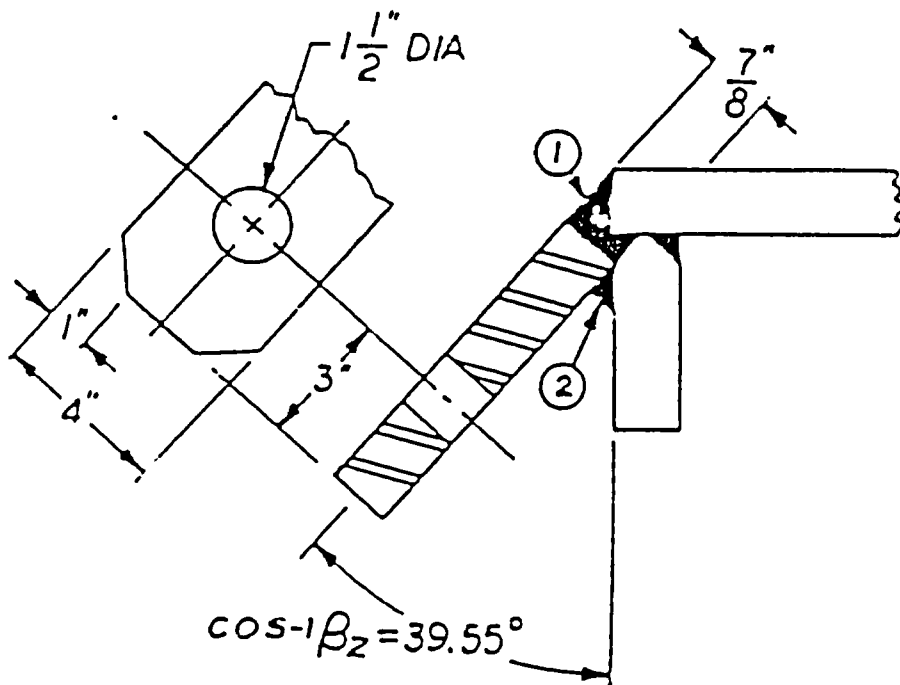
The results are:





2.5.2.2 Stresses in Tie-Down Lug

The tie-down lug is oriented precisely in line with the cable force vectors evaluated in the preceding section. As a consequence, the tie-down lug experiences inplane loads only; no bending loads are induced in this element.

(a) Tearout Stress

Using a conventional  $40^\circ$  tearout relation, the capability of the lug at yield stresses is estimated as:

$$P_A = 2 F_{sy} t (E_m - d/2 \cos 40^\circ) = 245060 \text{ lbs.}$$

Where:

$$F_{sy} = \frac{100000}{\sqrt{3}} = 57735 \text{ psi; ASTM-A514, Gr. 3}$$

$$t = 7/8 \text{ in.}$$

$$E_m = 3 \text{ in.}$$

$$d = 1.5 \text{ in.}$$

Thus, the factor of safety for lug tearout is

$$\text{F.S.} = \frac{245060}{148536} = 1.65$$

(b) Net Section Tension Stress

The net section tension yield load capacity is:

$$P_A = F_{ty}A \\ = (100000) (4-1.5) (.875) = 218750 \text{ lbs.}$$

Thus, the factor of safety for lug tension is:

$$\text{F.S.} = \frac{218750}{148536} = 1.47$$

(c) Welds to Frame

The tensile capacity of weld (1) is:

$$P_{w1} = (100000) (4) (.875) = 350000 \text{ lbs.}$$

The shear capacity of weld (2) is:

$$P_{w2} = (100000) (1/\sqrt{3}) (.707) (.875) = 35,716 \text{ lbs.}$$

Collectively, the weld capacity of the lug attachment is 385,722 lbs. Thus, the factor of safety is:

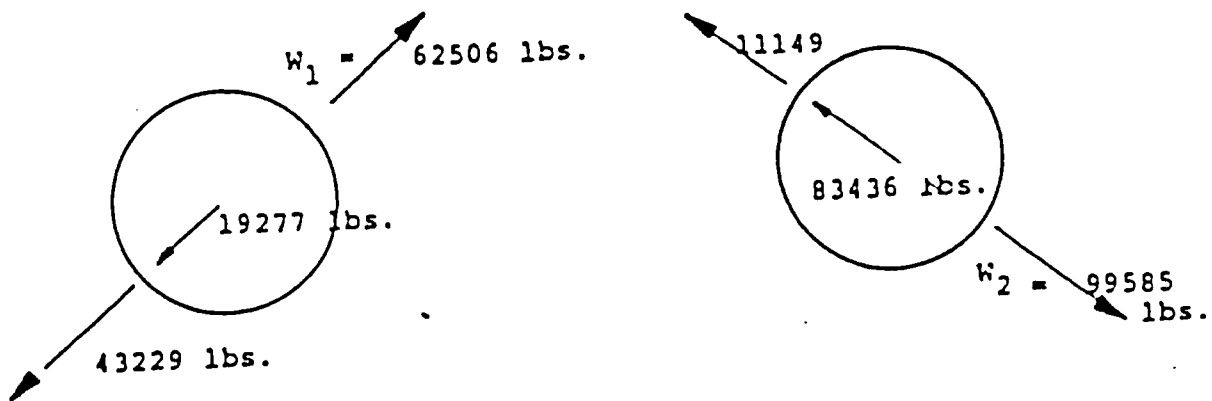
$$\text{F.S.} = \frac{385,722}{148,536} = 2.60$$

Therefore, should tie-down forces exceed the criteria specified in 10 CFR 71, the lug will fail at 240,625 lbs. (ultimate) in the net tensile section. This failure will not impair the ability of the cask or its contents to meet other provisions of 10 CFR 71.

#### 2.5.2.3 Tie-Down Frame Stresses

The reaction forces between the frame and cask are found from the forces of Section 2.5.2.1. The horizontal planar forces applied to the circular tie-down plate may be viewed as the superposition of two force sets as shown below.

The vectors external to the circles are applied by the tie-down cables; whereas the vectors within the circles are applied by cask reactions.

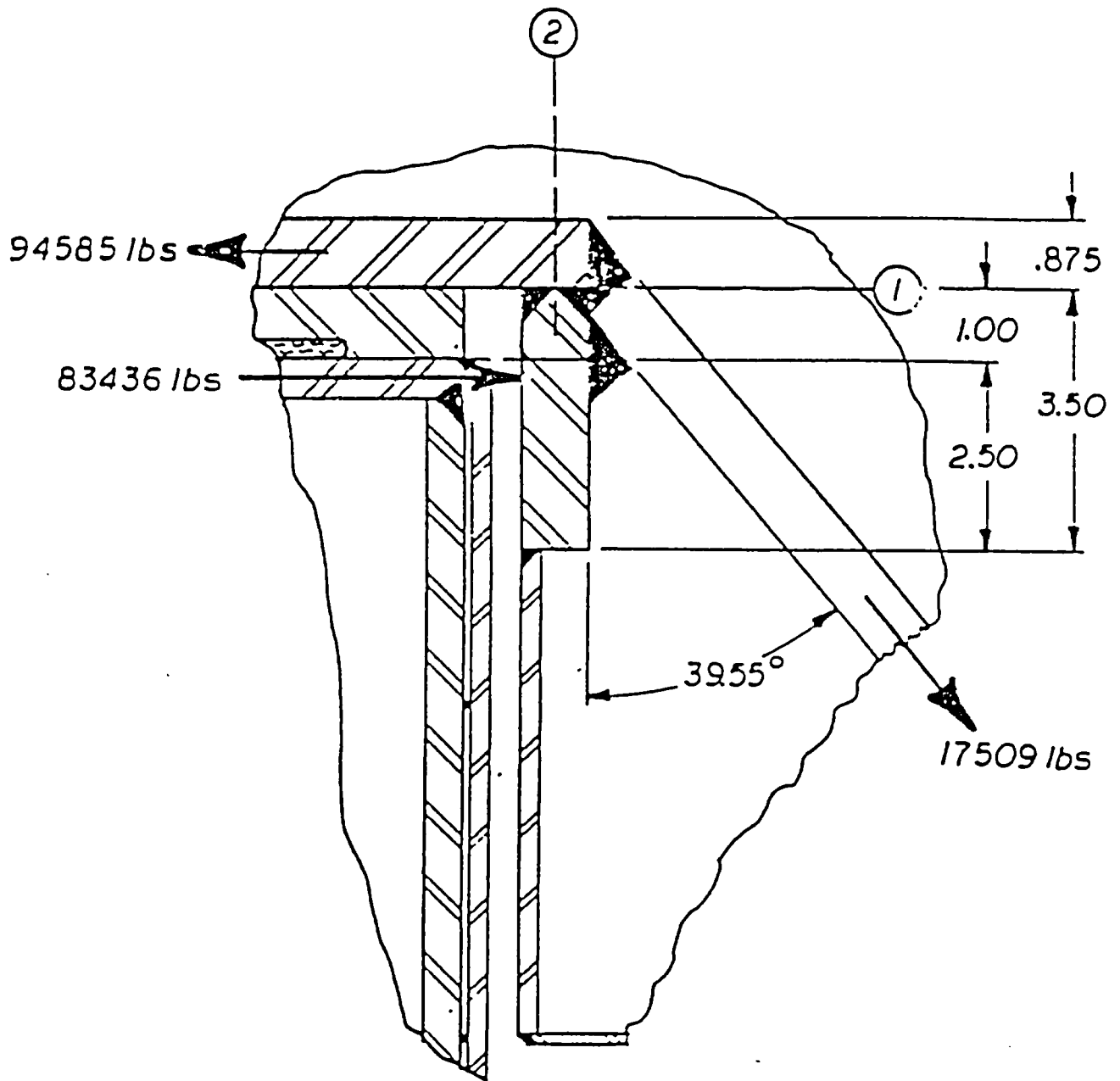


These planar horizontal reaction forces are applied to the cask as a lateral bearing load. The corresponding force acts on the tie-down frame as a lateral load applied to the 12 inch long cask restraint flanges located at each tie-down lug. Detail geometry and applied loads are shown in Figure 2.5.2-2.

Bending stresses are induced in the cask restraint flange by this cask to frame load. The moment area for this load is conservatively estimated assuming the center of pressure at mid depth of the cask body top plate. The previous sketch indicates two critical sections where flexural stresses will be checked.

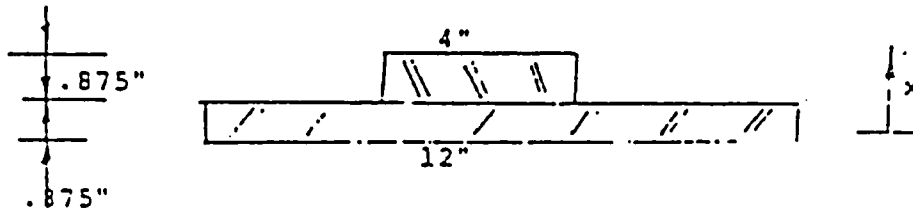
FIGURE 2.5.2-2

TIEDOWN LUG DETAILS



Section 1

The section properties are:



$$\Delta = (.875)(12) + (.875)(4) = 10.50 + 3.50 = 14.00 \text{ in.}^2$$

$$\bar{x} = \frac{(10.50)(.4375) + (3.50)(.875 + .4375)}{14} = .65625 \text{ in.}$$

$$\therefore c = 1.75 - .65625 = 1.09375 \text{ in.}$$

$$I = \frac{(12)(.875)^3}{12} + \frac{(4)(.875)^3}{12} + (3.50)(.65625 - 1.3125)^2$$

$$+ (10.5)(.65625 - .4375)^2 = 2.9030 \text{ in.}^4$$

The applied moment involves both the cask reaction force plus the cable force. Moment arms are scaled from the preceding sketch.

$$M_1 = (83436)(1.25) - (17509)(0.35) = 98167 \text{ in-lb.}$$

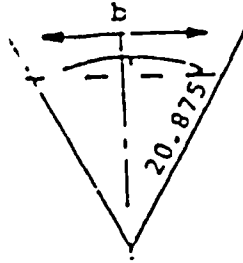
$$f_{b_1} = Mc/I = \frac{(98167)(1.09375)}{2.9030} = 36986 \text{ p.s.i.}$$

Section 2

The moment at Section 2 involves the cask reaction force plus the cable force. Applied moment is:

$$M_2 = (83436)(1.688) - (17509)(0.52) = 131,735 \text{ in-lb.}$$

The section is a single thickness of 7/8" plate with length b found as:



$$b = 2 \left[ (20.875)^2 - 20^2 \right]^{1/2} = 11.96''$$

Thus the bending stress:

$$f_{b_2} = \frac{6M}{bt^2} = \frac{(6)(131735)}{(11.96)(.875)^2} = 86319. \text{ psi}$$

The minimum factor of safety in the tie-down frame is therefore:

$$\text{F.S.} = \frac{100000}{86319} = 1.16$$

#### 2.5.2.4 Gask Tie-Down Stresses

The contact bearing stress due to lateral loads, calculated in paragraph 2.5.2.3, is:

$$f_{b_r} = \frac{83436}{(12)(2.5)} = 2,781 \text{ psi}$$

The vertical forces exerted on the cask are defined at the end of Paragraph 2.5.2.1 as the sum of:

13500 lbs.  
 75685 lbs.  
 114529 lbs.  
 52344 lbs.

These loads exert a total downward force on the cask external shell of 256,058 lbs.

The external shell is constructed of 1/2" thick 304 stainless steel. Resultant compressive stress is:

$$f_c = P/A = \frac{256058}{\pi (37.5)(.5)} = 4347 \text{ psi}$$

Since the lead provides adequate restraint to the outer shell, crippling need not be considered. The resultant cask factor of safety is:

$$F.S. = \frac{30000}{4347} = 6.90$$



## 2.6 Normal Conditions of Transport

The Model 1-13C II package has been designed and constructed, and the contents are so limited (as described in Section 1.2.3) that the performance requirements specified in 10 CFR 71 will be met when the package is subjected to the normal conditions of transport specified in 10 CFR 71. The ability of the Model 1-13C II Package to satisfactorily withstand the normal conditions of transport has been assessed as described below:

### 2.5.1 Heat

A detailed thermal analysis for normal conditions of transport can be found in Section 3.4. Internal heat loads up to 800 watts were considered.

The maximum cavity temperature was found to be 214.4<sup>o</sup>F. External package temperature was less than 156.3<sup>o</sup>F, assuming 100<sup>o</sup>F ambient air and full solar insolation. These temperatures will have no detrimental effects on the package.

### 2.6.6.1 Summary of Pressures and Temperatures

From Sections 3.4.2 and 3.4.4, it was found that the maximum temperatures and pressure are:

Pressure:

Pmax = 19 psig

Temperature:

Fire Shield	182.1 <sup>o</sup> F
Lift Lug	209.1 <sup>o</sup> F
Outer Shell	212.6 <sup>o</sup> F
Outer Ends	214.3 <sup>o</sup> F
Containment Cavity	214.4 <sup>o</sup> F

### 2.6.1.2 Differential Thermal Expansion

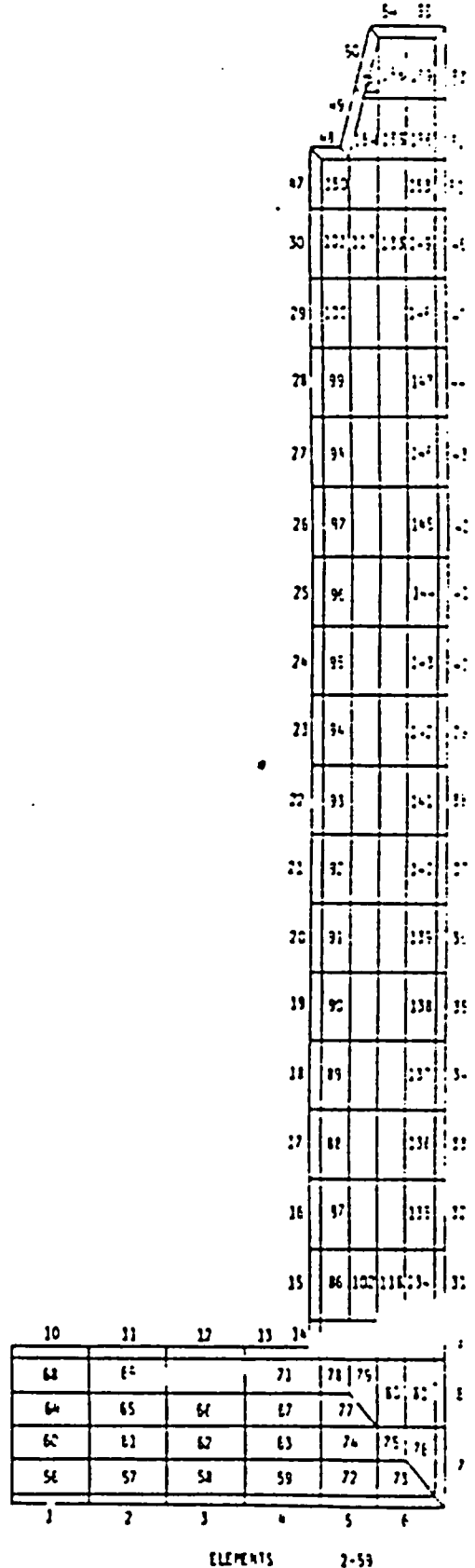
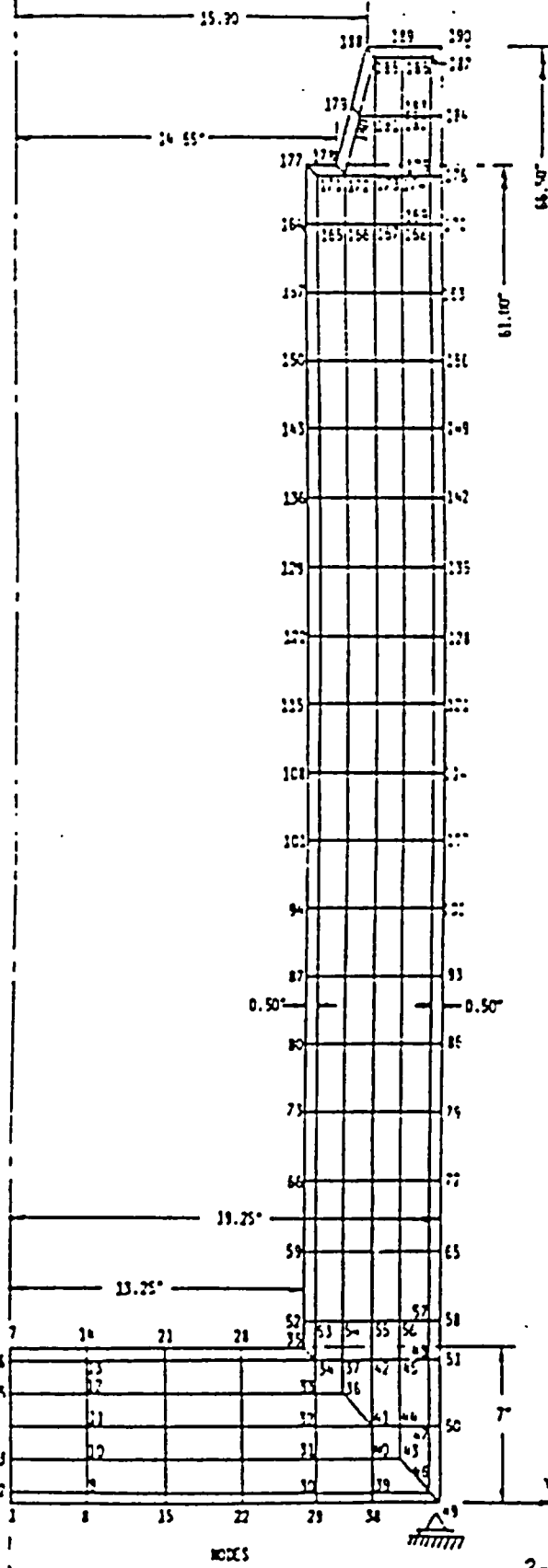
From the summary temperatures shown in Section 2.6.1.1 and Section 3.1 it can be seen that the temperature variations between the external shell and the inner containment vessel are small, i.e., 212.6°F vs. 214.4°F, respectively.

Since the lead bonding is not present, fabrication stresses are minimized because of the short term creep properties of lead. Therefore, a stress free temperature of 70°F was assumed.

The analysis of package stresses due to differential thermal expansion has been performed using a pair of axisymmetric finite element models, Figures 2.6.1-1 and 2.6.1-2, representing the cask and lid, respectively. These models are used for cask body analytic stress predictions throughout Section 2.6 and 2.7 of this report. The E3SAP program, described in Appendix 2.10.2.4, was used for all these analyses.

The referenced figures completed define model geometry. All material properties of the model are taken directly from Table 2.3-1 for stainless steel, Type 304, and lead. To represent the unbonded lead, the lead shear modulus has been reduced by a factor 10. This assures that only secondary shear forces are transmitted between steel shells and lead; yet permits proper treatment of direct stresses induced in steel shells due to differential thermal expansion effects.

FIGURE 2.5.1-1 AXISYMMETRIC FINITE ELEMENT MODEL OF CASK 1-13 C II



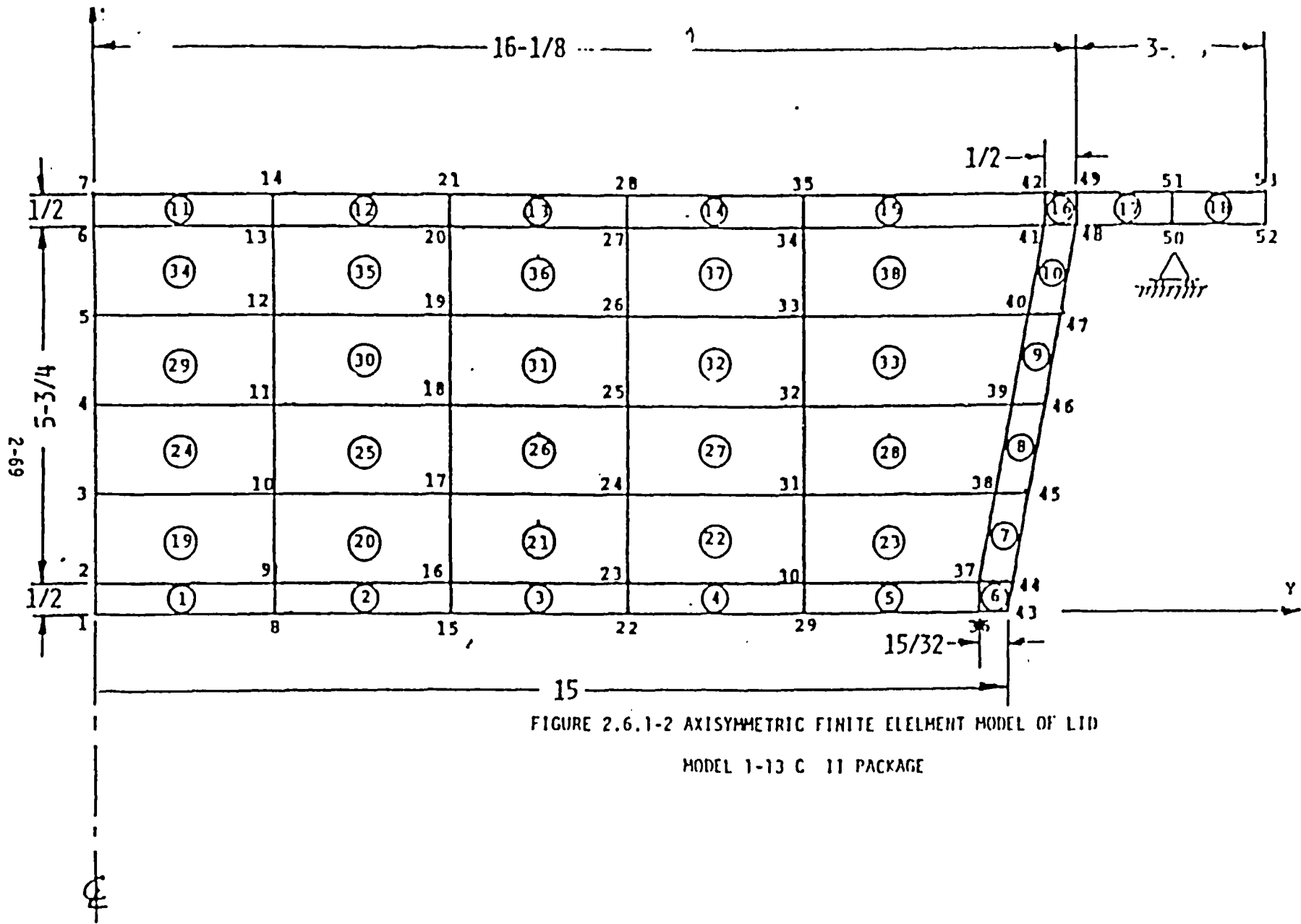


FIGURE 2.6.1-2 AXISYMMETRIC FINITE ELEMMENT MODEL OF LID

MODEL 1-13 C 11 PACKAGE

Comprehensive stress summaries for these two models are provided in Appendix 2.10.3. These summaries directly provide membrane (center) and surface stresses in terms of stress intensities as set forth in NRC Regulatory Guide 7.6. For differential expansion loads, stress intensity results are reported in Case 3\* (= Run 2, Case 1).

In the mid body region of the cask, stresses are modest, with little variation from inner to outer surfaces. Values at a typical section through elements 23/44, where inner shell stresses maximize, see Figure 2.6.1-i, are as follows:

Location	Element Number	STRESSES (psi)			(S.I.)
		Axial ( $\sigma_z$ )	Hoop ( $\sigma_\theta$ )	Radial ( $\sigma_r$ )	
<u>Inner Shell</u>	23	+11620	+ 4406.	-210	11830.
- I.D.		+11890	+ 4578	-294	12184.
- O.D.		+11350	+ 4225	-121	11471.
<u>Outer Shell</u>	44	12270	+18380	-265	18645.
- I.D.		12160	18590	-508	19098.
- O.D.		12390	18170	- 16	18186.

\*The seven reported cases were performed in two runs; Run 1 contains 4 cases; Run 2 contains 3 cases. For clarity and brevity, they are identified and discussed as 7 sequential cases in this report.

The axial variation of temperature induced stress intensity is illustrated by the following comparisons at top and bottom of cask.

LOCATION	ELEMENT	STRESS INTENSITY (psi)	
		CENTER	SURFACE
Top - Inner Shell	30	13671	16342
- Outer Shell	46	19503	19737
Base - Inner Shell	15	8005	9366
- Outer Shell	31	18464	19942

Stresses elsewhere in the cask body are less than these values excepting for localized stresses at the outer shell to base juncture, see elements 5 and 8. The membrane stresses here are:

ELEMENT	MEMBRANE S.I. (psi)
5 (Inner Shell)	19565.
8 (Outer Shell)	28261.

The stresses observed at elements 5 and 8 are highly localized; adjoining element stresses show extremely rapid decay of the obvious classical damped shell bending behavior. These high stresses, slightly in excess of yield, pose no threat to cask safety or integrity since they are self limiting secondary thermal stresses which disappear upon initial yielding of the outer shell. The only consequence of these stresses will be a slight outward ripple of cask outer surface subsequent to initial loading.

Stresses in the lid, Figure 2.6.1-2, are approximately of the same magnitude as in the cask body. The most highly stressed location occurs at element 8. The state of stress of element 8 is as follows:

Location	Stress (psi)			Intensity (S.I.)
	Axial ( $\sigma_z$ )	Hoop ( $\sigma_\theta$ )	Radial ( $\sigma_r$ )	
Center (Membrane)	10550	22450	+3174	19819
O.D.	32440	29580	6124	26331
I.D.	-4735	18140	4735	23405

As in the cask body, the dominant stress contributor is a bending stress arising from the connection of the conical shell sector to the flat inner end disk.

### 2.6.1.3 Stress Calculations

Combination of thermal stresses discussed in Section 2.6.1.2 with internal pressure (19 psig) stresses slightly increases the total state of stress.

Stress intensities for pressure and temperature phenomena at those locations discussed in Section 2.6.1.2 are obtained directly from case 7 of Appendix 2.10.2, as follows:

LOCATION	ELEMENT NUMBER	STRESS INTENSITY S.I. (psi)
<u>CASK BODY</u>		
Inner Shell - Center	28	11864.
- I.D.		12224.
- O.D.		11510.
Outer Shell - Center	44	18788.
- I.D.		19252.
- O.D.		18326.
Top - Inner Shell, Center	30	13696.
Surface	30	16331.
- Outer Shell, Center	46	19645.
Surface	46	19871.
Base - Inner Shell, Center	15	8255.
Surface	15	9592.
- Outer Shell, Center	31	18480
Surface	31	19957
Juncture, Outer Side	8	28265
Outer Base	5	19590
<u>LID</u>		
Center	8	19664
O.D.	8	26169
I.D.	8	23809



Maximum stress intensities and factors of safety are as follows:

1. Containment Vessel (Inner Shell)

(NRC Reg. Guide 7.6, Para. C.2)

a.  $S_m = 20 \text{ ksi @ } 214.4^\circ\text{F (Table 2.3-1)}$

Allowable Membrane Stress =  $S_m = 20 \text{ ksi}$

Allowable bending + membrane =  $1.5 S_m = 30 \text{ ksi}$

b. Maximum Membrane Stress @ El. 44

$f_m = 18.788 \text{ ksi}$

F.S. =  $20/18.788 = \underline{+1.06}$

c. Maximum Membrane + Bending @ El. 44

$f_b = 19.252 \text{ ksi}$

F.S. =  $30/19.252 = \underline{+1.56}$

2. Closure (Lid), El. 8

a. Maximum Membrane Stress

$f_m = 19.664 \text{ ksi}$

F.S. =  $20/19.664 = \underline{+1.02}$

b. Maximum Membrane + Bending

$f_b = 26.169 \text{ ksi}$

F.S. =  $30/26.169 = \underline{+1.15}$

3. Outer Shell

## a. Allowable Stress:

$$S_y = 24.64 \text{ ksi @ } 214.4^\circ\text{F (Table 2.3-1)}$$

## b. Maximum Stress at El. 31, excepting juncture:

$$f_y = 19.957 \text{ ksi}$$

$$\text{F.S.} = 24.64/19.957 = \underline{1.23}$$

## c. Maximum Stress at Base Juncture, El. 8

$$f_m = 28.265 \text{ ksi}$$

$$\text{F.S.} = 24.64/28.265 = \underline{0.87}$$

The slight (13%) overstress at Element 8 is highly localized as shown by the factors of safety for adjoining elements.

<u>Element Number</u>	<u>Z Location (inches)</u>	<u><math>f_m</math> (ksi)</u>	<u>F.S.</u>
7	1.75	7.610	3.24
8	5.00	28.265	0.87
9	7.38	19.843	1.24

This highly localized self-limiting thermal stress yielding will produce a slightly outward ripple on the exterior cask shell approximately 5 inches above the base, well beyond the heat affected zone of shell to base plate weld.

This initial yielding cannot lead to progressive collapse or shakedown rupture of the shell since subsequent load and unload cycles will always induce stresses within the elastic regime.

This fact is assured by the "Baushinger Effect"\* so long as the total stress range is less than twice yield stress. The ASME Boiler and Pressure Vessels Code, Section III, explicitly recognizes this fact by the allowable factor of  $3 S_m$  on combined primary and secondary stresses ( $S_m - 2/3 S_y$ ). In this instance, the zero to peak stress range is  $-1.147 S_y$ . Based on the "Baushinger Effect" the factor of safety is recomputed as:

$$F.S. = 2 S_y / 1.147 S_y = 1.74$$

This condition does not impair the effectiveness of the packaging to satisfy the requirements for Normal Conditions of Transport as set forth in 10 CFR 71, Part 71.71.

The pressure (19 psig) associated with normal transport produces insignificant loads upon the 12 1-1/4"-7 UNC closure bolts (ASTM SA 354, Gr. B). The loads are assessed as follows:

$$F.B. = (\pi/4) (12) (33^2) (19) = 1354 \text{ lbs.}$$

The effective section area of the bolts is  $0.968 \text{ in}^2$ , therefore, the stress is:

$$f_t = 1354 / 0.968 = 1400 \text{ psi}$$

The allowable tensile stress for the bolting material, Table 2.3-1, is 125 ksi. Therefore, the factor safety is:

$$F.S. = 125 / 1.4 = 89$$

Therefore, the Model 1-13C II packaging can safely satisfy the requirements of thermal and pressure loading of the Normal Conditions of Transport.

---

\* Timoshenko, S. P., Strength of Materials, Part II, "Advanced Theory and Problems" Third Edition, D. Van Nostrand Company, Inc., 1956, pp. 413.

2.6.2 Cold

The materials of construction for the packaging, including the stainless steel, carbon steel, overpack and the seals themselves are not significantly affected by an ambient temperature of  $-40^{\circ}\text{F}$ . Brittle fracture has been discussed in Section 2.1.2.3.1 and is not a physically plausible mechanism for the materials of construction.

There are two cold conditions corresponding to the  $-40^{\circ}\text{F}$  ambient air event - minimum decay heat and maximum decay heat and maximum decay heat. In the first instance, the differential thermal expansion coefficients between steel and lead cause the lead and steel to separate (gap) at temperatures below the  $70^{\circ}\text{F}$  stress-free temperature. Both lead and steel then experience an unconstrained shrinkage; hence, approach a stress free condition.

In the second instance with maximum decay heat, the predicted temperatures as summarized in Table 3.4.3-1 are as follows:

<u>LOCATION</u>	<u>NODE NO.</u>	<u>TEMPERATURE (<math>^{\circ}\text{F}</math>)</u>
Fire Shield	9	37.4
Lift Lug	2	74.8
Side Outer Shell	10	79.6
Top Outer Shell	3	81.4
Cavity	22	81.5

Except for the fire shield, all temperatures are very slightly above the  $70^{\circ}\text{F}$  stress-free temperatures; the maximum temperature differential above this stress-free temperature reference occurs at the cavity and is  $11.5^{\circ}\text{F}$ . The temperature gradient between the cavity and the exposed side outer shell is:

$$\Delta T = T_{22} - T_{10} = 1.9^{\circ}\text{F}$$

This is essentially identical to the maximum gradient reported for "hot" conditions in Table 3.4.2-1.

A conservative estimate of thermal expansion stresses in the steel shell induced by differential coefficients of thermal expansion between steel and lead is:

$$f = E_s \Delta T (\alpha_{pb} - \alpha_s)$$

$$= (28.3 \times 10^6)(11.5) (16.4 - 9.11) \times 10^{-6} = 2373 \text{ psi}$$

The stresses induced by the gradient through the wall can be approximated by assuming a thick cylinder of steel. The stress is given in Roark, 5th Edition, Case 16, Section 15.6, as:

$$F = \left( \Delta T E / 2(1 - \nu) \ln(c/b) \right) \cdot (1 - 2g^2/c^2 - b^2) \cdot \ln c/b = -393 \text{ psi}$$

where: b = inner radius = 13.25 in.  
 c = outer radius = 19.25 in.  
 g = b, for outer surface stress  
 = c, for inner surface stress

Assuming these two stresses are additive, the factor of safety is:

$$F.S. = 30,000 / (2373 + 393) = 10.8$$

### 2.6.3 Reduced External Pressure

10 CFR 71.71 (c)(3) requires that the package should be able to withstand a reduced external pressure of 3.5 psia. Conversely, the package should be able to withstand a 14.7 - 3.5 = 11.2 psi internal pressure. Assume the inner shell is supported by the lead in resisting the internal pressure.

(1) End Plates - From Roark

$$\sigma_c = 3/32(D/t)^2 P(3 + \nu) \quad (\text{Free Ends})$$

D = Mean Diameter = 27 in.

P = 11.2 psig

Steel : t = 0.5 in. ;  $\nu = 0.3$

Lead : t = 5 in. ;  $\nu = 0.45$

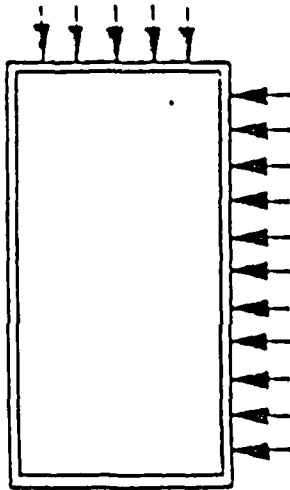
$$\text{Lead : } \sigma_c = 3/32(27/5)^2 (11.2)(3 + 0.45) =$$

$$\sigma_c \text{ yield} = 105.63 \text{ psi for lead}$$

For the lead and steel shells in contact, the yield of the steel plate will not be exceeded as entire pressure can be taken by the lead without yield.

### 2.6.4 Increased External Pressure

The requirement for external pressure is that the cask must be able to withstand an external pressure of 25 psig without the loss of contents. Assume the outer shell is supported by the lead in resisting the external pressure.



(a) End Plates\*

$$\sigma_t = 3/32 (D/t)^2 P(3+\nu) \text{ (Free Ends)}$$

D = Mean Diameter = 37.5 in.

P = 25 psig = 0.50 in.

Steel: t = 0.50 in;  $\nu = 0.30$ Lead: t = 5.75 in;  $\nu = 0.45$ 

$$\text{Lead: } \sigma_f = 3/32 (37.5/5.75)^2 (25) (3+.45) = 344 \text{ psi}$$

$$\sigma_{\text{yield}} = 1130 \text{ psi for Lead}$$

For the lead and steel shells in contact, the yield of the steel plate will not be exceeded as entire pressure can be taken by the lead without yield.

(b) Cylindrical Shell - Buckling\*

$$P_c = \frac{2t}{D} \left( \frac{\sigma_y}{1 + \frac{\sigma_y}{E} \left( \frac{D}{t} \right)^2} \right)$$

E = Modulus of Elasticity =  $28 \times 10^6$  psi $\sigma_y$  = Yield Strength = 30,000 psi

D = 37.5 in.

t = 0.50 in.

$$P_c = \frac{(2)(.50)}{(37.5)} \left( \frac{30,000}{1 + \frac{30,000}{28 \times 10^6} \left( \frac{37.5}{.5} \right)^2} \right)$$

$$= 114 \text{ psi}$$

$$\text{Safety Factor: } SF = \frac{114}{25} = 4.6$$

\*Roark, R. J., Formulas for Stress and Strain, Fourth Edition. McGraw-Hill Book Co., New York, 1965 Chapter 12, page 298, Case 1.

### 2.5.5 Vibration

Section 1.i observes that the Model 1-13C II is an improved lineal descendant of a proven package with well over ten years of operational use in a transport environment. This experience conclusively demonstrates that vibrations normally incident to transport will have no effect upon the Model 1-13C II package.

### 2.5.6 Water Spray

Since the package exterior is constructed of steel, this test is not required.

### 2.5.7 Free Drop

The package weight of 27000 pounds indicates that the Model 1-13C II package must survive a two foot free fall without substantially reducing its effectiveness in reacting subsequent accident conditions. The package has been designed and successfully tested to withstand 30 foot drops, see Section 2.7.1 and 2.11. Energies generated during the 30 foot drop are  $9.72 \times 10^6$  in-lbs. Energies associated with the two foot drop are:

$$KE = (27000 \text{ lbs}) (24 \text{ in}) = 648,000 \text{ in-lbs.}$$

For impact energies of this magnitude, the computer generated data shown in Section 2.7.1 and described in Appendix, Section 2.10.1.1 provides maximum impact accelerations. These loads are summarized below:

<u>Condition</u>	<u>2 Foot Drop (g's)</u>
End	62.2 (EYDROP)
Corner	14.2 (CYDROP)
Side	28.3 (SYDROP)



These energy balance load predictions were verified by performing package dynamic analyses for a full range of impact orientations from near vertical to near horizontal, as described in Appendix Section 2.10.2.2. Load results from the dynamic analyses compare with the energy balance results, as follows:

<u>Orientation</u>	<u>Energy Balance</u>	<u>Dynamic Analysis</u>
End	62.2g	25.7g (@2.5 <sup>0</sup> )
Corner (29.7 <sup>0</sup> wrt. Vert.)	14.2g	14.2g
Side	28.3g	N/A

The corner orientation values agree precisely. For an end impact orientation, the difference appears to exceed a factor of two. The plotted dynamic response results, Figures 2.6.7-1 and 2.6.7-2, show why. As the orientation angle approaches 0°, the dynamic response force predictions increase very steeply while the predicted deformation of the energy absorbing overpack decreases very rapidly. For assessment of stresses, the most conservative of the alternative load predictions are employed.

#### 2.6.7.1 End Impact

End impacts produce the largest forces on the Model 1-13C II Package. At other orientations, the forces rapidly decrease. The end impact acceleration of 62.2g induces stresses in the cask and lid as reported in Case 3, Appendix Section 2.10.3. Case 3 stresses are developed for 30 foot drop accident conditions with an acceleration of 100.184g's. Case 3 stresses must therefore be multiplied by the ratio of (62.2/100.184) = .6209 to correspond with the 2 foot drop provisions for normal conditions of transport. Maximum stresses are as follows:

FIGURE 2.6.7-1

IMPACT FORCES (LBS) -2 FT DROP

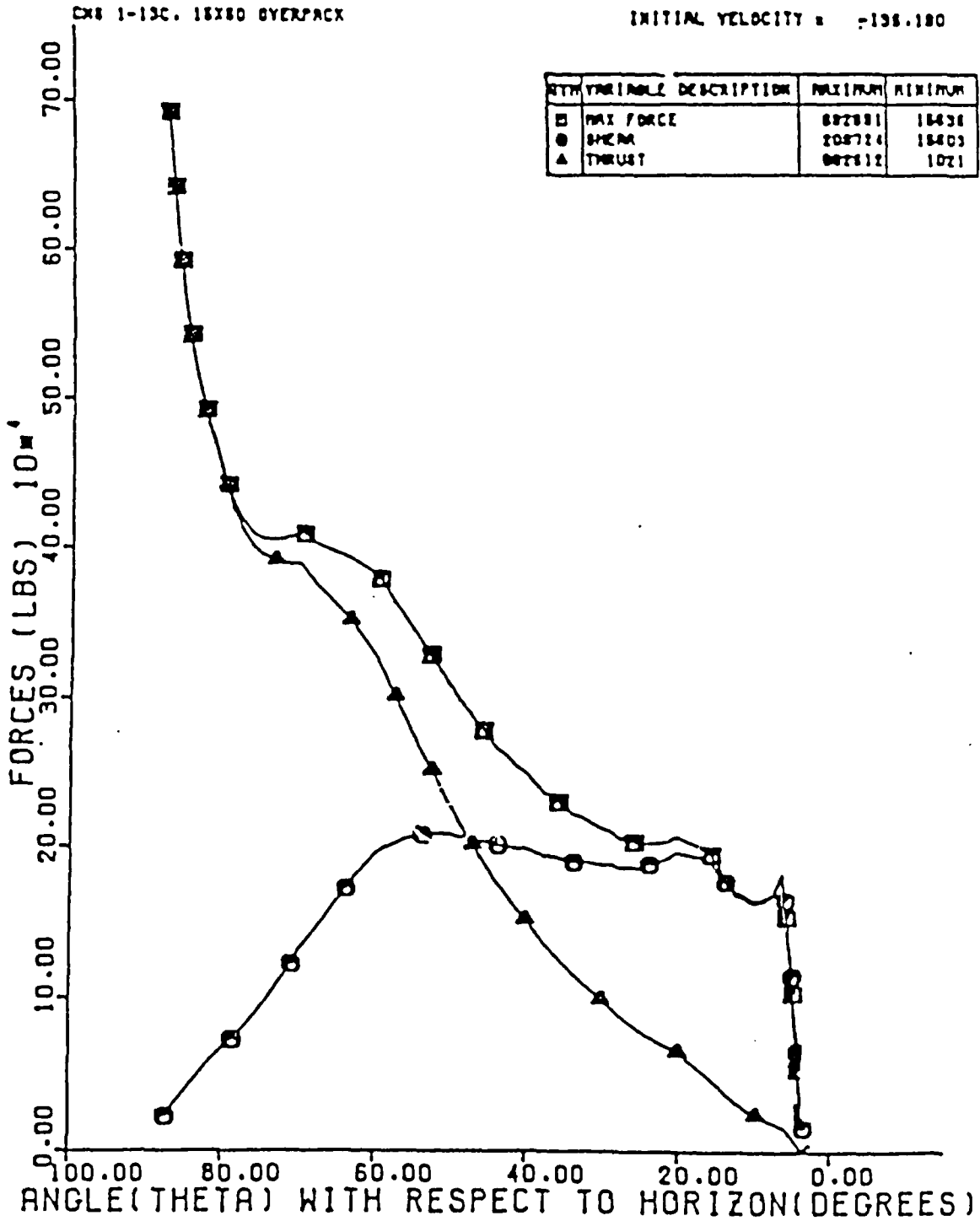
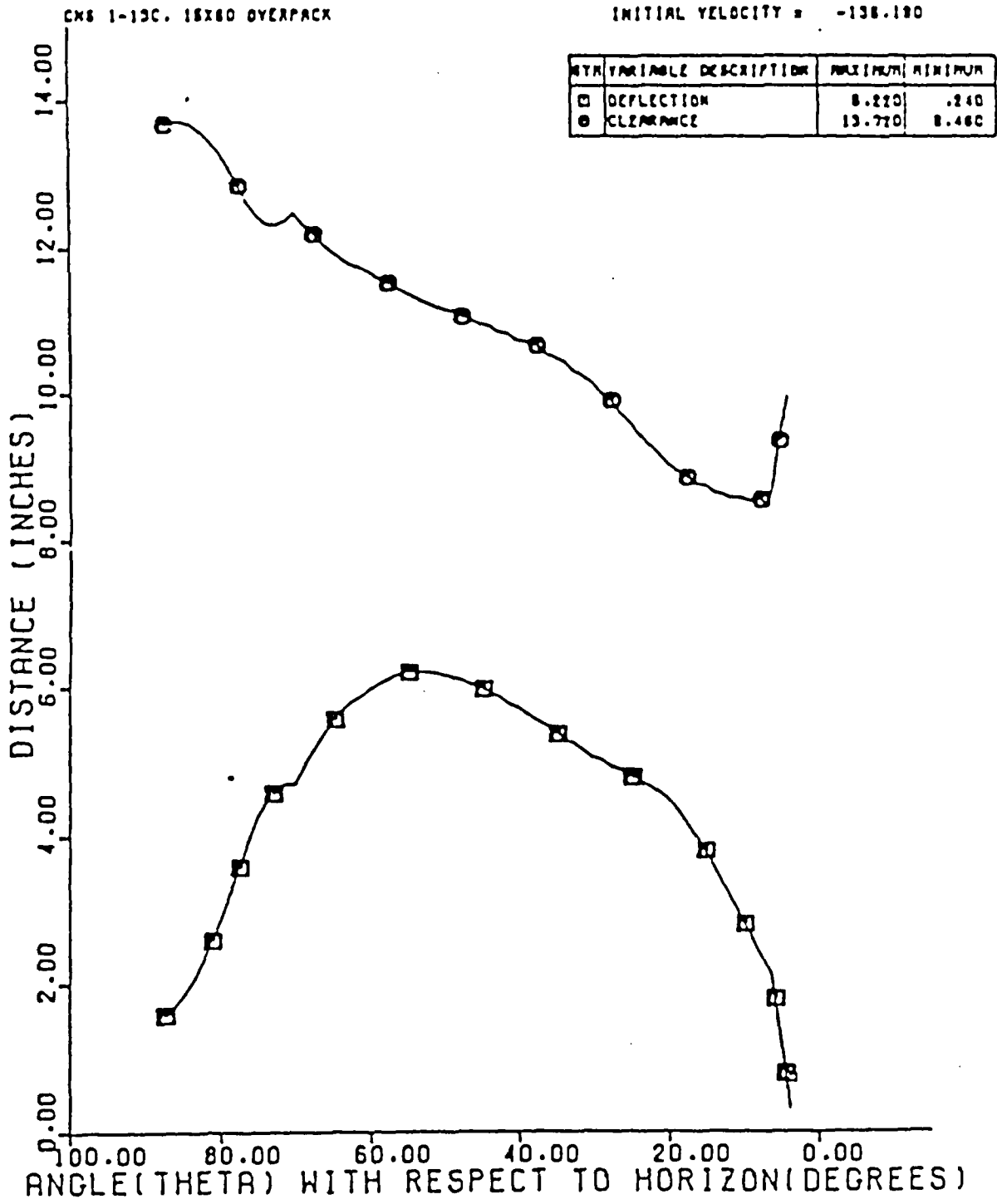


FIGURE 2.6.7-2

OVERPACK DEFLECTION AND RESIDUAL CLEARANCE -2 FT DRCP



LOCATION	El. Nr.	STRESS INTENSITY (psi)	
		SURFACE	CENTER
<u>Cask Body</u>			
o Inner Shell	14	7150.	4326.
o Outer Shell*	8	12304.	9574.
<u>Lid</u>			
	16	18082	10365.
	17	22493	4791.

\*Stresses at element 7 are neglected due to the unrealistic concentrated support of the cask at the lower end of this element.

For the containment elements of the package, the minimum factors of safety in membrane and combined stress states of stress are:

- o Membrane (Cask Element 14)

$$\text{F.S.} = \frac{20}{4.326} = \underline{+4.62}$$

- o Combined Membrane + Bending (Cask Element 14)

$$\text{F.S.} = \frac{30}{7.150} = \underline{+4.20}$$

For the outer shell and lid, the minimum factor of safety is at lid element 17:

$$F.S. = \frac{24.64}{22.493} = \underline{+1.10}$$

( $S_y = 24.64$  ksi @  $214.4^\circ\text{F}$  per Table 2.3-1)

When these maximum stresses are combined with normal temperature and pressure stresses, Case 7, the minimum factors of safety become:

o Cask Element 14 - Membrane:

$$F. S. = \frac{20}{(4.326+6.095)} = \underline{+1.92}$$

o Cask Element 14 - Combined:

$$F. S. = \frac{30}{(7.150+6.507)} = \underline{+2.20}$$

o Lid Element 17 (Top Surface)

Load	$\sigma_r$	$\sigma_z$	$\tau_{rz}$	$\sigma_\theta$	S.I.
Drop	1176	-20831	-2328	-9779	22494
Press + Temp	-849	+ 1510	166	5566	6427
Combined	+327	-19321	-2162	-4213	20118

$$F.S. = \frac{24.64}{20.118} = \underline{+1.22}$$

It is concluded that the Model 1-13C II Package, including overpack, safely withstand the end drop requirements for normal transport conditions.

2.6.7.2 Side Impact

Predicted side impact acceleration under normal conditions is 28.3g's, per Section 2.6.7. This lateral acceleration induces bending stresses in the package as it lands upon the overpack protected ends. The magnitude of the bending moment at mid length is:

$$\begin{aligned} M &= Wl/8; & W &= (27000)(28.3) \text{ lbs.} \\ l &= 68 \text{ inches} \\ & & &= 6.495 \times 10^6 \text{ in-lb.} \end{aligned}$$

The moment of inertia of the steel segments of the cask are:

$$\begin{aligned} I &= \pi/4 (R_o^4 - R_i^4) = \pi/4 [(13.74^4 - 13.25^4) + (14.25^4 - 18.75^4)] \\ &= 14,642 \text{ in}^4 \end{aligned}$$

The bending stresses in the outer shell and inner shell are:

$$\begin{aligned} f_{bo} &= \frac{(6.495 \times 10^6)(19.1)}{14642} = 8428 \text{ psi} \\ f_{bi} &= \frac{(6.495 \times 10^6)(13.5)}{14642} = 5988 \text{ psi} \end{aligned}$$

These bending stresses must be added to the normal pressure stresses summarized in Case 7, Appendix Section 2.10.2. Elements 23 and 29 correspond to the mid-length where the above bending stresses are calculated.

Stresses are summarized as follows:

STRESSES (psi)					
LOCATION	$\sigma_r$	$\sigma_z$	$\tau_{rz}$	$\sigma_\theta$	S.I.
<u>Outer Shell (El. 19)</u>					
- Bending	0	$\pm 8428$	0	0	-
- Case 7 (Pres&Ther)	-285	13530	-11	19140	19425
- Combined	-	+21958	-11	19140	22243
<u>Inner Shell El. 23)</u>					
- Bending	0	$\pm 5988$	0	0	-
- Case 7 (Pres&Ther)	53	11300	-11	4704	11247
- Combined	53	17288	-11	4704	17235

The minimum factors of safety under side impact and pressure and temperature conditions are:

- o The Inner Shell (Containment Vessel):

$$F.S. = \frac{20}{17.235} = \underline{+1.16}$$

- o The Outer Shell:

$$F.S. = \frac{24.64}{22.243} = \underline{+1.11}$$

It is concluded that the Model 1-13C II Package, including overpack, can safely withstand the side drop requirements for normal transport conditions.

2.5.7.3 Corner Impact

Corner Impact accelerations are a rather modest 14.2g's. As outlined in Appendix 2.10.1.2, moments are introduced into the cask body by these oblique impacts. Figure 2.6.7-3 depicts the moments produced in the cask body as a function of orientation angle. The maximum moment is found as:

$$M = 2.1594 \times 10^6 \text{ in-lb @ } 51.3^\circ \text{ wrt horizontal}$$

This is approximately a factor of three less than the moments examined for side impact, Section 2.6.7.2, and consequently will result in stresses less than those examined in that section.

It is concluded that the Model 1-13C II Package, including overpack, safely withstand the corner and oblique force drop requirements for normal transport conditions.

2.6.7.4 Summary of Results

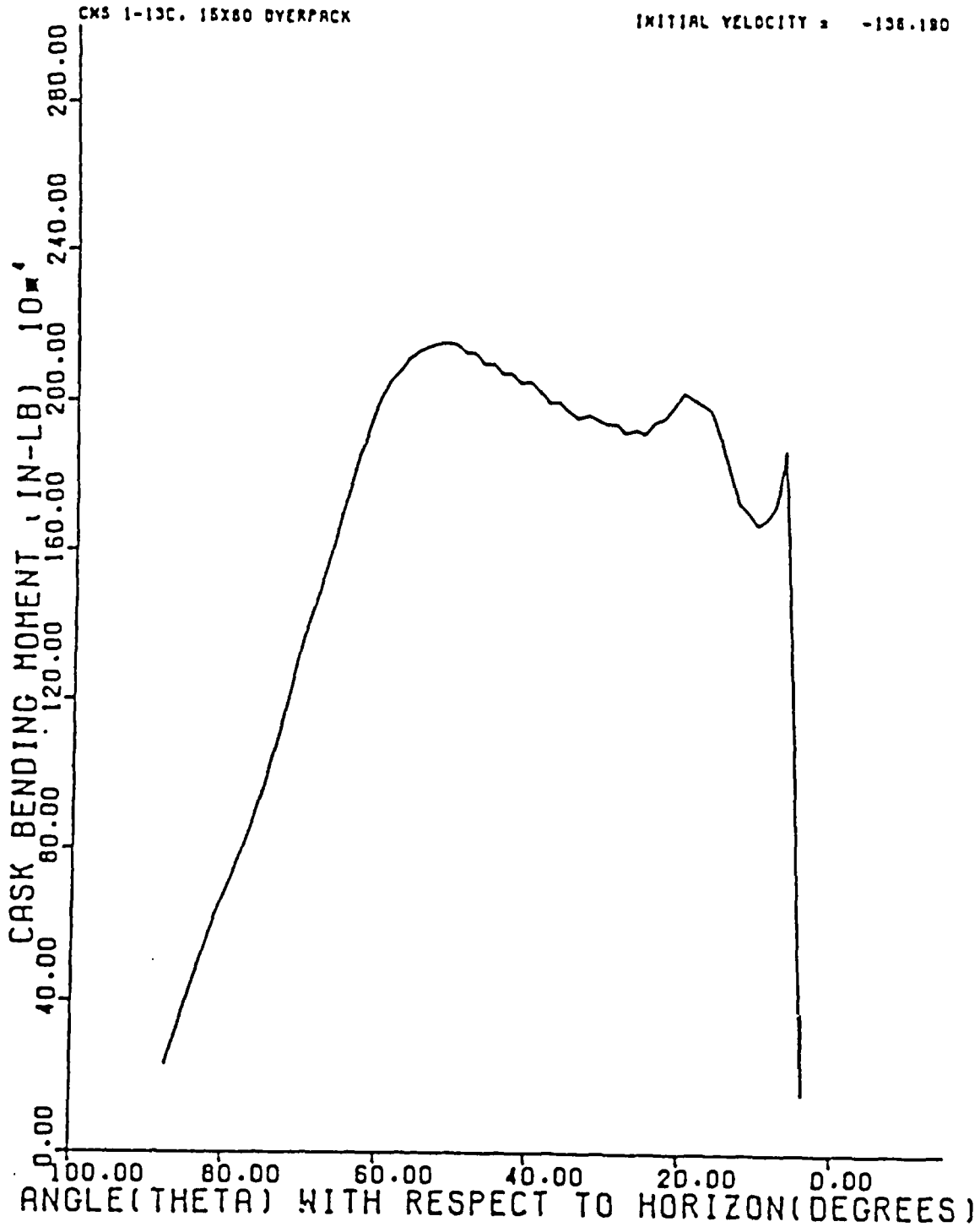
Drop Orientation	External Shell		Containment Vessel	
	Stress	Factor of Safety	Stress	Factor of Safety
End	20118	+1.22	10421	+1.92
Corner	-	-	-	-
Side	22243	+1.11	17235	+1.16

From the above it can be concluded that the package experience no inelastic deformation and all stresses are well below yield. Therefore, the Model 1-13C II Packaging can safely satisfy the loading due to the drop condition associated with Normal Conditions of Transport.



FIGURE 2.6.7-3

CASK BENDING MOMENT (IN-LB) -2 FT DROP



2.6.8 Corner Protector

This requirement is not applicable since the Model 1-13C II Packaging is fabricated of steel and weighs more than 110 lbs.

2.6.9 Compression

Not applicable since package weighs more than 10,000 lbs.

2.6.10 Penetration

Impact energies resulting from a 13 pound rod dropping from a height of 40 inches will have no significant effect on the exterior of the cask. The overpack fully protects both ends of the package leaving only the central cask body which is manufactured from 1/2 inch thick steel and backed with over 5 inches of lead. No valves, valve covers or fragile protrusions exist.

2.6.11 Conclusions

As the result of the above assessment, it is concluded that under normal conditions of transport the package complies with criteria in 10 CFR 71, as follows:

- 1) There will be no release of radioactive material from the containment vessel;
- 2) The effectiveness of the packaging will not be substantially reduced;
- 3) There will be no mixture of gases or vapors in the package which could, through any credible increase in pressure or an explosion, significantly reduce the effectiveness of the package.

## 2.7 Hypothetical Accident Conditions

The Model 1-13C II package has been designed and its contents are so limited that the performance requirements specified in 10 CFR will be met if the package is subjected to the hypothetical accident conditions specified in 71.73 of 10 CFR 71.

To demonstrate the structural integrity of the package and its ability to withstand accident conditions, a comprehensive full scale drop test program has been conducted. These tests employed an existing 1-13C II package modified to bring the assembly into conformance with the configuration detailed in Section 1.3.1.1. Analytic predictions are used to augment test data where topics have not been directly measured in tests.

### 2.7.1 Free Drop

Section 71.73 of 10 CFR 71 requires that the package survive a 30 foot drop onto a flat essentially unyielding surface. The test and analysis methods used to demonstrate this capability closely parallel the techniques used for past Type B packages. Analytic techniques are completely described in Appendix Section 2.10.1. Test methods, plans, data, results, conclusions and interpretations are consolidated in a special drop test Appendix, Section 2.11.

As described in Section 1.2, the Model 1-13C II package features circular energy absorbing overpacks surrounding each end of the cask body. These overpacks are designed to minimize damages to the cask body during 30 foot drops at any orientation upon unyielding surfaces. Test results, described in Section 2.11, demonstrate that these overpacks function as designed; the cask body experience no damage and incurs no measurable strains in excess of yield. This behavior under tested 30 foot drop conditions assures the complete effectiveness of the cask closure features essential for preservation of package containment integrity.

Overpacks loads and performance analyses preceded and followed the drop tests. Analysis prior to test were conducted to refine the geometry and properties of the overpacks and to select the most critical drop orientations for these tests. Analyses subsequent to test were conducted using actual physical properties of the test articles. These post-test analyses were used to derive essential parameters not directly measured by test. An important result of these tests was the validation of analytic overpack performance prediction methods described in Section 2.10.2.

Prior to conduct of the two drop tests described in Section 2.11, a full scale engineering prototype drop test was conducted in July, 1980, using a simulated cask and prototype overpack. This engineering development test, like the test described in Section 2.11, was completely successful and the simulated cask suffered no damage. Notably, the simulated cask was fabricated of materials with significantly less robust structural properties than the actual 1-13C II cask. This engineering development test resulted in slight modifications of crushable foam properties and overpack shell thicknesses to improve overpack performance. This development test data also resulted in slight modifications of predictive methods for oblique impacts, Section 2.10.2.2, to improve the accuracy of pitching moment calculations. That is, the location of the effective impact force was changed to allow variation as a function of crushed overpack footprint geometry.

Using the methods of Section 2.10.1.1, three drop conditions for the package have been evaluated, i.e., end, corner, and side. For each, relevant test results are discussed. Analytic values are then correlated with these data and combined with appropriate analytic temperature and pressure data. These combined results are then compared with applicable criteria to demonstrate compliance of the Model 1-13C II package with requirements for hypothetical accident conditions.

2.7.1.1 Free Drop Impact, End Drop

The first of two drop tests, discussed in Section 2.11 was an end impact upon the package base. Of all the potential orientation angles, end drop produces one of the largest package deceleration forces.

These deceleration forces induce large edge bending forces on the edge supported and sealed lid. Test results indicated no degradation of containment integrity, and no measurable change to the closure geometry.

These deceleration forces together with edge prying forces potentially induce severe loadings in the closure bolts. Test results, including instrumented bolt force measurements, indicate surprisingly modest forces in closure bolts; at or below yield.

These deceleration forces also provide large forces which could induce slump of the unbonded lead shield. Gamma scan test results indicated no lead slump; in fact, there was no measurable change to the lead shield configuration of any fashion.

For a thirty foot end impact drop, measured dynamic deformation of the overpack amounted to 4.46 inches. Post-test analytic predictions were adjusted to agree precisely with this value, as outlined in Section 2.11.5.2. These analytic predictions employed the computer program EYDROP, described in Section 2.10.1, and the energy absorbing foam properties of Figure 2.3-1. EYDROP output results are shown in Table 2.7.1-1. Peak deceleration of 95.56g was calculated. A slightly higher deceleration of 100.18g was forecast by the oblique dynamic analyses. For conservatism, the higher value has been used for stress calculation purposes.

ENDROP (END)

CHST 1-13C OVERPACK END DROP ANALYSIS 16.5 PCF FOAM

PACKAGE WEIGHT : 27000 (LBS)  
 PACKAGE DIAMETER : 57.36 (IN)  
 OVERPACK DEPTH : 15.00 (IN)  
 DROP HEIGHT : 30.00 (FT)

CRUSH DEPTH (IN)	STRAIN	IMPACT		ENERGY		
		FORCE (LBS)	ACCEL. (G)	KINETIC (IN-LB)	STRAIN (IN-LB)	RATIO (SE/SE)
.50	.033	1317500.	4.0	5733500.	324192.	.034
1.00	.067	2255300.	14.7	9747000.	1720736.	.126
1.50	.100	2454800.	90.9	9711500.	2415609.	.247
2.00	.133	2511270.	93.0	9774000.	3656951.	.374
2.50	.167	2502614.	97.9	9787500.	4911924.	.502
3.00	.200	2490720.	91.0	9801000.	6159200.	.628
3.50	.233	2500150.	92.6	9814500.	7404409.	.754
4.00	.267	2533049.	93.4	9825000.	8662799.	.881
4.50	.300	2544093.	95.7	9841500.	9942081.	1.010
5.00	.333	2624407.	98.7	9855000.	11254230.	1.147
5.50	.367	2767351.	102.5	9864500.	12612314.	1.278
6.00	.400	2854174.	107.2	9882500.	14027323.	1.420
6.50	.433	2837745.	112.5	9895500.	15510806.	1.567
7.00	.467	3232921.	117.7	9905000.	17078469.	1.724
7.50	.500	3488570.	129.2	9922500.	18758867.	1.891
8.00	.533	3798256.	140.7	9930000.	20500573.	2.071
8.50	.567	4171675.	154.5	9945000.	22573110.	2.269
9.00	.600	4651306.	172.3	9963000.	24778927.	2.487
9.50	.633	5309833.	196.7	9976500.	27269277.	2.733
10.00	.667	6252617.	231.4	9995000.	30155907.	3.019
10.50	.700	7245552.	279.5	10005000.	33609507.	3.380
11.00	.733	9147052.	338.6	10017000.	37787250.	3.772
11.50	.767	11510380.	426.3	10030500.	42947016.	4.282
12.00	.800	14987740.	555.1	10044000.	49571556.	4.935
12.50	.833	19723895.	730.5	10057500.	58244455.	5.742
13.00	.867	27145739.	1005.4	10071000.	69986803.	6.947
13.50	.900	37727700.	1297.3	10084500.	84165238.	8.240
14.00	.933	51056570.	1841.0	10099000.	100301322.	10.733
14.50	.967	68834511.	2467.9	10111500.	137804094.	13.826
15.00	1.000	13961021.	3110.5	10125000.	175428479.	17.329

21" drop:  $S = .637$   
 $F = 1,677,952 \text{ lbs.}$   
 $G = 62.2 g$

30" drop:  $S = 4.16$   
 $F = 2,550,037 \text{ lbs.}$   
 $G = 75.56 g$

2-95

Revision 0

TABLE 2.7.1-1

Detailed cask stress calculations were conducted using the cask and lid finite element models discussed in Section 2.6.1, see Figures 2.6.1-1 and 2.6.1-2. The stresses associated with an end impact deceleration of 100.18g's must be combined with maximum normal temperature and pressure stresses, as outlined in NRC Regulatory Guide 7.8. Combined stresses for this set of conditions are found in Case 6, Appendix Section 2.10.3.

Maximum stresses are summarized on the following page.

Center Location	Stress Intensity (psi)	
	(Membrane)	Surface
<u>Cask Body (Fig. 2.6.1-1)</u>		
Base - Inner Shell	9554 (12)*	14497 (12)
- Outer Shell	27257 (5)	60493 (5)
Side - Lower Quarter		
- Inner Shell	10935 (15)	13110 (14)
- Outer Shell	44009 (9)	65270 (7)
Side - Mid Height		
- Inner Shell	10372 (25)	10478 (25)
- Outer Shell	18703 (40)	19197 (40)
Side - Top Quarter		
- Inner Shell	13522 (30)	16223 (30)
- Outer Shell	18703 (41)	19197 (41)
<u>Lid (Fig. 2.6.1-2)</u>		
- Base Plate	14181 (2)	27806 (4)
- Side Cone	21238 (9)	34815 (9)
- Top Plate	11472 (16)	38091 (16)

\*( ) Denotes element number.

Factors of safety are calculated using allowable stresses at a temperature of 214.4°F, based on material properties from Table 2.3-1, as follows:



o Containment Vessel (Inner Shell)

(NRC Reg. Guide 7.6)

$$S_m = 20 \text{ ksi}$$

$$S_u = 70.28 \text{ ksi}$$

- Membrane

$$2.4 S_m = (2.4) (20) = 48 \text{ ksi}$$

$$0.7 S_u = (.7) (70.28) = 49.20 \text{ ksi}$$

- Membrane + Bending

$$3.6 S_m = (3.6) (20) = 72 \text{ ksi}$$

$$S_u = 70.28 \text{ ksi}$$

o Outer Shell

$$S_u = 70.28 \text{ ksi}$$

For the containment vessel the minimum factors of safety are:

o Membrane (Lid Cone):

$$\text{F.S.} = \frac{48}{21.238} = \underline{+2.26}$$

o Membrane + Bending (Lid Cone)

$$\text{F.S.} = \frac{70.28}{34.815} = \underline{+2.02}$$

For the exterior shell, the minimum factor of safety (at lower cask side, Element 7) is:

$$\text{F.S.} = \frac{70.28}{65.27} = \underline{+1.08}$$

2.7.1.2 Free Drop Impact, Corner Drop

The second of the two drop tests, discussed in Section 2.11 was a corner drop, lid end down, with package oriented at  $40^\circ$  with respect to a horizontal plane. This orientation angle was chosen for two reasons:

- o To minimize overpack clearance margins, see Figure 2.7.1-2.
- o To maximize secondary "slap-down" loads on the lid closure and thereby maximize closure bolt loads.

Of note, the earlier engineering development test conducted in July, 1980, was conducted at an orientation angle of about  $60^\circ$  with respect to horizontal plane. This corresponded to the traditional c.g. over struck corner orientation.

The test results indicated no change to the cask and no measurable residual strains excepting for a single closure bolt that could have experienced a strain of as much as 0.44%; about twice the value of yield strain. See Section 2.11.5.1.3 for details on closure bolt experimental strains.

Analytic predictions of package performance, used to determine cask loads, employed two computer programs described in Appendix Section 2.10.1 - CYDROP and OBLIQUE. CYDROP uses an energy balance technique to determine loads and deformations of the overpack. Since CYDROP assumes all drop energy is absorbed in deformation of the overpack, it provides valid results at the c.g. over struck corner orientation (no rotational motions). CYDROP output for this orientation is provided in Table 2.7.1-2.

At other orientation angles, the force-deflection values generated by CYDROP are used in OBLIQUE, a dynamic analyses model that properly treats rotational motion effects. Figures 2.7.1-1 to 2.7.1-3 summarize predicted overpack responses for all orientation angles from near vertical to near horizontal. Figure 2.7.1-1 clearly shows that near vertical orientation produce maximum forces on the cask. Figure 2.7.1-2 shows that the tested 40° orientation corresponds to minimum clearance between the impact plane and cask "hard points." Figure 2.7.1-3 maps bending moments induced in the cask body.

At the tested orientation, predicted dynamic overpack deformation amounts to 13.9 inches. Post-test measurements of the deformed overpack, Figure 2.11.4-6, shows about 9.1 inches residual deformation following recovery. The foam utilized in these overpacks recovers about 30% following removal of load. This gives a test based dynamic deformation estimated at  $(9.2/.7) = 13.1$  inches; about 6% lower than the analytic predictions.

For cask stress evaluation purpose, moment and thrust forces are a maximum at 53.75° with respect to a horizontal plane. At this orientation, cask loads are:

$$\text{Moment} = 12.634 \times 10^6 \text{ in-lb.}$$

$$\text{Thrust} = 1.399 \times 10^6 \text{ lbs (51.8g)}$$

CYCLIC IMPACT

10.35.51 01/03/71 PAGE 22

CMS 1-11C PACIFIC, 15340 OVERPACK, 20.5 PER FOAM, 29.49 DECC

CRUSH DEPTH (IN)	AREA (IN <sup>2</sup> )	VOLUME (IN <sup>3</sup> )	FORCE (LBS)	ACCEL. (G)	KINETIC (IN-LB)	STRAIN (IN-LB)	RATIO (S <sup>2</sup> /FE)	DISTRIBUTION OF STRAIN RATIOS BY PERCENT OF CONTACT AREA				
								LE.70	CL.70	CE.50	CL.50	CE.45
0.25	12.0	3.0	207.	0.0	9733500.	52.	0.00	100.00	0.00	0.00	0.00	0.00
1.00	33.5	14.	7791.	0.3	9747000.	2651.	0.00	100.00	0.00	0.00	0.00	0.00
1.50	51.1	36.	24964.	0.9	9766500.	10225.	0.00	100.00	0.00	0.00	0.00	0.00
2.00	67.2	77.	44259.	1.6	9774000.	24766.	0.00	100.00	0.00	0.00	0.00	0.00
2.50	125.5	132.	79430.	2.4	9787500.	60845.	0.00	100.00	0.00	0.00	0.00	0.00
3.00	144.0	201.	111521.	5.1	9801000.	102204.	0.01	100.00	0.00	0.00	0.00	0.00
3.50	204.4	301.	143320.	5.5	9814500.	173247.	0.01	100.00	0.00	0.00	0.00	0.00
4.00	257.4	417.	190043.	7.0	9828000.	257453.	0.02	100.00	0.00	0.00	0.00	0.00
4.50	299.9	522.	235845.	8.7	9841500.	344317.	0.03	100.00	0.00	0.00	0.00	0.00
5.00	347.9	717.	284714.	10.5	9855000.	444423.	0.05	100.00	0.00	0.00	0.00	0.00
5.50	397.3	903.	327017.	12.1	9868500.	544423.	0.05	100.00	0.00	0.00	0.00	0.00
6.00	447.0	1115.	363594.	14.5	9882000.	644423.	0.05	100.00	0.00	0.00	0.00	0.00
6.50	494.6	1351.	445035.	16.5	9895500.	744423.	0.05	100.00	0.00	0.00	0.00	0.00
7.00	552.3	1614.	502853.	18.7	9909000.	844423.	0.05	100.00	0.00	0.00	0.00	0.00
7.50	602.7	1904.	563265.	20.9	9922500.	944423.	0.05	100.00	0.00	0.00	0.00	0.00
8.00	659.7	2220.	624924.	23.2	9936000.	1044423.	0.05	100.00	0.00	0.00	0.00	0.00
8.50	714.2	2564.	697144.	25.3	9949500.	1144423.	0.05	100.00	0.00	0.00	0.00	0.00
9.00	768.9	2924.	772397.	27.1	9963000.	1244423.	0.05	100.00	0.00	0.00	0.00	0.00
9.50	822.7	3333.	853017.	28.9	9976500.	1344423.	0.05	100.00	0.00	0.00	0.00	0.00
10.00	878.5	3784.	940045.	31.4	9990000.	1444423.	0.05	100.00	0.00	0.00	0.00	0.00
10.50	933.2	4277.	924445.	34.5	10003500.	1544423.	0.05	100.00	0.00	0.00	0.00	0.00
11.00	987.5	4811.	1024453.	39.3	10017000.	1644423.	0.05	100.00	0.00	0.00	0.00	0.00
11.50	1041.4	5398.	1123472.	47.7	10030500.	1744423.	0.05	100.00	0.00	0.00	0.00	0.00
12.00	1094.7	5737.	1222129.	44.4	10044000.	1844423.	0.05	100.00	0.00	0.00	0.00	0.00
12.50	1147.3	6293.	1329172.	20.3	10057500.	1944423.	0.05	100.00	0.00	0.00	0.00	0.00
13.00	1199.0	6879.	1479101.	54.3	10071000.	2044423.	0.05	100.00	0.00	0.00	0.00	0.00
13.50	1249.7	7492.	1616171.	59.9	10084500.	2144423.	0.05	100.00	0.00	0.00	0.00	0.00
14.00	1299.3	8129.	1777357.	65.8	10098000.	2244423.	0.05	100.00	0.00	0.00	0.00	0.00
14.50	1347.6	8791.	1967351.	72.2	10111500.	2344423.	0.05	100.00	0.00	0.00	0.00	0.00
15.00	1394.2	9559.	2239064.	82.5	10125000.	2444423.	0.05	100.00	0.00	0.00	0.00	0.00
15.50	1438.7	10554.	2411327.	89.3	10138500.	2544423.	0.05	100.00	0.00	0.00	0.00	0.00
16.00	1482.2	11524.	2536593.	97.9	10152000.	2644423.	0.05	100.00	0.00	0.00	0.00	0.00
16.50	1533.4	12530.	2744444.	103.4	10165500.	2744423.	0.05	100.00	0.00	0.00	0.00	0.00
17.00	1584.7	13567.	2921378.	109.2	10179000.	2844423.	0.05	100.00	0.00	0.00	0.00	0.00
17.50	1626.0	14723.	3129035.	115.9	10192500.	2944423.	0.05	100.00	0.00	0.00	0.00	0.00

TABLE 2.7.1-2

2-101

FIGURE 2.7.1-1

IMPACT FORCES (LBS) -30 FT DROP

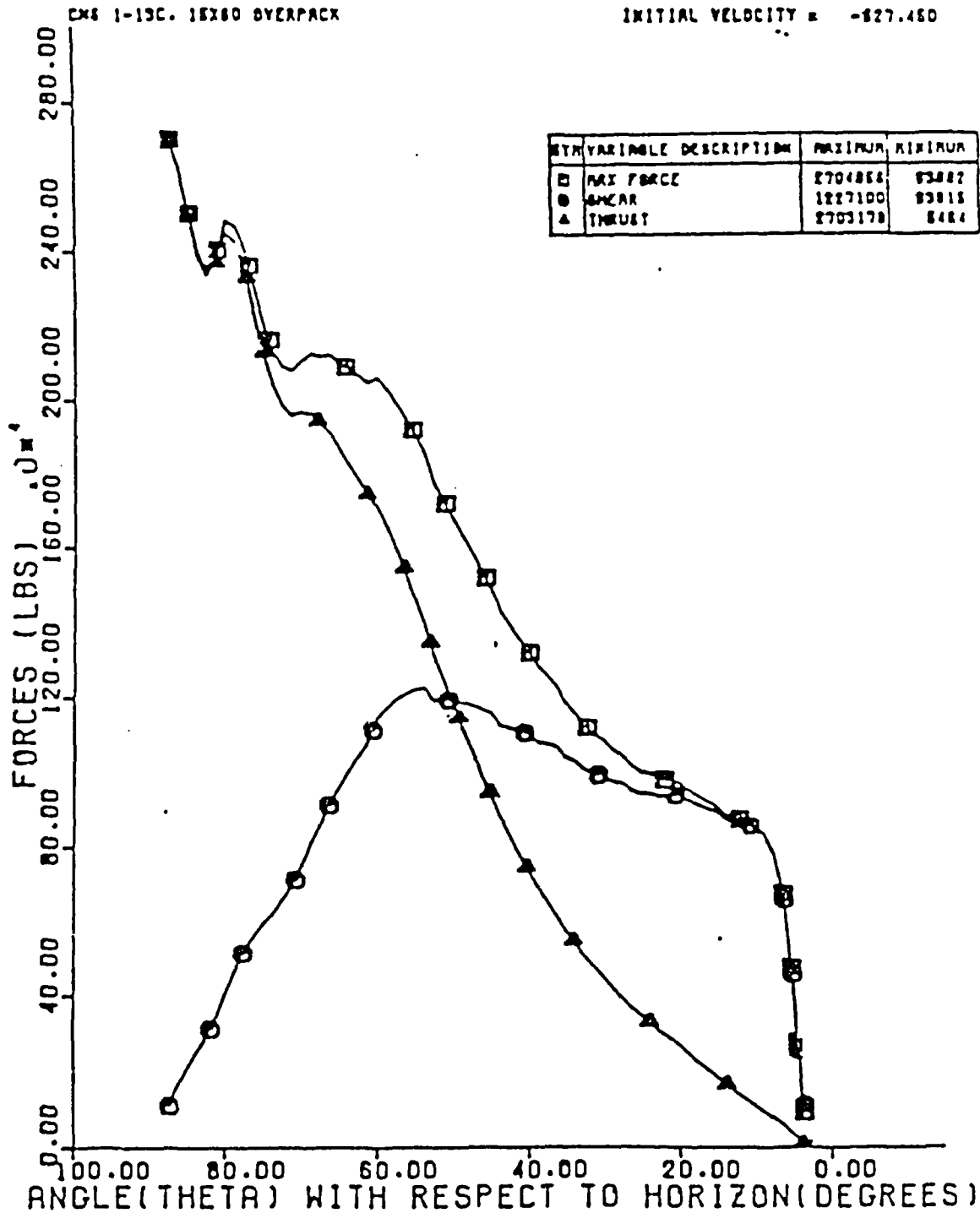


FIGURE 2.7.1-2

OVERPACK DEFLECTION AND RESIDUAL CLEARANCE -30 FT DROP

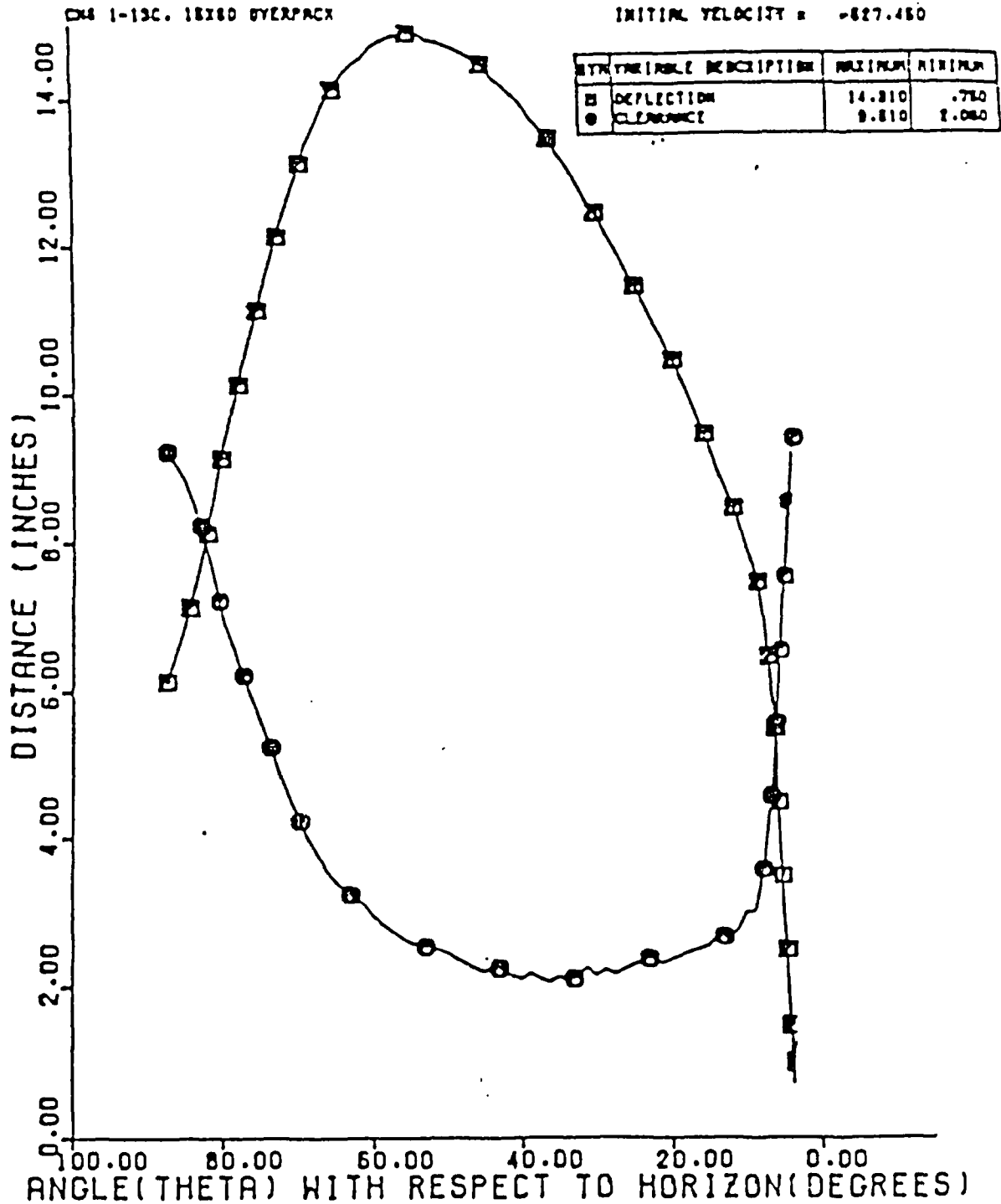
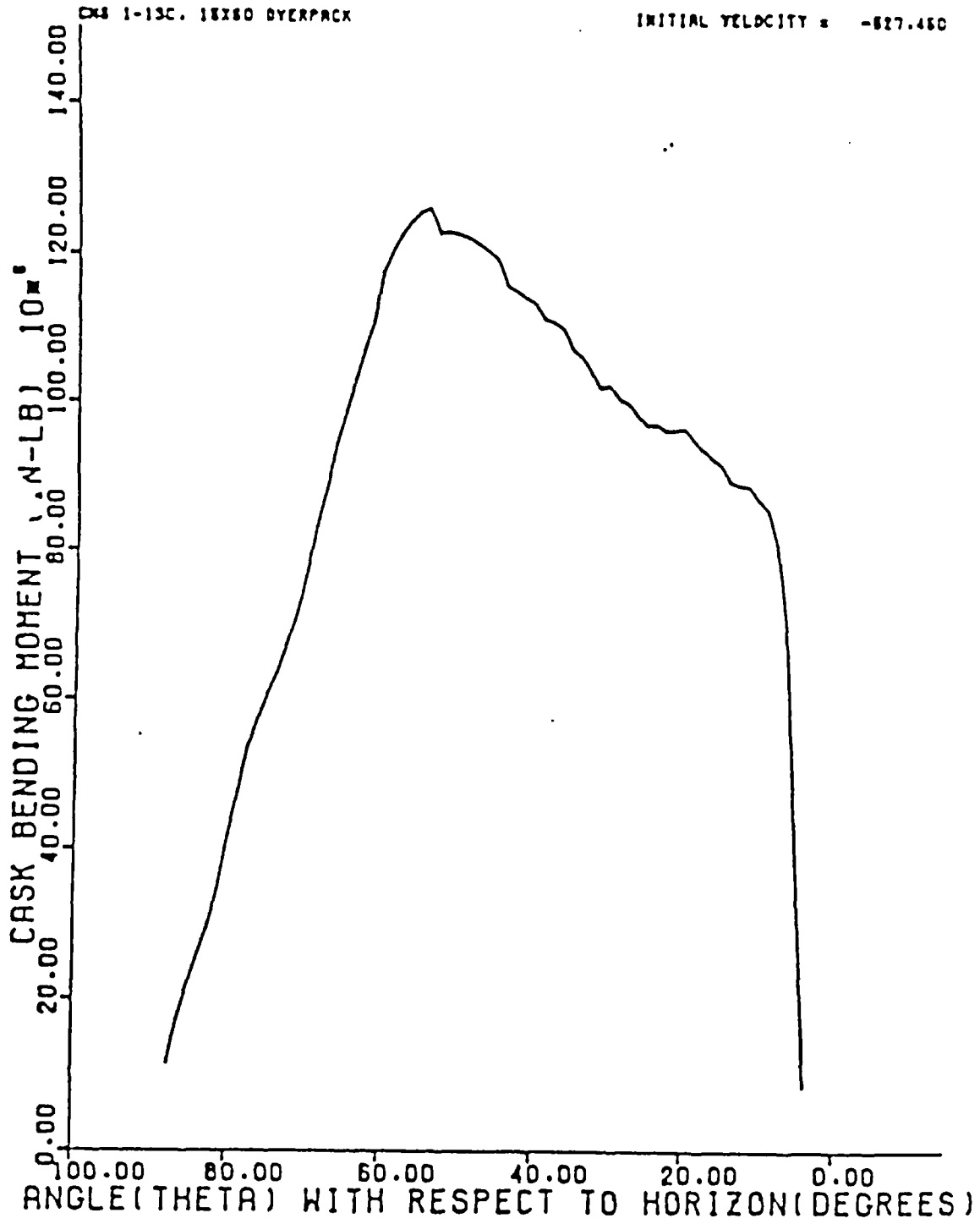


FIGURE 2.7.1-3

CASK BENDING MOMENT (IN-LB) -30 FT DROP



The moment load produces a maximum bending stresses at the lower 1/3 point of the cask height (68/3 = 22.7"); corresponding to cask model elements 19 and 35, see Figure 2.6.1-1. At this location, the bending stresses are:

$$f_b = Mc/I = 11,649 \text{ psi, inner shell}$$

$$16,394 \text{ psi, outer shell}$$

Where:  $M = 12.634 \times 10^6 \text{ in-lb.}$   
 $c = 13.50 \text{ in.} - \text{inner shell}$   
 $19.00 \text{ in.} - \text{outer shell}$

$$I = \bar{y}_4 (I_o^4 - R_i^4) = \bar{y}_4 [19.25^4 - 18.75^4 + 13.75^4 - 13.25^4]$$

$$= 14642 \text{ in.}^4$$

Stresses for thrust load effects are obtained by multiplying results for Case 3, Section 2.10.3, by the factor  $51.8/100.184 = .5170$ .

Stresses for maximum normal pressure and temperature are obtained from Case 7. Stress predictions are shown below.

		Stresses (psi)					
Locations (Element Number)	Load	$\sigma_r$	$\sigma_z$	$\tau_{rz}$	$\sigma_\theta$	S.I.	
<u>Inner Shell</u> (19) (Containment)	Bending	-	$\pm 11649$	-	-	-	
	Press & Temp (7)	47.	10550	-16	4566	10503	
	Thrust (3)	0	-405	18	627	1033	
	Combined	+47.	21794 -1504	+ 2	5193	21747. 6697	
<u>Outer Shell</u> (35)	Bending	-	$\pm 16394$	-	-	-	
	Press & Temp (7)	-289	13750	0	19180	19469	
	Thrust (3)	13	-6178	45	-719	6192	
	Combined	-276	23966 -8822	45	18461	24242 27283	



The resultant factors of safety using allowables defined in Section 2.7.1.1 are:

- o Containment: F.S. =  $\frac{48}{21.747} = +2.21$  .
- o Outer Shell: F.S. =  $\frac{70.28}{27.283} = +2.58$

### 2.7.1.3 Free Drop Impact, Side Drop

Side drop impacts were not tested in the drop test program; however, the rather shallow angle oblique impact ( $40^\circ$ ) induced significant impact upon the second overpack. This test approximately simulated a side drop event. As noted previously, the cask experienced no damage in these tests.

The most critical phenomena investigated in a side drop evaluation are the bending stresses induced in the cask body by the impacts upon the end mounted overpacks. Behavior of the overpacks has been evaluated using the program, SYDROP, described in Section 2.10.1. Results are shown in Table 2.7.1-3. Peak acceleration of 137.4g was calculated. This produces a midsection bending moment of:

$$M = Wl/8 = (27000)(137.4g)(68)/8 = 31.5 \times 10^6 \text{ in-lb.}$$

Using the cask cross section properties gives bending stresses of:

<u>Location</u>	<u>Bending Stress (psi)</u>
Inner Shell	$\pm 29,075$
Outer Shell	$\pm 40,918$

These bending stresses must be superimposed upon the maximum normal pressure and temperature stresses found in Case 7, Section 2.10.2. For midsection elements 23 and 39, the resultant stresses are:

CRUSH DEPTH (IN)	CRUSH PLANE		IMPACT		ENERGY			DISTRIBUTION OF STRAIN PATTERNS BY PERCENT OF CONTACT AREA				
	AREA (IN <sup>2</sup> )	VOLUME (IN <sup>3</sup> )	FORCE (LBS)	ACCEL. (G)	POTENTIAL (IN-LBS)	STRAIN (IN-LBS)	RATIO (%)	11.70	11.70	11.45	11.45	11.45
0.25	267.6	22.0	26220.	1.3	3726720.	6271.	0.00	100.00	0.00	0.00	0.00	0.00
0.50	495.6	41.0	27992.	2.6	9733260.	32304.	0.04	100.00	0.00	0.00	0.00	0.00
0.75	822.6	68.0	2812.	14.9	9740220.	718437.	0.07	100.00	0.00	0.00	0.00	0.00
1.00	1150.6	95.0	523911.	13.6	9747180.	234204.	0.04	100.00	0.00	0.00	0.00	0.00
1.25	1478.6	122.0	122642.	21.1	9753120.	377627.	0.03	100.00	0.00	0.00	0.00	0.00
1.50	1806.6	149.0	706210.	28.2	9760060.	542733.	0.02	100.00	0.00	0.00	0.00	0.00
1.75	2134.6	176.0	373577.	27.5	9767000.	726718.	0.05	100.00	0.00	0.00	0.00	0.00
2.00	2462.6	203.0	1121.	31.2	9773940.	911555.	0.05	100.00	0.00	0.00	0.00	0.00
2.25	2790.6	230.0	602333.	33.6	9780880.	1149824.	0.08	100.00	0.00	0.00	0.00	0.00
2.50	3118.6	257.0	913314.	32.6	9787820.	1372264.	0.08	100.00	0.00	0.00	0.00	0.00
2.75	3446.6	284.0	1616414.	32.0	9794760.	1630411.	0.08	100.00	0.00	0.00	0.00	0.00
3.00	3774.6	311.0	2079494.	32.9	9801700.	1822769.	0.08	100.00	0.00	0.00	0.00	0.00
3.25	4102.6	338.0	1137873.	42.2	9808640.	2186844.	0.07	100.00	0.00	0.00	0.00	0.00
3.50	4430.6	365.0	1219452.	44.5	9815580.	2452257.	0.05	100.00	0.00	0.00	0.00	0.00
3.75	4758.6	392.0	1245537.	44.9	9822520.	2726237.	0.02	100.00	0.00	0.00	0.00	0.00
4.00	5086.6	419.0	1327714.	49.6	9829460.	3055325.	0.05	100.00	0.00	0.00	0.00	0.00
4.25	5414.6	446.0	1414314.	52.0	9836400.	3437419.	0.06	100.00	0.00	0.00	0.00	0.00
4.50	5742.6	473.0	1483311.	54.5	9843340.	3776474.	0.06	100.00	0.00	0.00	0.00	0.00
4.75	6070.6	500.0	1576311.	59.2	9850280.	4181472.	0.04	100.00	0.00	0.00	0.00	0.00
5.00	6398.6	527.0	1666414.	61.2	9857220.	4574794.	0.04	100.00	0.00	0.00	0.00	0.00
5.25	6726.6	554.0	1773314.	63.2	9864160.	5014774.	0.05	100.00	0.00	0.00	0.00	0.00
5.50	7054.6	581.0	1842114.	70.1	9871100.	5473337.	0.05	100.00	0.00	0.00	0.00	0.00
5.75	7382.6	608.0	2021814.	75.2	9878040.	5982117.	0.04	100.00	0.00	0.00	0.00	0.00
6.00	7710.6	635.0	2061611.	81.4	9884980.	6462276.	0.05	100.00	0.00	0.00	0.00	0.00
6.25	8038.6	662.0	2167514.	84.0	9891920.	7166413.	0.05	100.00	0.00	0.00	0.00	0.00
6.50	8366.6	689.0	2147101.	82.1	9898860.	7497443.	0.02	100.00	0.00	0.00	0.00	0.00
6.75	8694.6	716.0	2542270.	100.2	9905800.	8396916.	0.04	82.47	17.33	0.00	0.00	0.00
7.00	9022.6	743.0	3316610.	122.8	9912740.	9179910.	0.02	74.00	24.00	0.00	0.00	0.00
7.25	9350.6	770.0	2709811.	137.6	9919680.	9916617.	0.05	71.59	28.41	0.00	0.00	0.00
7.50	9678.6	797.0	2762244.	145.3	9926620.	10668524.	0.05	70.47	29.33	0.00	0.00	0.00
7.75	10006.6	824.0	2854701.	145.0	9933560.	11099581.	0.05	61.67	24.00	7.33	0.00	0.00
8.00	10334.6	851.0	5682259.	210.3	9940500.	12368900.	0.04	63.33	18.47	14.00	6.00	0.00
8.25	10662.6	878.0	6328224.	227.6	9947440.	13844225.	0.03	60.67	15.33	24.00	0.00	0.00
8.50	10990.6	905.0	4721770.	170.6	9954380.	15207099.	0.02	58.00	13.33	21.87	0.00	0.00
8.75	11318.6	932.0	4147770.	153.6	9961320.	15536673.	0.03	52.33	12.47	21.33	10.67	0.00
9.00	11646.6	959.0	3712110.	134.3	9968260.	17277811.	0.02	52.33	11.33	14.67	10.67	0.00
9.25	11974.6	986.0	3416770.	128.7	9975200.	18720197.	0.02	52.00	10.00	14.00	12.00	12.00
9.50	12302.6	1013.0	1220011.	119.2	9982140.	15037601.	0.01	50.00	10.00	12.00	9.33	14.47

TABLE 2.7.1-3

2-108

Locations (Element Number) Load		Stresses (psi)				
		$\sigma_r$	$\sigma_z$	$\tau_{rz}$	$\sigma_\theta$	S.I.
<u>Inner Shell</u> (23) (containment)	Bending	-	$\pm 29075$	-	-	-
	Press & Temp	68.	11240	-12	4440	11172
	Combined	68.	40315 -17835	-12	4440	40247 22275
<u>Outer Shell</u> (35)	Bending	-	$\pm 40918$	-	-	-
	Press & Temp	-283	13560	-12	19010	19293
	Combined	-283	54478 -27358	-12	19010	54761 46368

The resultant factors of safety, using allowables defined in Section 2.7.1.1 are:

$$\circ \text{ Containment: F.S.} = \frac{48}{40.247} = \underline{+1.19}$$

$$\circ \text{ Outer Shell: F.S.} = \frac{70.28}{54.761} = \underline{+1.28}$$

## 2.7.2 Puncture

A 40 inch drop onto a 6 inch diameter pin can occur only on the cylindrical body or side wall between the overpacks.

The Helms\* puncture relation is given as:

$$t = (W/S)^{0.71}$$

Where:  $t$  = shell thickness = 1/2 (outer shell) and  
1/4 (fireshield)

$W$  = cask weight - lbs.

$S$  = ultimate tensile strength of outer shell

$$= 70,280 \text{ psi @ } 214.4^{\circ}\text{F}$$

The package weight causing puncture is:

$$W = St^{1.4}$$

Upon impact, the fireshield is deformed and brought into direct contact with the outer shell. At this point in the impact scenario, the fireshield is effectively "backed" by the outer shell and lead. The package weight to cause puncture of this 1/4" fireshield is:

$$W_f = (70,280)(.25)^{1.4} = 10,091 \text{ lbs.}$$

The corresponding weight to cause puncture of the 1/2" outer shell is:

$$W_s = (70,280)(.5)^{1.4} = 26,631 \text{ lbs.}$$

---

\*Shappert, L.B., "Cask Designers Guide", ORNL-NSIC-68, Page 18.

Thus, the total weight at which puncture of both fire shield and outer shell occurs is:

$$W = W_f + W_s = 36,722 \text{ lbs.}$$

The actual package weight is 27,000 lbs; therefore, the factor of safety for puncture resistance on an energy basis is:

$$\text{F.S.} = \frac{36,720}{27,000} = \underline{+1.36}$$

When the cask impacts the puncture pin the force imposed upon the cask is estimated as:

$$F_I = k_s A_I$$

$$k_s = \text{Dynamic flow pressure of stainless} = 45,000 \text{ psi} *$$

$$A_I = \pi/4 (R_c)^2 = \pi/4 (6.0)^2 = 28.27 \text{ in}^2$$

$$F_I = (45,000) (28.27) \\ = 1.272 \times 10^6 \text{ lbs.}$$

This force induces a moment at the midsection of the cask. The moment is estimated as:

$$M = \frac{F l}{8} = \frac{(1.272 \times 10^6)(68)}{8} = 10.8 \times 10^6 \text{ in-lb.}$$

---

\*Shappert, L.B., "Cask Designers Guide", ORNL-NSIC-68, Page 64.

Using the section properties from Section 2.7.1.3 to calculate bending stresses and the pressure and temperature stresses reported gives stress intensities and factors of safety of:

	Stresses (psi)		F.S.
	Bending	S.I.	
o Inner Shell (Containment)	$\pm 9958$	21130	$48/21.13 = 2.27$
o Outer Shell	$\pm 14014$	27857	$70.28/27.86 = 2.52$

### 2.7.3 Thermal

#### 2.7.3.1 Summary of Pressures and Temperatures

The maximum temperatures and pressures resulting from the hypothetical accident conditions presented in Section 3.5.3 and 3.5.4 are summarized below:

Maximum Containment Vessel Pressure = 184.4 psig Temperatures:

- o Cavity (Inner Shell) = 371.43°F
- o Outer Shell Sides = 434.56°F
- o Outer Shell Ends = 363.35°F

2.7.3.2 Differential Thermal Expansion

Differential thermal expansion between the two shells of the cask and the lead shield produces significant stresses. Stresses have been assessed by use of the finite element models discussed in Section 2.6.1, see Figure 2.6.1-1 and 2.6.1-2.

2.7.3.3 Stress Calculations

Stress calculations for pressure and thermal loads were performed using the conditions summarized in Section 2.7.3.1, as Cases 2 and 1 of Appendix Section 2.10.3, respectively. These two cases are combined as Case 4 of the referenced section.



Maximum Stresses are summarized as follows:

Location	Stress Intensity (ksi)	
	Center	Surface
<u>Cask Side (Figure 2.6.1-1)</u>		
o Lower Quarter		
	*	
- Inner Shell	27740 (18)	29042 (18)
- Outer Shell	53380 (9)	62805 (9)
o Mid Height		
- Inner Shell	32049 (26)	33611 (25)
- Outer Shell	34901 (35)	36641 (35)
o Top Quarter		
- Inner Shell	36322 (30)	44216 (30)
- Outer Shell	36860 (46)	37917 (46)
<u>Lid (Figure 2.6.1-2)</u>		
- Base Plate	18760 (5)	33325 (5)
- Side Cone	37963 (8)	58210 (10)
- Top Plate	31120 (16)	53494 (14)

\* ( ) Denotes element number.

2.7.4 Comparison With Allowable Stresses

Allowable stresses based upon the temperatures of Section 2.7.3.1 and Table 2.3-1 are as follows:

- o Containment Vessel (Inner Shell) (T=371.43°F)

$$S_m = 19.07 \text{ ksi}$$

$$S_u = 64.86 \text{ ksi}$$

- Membrane:

$$2.4S_m = 45.77 \text{ ksi}$$

$$.7S_u = 45.40 \text{ ksi}$$

- Membrane + Bending

$$3.6S_m = 68.65 \text{ ksi}$$

$$S_u = 64.86 \text{ ksi}$$

- o Outer Shell (T=434.56°F)

$$S_u = 64.09 \text{ ksi}$$

For the containment vessel, the minimum factors of safety are:

- o Membrane  $F.S. = \frac{45.40}{37.963} = 1.20$

- o Membrane + Bending:  $F.S. = \frac{64.86}{58.21} = 1.11$

For the outer shell, the minimum factor of safety is:

$$F.S. = \frac{64.09}{62.805} = 1.02$$

Therefore, it is safe to conclude that the containment vessel can safely react any anticipated loading condition without experiencing detrimental stresses.

#### 2.7.4 Immersion-Fissile Material

The requirement of 10 CFR 71.73 (c)(4) is not applicable, since no arrangement of the TMI-2 core debris samples contained in the shielded debris canisters can result in a critical configuration under any normal or accident conditions with the total mass limited to 29kg by the volume restriction. The actual mass of approximately 15 kg will provide a safety factor of five.

#### 2.7.5 Immersion - All Packages

10 CFR 71.73 (c) (5) requires an immersion in water with a pressure of 21 psig for eight hours. Review of the stresses in Section 2.6.4 for a 25 psig pressure indicates the stresses are low, and this test will have no significant effect on the package.

#### 2.7.6 Summary of Damage

The structural integrity of the Model 1-13C II Package has been substantiated for normal transport conditions as well as hypothetical accident conditions.

Damage to the Model 1-13C II Package that results from the hypothetical accident condition is:

1. Impact limiters crush during the 30 foot drop condition producing a maximum bolt load on the containment vessel. Bolt stresses are maintained at or below yield. Vessel stresses are less than those prescribed by NRC Regulatory Guide 7.6.

2. Small local deformations to the external shell may result during the 40 inch puncture condition. There will be no loss of shielding and the containment vessel will not be deformed.
  
3. Presence of the overpack and heat shield limit temperatures in the containment vessel walls to less than 372<sup>o</sup>F, and internal pressures to 185 psig. Geometry and temperature integrity of the seals is maintained.

#### 2.8 Special Form

Not applicable since no special form is claimed.

#### 2.9 Fuel Rods

Not applicable since fuel rod cladding is not considered to provide containment of radioactive material.

#### 2.10 Structural Evaluation Appendices

This section contains three blocks of informational appendices supporting the structural evaluations of the 1-13C II Cask presented in Sections 2.1 through 2.9.

- o Section 2.10.1 - Summarizes the methodology of computer programs utilized to demonstrate structural compliance of the package with applicable provisions.
  
- o Section 2.10.2 - Contains finite element stress summaries for the cask under normal and accident conditions.
  
- o Section 2.10.3 - contains finite element stress summaries for the cask lifting lug support ring.

### 2.10.1 Analytic Methods

This section briefly documents the methodology employed for computer programs used to demonstrate compliance of the package with applicable provisions of 10 CFR 71 under normal and accident conditions. The first three subsections deal with the calculation of external and internal forces imposed upon the package, when subjected to drop events. These three subsections describe techniques and computer programs developed by Nuclear Packaging, Inc., of Tacoma, Washington.

The fourth section describes the E3SAP finite element code employed for detailed evaluation of package stresses under normal and accident conditions. The E3SAP program was developed by Boeing Computer Services Company based upon the well known SAP IV program developed by Dr. E. L. Wilson.

#### 2.10.1.1 Overpack Deformation Behavior

The package is protected by foam filled energy absorbing end buffers, called overpacks. For purposes of analysis, the overpacks are assumed to absorb, in plastic deformation of foam, the potential energy of the drop event. That is, the analyses assume that none of the drop potential energy is transferred to kinetic or strain energy of the target (the "unyielding surface" assumption of 10 CFR 71) nor strain energy in the package body itself.

There are three orientations of the package where the potential energy of drop is assumed totally absorbed by plastic deformation of the overpacks. At other orientations, where rotational effects are important, the methods outlined in Section 2.10.1.2 are employed. These three orientations where rotational (or pitch) motions play no role in the evaluation of the impact event are:

- o End Drop - on the circular end surface of the overpack.
- o Side Drop - on the cylindrical side surface of the overpacks.
- o Corner Drop - with package center of gravity directly above the struck corner of the overpack.

For these three orientations, the prediction of overpack behavior can be approached from straightforward energy balance principles:

$$E = W(h + \delta) = \int_0^{\delta} F_x dx \quad (1)$$

Where: W = Package weight

h = Drop height

$\delta$  = Maximum overpack deformation

$F_x$  = Force imposed upon target and package by the overpack at a deflection equal to x.

The left-hand term represents the potential energy of the drop. The right hand term represents the strain energy of the deformed overpack.

Each of these three orientations is treated by an individual computer program reflecting the differing geometry characteristics of each event. All three employ common energy balance techniques to assess maximum overpack deformations. All three employ a common description of the crushable energy absorbing foam.

This foam typically exhibits a stress-strain plateau of nearly constant stress up to a total strain of 40-60%. Above this strain value, pronounced strain hardening effects commence reflecting the collapse or consolidation of the entrapped bubbles within the foam. Accordingly, a tabular definition of foam stress-strain relations is employed in each of the three computer programs. This tabular definition is taken directly from measured properties and accurately reflects the strain hardening behavior of the foam up to strains of 90-95%.

This discussion of these three computer programs proceeds from the geometrically simple (end drop) to the most complex (corner drop).

1. End Drop (EYDROP)

The force produced by the overpack is simply:

$$F_x = A\sigma_e \quad (2)$$

Where:  $A = \frac{\pi D^2}{4}$ , the end area of the package.

$D =$  effective diameter of package

$\sigma_e = \beta(e)$ , the foam crush stress at a strain of  $e$  (3)

$\beta(e) =$  the tabular definition of foam stress strain properties

$e = x/x_u$ ,

$x =$  deformation

$x_u =$  end thickness of overpack.

EYDROP performs the calculations outlined in Equations (1) to (3) for a trial range of deformation values,  $\delta$ . For each trial value of total deformation, the energy balance of Equation (1) is monitored and reported. Solution for total overpack deformation is found by an interpolated balance of Equation (1).

2. Side Drop (SYDROP)

SYDROP differs from the end drop solution only in the fact that both deformation and strain vary from point to point and total force, at a given crush depth, must be found by geometric integration over these points. The details on this geometry are found in Figure 2.10.2-1. For each trial deformation value, the force is found as:

$$F_{\delta} = 2L \int_0^{x_{\max}} \sigma_{ex} dx$$

Where: L = effective length of overpack

$$x_{\max} = [r_0^2 - (r_0 - \delta)^2]^{1/2} \quad (5)$$

$\sigma_{ex} = f(e_x)$ , tabular definition of foam  
stress-strain properties.

$e_x$  = The foam strain at location x.

The strain at a point x is found by reference to Figure 2.10.2-1 as:

$$e_x = \frac{\text{Crush Depth}}{\text{Original Thick.}} = \frac{\delta - r_0 (1 - \cos\theta)}{r_0 \cos\theta - r_1 \cos\psi}$$

$$\text{Where: } \theta = \sin^{-1} (x/r_0)$$

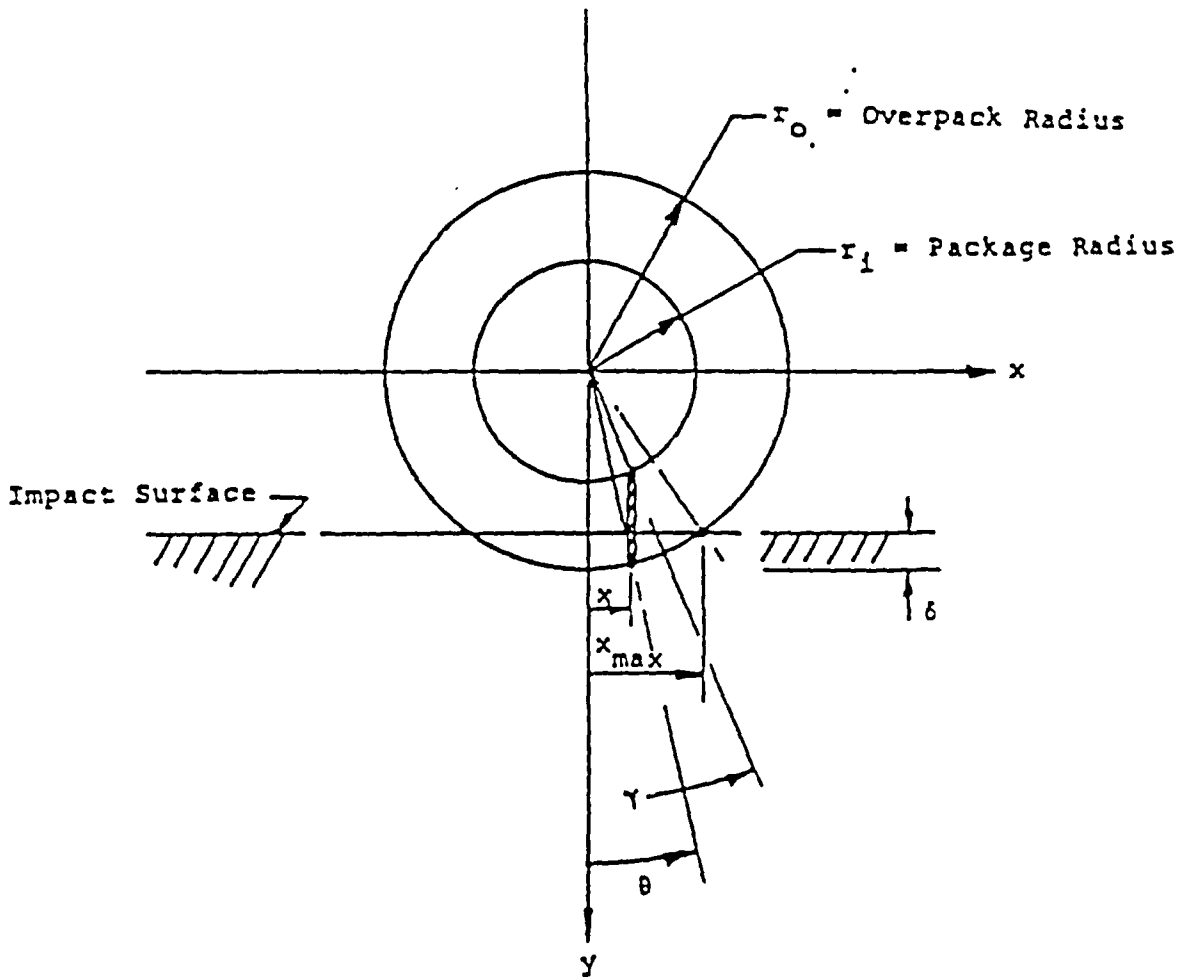
$$\psi = \sin^{-1} (x/r_1)$$

3. Corner Drop (CYDROP)

CYDROP is like SYDROP excepting that a two dimensional geometric integration is required to assess the overpack crush force at each deformation. A detailed explanation follows.



FIGURE 2.10.1-1  
SIDE DROP GEOMETRY  
(SYDROP)



CYDROP treats the corner impact of a cylindrical package upon an unyielding surface. The package itself consists of a cylindrical payload portion surrounded by a larger cylindrical volume composed of a crushable media. So long as the deformations of the crushable media are modest, the problem may be approximately solved by assuming a uniform crush stress exists over the elliptical surface of the crush plane (contact surface). CYDROP was developed specifically to address problems of large deformations of this crushable media and to treat geometries where the cylindrical overpack envelope possesses axisymmetric cylindrical voids (e.g. does not completely cover the cylindrical ends of the payload package).

The large deformation behavior of the crushable media is accommodated by determining the actual strain of the crushable media at a point. This strain is used to determine the corresponding stress from an implicit tabular definition of media stress-strain characteristics. The total crush force is found by a double integration over the contact area of the crush plane.

Strain energy absorbed by the crushable media is determined by integrating the crush force and its associated deformation. The package is assumed to be at "rest" when the computed strain energy value equals the applied drop energy.

The geometric calculations for the contact surface and the associated strains are carried out using a moving (x, y, z) coordinate system in which the x-y plane corresponds to the crush plane, see Figure 2.10.1-2. The crush plane itself represents a segment of an ellipse. The contact area is this ellipse segment, provided no cylindrical end void exists. When a cylindrical end void exists, the contact area of the crush plane is reduced by the removal of a second elliptical region associated with the projection of this void into the contact plane.

Calculation of strain is somewhat more complex. In principal, the distance from point (x,y) in the crush lane to the payload is found and denoted,  $Z_{top}$ . Similarly the distance to the undeformed external overpack envelope is found and denoted,  $Z_{bot}$ . The strain represents deformation divided by original thickness, or:

$$= \frac{Z_{bot}}{Z_{bot} + Z_{top}}$$

At any point (x, y), the calculation of Ztop may follow three branches, according to location. The three possible branches relate to the payload surface intercepted. They are:

#### The Circular Bottom of the Payload

The bottom of the payload cylinder describes an ellipse in the crush plane. If (x,y) is inside this ellipse, the point is considered "backed" by the bottom of the payload. An exception to this general statement is noted in the discussion of the "Unbacked Region," see below.

#### The Cylindrical Surface of the Payload

The cylindrical surface of the payload describes a rectangular region tangent to the payload bottom ellipse at its major axes. If (x,y) is outside the bottom ellipse yet possesses an x coordinate less than the radius of the payload bottom, the point is considered "backed" by the payload cylinder.

#### Unbacked Regions

Unbacked regions are of two forms - those associated with the cylindrical end void and those near the external surface of the overpack. The unbacked region associated with the end void is a point in the crush plane which lies within the ellipse defined by the void circle lying in the plane of the payload bottom. The unbacked region associated with points near the overpack extrimities is defined by those points (x, y) where the x coordinate exceeds the radius of the payload volume. Points which are "unbacked" employ a nominal crush stress for force integration purposes.

The calculation of  $Z_{\text{bot}}$ , the distance to the undeformed overpack envelope, may follow two branches. These branches correspond to intercepts with either the cylindrical surface of the overpack or the circular end of the overpack.

The analytics describing the geometry discussed above, consists of the sequential application of a series of geometric transformations of surfaces described in the coordinates of the cylindrical package (X, Y, Z) to the coordinates of the contact plane (x, y, z). The surfaces in package coordinates are:

Overpack Cylinder

$$X^2 + Y^2 = R_c^2$$

Overpack Bottom Circle

$$X^2 + Y^2 = R_c^2$$

$$Z = -1_c/2$$

Payload Cylinder

$$X^2 + Y^2 = R_p^2$$

Payload Bottom Circle

$$X^2 + Y^2 = R_p^2$$

$$Z = -1_p/2$$

Void Circle at Payload

$$X^2 + Y^2 = R_f^2$$

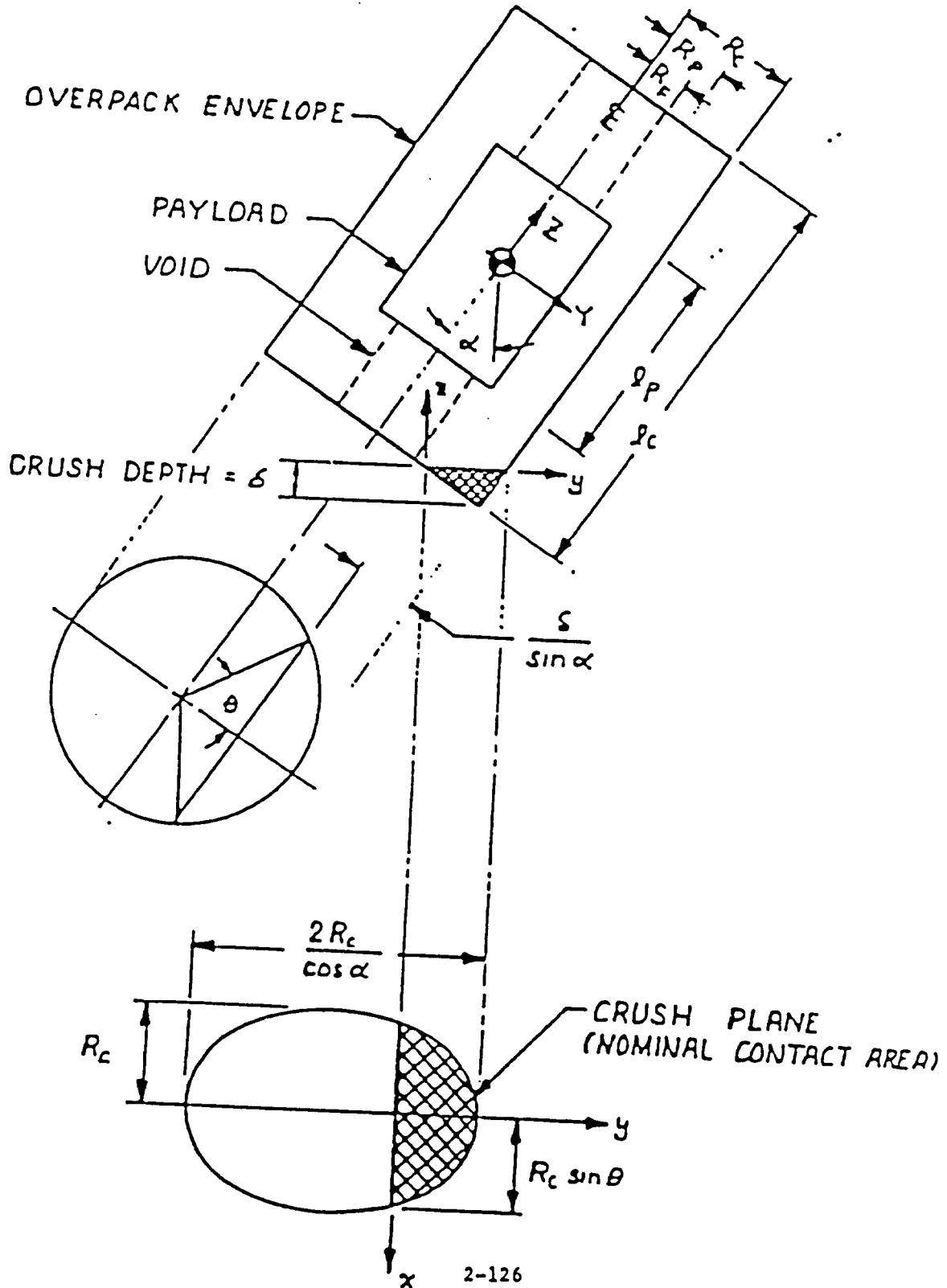
$$Z = -1_p/2$$

Void Circle at Overpack Exterior

$$X^2 + Y^2 = R_f^2$$

$$Z = -1_c/2$$

FIGURE 2.10.1-2  
CORNER CYLINDER IMPACT GEOMETRY



2.10.1.2 Oblique Impact Dynamic Analysis

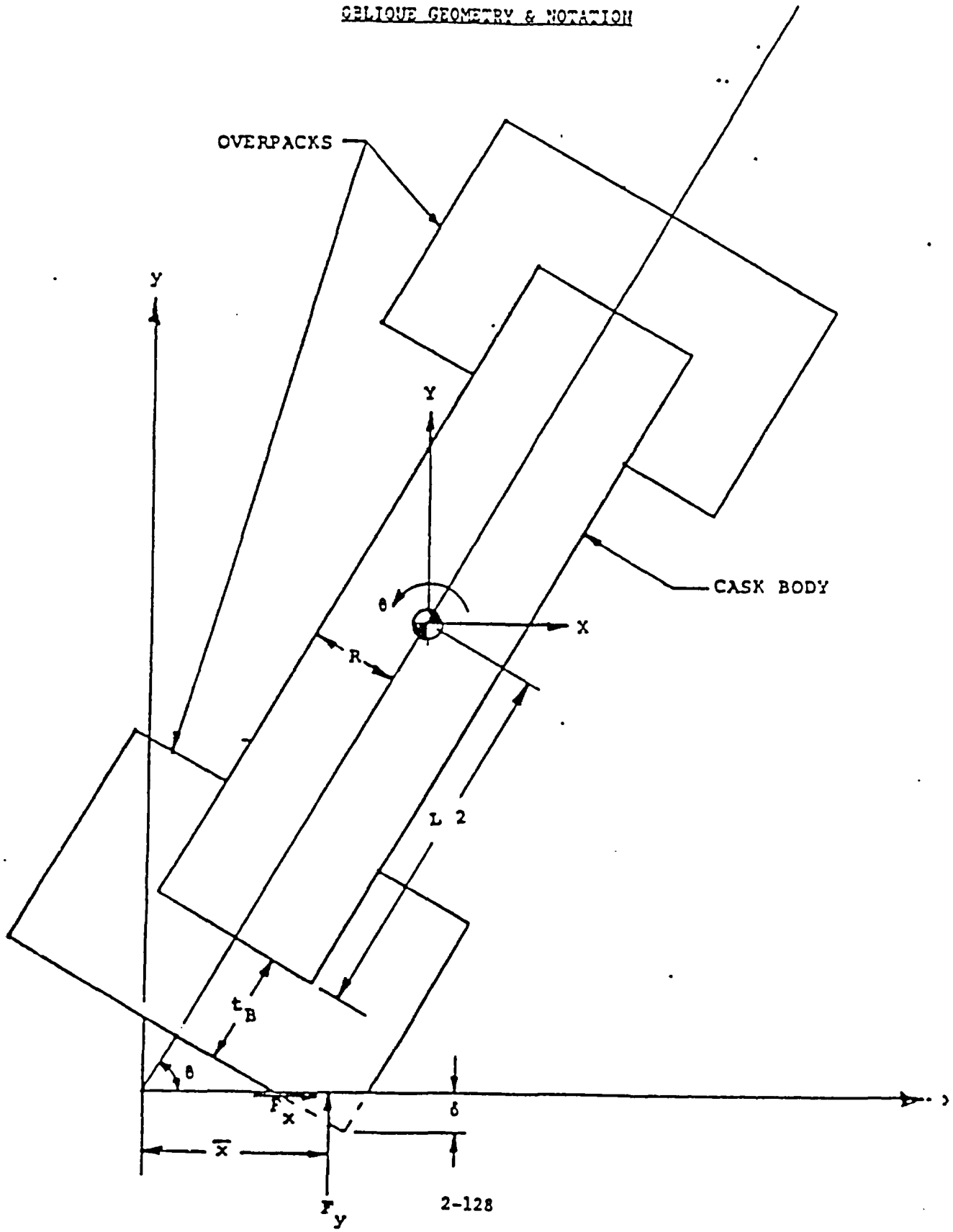
Impact at arbitrary orientation angles differ in two major respects from those that occur at angles corresponding to stable or neutral equilibrium (end, side, and c.g. over struck corner). In the neutral equilibrium conditions the entire initial kinetic energy of drop is transformed into strain energy associated with plastic deformation of the overpack. At arbitrary orientation angles, only a portion of this kinetic energy is transformed into strain energy at the impacted end. The remainder of this kinetic energy becomes rotational motion of the package. The solution approach must properly reflect the continually changing transformation of initial translational kinetic energy into rotational kinetic energy and plastic deformation of the overpack energy absorber.

The second major difference between neutral equilibrium impacts and arbitrary angle impacts relates to the rather different load-deflection behavior of the overpacks at low angle ( $10-30^{\circ}$  from horizontal) orientations. Under neutral equilibrium conditions a major portion of the crush footprint is backed by the cylindrical body of the package, allowing strain hardening effects to stiffen the overpack load-deflection relation. At low angle orientations ( $10-30^{\circ}$  from horizontal) much of the overpack crush footprint is unbacked. Thus, the low angle load-deflection relations are initially quite soft, then abruptly harden as portions of the crush footprints approach horizontal attitudes, this terminal stiffening phenomena becomes more pronounced.

There are two potential solution paths to problems of this nature - a momentum formulation or a direct solution of the equations of motion.

The momentum approach provides an easy and simple means to assess the transformation of translational initial velocities into rotary velocities; hence, total plastic strain energy absorbed by the overpack energy absorber. Unfortunately, this momentum formulation does not produce intermediate values of crush force and crush deformation needed to assess overpack attachment forces nor does it conveniently provide a means to incorporate the varying load-deflection relationships of the overpack as a function of orientation angle. Thus, a direct solution of the equations of motion was selected. The model is illustrated on the following page.

RELIGNE GEOMETRY & NOTATION



The three key problem variables (crush force,  $F$ , crush depth,  $\delta$ ; and orientation angle,  $\theta$ ) all vary with time for a given orientation angle,  $\theta_0$ . The crush force is assumed to act at the centroid of the elliptical crush footprint. For the model shown in the sketch, three independent second order differential equations of motion can be formed:

$$M\ddot{X} = F_x$$

$$M\ddot{Y} = F_y - Mg$$

$$I\ddot{\theta} = \begin{bmatrix} \left( \frac{\delta}{\sin\theta} \cdot \frac{(a-c)}{c} + t_B + L/2 \right) \sin\theta \\ \left[ \bar{x} \left( \frac{\delta}{\sin\theta} \cdot \frac{(a-c)}{c} + t_B + L/2 \right) \cos\theta \right] \end{bmatrix} \begin{matrix} F_x - \\ F_y \end{matrix}$$

Where:  $M$  = the package mass =  $pl$

$F$  = the crush force

$g$  = the gravitational constant, =  $386.4 \text{ in/sec}^2$

$I$  = the rotational mass moment of inertia =  $(pl^3/12)$

$R$  = the radius of the body

$L$  = the length of the body

$t_B$  = overpack bottom thickness

$\theta$  = the instantaneous orientation angle of the package with respect to the horizon

$p$  = the mass per unit length

$a$ ,  $c$ ,  $t_B$ ,  $\bar{x}$  are footprint geometry quantities defined in Section 2.10.2.3.



These differential equations are integrated subjected to initial conditions, associated with the moment of impact,  $t = 0$ , of:

$$X = 0, Y = 0, \theta = \theta_0$$

$$\dot{X} = 0, \dot{Y} = \dot{Y}_0, \dot{\theta} = 0$$

$$\theta_0 = \text{impact angle, varies}$$

$$\dot{Y}_0 = \sqrt{2gh}$$

$$h = \text{drop height}$$

Each of the above differential equations requires a continuously updated value of force,  $F$ , reflecting both crush depth and package orientation, or:

$$F = \psi(\delta_y; \theta)$$

This continuously updated value of force,  $F$ , is supplied to the integration process by means of a two dimensional Lagrangian interpolation of crush depth,  $\delta_y$ , and orientation angle,  $\theta$ . The tabular data used in this interpolation consists of a series of complete force-deflection relations for separate orientation angles developed via the CYDROP (and SYDROP) computer programs, described in Section 2.10.2.1. The deflection,  $\delta_y$ , is expressed in terms of problem variables as:

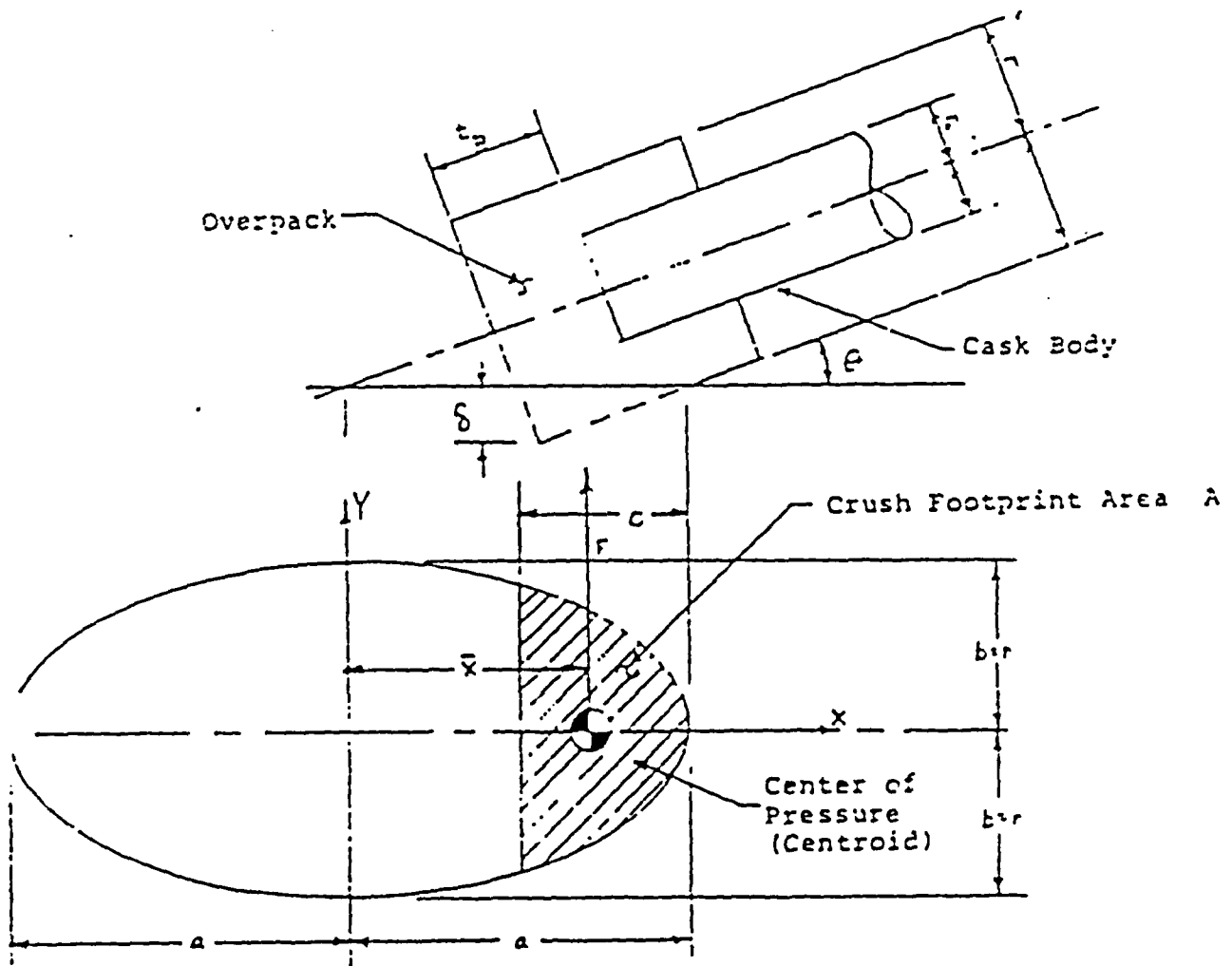
$$\delta_y = \frac{L}{2} (\sin\theta - \sin\theta_0) + R (\cos\theta - \cos\theta_0) - Y$$

The foregoing analysis process for evaluating impacts at oblique orientations was consolidated in a NuPac developed computer program, OBLIQUE. OBLIQUE integrates the equations of motion for each value of orientation angle versus time until maximum values are found for crush force, crush deformation, shear and body bending moment. At each incremental time step (incremental crush deformation) overpack attachment moments are computed, scanned for maximum values and output. By sweeping through a series of initial orientation angles, the maximum values of all internal loads are found.

#### 2.10.1.3 Overpack Force Analyses

This section treats both external and internal forces imposed upon the package. Key to the treatment of external force application locations is an understanding of crush footprint geometry.

The crush footprint is a sector of the ellipse shown the next page. The location of the centroid,  $\bar{x}$ , is calculated relative to the ellipse origin.



From the above sketch, the geometric properties of the elliptical crush footprint are:

$$a = r / \sin \theta$$

$$c = \delta / (\sin \theta \cos \theta)$$

The area,  $A$ , and the centroidal offset,  $\bar{x}$ , of the crush footprint are derived as:

When  $c < a$ :

$$\lambda = 2 \int_{(a-c)}^a y dx ; y = \frac{b}{a} \sqrt{a^2 - x^2}$$

$$\lambda = \frac{2b}{a} \int \sqrt{a^2 - x^2} dx$$

$$\lambda = \frac{b}{a} \left[ \frac{\pi a^2}{2} - (a-c)(2ac-c^2)^{1/2} - a^2 \sin^{-1} \left( \frac{a-c}{a} \right) \right]$$

$$\bar{\lambda x} = \frac{2b}{a} \int_{(a-c)}^a x \sqrt{a^2 - x^2} dx$$

$$\bar{x} = \frac{2b}{3a} (2ac-c^2)^{3/2} / \lambda$$

When  $a < c < 2a$ :

$$\lambda = \pi ab - \lambda^*$$

$$\bar{x} = \frac{\lambda^* \bar{x}^*}{\lambda}$$

$\lambda^*$  and  $\bar{x}^*$  are as defined for  $\lambda$  and  $\bar{x}$ , except that  $c^*$  replaces  $c$ .

$$c^* = 2a - c$$

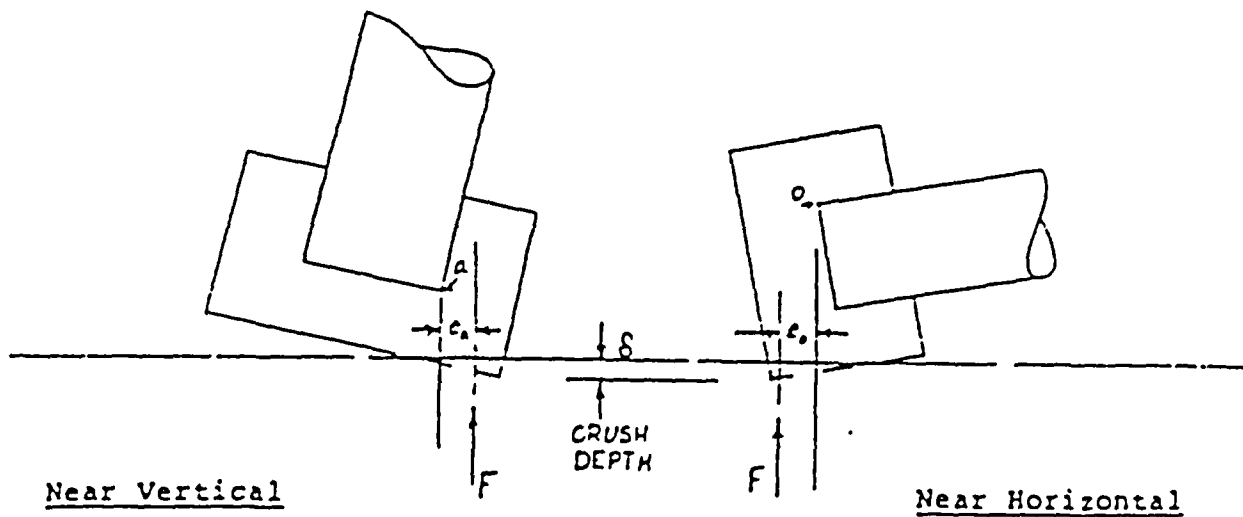
When  $c > 2a$ :

$$\lambda = \pi ab$$

$$\bar{x} = 0$$

### Overpack Attachment Forces

For most orientations and crush depths, the overpack crush force is transmitted to the cask body in direct compression; hence, the forces transmitted to the circumferential overpack attachments are near zero. This is not true for near vertical and near horizontal orientations of the package, at very modest crush deformations and crush forces. In these very limited situations, the center of pressure of the crush force can lie beyond the outer extremities of the cask body and exert a resultant moment force upon the overpack attachments. Significantly, these moments exist only for very modest crush deformations and crush forces, regardless of orientation angle. This is because larger crush deformations move the center of pressure toward the cask body. At maximum crush depth and maximum crush force, for all angles of orientation, there are no overpack attachment moments because the overpack interface forces are all direct compression. The near vertical and near horizontal orientations where attachment moments exist are sketched below:



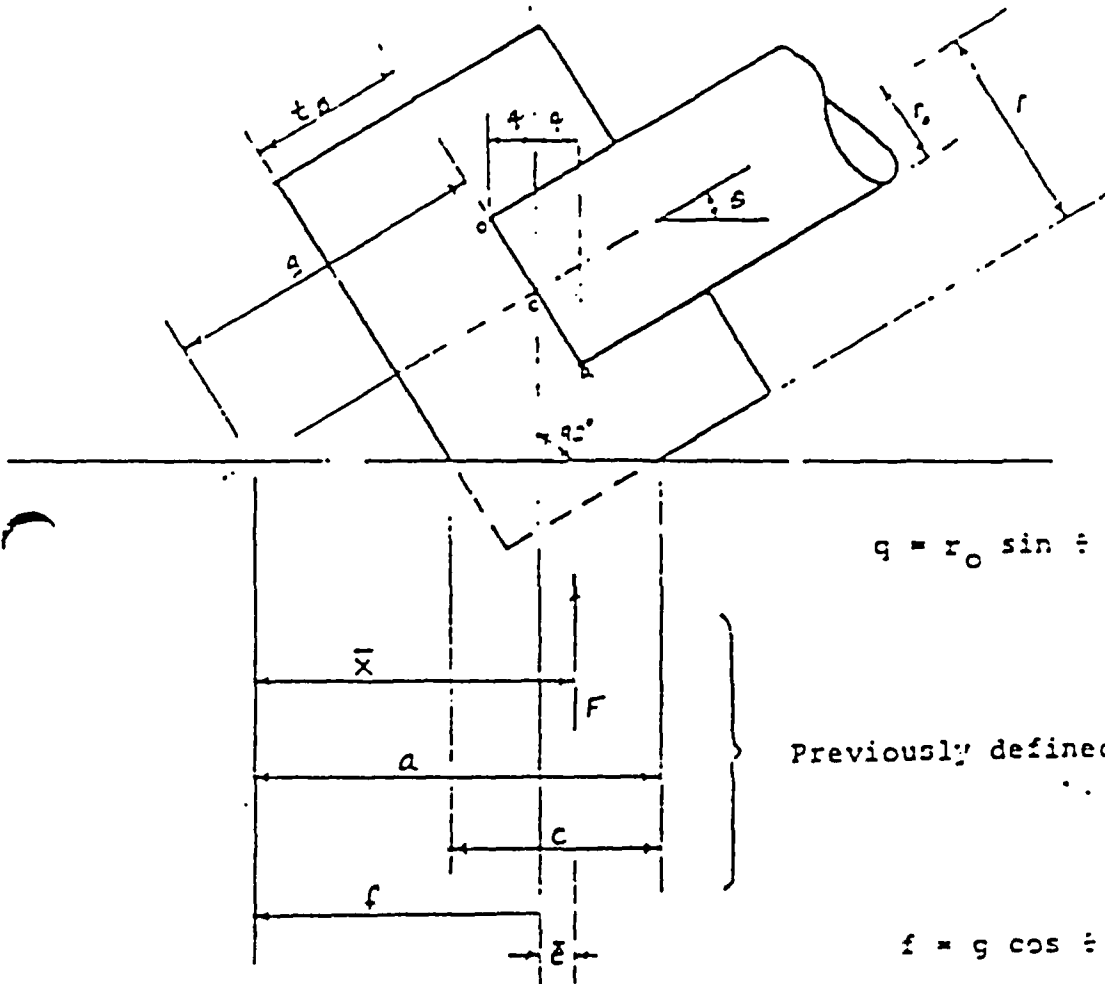
Attachment Moment =  $M = F \cdot e_a$  or  $F \cdot e_o$

Where:  $e_a$  = Moment Arm about adjacent corner

$e_o$  = Moment Arm about opposite corner

The location of the crush force can be approximated as the centroid of the crush footprint area. This approximation is consistently conservative. Specifically, for both near vertical and near horizontal orientations, foam strain hardening effects tend to move the center of force from the geometric center of the crush footprint toward the cask body. In both instances, this tendency reduces the actual moment arm of the crush force to less than that predicted by the location of the crush footprint centroid. The moment arm, as defined by crush footprint geometry is found below.

The location of the center of pressure relative to the opposite and adjacent corners of the cask body can be obtained from the geometry of the sketch shown on the following page.



$$g = r_0 \sin \phi$$

Previously defined

$$f = g \cos \phi$$

$$g = t_g = (a-c) \cos \phi$$

$$\bar{e} = \bar{x} - f$$

The location of the center of pressure measured from a normal to the crush plane passed through the intercept of package center line and body baseplate (point c) is:

$$\bar{e} = \bar{x} - [t_B + (a-c) \cos \theta] \cos \theta$$

The moment arms,  $e_o$  and  $e_a$ , representing the distance from the center of pressure to the corners of the cask body, are thus given as:

$$e_o = - (e+c) ; \text{ Moment Arm about opposite corner}$$

$$e_a = (e-q) ; \text{ Moment Arm about adjacent corner}$$

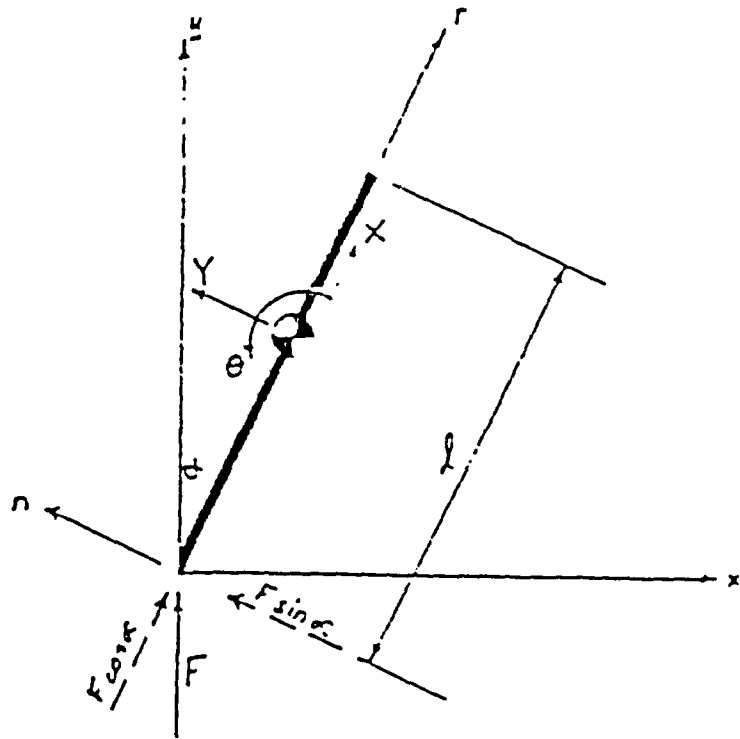
Sign convention for these arms is such that the moment ( $F \cdot e_o$ ) produces a clockwise (separation) moment about the opposite corner and moment ( $F \cdot e_a$ ) produces a counter-clockwise (separation) moment about the adjacent corner. In other words, a positive moment must be resisted by overpack attachment bolts whereas a negative moment implies that the center of pressure is totally resisted by compressive interface forces and there are no attachment bolt loads.

In summary, the attachment moment interface forces between the overpack and body have been derived in terms of package geometry and three problem variables: orientation angle, crush force and crush deformation.



Internal Forces

The cask is idealized as a beam impacting on the lower end. The equations of motion are formed and used to define state-wise accelerations. These accelerations, in conjunction with the unit mass of the package, form forces which vary along with the length of the package. When integrated, these forces provide a complete definition of internal thrusts, shears and moments for the package as a function of total impact force and orientation angle. The derivation is as follows:



For a planar rigid body system, the behavior is totally defined by a solution of the three equations of equilibrium written at the c.g. of the rigid body. In the above sketch, local coordinates are defined at the c.g. with axes parallel and normal to the beam. The end impact force is resolved into components parallel to these local axes. Summation of forces at the c.g. leads to three rigid body equations of motion:

$$\text{Sum of Normal Forces} - M\ddot{Y} = F \sin \alpha,$$

$$\text{Sum of Longitudinal Forces} - M\ddot{X} = F \cos \alpha,$$

$$\text{Sum of Moments} - I\ddot{\theta} = -Fl/2 \sin \alpha.$$

Where:

$M = pl$ , the mass of the body

$I = Ml^2/12 = pl^3/12$ ; the mass moment of inertia of the body

$p$  = the mass per unit length of the body

$\alpha$  = the vertical orientation angle

Substituting for the mass and inertia terms:

$$\ddot{Y} = F/pl \sin \alpha$$

$$\ddot{X} = F/pl \cos \alpha$$

$$\ddot{\theta} = -6F/pl^2 \sin \alpha$$

The normal and longitudinal acceleration at a point  $r$  are:

$$\begin{aligned}\ddot{S}_n &= \ddot{Y} + (r-i/2)\ddot{\theta} \\ &= \frac{F \sin \alpha}{\rho l^2} [i - 6(r-i/2)] \\ &= \frac{2F \sin \alpha}{\rho l^2} (-3r+2i), \text{ (varies with } r\text{)} \\ \ddot{S}_r &= \ddot{X} = \frac{F \cos \alpha}{\rho l} , \text{ (a constant)}\end{aligned}$$

The lateral inertial force acting on the body at the  $r$ th location is:

$$\frac{dV}{dr} = -\rho \ddot{S}_n$$

The corresponding expression for shear is found by integrating this lateral force from the free end to the  $r$ th location:

$$\begin{aligned}V_r &= \frac{2F \sin \alpha}{\rho l^2} \int_i^r (-3r+2i) dr = \frac{2F \sin \alpha}{\rho l^2} \left[ -\frac{3}{2}(r^2-i^2) + 2i(r-i) \right] \\ &= \frac{2F \sin \alpha}{\rho l^2} \left[ -\frac{3}{2}r^2 + \frac{3}{2}i^2 + 2ir - 2i^2 \right]\end{aligned}$$

$$V_r = \frac{F \sin \alpha}{\rho l^2} (3r^2 - 4ir + 2i^2)$$

Similarly, the corresponding moment is found by integration of the shear expression:

$$\frac{dM_r}{dr} = V_r$$

$$M_r = \frac{F \sin \alpha}{i^2} \int_i^r (3r^2 - 4ir + i^2) dr$$

$$M_r = \frac{F \sin \alpha}{i^2} [(r^3 - i^3) - 2i(r^2 - i^2) + i^2(r - i)]$$

$$= \frac{F \sin \alpha}{i^2} [r^3 - i^3 - 2ir^2 + 2i^3 + i^2r - i^3]$$

$$M_r = \frac{F \sin \alpha}{i^2} [r^3 - 2ir^2 + i^2r]$$

In order to verify these expressions for shear and moment, they are evaluated at the boundaries,  $r = 0, l$ .

$$r = l:$$

$$V_r = \frac{F \sin \alpha}{i^2} (3r^2 - 4ir + i^2)$$

$$= \frac{F \sin \alpha}{i^2} (3i^2 - 4i^2 + i^2) = 0:$$

$$\begin{aligned}
 M_r &= \frac{F \sin \alpha}{l^2} [r^3 - 2ir^2 + i^2 r] \\
 &= \frac{F \sin \alpha}{l^2} [i^3 - 2i^3 + i^3] = 0:
 \end{aligned}$$

$$r = 0:$$

$$\begin{aligned}
 V_r &= \frac{F \sin \alpha}{l^2} (3r^2 - 4ir + i^2) \\
 &= \frac{F \sin \alpha}{l^2} (i^2) = F \sin \alpha;
 \end{aligned}$$

$$M_r = \frac{F \sin \alpha}{l^2} [r^2 - 2ir^2 + i^2 r] = 0;$$

Maximum moment occurs when the shear term,  $V_r$ , equals zero. For this to occur

$3r^2 - 4ir + i^2 = 0$ , and the location of the moment mini/max is found as:

$$r = \frac{4i \pm \sqrt{16i^2 - 4(3)(i^2)}}{6} = \frac{4i - 2i}{6} = i, \frac{l}{3}$$

Substituting  $r = l/3$  into the moment expression:

$$\begin{aligned}
 M_r &= \frac{F \sin \alpha}{l^2} [r^3 - 2ir^2 + i^2 r] \\
 M_{\max} &= \frac{F \sin \alpha}{l^2} \left[ \frac{l^3}{27} - \frac{2il^3}{9} + \frac{l^3}{3} \right] \\
 &= F l \sin \alpha \frac{1 - 6 + 9}{27}
 \end{aligned}$$

$$M_{\max} = \frac{4}{27} F l \sin \alpha, \text{ at } r = l/3$$

The location of minimum shear can be found where the lateral force expression equals zero:

$$\frac{dV_r}{dr} = \frac{-2F \sin \alpha}{l^2} (-3r+2i)$$

$$r = \frac{2}{3} i.$$

The magnitude of axial forces can be found as a function of location as:

$$\frac{dT}{dr} = -\rho S_r \quad (\text{a constant})$$

$$T = -\rho S_r \int_r^i dr = -\rho S_r (r-i)$$

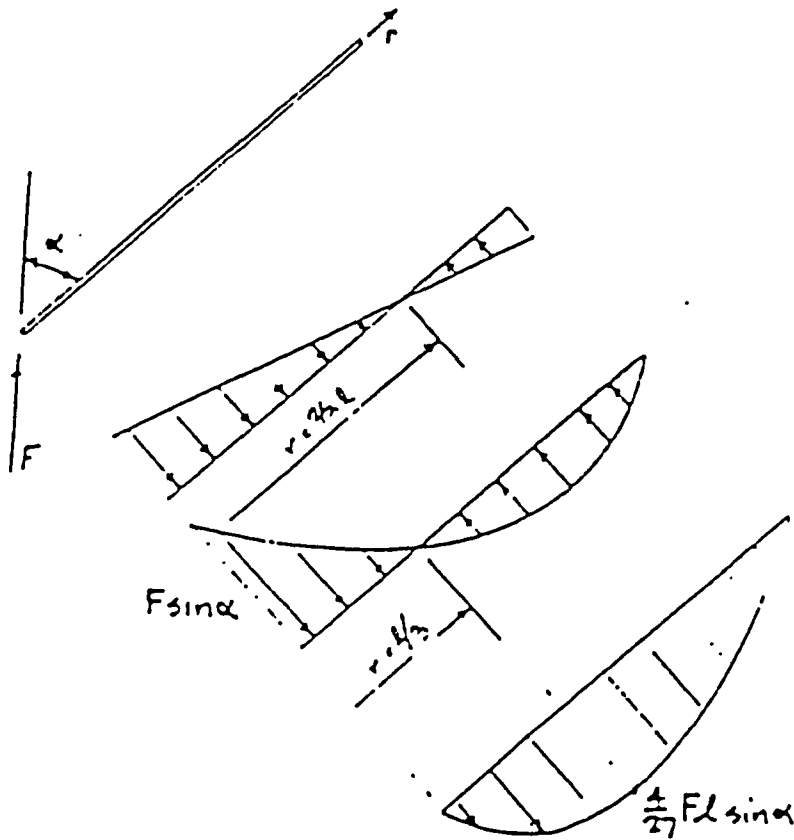
$$T = F \cos \alpha (1-r/i)$$

For convenience, the package internal forces are summarized as:

<u>Force</u>	<u>Expression</u>	<u>Maximum</u>	<u>Minimum</u>
• Thrust	$F \cos \alpha (1-r/i)$	$F \cos \alpha$ ( $r=0$ )	$0$ ( $r=i$ )
• Moment	$\frac{F \sin \alpha}{l^2} (r^3 - 2lr^2 + l^2 r)$	$\frac{4}{27} Fl \sin \alpha$ ( $r=l/3$ )	$0$ ( $r=0, l$ )
• Shear	$\frac{F \sin \alpha}{l^2} (3r^2 - 4lr + l^2)$	$F \sin \alpha$ ( $r=0$ )	$0$ ( $r=2/3l, l$ )

These forces are graphically illustrated on the next page.

PACKAGE INTERNAL FORCES UNDER END IMPACT



## Product Newsletter

### E<sup>3</sup>SAP

#### GENERAL INFORMATION

E<sup>3</sup>SAP (the Easy, Efficient, and Enhanced Structural Analysis Program) was originally developed as SAP IV at the University of California. E<sup>3</sup>SAP, pronounced E-three-SAP, is the BCS version of the program incorporating extensive modifications and enhancements which provide

- Greater convenience
- Improved utility
- Lower cost solutions

#### ANALYSIS CAPABILITIES

The purpose of E<sup>3</sup>SAP is to perform linear, static, and dynamic analysis of engineering structures and piping systems. E<sup>3</sup>SAP offers comprehensive structural capabilities while providing a problem solving method that is easy to learn and easy to use. The analysis capabilities and assumptions inherent in E<sup>3</sup>SAP may be broadly categorized as:

- Linear static analysis
- Natural frequency and mode shape determination
- Response spectrum analysis for earthquake shock studies
- Time history response to arbitrary force or acceleration functions
- Solution approaches based on proven state-of-the-art finite element methods
- Orthotropic and temperature dependent material properties for a number of situations

### MAINSTREAM-EKS

- Theoretical derivations assuming linear and reversible materials

#### TYPICAL APPLICATIONS

E<sup>3</sup>SAP, one of the most widely applicable structures programs available today, is used to evaluate a variety of structures, including

- Framed Structures
  - Buildings
  - Bridges
  - Off-shore oil rigs
  - Piping systems
  - Railcars
  - Transmission towers
- Plate and Shell Structures
  - Nuclear containment structures
  - Pressure vessels
  - Storage tanks
  - Ships and barges
- Solid Bodies
  - Dams
  - Tunnels
- Axisymmetric Structures
  - Rotating machinery
  - Pressure vessels
  - Storage tanks



## BCS ENHANCEMENTS

BCS enhancements provide important benefits. For example:

- Greater Convenience
  - Problems may be solved interactively for quick real-time answers or in batch for minimum cost
  - Simplified control card procedures are provided for both normal and restart runs
  - Concentrated loads may be specified in arbitrary order
  - Nodal data may be specified using the mesh generation feature
- Comprehensive Debug Aids
  - Exhaustive error checking is performed to lessen manual debugging
  - Automatically generated model details are "tagged" for easier identification
  - Stiffness matrix printout is provided to assist in debugging
  - Auxiliary element characteristics (length, area, volume, weight) are provided to aid in interpretation and debugging
- Improved Reliability
  - Known SAP IV errors have been removed
- Enhanced Output
  - Output formats have been reorganized for clarity
  - Simplified result file has been incorporated for ease of post-processing
  - Interactive and hardcopy plots of the model and output results are available for checking and interpretation. Users are free to select from a variety of devices, such as Tektronix

interactive graphics terminals and CalComp, Gerber, or Comp80 plotters.

- Lower Cost and Greater Efficiency
  - Automatic bandwidth resequencing features assure an efficient set of equations—solved at a low cost
  - During execution, core memory is dynamically allocated to minimize user cost and simplify the job control statements
  - Improved solution algorithms and file management for lower run cost

## FEATURES

### Input/Output

E<sup>3</sup>SAP data follows a fixed format and consists of a description of the model, its properties, and the loading conditions relative to the selected analysis. Model geometry may be expressed in either cartesian, cylindrical or spherical coordinates. Input to E<sup>3</sup>SAP is generally a deck of punched cards or a disk file containing card images. CMEDIT, the powerful editor offered on the interactive (KIT) system of EKS, provides the means for conversationally creating and modifying data files for use with E<sup>3</sup>SAP.

Output is tabular, and the input data, as well as the "tagged" generated and computed quantities, are listed. Results, such as displacements, stress, reaction, frequencies and mode shapes, and dynamic time histories are conveniently displayed for easy interpretation. The output may optionally be scanned and spot-checked at a low speed terminal prior to routing to an RJE terminal or to the BCS Data Center for printing. Additionally, graphic displays of displacements and mode shapes are available if desired.

### Multiple Job Processing

Multiple jobs can be processed within a single computer run by appropriate stacking of the input data. This time saving feature is particularly useful for the parametric evaluation of a structure.

### Execution Options

E<sup>3</sup>SAP may be executed interactively or in batch mode. Interactive execution of E<sup>3</sup>SAP directs solution results to the user's output file in real-time. When time is not a factor, however, economical solutions may be achieved by executing E<sup>3</sup>SAP in the batch mode.

Input requirements for both modes are identical, and only minor differences occur within the job control statements. As a result, users may alternate between the two modes with ease.

### Extensive Element Library

E<sup>3</sup>SAP maintains a comprehensive, state-of-the-art inventory of finite elements needed to perform most linear structural analysis, including:

- Three-dimensional truss
- Three-dimensional beam
- Two-dimensional membrane
- Two-dimensional axisymmetric solid
- Three-dimensional solid
- Thin-plate or thin-shell
- Three-dimensional variable-number-of-nodes solid
- Boundary (or foundation) springs
- Three-dimensional pile
- Three-dimensional pipe (tangent and bend)

### SPECIAL FEATURES

#### User-Defined Motion Features

E<sup>3</sup>SAP permits the linking of "slave" and "master" degrees of freedom. This allows the realistic and accurate treatment of rigid body portions of a structure such as rigid or very stiff beams, diaphragms, and slabs.

In addition, skewed boundary degrees of freedom may easily be specified using the boundary spring features.

### Diagnostic Aids

The E<sup>3</sup>SAP program may be run in a data check mode. In this mode, the complete data input stream is checked and error messages are printed to indicate probable causes of any detected errors.

As an additional diagnostic aid, E<sup>3</sup>SAP logs important solution job-step summary information in the user's EKS system dayfile. A quick examination of this dayfile via an interactive terminal not only indicates whether or not the run is successful, but also what and where the probable cause of the error might be.

### Comprehensive Result File

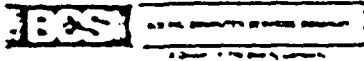
Frequently, there is a need to perform post-processing analyses using E<sup>3</sup>SAP output. To facilitate this need, E<sup>3</sup>SAP features an easy to read result file containing complete geometry information, as well as computed quantities such as displacements, stresses, and mode shapes.

### PROGRAM CAPACITIES

Because its memory requirements are completely dynamic, there are no fixed capacity limits for E<sup>3</sup>SAP. Utilizing the maximum computer capacity of MAINSTREAM-EKS, static analysis problems as large as 6000 nodes with a virtually unlimited number of elements or load cases can be solved with E<sup>3</sup>SAP. For dynamic analyses, the maximum problem size is governed by the product of the total number of nodes and the number of frequencies.

### MAINSTREAM-EKS OPERATING ENVIRONMENT

E<sup>3</sup>SAP and MAINSTREAM-EKS offer the flexibility for selecting the operational mode which best satisfies your solution needs. Both processing modes, interactive and batch, offer specific benefits. Interactive solutions provide real-time answers, whereas batch solutions provide results at a minimum of cost.



#### PROGRAM SUPPORT

BCS provides in-depth technical support for users of E<sup>3</sup>SAP. This support is provided by personnel with structural engineering degrees who are familiar with both the program code and real-life engineering problems.

#### DOCUMENTATION

The following documentation is available through your local BCS Representative

*E<sup>3</sup>SAP User's Manual* 10205-043

Contact your BCS Representative for further information regarding E<sup>3</sup>SAP.

\*MAINSTREAM IS A REGISTERED SERVICEMARK OF THE BOEING COMPANY  
COPYRIGHT © THE BOEING COMPANY 1978

## Product Newsletter

### STARDYNE<sup>®</sup>

#### GENERAL INFORMATION

The STARDYNE Analysis System consists of a series of compatible programs for the static and dynamic analysis of structures.

The static capability includes the computation of structural deformations and member loads and stresses caused by an arbitrary set of thermal, nodal applied loads and prescribed displacements.

Using the direct integration or the normal mode techniques, dynamic response analyses can be performed for a wide range of loading conditions, including transient, steady-state harmonic, random and shock spectra excitation types. Dynamic response results can be presented as structural deformations (displacements, velocities or accelerations) and/or internal member loads and stresses.

To aid the user in the interpretation of results, plots of stress contours, deformed and undeformed model geometry are available. Complete time histories of stresses, internal member loads, displacements, velocities and accelerations may also be plotted.

Automated node and element generation capabilities reduce the time and effort required for data input.

#### ANALYSIS CAPABILITIES

The STARDYNE system provides the following capabilities:

##### Static Analysis

The static analysis is based on the "Stiffness" ("Displacement") method and conforms to small displacement theory.

### MAINSTREAM:EKS

#### Substructure Analysis

An unlimited number of substructures may be individually modeled and subsequently tied together. Hence, there is no limit to the size of a complete structure for static analysis.

#### Lift-off

The static response of structures containing lift-off and bottom-out points, as well as tension only and compression only members, may be solved in a non-iterative exact solution, with the static analysis.

#### Extraction of Eigenvalues and Eigenvectors for the Structural System

Procedures include LANCZOS, Householder-QR, Inverse Iteration and H-QR Guyan.

#### Complete Seismic Analysis

Earthquake response may be analyzed as a transient response in the time domain or as a random response using Power Spectral Density inputs or utilizing the shock response capability. Many standard earthquakes are built into the program.

#### Piping System Analysis

A curved pipe and a straight pipe are available as finite elements and can be subjected to any of the static or dynamic analyses. The stiffness matrix can be formulated using the ASME flexibility factors at the user's option. Piping elements may be combined with any other elements in the STARDYNE library.

#### Dynamic Response Analysis (DYNRE) Programs

Program modules for the various dynamic analyses include:

#### DYNRE1—Transient Response Analysis, Modal Method, Time Domain Solution

The stresses, internal loads, and coordinate responses are calculated for any time-dependent forces applied to the structure. Base motion response can be computed in either relative or absolute coordinates. Sinusoidal forcing functions may be automatically generated.

#### DYNRE2—Steady State Harmonic Response Analysis, Frequency Domain Solution

The coordinate displacement, velocity and acceleration and stress responses are computed for a steady state sinusoidal forcing functions or sinusoidal base motion. Point-to-point transfer functions are calculated for unit sinusoidal excitations.

#### DYNRE3—Stationary Random Vibration Analysis

Calculates RMS nodal responses, element forces, stresses and Nodal Response Power Spectral Density (PSD) due to a user supplied PSD input forcing function.

#### DYNRE4—Shock Analysis

Stresses, internal loads and coordinate responses are calculated for either user-supplied shock spectra or standard earthquake spectra internally supplied by the program. The program will do an absolute upper bound or a root sum square or let the user select from a variety of other modal combination methods currently in use by the engineering community.

#### DYNRE5—Shock Spectra Calculation

Using a DYNRE acceleration time history or one supplied by the user, the program will calculate shock spectra which can be used as input to DYNRE4.

#### DYNRE6—Transient Response Analysis, Direct Integration, Time Domain Solution

In addition to the linear elastic structural components, the model may contain non-linear, one-dimensional elements to simulate such phenomena as gapping, bottoming out and soil.

#### TYPICAL APPLICATIONS

- Gearbox analysis and design
- Building frames subjected to seismic loads
- Industrial piping systems
- Nuclear pressure vessels
- Solar collectors
- Offshore drilling platforms
- Electronic component housings
- Heavy equipment design and manufacture

#### FEATURES

##### Input Data Generation

Input data generation features are available for node points and finite elements on curved or flat planes.

##### Graphic Output

Plots of the original model as well as the deformed structural shape and stress contours are available on many different plotting devices. Complete time histories of stress, internal member loads, displacements, velocities and accelerations may also be plotted.

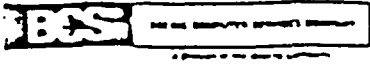
##### Load Case Combination

A post processor for complex load case combinations provides searches, output by load case or by element and stresses for "worst direction" of wind or wave loadings.

##### Extensive Finite Element Library

STAR DYNE provides a comprehensive, state-of-the-art inventory of finite elements needed to perform most structural analyses including:

- Beam and Pipe elements with shear stiffness in 3-D space
- Two Triangular Plate Elements (thick plate and thin plate)
  - Plate Bending
  - Sandwich (thick plate only)
  - In-plane (constant strain)
  - Shear Only (thick plate only)
- Quadrilateral Plate Element (isoparametric in-plane)



### Infinitely Rigid Members

Members, non-standard elements or substructures may be entered in numerical form by direct alterations to the stiffness matrix.

- Hexahedron (Brick) Solid Element (isoparametric)
- Wedge Solid Element (isoparametric)
- Tetrahedron Solid Element (constant strain)
- Nonlinear Springs

### Calculation of Hydrodynamic Forces

STARDYNE may be used to compute hydrodynamic forces on the tubular and circular beam members contained in the submerged portion of the model. The fluid forces can result from both wave motion and a steady current. The wave motion is defined by a Stoke's 5th order theory.

### Nonlinear Foundation Analysis

The program may be used to determine loads and deformations in a linear elastic structure supported on a nonlinear foundation and subjected to a static loading.

### Extensive Program Checks

Numerous error, consistency and validity checks are performed throughout the program.

### Automatic Bandwidth Reduction

Nodes are reordered internally so as to produce a minimum bandwidth. This does not effect either input or output of data and can produce a substantial savings in run time and cost.

### Geometry Phase Checks

The user may complete an entire analysis in a single run; however on larger problems, it is advisable to terminate the run after the geometry phase in order to check the run time estimates and to inspect node and element data. Additional validation performed during this phase includes checks for problem size, duplicate or badly shaped elements and data inconsistency.

### PROBLEM SIZE

There is no practical limit to the number of elements which may be used in a single model or substructure nor in the number of nodes used in most dynamic analyses. Limitations on program capacity are imposed only by available memory storage.

### MAINSTREAM-EKS OPERATING ENVIRONMENT

STARDYNE on MAINSTREAM-EKS offers the flexibility for selecting the operational mode which best satisfies a user's solution needs. Both processing modes, interactive and batch, offer specific benefits. Interactive solutions provide real-time answers, whereas batch solutions provide results at a minimum of cost.

### SUPPORT

#### User Documentation

Manual for the use of STARDYNE on MAINSTREAM-EKS is:

*MAINSTREAM-EKS STARDYNE User Information Manual* 10208-136

Contact your BCS local representative for this document and for other information on MAINSTREAM-EKS.

#### Technical Support

BCS provides in-depth technical support for users of STARDYNE both at National Support Headquarters and in a large number of BCS sales offices throughout the nation. The support staff consists of engineers who have a thorough understanding of STARDYNE and its application to a variety of practical engineering problems. Staff members can help you select an appropriate solution process from several options and assist in debugging and in the interpretation of results.

© COPYRIGHT The Boeing Company 1980

E<sup>®</sup> a proprietary program developed by System Development Corporation.

MAINSTREAM-EKS IS A REGISTERED SERVICEMARK OF THE BOEING COMPANY

### 2.10.2 Finite Element Stress Summary

This section provides results of cask and lid stress analyses using models depicted in Figures 2.6.1-1 and -2. Results were developed using the EJSAP program described in Section 2.10.1.4. A common organization of results is used for both cask and lid analyses. Each analysis consists of two runs for a total of seven loading cases. The two runs were used to reflect both accident and normal temperature distributions, respectively. The seven cases are described as follows:

o Case 1 - Accident (Fire) Thermal Stresses

Decay Heat = 800 watts

Stress-free temperature = 70°F

Other controlling temperatures:

Component	Temperature
-----	<u>(Table 3.5.3-1)</u>
Cavity	371.43°F
Outer Shell	343.56°F
Bottom Outer Shell	363.35°F

o Case 2 - Accident (Fire) Pressure Stresses

Internal Pressure = 184.40 psig

(Section 3.5.4)

o Case 3 - Accident (30 foot drop) Impact Stresses

(Section 2.7.1)

$$n_g = \frac{2,704,956}{27,000} = 100.184g's$$

o Case 4 - Accident (Fire) Combined Temperature & Pressure Stresses

Case 1 + Case 2

o Case 5 - Normal Thermal Stresses

Stress Free Temperature =  $70^{\circ}\text{F}$

Decay Heat = 800 watts

Ambient Air Temperature =  $130^{\circ}\text{F}$

Body Temperature =  $214.4^{\circ}\text{F}$

(Table 3.4.2-1)

o Case 6 - Accident (Impact) Combined Stresses

Body Temperature =  $214^{\circ}\text{F}$

Internal Pressure = 19 psig

Axial Load = 100.184g

Case 6 = Case 5 +  $(19/184.4) \cdot$  Case 2 + Case 3

o Case 7 - Normal Combined Temperatures and Pressures

Body Temperature =  $214.4^{\circ}\text{F}$

Internal Pressure = 19 psig



2.10.2.1 Cask Stresses

Cask stresses are provided in Microfiche form in Section 2.12. These data include complete results of finite element stress analyses of cask and lid for all cases described in Section 2.10.1. The information is contained on the microfiche entitled "2.10.3 Finite Element Stress Analysis 1-13C II Cask, and on the Microfiche entitled "Appendix 2.10.4 Lift Lug Analysis, August 1981.

30 BASE NODE LOAD  
 QUAD-PLATE CORNER FORCES FOR CASE 1  
 NODE FORCES

		FX1	FX2	FX3	MX1	MOMENTS MX2	MX3
1 MM							
GLOBAL	J1	.150443E+03	-.149510E+04	.222962E+04	-.427402E+02	.653273E+02	.199878E+04
	J2	-.419456E+03	.314412E+04	.752348E+03	.675841E+02	-.496151E+03	-.166277E+04
	J3	.269014E+03	.143215E+04	-.298197E+04	.582780E+02	-.278100E+03	-.200471E+04
	J4	.288128E-08	-.308117E+04	.150030E-07	-.521726E+02	.261934E-09	.274394E+04
2 MM							
GLOBAL	J1	.456252E+03	-.778929E+03	.207237E+03	.112274E+03	-.271053E+03	.139334E+04
	J2	-.101720E+04	.211801E+04	-.180285E+04	-.933765E+02	.225431E+03	-.346288E+03
	J3	.781094E+03	.102661E+02	-.436347E+03	.176078E-08	-.232831E-08	-.302041E+03
	J4	-.220146E+03	-.134935E+04	.203196E+04	-.190613E+01	.460182E+01	.221275E+04
3 MM							
GLOBAL	J1	-.579590E+02	.551513E+03	-.601418E+02	.980495E+01	-.127781E+02	.801897E+02
	J2	-.624792E+02	-.336476E+03	-.521904E+03	-.174459E+03	.227359E+03	.465548E+03
	J3	.901532E+03	-.204771E+03	.145697E+03	.168802E-08	-.337604E-08	.819648E+03
	J4	-.781094E+03	-.102661E+02	.436347E+03	-.276486E-08	.465661E-08	.302041E+03
4 MM							
GLOBAL	J1	-.827742E+02	.423813E+03	-.569197E+03	-.105573E+03	.810088E+02	-.697301E+03
	J2	.489886E+03	-.654660E+03	.331586E+03	-.287044E+03	.220257E+03	.834899E+03
	J3	.494421E+03	.260743E+02	.383310E+03	-.756700E-08	.298314E-08	-.118062E+04
	J4	-.901532E+03	.204771E+03	-.145699E+03	-.260479E-08	.379805E-08	-.819648E+03
5 MM							
GLOBAL	J1	-.321902E+03	.346851E+03	-.133345E+03	-.211008E+03	.874023E+02	-.103042E+04
	J2	.662560E+03	-.399780E+03	.376144E+03	-.364750E+03	.151084E+03	.102896E+04
	J3	.153763E+03	.790057E+02	.140512E+03	.183718E-08	-.851237E-09	.126163E+04
	J4	-.494421E+03	-.260763E+02	-.383310E+03	.749424E-08	-.421460E-08	-.118062E+04
6 MM							
GLOBAL	J1	-.593238E+03	.175543E+03	.189084E+02	-.311266E+03	.409789E+02	-.113945E+04
	J2	.683183E+03	-.965375E+02	.121603E+03	-.371855E+03	.489557E+02	.112870E+04
	J3	.638382E+02	-.282307E-08	-.325963E-08	.677232E-09	-.541434E-11	.178128E+04
	J4	-.153763E+03	-.790057E+02	-.140512E+03	.141426E-09	.386081E-09	-.126163E+04
7 MM							
GLOBAL	J1	-.445869E+04	.133826E+05	.260265E+04	.464929E+03	-.225568E+04	.295498E+04
	J2	.428032E+04	-.127822E+05	-.348434E+02	-.377636E+03	.183216E+04	.592959E+03
	J3	.135683E+04	-.511521E+04	-.211225E+04	.984254E+02	-.477527E+03	-.114482E+04
	J4	-.117895E+04	.451486E+04	-.455554E+03	-.103839E+03	.503794E+03	.183956E+04
8 MM							
GLOBAL	J1	-.344635E+04	.697641E+04	.162393E+04	.507776E+03	-.122588E+04	.200479E+04
	J2	.223919E+04	-.416113E+04	-.401025E+04	-.377905E+03	.912342E+03	.127225E+04
	J3	.163560E+04	-.273689E+04	-.713835E+03	.933765E+02	-.225431E+03	-.968240E+01
	J4	-.428447E+03	-.783895E+02	.310016E+04	-.112274E+03	.271053E+03	.139546E+04
9 MM							
GLOBAL	J1	-.141380E+04	.144392E+04	-.195303E+04	.531648E+03	-.692857E+03	.121223E+04
	J2	.110220E+04	-.117323E+04	-.175293E+04	-.312475E+03	.407225E+03	.115102E+04
	J3	.872043E+03	-.338060E+03	.112913E+04	.174459E+03	-.227359E+03	.566417E+03
	J4	-.560444E+03	.673642E+02	.257683E+04	-.980495E+01	.127781E+02	.275780E+03
10 MM							
GLOBAL	J1	-.335624E+03	-.130361E+03	-.779337E+03	.778610E+03	-.597449E+03	.963141E+03
	J2	.671675E+03	-.302236E+03	.428913E+03	-.329875E+03	.253122E+03	.121067E+04
	J3	.390739E+03	.181874E+03	.388458E+03	.287044E+03	-.220257E+03	.835138E+03
	J4	-.726790E+03	.250724E+03	-.380342E+02	.105573E+03	-.810088E+02	-.334664E+03
11 MM							
GLOBAL	J1	.232050E+03	-.394000E+03	.975805E+02	.762551E+03	-.315859E+03	.486924E+03
	J2	-.766720E+00	.123674E+03	.587456E+03	-.198716E+03	.823109E+02	.102925E+04
	J3	.327439E+03	.144390E+03	-.983377E+02	.364750E+03	-.151064E+03	.103189E+04

2-155

APPENDIX 2.10.3 LIFT LUG ANALYSIS

	12	- .358722E+03	.125936E+03	-.586699	211008E+03	-.874023E+02	-.699616E+03
NNQU.	LATE HO	12					
GLOBAL	1	20	.535102E+03	-.230478E+03	.18818	.488213E+03	-.642745E+02
	2	21	-.487346E+03	.540935E+02	.230137	.107740E+03	-.141843E+02
	J3	14	.348986E+03	.965375E+02	-.121603E+03	.371855E+03	-.489557E+02
	J4	13	-.396741E+03	.798468E+02	-.296715E+03	.311266E+03	-.409789E+02
NNQUAD-PLATE HO		14					
GLOBAL	J1	23	-.199511E+04	.638152E+04	.718795E+04	-.716967E+02	.173091E+03
	J2	24	-.255380E+04	.462336E+04	-.110214E+05	.697454E+02	-.168380E+03
	J3	17	.519986E+04	-.106193E+05	-.818503E+04	.833384E+02	-.201197E+03
	J4	16	-.650948E+03	-.385593E+03	.120185E+05	-.108126E+03	.261039E+03
NNQUAD-PLATE HO		15					
GLOBAL	J1	24	-.404610E+04	.593172E+04	.108522E+05	.468095E+01	-.610033E+01
	J2	25	-.445361E+04	.505106E+04	-.110309E+05	.129A02E+03	-.169161E+03
	J3	18	.601565E+04	-.679319E+04	-.115183E+05	.137355E+03	-.179005E+03
	J4	17	.248406E+04	-.418959E+04	.115470E+05	.759469E+01	-.989759E+01
NNQUAD-PLATE HO		16					
GLOBAL	J1	25	-.333555E+04	.295257E+04	.106223E+05	.886462E+02	-.680207E+02
	J2	26	-.682521E+04	.475855E+04	-.974826E+04	.143650E+03	-.110227E+03
	J3	19	.492402E+04	-.309171E+04	-.108248E+05	.153258E+03	-.117599E+03
	J4	18	.523675E+04	-.461941E+04	.995082E+04	.450213E+02	-.345462E+02
NNQUAD-PLATE HO		17					
GLOBAL	J1	26	-.440279E+03	.408392E+03	.745677E+04	.972918E+02	-.482996E+02
	J2	27	-.776374E+04	.292269E+04	-.648326E+04	.1	-.564005E+02
	J3	20	.204125E+04	-.431335E+03	-.737783E+04	.1	-.720972E+02
	J4	19	.616277E+04	-.289974E+04	.682433E+04	.509363E+02	-.210985E+02
NNQUAD-PLATE HO		18					
GLOBAL	J1	27	.338997E+04	-.391181E+03	.243882E+04	.105652E+03	-.139093E+02
	J2	28	-.652446E+04	.739910E+03	-.271696E+04	.122301E+03	-.161012E+02
	J3	21	-.170875E+04	.383203E+03	-.236883E+04	.164734E+03	-.216877E+02
	J4	20	.484324E+04	-.731932E+03	.264696E+04	.118071E+03	-.144911E+02
NNQUAD-PLATE HO		19					
GLOBAL	J1	91	.896482E+03	-.256518E+04	.155099E+03	-.194780E+03	.945009E+03
	J2	30	-.127091E+04	.468379E+04	-.740482E+04	.154278E+03	-.748505E+03
	J3	23	-.309236E+04	.800370E+04	-.101205E+04	-.466149E+03	.226160E+04
	J4	65	.346679E+04	-.101223E+05	.826177E+04	.399582E+03	-.193864E+04
NNQUAD-PLATE HO		20					
GLOBAL	J1	30	-.125348E+02	.100440E+04	.583400E+03	-.149549E+03	.361043E+03
	J2	31	-.147458E+04	.260285E+04	-.483444E+04	.147523E+03	-.356151E+03
	J3	24	-.757034E+03	.807685E+03	-.200937E+04	-.432473E+03	.104408E+04
	J4	23	.224414E+04	-.441493E+04	.634041E+04	.412785E+03	-.996550E+03
NNQUAD-PLATE HO		21					
GLOBAL	J1	31	-.179786E+03	.893403E+03	.273878E+04	-.322309E+02	.420041E+02
	J2	32	-.118250E+04	.856413E+03	-.703937E+03	.155147E+03	-.202191E+03
	J3	25	.323304E+03	-.205951E+03	-.318568E+04	-.139308E+03	.181550E+03
	J4	24	.103898E+04	-.154387E+04	.115064E+04	.987471E+02	-.128690E+03
NNQUAD-PLATE HO		22					
GLOBAL	J1	32	.250967E+03	.199746E+03	.230824E+04	.948944E+02	-.728150E+02
	J2	33	-.120298E+04	.395274E+03	.116264E+03	.228002E+03	-.174952E+03
	J3	26	-.952208E+03	.957463E+03	-.207641E+04	.110424E+03	-.847314E+02
	J4	25	.190422E+04	-.155248E+04	-.348093E+03	.308579E+03	-.236781E+03
NNQUAD-PLATE HO		23					
GLOBAL	J1	33	.983929E+03	-.222630E+03	.839695E+03	.205002E+03	-.849145E+02
	J2	34	-.157400E+04	.276176E+03	-.475186E+03	.314273E+03	-.130176E+03
	J3	27	-.297422E+04	.141861E+04	-.516967E+03	.372961E+03	-.154485E+03
	J4	26	.356427E+04	-.147216E+04	.152461E+03	.525133E+03	-.217517E+03
NNQUAD-PLATE HO		24					
GLOBAL	J1	34	.158023E+04	-.221165E+03	-.410683E+03	.303437E+03	-.399482E+02
	J2	35	-.178420E+04	.320680E+02	-.864646E+03	.348770E+03	-.459164E+02
	J3	28	-.444759E+04	.724146E+03	.553237E+03	.569777E+03	-.750126E+02

2-156

	J4	27	.485156E+04	-.535049E+03	.727	.624769E+03	-.822525E+02	-.258268E
M	1-PLATE NO	25	MM					
GLL	J1	36	.367835E+02	.518089E+03	-.486756E+04	-.895286E+02	.514685E+03	-.233648E+04
	J2	37	-.773977E+02	-.714337E+03	-.308993E+04	.165509E+02	.985136E+01	.191563E+04
	J3	91	.120517E+03	-.138432E+04	.618225E+04	.627990E+02	-.371654E+03	.143866E+04
	J4	29	-.599024E+02	.158057E+04	.177548E+04	.146165E+02	-.259196E+03	-.209374E+04
MMQUAD-PLATE NO		26	MM					
GLOBAL	J1	37	-.324120E+03	.218056E+04	-.431957E+03	-.290923E+03	.782351E+03	-.186994E+04
	J2	38	-.977231E+03	.113959E+04	-.546543E+04	.615925E+02	-.148697E+03	.611255E+03
	J3	31	.915012E+03	-.203457E+04	-.788437E+03	-.147523E+03	.356151E+03	.299491E+03
	J4	30	.386339E+03	-.128557E+04	.668582E+04	.149549E+03	-.361043E+03	-.102469E+04
MMQUAD-PLATE NO		27	MM					
GLOBAL	J1	38	-.230014E+03	.125402E+04	.153034E+04	-.262171E+03	.341668E+03	-.597176E+03
	J2	39	-.127602E+04	.762644E+03	-.233360E+04	.211104E+03	-.275116E+03	-.394494E+03
	J3	32	.766682E+03	-.554981E+03	-.208084E+04	-.155147E+03	.202191E+03	-.221281E+03
	J4	31	.739350E+03	-.146168E+04	.288410E+04	.322309E+02	-.420041E+02	-.942738E+02
MMQUAD-PLATE NO		28	MM					
GLOBAL	J1	39	-.584088E+02	.646614E+03	.126035E+04	-.868665E+02	.666550E+02	.396586E+03
	J2	40	-.715697E+03	-.288219E+02	-.549712E+03	.279438E+03	-.214420E+03	-.103017E+04
	J3	33	.609258E+03	-.116614E+03	-.116718E+04	-.228002E+03	.174952E+03	-.681603E+03
	J4	32	.164848E+03	-.501178E+03	.476540E+03	-.948944E+02	.728150E+02	.421506E+03
MMQUAD-PLATE NO		29	MM					
GLOBAL	J1	40	-.769998E+02	.374712E+03	.204044E+03	.721197E+02	-.298730E+02	.103249E+04
	J2	41	-.144607E+03	-.261269E+03	-.537367E+03	.286377E+03	-.118621E+03	-.141311E+04
	J3	34	.611815E+03	-.574142E+02	.102101E+03	-.314273E+03	.130176E+03	-.971273E+03
	J4	33	-.390208E+03	-.560294E+02	.231222E+03	-.205002E+03	.849145E+02	.778355E+03
MMQUAD-PLATE NO		30	MM					
GLOBAL	J1	41	-.137525E+03	.139279E+03	-.720226E+03	.181695E+03	-.239206E+02	.141492E+04
	J2	42	.104892E+03	-.109615E+03	-.928188E+03	.253564E+03	-.333824E+02	-.154838E+04
	J3	35	.650685E+03	-.320680E+02	.864646E+03	-.348770E+03	.459164E+02	-.109773E+04
	J4	34	-.618052E+03	.240306E+01	.783768E+03	-.303437E+03	.399482E+02	.102364E+04
MMQUAD-PLATE NO		31	MM					
GLOBAL	J1	43	.846034E+02	.110020E+04	-.231892E+04	-.916416E+02	.696087E+03	-.322706E+04
	J2	44	-.255527E+03	.342990E+03	-.418138E+04	-.375743E+02	.285405E+03	.260323E+04
	J3	37	.187708E+03	-.146298E+04	.163250E+04	.399793E+02	-.303673E+03	.220919E+04
	J4	36	-.167835E+02	.197916E+02	.486780E+04	.677596E+02	-.514685E+03	-.264396E+04
MMQUAD-PLATE NO		32	MM					
GLOBAL	J1	44	.605762E+02	.114595E+04	-.564717E+03	-.294364E+03	.718658E+03	-.260980E+04
	J2	45	-.755698E+03	.531668E+03	-.363923E+04	.577230E+02	-.139356E+03	.121170E+04
	J3	38	.440723E+03	-.125362E+04	.454037E+03	-.615925E+02	.148697E+03	.836464E+03
	J4	37	.254399E+03	-.423998E+03	.374991E+04	.298946E+03	-.721720E+03	-.225205E+04
MMQUAD-PLATE NO		33	MM					
GLOBAL	J1	45	-.322045E+02	.111530E+04	.312055E+03	-.371951E+03	.484736E+03	-.121884E+04
	J2	46	-.127834E+04	.604865E+03	-.304296E+04	.281434E+03	-.386772E+03	-.350416E+03
	J3	39	.544018E+03	-.580175E+03	-.750146E+03	-.211104E+03	.275116E+03	-.395214E+03
	J4	38	.766521E+03	-.113999E+04	.348105E+04	.262171E+03	-.341668E+03	-.850543E+03
MMQUAD-PLATE NO		34	MM					
GLOBAL	J1	46	.127224E+02	.735991E+03	.559317E+03	-.201153E+03	.154350E+03	.341181E+03
	J2	47	-.109747E+04	.817915E+02	-.172769E+04	.473507E+03	-.363335E+03	-.156034E+04
	J3	40	.294335E+03	.112999E+02	-.455024E+03	-.279438E+03	-.214420E+03	-.123266E+04
	J4	39	.790408E+03	-.829082E+03	.182340E+04	.868665E+02	-.666550E+02	.393121E+03
MMQUAD-PLATE NO		35	MM					
GLOBAL	J1	47	.720192E+02	.388676E+03	-.123500E+03	.876848E+02	-.363202E+02	.155204E+04
	J2	48	-.547130E+03	-.228871E+03	-.113746E+04	.545507E+03	-.225956E+03	-.223285E+04
	J3	41	-.232513E+02	.197385E+03	.260272E+03	-.286377E+03	.118621E+03	-.172646E+04
	J4	40	.498362E+03	-.357190E+03	.100069E+04	-.721197E+02	.298730E+02	.123034E+04
MMQUAD-PLATE NO		36	MM					
GLOBAL	J1	48	.701119E+02	.109671E+03	-.835059E+03	.340628E+03	-.448445E+02	.227843E+04
	J2	49	-.167923E+03	-.143890E+03	-.109045E+04	.497389E+03	-.654825E+02	-.252054E+04
	J3	42	-.207573E+03	.109615E+03	.928188E+03	-.253564E+03	.333824E+02	-.189419E+04

		41	.305384E+03	-.753953E+02	.997321E	-.181695E+03	.239206E+02	.172465E+04
NNQUAD	TE HO	37	MM					
GLOBAL		50	.153930E+02	.172684E+04	-.155994E	-.132928E+03	.100969E+04	-.412533E+04
	J2	51	.692765E+01	-.128746E+04	-.236452E+04	-.865436E+02	.657364E+03	.347176E+04
	J3	44	.622828E+02	-.128389E+04	.168554E+04	.375743E+02	-.285405E+03	.290578E+04
	J4	43	-.846034E+02	.844515E+03	.231892E+04	.916416E+02	-.696087E+03	-.357658E+04
NNQUAD-PLATE HO		38	MM					
GLOBAL	J1	51	-.768902E+02	.171574E+04	-.709954E+03	-.409910E+03	.989610E+03	-.347615E+04
	J2	52	-.391627E+03	-.409910E+03	-.293393E+04	-.493529E+02	.119148E+03	.180567E+04
	J3	45	.335849E+03	-.110079E+04	.503323E+03	-.577230E+02	.139356E+03	.144661E+04
	J4	44	.132668E+03	-.205043E+03	.314056E+04	.294364E+03	-.710658E+03	-.289921E+04
NNQUAD-PLATE HO		39	MM					
GLOBAL	J1	52	.110292E+02	.120117E+04	-.191158E+03	-.469599E+03	.611994E+03	-.181533E+04
	J2	53	-.903651E+03	.578503E+01	-.272216E+04	-.238278E+03	-.310531E+03	-.241477E+03
	J3	46	.440567E+03	-.660780E+03	.894674E+02	-.281434E+03	.366772E+03	-.303684E+03
	J4	45	.452054E+03	-.546179E+03	.282385E+04	.371951E+03	-.484736E+03	-.143948E+04
NNQUAD-PLATE HO		40	MM					
GLOBAL	J1	53	.335764E+03	.618554E+03	-.211782E+03	-.221047E+03	.169615E+03	.228532E+03
	J2	54	-.133302E+04	.125634E+03	-.229074E+04	.608598E+03	-.466994E+03	-.205954E+04
	J3	47	.172216E+03	-.641126E+02	.108347E+03	-.473507E+03	.363335E+03	-.174433E+04
	J4	46	.825045E+03	-.680076E+03	.239418E+04	.201153E+03	-.154350E+03	.312919E+03
NNQUAD-PLATE HO		41	MM					
GLOBAL	J1	54	.751564E+03	.194439E+03	-.576473E+03	.232225E+03	-.961908E+02	.204719E+04
	J2	55	-.138794E+04	.684503E+01	-.175462E+04	.863688E+03	-.357751E+03	-.324149E+04
	J3	48	-.216854E+03	.205071E+03	.588255E+03	-.545507E+03	.225956E+03	-.263381E+04
	J4	47	.853230E+03	-.406355E+03	.174284E+04	-.876848E+02	.363202E+02	.175313E+04
NNQUAD-PLATE HO		42	MM					
GLOBAL	J1	55	.105263E+04	-.175808E+01	-.106458E+04	.660001E+03	-.868908E+02	.323405E+04
	J2	56	-.124410E+04	-.562604E+02	-.141014E+04	.889747E+03	-.117137E+03	-.364079E+04
	J3	49	-.502400E+03	.143890E+03	.109045E+04	-.497389E+03	.654825E+02	-.293127E+04
	J4	48	.693872E+03	-.858719E+02	.138427E+04	-.340628E+03	.448445E+02	.263823E+04
NNQUAD-PLATE HO		43	MM					
GLOBAL	J1	57	.139698E-08	.785843E+03	-.148250E+04	.100772E-08	-.424916E-08	-.447888E+04
	J2	58	-.197378E+03	-.687300E+03	-.153922E+04	-.152795E-08	.942964E-08	.383418E+04
	J3	51	.212771E+03	-.142548E+04	.146178E+04	.865436E+02	-.657364E+03	.371552E+04
	J4	50	-.153930E+02	.148694E+04	.155994E+04	.132928E+03	-.100969E+04	-.436296E+04
NNQUAD-PLATE HO		44	MM					
GLOBAL	J1	58	.197378E+03	.687300E+03	-.142578E+04	-.148430E-08	.803266E-08	-.383418E+04
	J2	59	-.365600E+03	-.641640E+03	-.160414E+04	-.675209E-08	.115251E-07	.211334E+04
	J3	52	.311030E+03	-.104286E+04	.141723E+04	.493529E+02	-.119148E+03	.198452E+04
	J4	51	-.142808E+03	.997202E+03	.161269E+04	.409910E+03	-.989610E+03	-.371112E+04
NNQUAD-PLATE HO		45	MM					
GLOBAL	J1	59	.365600E+03	.641640E+03	-.136886E+04	.250293E-08	-.756700E-09	-.211334E+04
	J2	60	-.520682E+03	-.511280E+03	-.164674E+04	-.130385E-07	.137952E-07	-.133158E+03
	J3	53	.855142E+02	-.381959E+03	.129974E+04	-.238278E+03	.310531E+03	-.188119E+03
	J4	52	.695676E+02	.251599E+03	.170786E+04	.469599E+03	-.611994E+03	-.197487E+04
NNQUAD-PLATE HO		46	MM					
GLOBAL	J1	60	.520682E+03	.511280E+03	-.131826E+04	.809086E-08	-.867294E-08	.133158E+03
	J2	61	-.629403E+03	-.357084E+03	-.160631E+04	.186847E-07	-.104774E-07	-.224477E+04
	J3	54	-.373651E+03	.881805E+02	.129037E+04	-.608598E+03	.466994E+03	-.217626E+04
	J4	53	.482373E+03	-.242381E+03	.163420E+04	.221047E+03	-.169615E+03	.201064E+03
NNQUAD-PLATE HO		47	MM					
GLOBAL	J1	61	.629403E+03	.357080E+03	-.135869E+04	-.222062E-07	.127693E-07	.224477E+04
	J2	62	-.692134E+03	-.183517E+03	-.155136E+04	-.483124E-08	.844011E-09	-.370114E+04
	J3	55	-.892381E+03	.234690E+03	.133320E+04	-.863688E+03	.357751E+03	-.350533E+04
	J4	54	.955112E+03	-.408253E+03	.157625E+04	-.232225E+03	.961908E+02	.210861E+04
NNQUAD-PLATE HO		48	MM					
GLOBAL	J1	62	.692134E+03	.183517E+03	-.141364E+04	.167165E-08	-.226464E-09	.370114E+04
	J2	63	-.709583E+03	.861473E-08	-.148250E+04	.117325E-09	-.144382E-10	-.421385E+04
	J3	56	-.121024E+04	.562604E+02	.141014E+04	-.889747E+03	.117137E+03	-.396627E+04

2-158

		53	.122769E+04	-.239777E+03	.148600E+03	-.660001E+03	.868908E+02	.351277E+04		
NNQUAD	TE	NO	49	MM						
GLOBAL			68		.125789E+05	.290403E+04	.101263E+	.240057E+03	-.120928E+05	.131499E+05
	J2	66	-.766416E+03	.395120E+04	.814338E+04	.166767E+03	-.672390E+04	.593180E+04		
	J3	64	.128053E+05	-.812792E+04	-.897717E+04	.439266E+02	-.900607E+03	-.100407E+03		
	J4	15	.539953E+03	.127268E+04	-.178844E+03	-.356738E+03	.498841E+03	.138343E+05		
NNQUAD-PLATE	NO		50	MM						
GLOBAL			J1	69	.155215E+05	-.426568E+04	-.351073E+04	-.599089E+03	.129997E+05	-.759159E+04
	J2	67	-.624054E+04	.439239E+04	-.542184E+04	-.384805E+03	.834992E+04	-.139936E+04		
	J3	66	.582444E+04	.652001E+04	.602341E+04	-.235624E+03	.511284E+04	-.581214E+04		
	J4	68	-.151054E+05	-.664673E+04	.290916E+04	-.275239E+03	.597244E+04	.149548E+05		
NNQUAD-PLATE	NO		51	MM						
GLOBAL			J1	67	.142994E+05	-.110271E+05	-.692281E+02	-.335846E+03	.282277E+04	.470674E+03
	J2	65	-.800561E+04	.535837E+04	-.288978E+04	.992664E+03	-.834331E+04	-.585177E+04		
	J3	64	.182811E+04	.128275E+04	.798103E+04	-.111583E+04	.937849E+04	-.189647E+05		
	J4	66	-.812186E+04	.438595E+04	-.502202E+04	.109343E+04	-.917022E+04	.189967E+05		
NNQUAD-PLATE	NO		52	MM						
GLOBAL			J1	65	.572870E+03	.229691E+04	.856438E+04	-.208729E+03	.101268E+04	-.765470E+03
	J2	23	-.143386E+04	.286168E+04	-.105214E+05	.200915E+02	-.974773E+02	-.528965E+03		
	J3	16	.348639E+04	-.124264E+05	-.828694E+04	-.214965E+02	.104294E+03	.143923E+03		
	J4	64	-.262541E+04	.726777E+04	.102440E+05	-.109309E+03	.532757E+03	.132711E+04		
NNQUAD-PLATE	NO		53	MM						
GLOBAL			J1	22	-.717577E+03	-.874037E+04	-.748497E+04	-.144366E+03	.621105E+03	-.129146E+05
	J2	65	-.645020E+04	.907041E+04	-.624027E+04	-.534082E+03	.794928E+04	.548631E+04		
	J3	67	-.368263E+04	.590535E+04	.744651E+04	.101845E+04	-.139405E+04	.101934E+04		
	J4	69	.108504E+05	-.623537E+04	.7873E+04	.101778E+04	-.156439E+05	-.151222E+05		
NNQUAD-PLATE	NO		54	MM						
GLOBAL			J1	73	.412525E+04	.571176E+04	.100463E+05	-.200092E+02	.434182E+03	-.341720E+04
	J2	71	-.437620E+04	.729320E+03	-.295544E+04	.419766E+02	-.910855E+03	-.150157E+04		
	J3	70	.306384E+04	-.148572E+05	-.914477E+04	.267857E+02	-.581226E+03	-.271421E+03		
	J4	72	-.281289E+04	.841608E+04	.205395E+04	-.561381E+02	.121815E+04	.153332E+04		
NNQUAD-PLATE	NO		55	MM						
GLOBAL			J1	75	.465661E-08	0.	-.125729E-07	0.	0.	0.
	J2	73	-.304971E+05	0.	-.118143E+05	0.	0.	0.	0.	
	J3	72	.304971E+05	0.	-.597574E+04	0.	0.	0.	0.	
	J4	74	-.521541E-07	0.	.177900E+05	0.	0.	0.	0.	
NNQUAD-PLATE	NO		62	MM						
GLOBAL			J1	83	.110331E+05	-.105157E+05	-.996890E+04	-.169027E+04	.820062E+04	-.432781E+04
	J2	84	-.821753E+04	.444357E+04	.134782E+05	.236695E+03	-.114837E+04	-.460568E+04		
	J3	77	.525920E+04	.135095E+05	.109339E+05	-.159268E+03	.772714E+03	.136844E+04		
	J4	76	-.807482E+04	-.743737E+04	-.144432E+05	-.861071E+03	.417763E+04	.111169E+05		
NNQUAD-PLATE	NO		63	MM						
GLOBAL			J1	84	.124947E+05	-.172755E+05	-.154731E+05	-.518960E+03	.125288E+04	-.227391E+04
	J2	85	-.520055E+04	-.154499E+03	.154619E+05	.511480E+03	-.123482E+04	-.552254E+04		
	J3	78	.163495E+04	.123218E+05	.162657E+05	.671090E+03	-.162016E+04	.526450E+04		
	J4	77	-.892912E+04	.510827E+04	-.162545E+05	-.874060E+03	.211017E+04	.902093E+04		
NNQUAD-PLATE	NO		64	MM						
GLOBAL			J1	85	.115185E+05	-.966441E+04	-.144342E+05	.133202E+03	-.173593E+03	-.696387E+03
	J2	86	-.168937E+04	-.388548E+04	.137390E+05	.928786E+03	-.121042E+04	-.326760E+04		
	J3	79	.315124E+03	.834556E+04	.143597E+05	.107306E+04	-.139344E+04	.614620E+04		
	J4	78	-.101443E+05	.520432E+04	-.136644E+05	.597211E+02	-.778300E+02	.555899E+04		
NNQUAD-PLATE	NO		65	MM						
GLOBAL			J1	83	.725100E+04	-.235972E+04	-.974652E+04	.800803E+03	-.614478E+03	-.130375E+04
	J2	87	.197183E+04	-.538795E+04	.101920E+05	.101037E+04	-.775670E+03	-.192889E+04		
	J3	80	.311127E+04	.337704E+04	.100144E+05	.121908E+04	-.935433E+03	.667307E+04		
	J4	79	-.123341E+05	.437062E+04	-.104599E+05	.346589E+03	-.265947E+03	.370128E+04		
NNQUAD-PLATE	NO		66	MM						
GLOBAL			J1	87	.268158E+04	.735700E+03	-.597658E+04	.850638E+03	-.352346E+03	-.155996E+04
	J2	88	.401685E+04	-.404294E+04	.630759E+04	.979272E+03	-.405628E+03	-.783762E+03		
	J3	81	.840334E+04	-.341177E+01	.620938E+04	.140679E+04	-.582712E+03	.615412E+04		

APPENDIX 2.10.3 WITH IUG ANALYSIS cont'd.

Revision 6

		80	-.151018E+05	.331065E+04	-.654038E+04	.400487E+03	-.165887E+03	.102366E+04
		MMQUAD-PLATE NO	67 MM					
GLOBAL	J1	88	-.132043E+04	.627872E+03	-.204827E+04	.866824E+03	-.114119E+03	-.113567E+04
	J2	39	.379465E+04	-.146406E+04	.216372E+04	.930713E+03	-.122531E+03	.274971E+03
	J3	82	.133479E+05	-.437297E+03	.213869E+04	.133154E+04	-.175301E+03	.450470E+04
	J4	81	-.158222E+05	.127348E+04	-.225414E+04	.884928E+03	-.116503E+03	-.176476E+04
		MMQUAD-PLATE NO	68 MM					
GLOBAL	J1	15	-.539953E+03	.562827E+04	.178844E+03	.361634E+02	-.498841E+03	.133386E+04
	J2	64	.525487E+03	-.636781E+04	.259271E+04	.154744E+02	-.213455E+03	-.980046E+03
	J3	90	.164908E+03	-.176926E+04	-.541928E+03	-.188155E+02	.259542E+03	-.155081E+04
	J4	8	-.150443E+03	.250880E+04	-.222962E+04	.473590E+01	-.653273E+02	.147240E+04
		MMQUAD-PLATE NO	69 MM					
GLOBAL	J1	29	.599024E+02	.183294E+04	-.177548E+04	-.187904E+02	.259196E+03	-.153978E+04
	J2	91	-.160479E+03	-.323505E+02	-.798228E+04	-.743951E+01	.103311E+03	.107067E+04
	J3	65	-.617001E+03	.391233E+04	.227280E+04	-.375423E+02	.517860E+03	.353435E+03
	J4	22	.717577E+03	-.571291E+04	.748497E+04	.450269E+02	-.621105E+03	-.124416E+04

30 E MODE LOAD

Nodes	QUADRILATERAL ELEMENT FORCES	STRESSSES	AND FORCES MAX	FOR OUTPUT VECTOR MIN	PRINCIPAL STRESSES	MAX SHEAR	1 ANGLE
X2. 1 QUAD 1 8.-----X1	FX = 5.624E+02 FY = -8.057E+02 FXY = -3.825E+02 MX = -5.571E+02 MY = 2.324E+00 MXY = -1.022E+02	+ZFACE SX = -1.225E+04 SY = -1.556E+03 SXY = -3.218E+03 -ZFACE SX = 1.450E+04 SY = -1.667E+03 SXY = 1.688E+03	+ZFACE -6.615E+02	-1.314E+04	6.239E+03 VM 1.282E+04	8.256E+03 VM 1.567E+04	-74.474 5.901
X2. 2 QUAD 2 9.-----X1	FX = 2.688E+02 FY = 3.217E+02 FXY = -2.927E+02 MX = -2.781E+02 MY = -5.480E+00 MXY = -1.771E+02	+ZFACE SX = -6.136E+03 SY = 5.119E+02 SXY = -4.835E+03 -ZFACE SX = 7.211E+03 SY = 7.749E+02 SXY = 3.465E+03	+ZFACE 3.056E+03	-8.680E+03	5.868E+03 VM 1.054E+04	4.877E+03 VM 9.343E+03	-62.253 24.355
X2. 3 QUAD 3 10.-----X1	FX = -1.229E+02 FY = 1.173E+02 FXY = -4.918E+01 MX = 5.902E+01 MY = 2.727E+01 MXY = -1.946E+02	+ZFACE SX = 1.171E+03 SY = 8.891E+02 SXY = -4.769E+03 -ZFACE SX = -1.662E+03 SY = -4.197E+02 SXY = 4.573E+03	+ZFACE 5.801E+03	-3.742E+03	4.771E+03 VM 8.328E+03	4.615E+03 VM 8.060E+03	-44.155 48.869
X2. 4 QUAD 4 11.-----X1	FX = -1.521E+02 FY = 4.791E+01 FXY = 9.345E+01 MX = 2.309E+02 MY = 4.989E+01 MXY = -1.463E+02	+ZFACE SX = 5.237E+03 SY = 1.293E+03 SXY = -3.323E+03 -ZFACE SX = -5.845E+03 SY = -1.101E+03 SXY = 3.697E+03	+ZFACE 7.129E+03	-5.993E+02	3.864E+03 VM 7.447E+03	4.393E+03 VM 8.364E+03	-29.659 61.341
X2. 5 QUAD 5 12.-----X1	FX = -1.146E+02 FY = -4.895E+01 FXY = 6.754E+01 MX = 2.942E+02 MY = 6.282E+01 MXY = -8.333E+01	+ZFACE SX = 6.832E+03 SY = 1.410E+03 SXY = -1.865E+03 -ZFACE SX = -7.291E+03 SY = -1.606E+03 SXY = 2.135E+03	+ZFACE 7.412E+03	8.304E+02	-3.291E+03 VM 7.033E+03	3.555E+03 VM 7.596E+03	-17.261 71.545
X2. 6 QUAD 6 13.-----X1	FX = -9.846E+01 FY = -2.833E+01 FXY = 1.590E+01 MX = 3.144E+02 MY = 6.946E+01 MXY = -2.662E+01	+ZFACE SX = 7.350E+03 SY = 1.610E+03 SXY = -6.070E+02 -ZFACE SX = -7.744E+03 SY = -1.724E+03 SXY = 6.706E+02	+ZFACE 7.413E+03	1.547E+03	2.933E+03 VM 6.774E+03	3.084E+03 VM 7.137E+03	-5.971 83.720
X2. 7 QUAD 7 14.-----X1	FX = -2.440E+03 FY = -1.155E+03 FXY = -2.807E+02 MX = -3.494E+02 MY = -1.033E+02 MXY = -1.079E+02	+ZFACE SX = -1.327E+04 SY = -4.789E+03 SXY = -3.150E+03 -ZFACE SX = 3.506E+03 SY = 1.683E+02 SXY = 2.028E+03	+ZFACE -3.747E+03	-1.431E+04	5.281E+03 VM 1.285E+04	2.626E+03 VM 4.905E+03	-71.690 25.272
X2. 8 QUAD 8 15.-----X1	FX = -1.027E+03 FY = 4.811E+02 FXY = -6.175E+02 MX = -1.397E+02	+ZFACE SX = -5.407E+03 SY = 2.170E+01 SXY = -5.480E+03 -ZFACE SX = 1.299E+03	+ZFACE 3.423E+03	-8.808E+03	6.115E+03 VM 1.093E+04		-58.175

2-161



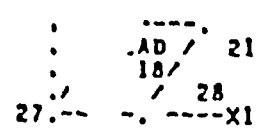
16.-----X1	17	MY = -3.919E+01 MXY = -1.769E+02	SY = 1.903 SXY = 3.010E	-ZFACE 4.626E+03	-1.424E+03	3.025E+03	47.
						5.479E+03	
X2. 10	11	FX = -3.138E+02 FY = 7.472E+02 FXY = -8.154E+01	+ZFACE SX = -2.678E+02 SY = 1.278E+03 SXY = -4.965E+03	+ZFACE 5.529E+03	-4.519E+03	5.024E+03	-49.423
						8.717E+03	
17.-----X1	18	MX = 1.499E+01 MY = -9.028E+00 MXY = -2.001E+02	-ZFACE SX = -9.875E+02 SY = 1.711E+03 SXY = 4.638E+03	-ZFACE 5.192E+03	-4.469E+03	4.831E+03	53.110
						8.375E+03	
X2. 11	12	FX = -1.198E+02 FY = 7.065E+01 FXY = 1.068E+02	+ZFACE SX = 2.078E+03 SY = -2.983E+01 SXY = -3.794E+03	+ZFACE 4.962E+03	-2.913E+03	3.938E+03	-37.238
						6.896E+03	
18.-----X1	19	MX = 9.656E+01 MY = -7.131E+00 MXY = -1.670E+02	-ZFACE SX = -2.557E+03 SY = 3.124E+02 SXY = 4.221E+03	-ZFACE 3.336E+03	-5.381E+03	4.458E+03	54.386
						7.803E+03	
X2. 12	13	FX = -2.604E+01 FY = -1.381E+02 FXY = 6.394E+01	+ZFACE SX = 3.315E+03 SY = -2.450E+02 SXY = -2.402E+03	+ZFACE 4.685E+03	-1.415E+03	3.050E+03	-25.974
						5.530E+03	
19.-----X1	20	MX = 1.486E+02 MY = 1.391E+00 MXY = -1.054E+02	-ZFACE SX = -3.619E+03 SY = -3.074E+02 SXY = 2.657E+03	-ZFACE 1.168E+03	-5.094E+03	3.131E+03	60.963
						5.767E+03	
X2. 13	14	FX = 2.050E+01 FY = -8.434E+01 FXY = 1.419E+01	+ZFACE SX = 4.228E+03 SY = 4.403E+01 SXY = -8.249E+02	+ZFACE 4.386E+03	-1.135E+02	2.250E+03	-10.783
						4.443E+03	
20.-----X1	21	MX = 1.745E+02 MY = 8.863E+00 MXY = -3.564E+01	-ZFACE SX = -4.146E+03 SY = -3.814E+02 SXY = 8.836E+02	-ZFACE -1.843E+02	-4.343E+03	2.079E+03	77.427
						4.254E+03	
X2. 16	17	FX = -8.190E+02 FY = 7.729E+02 FXY = -2.401E+03	+ZFACE SX = -2.897E+03 SY = 1.401E+03 SXY = -8.058E+03	+ZFACE 7.592E+03	-9.088E+03	8.340E+03	-52.466
						1.646E+04	
23.-----X1	24	MX = -5.244E+01 MY = -6.016E+00 MXY = -1.357E+02	-ZFACE SX = -3.795E+02 SY = 1.490E+03 SXY = -1.545E+03	-ZFACE 2.515E+03	-1.204E+03	1.839E+03	-61.908
						3.287E+03	
X2. 17	18	FX = -2.916E+02 FY = 4.611E+01 FXY = -2.800E+03	+ZFACE SX = -9.386E+02 SY = 1.338E+02 SXY = -8.597E+03	+ZFACE 8.211E+03	-9.016E+03	8.614E+03	-46.785
						1.493E+04	
24.-----X1	25	MX = -1.481E+01 MY = 1.733E+00 MXY = -1.249E+02	-ZFACE SX = -2.279E+02 SY = 5.062E+01 SXY = -2.602E+03	-ZFACE 2.518E+03	-2.695E+03	2.686E+03	-46.531
						4.515E+03	
X2. 18	19	FX = 3.154E+02 FY = -1.762E+02 FXY = -2.572E+03	+ZFACE SX = 1.050E+03 SY = -4.562E+02 SXY = -7.623E+03	+ZFACE 7.957E+03	-7.363E+03	7.660E+03	-42.178
						1.327E+04	
25.-----X1	26	MX = 1.748E+01 MY = -4.322E+00 MXY = -1.033E+02	-ZFACE SX = 2.111E+02 SY = -2.487E+02 SXY = -2.664E+03	-ZFACE 2.655E+03	-2.693E+03	2.674E+03	-42.534
						4.631E+03	
X2. 19	20	FX = 7.800E+02 FY = -1.116E+02 FXY = -1.785E+03	+ZFACE SX = 2.619E+03 SY = -2.453E+02 SXY = -5.231E+03	+ZFACE 6.611E+03	-4.237E+03	5.424E+03	-37.344
						9.469E+03	
26.-----X1	27	MX = 4.414E+01 MY = -9.231E-01 MXY = -6.921E+01	-ZFACE SX = 5.007E+02 SY = -2.010E+02 SXY = -1.909E+03	-ZFACE 2.091E+03	-1.791E+03	1.941E+03	-39.793
						3.365E+03	
X2. 20		FX = 1.039E+03	+ZFACE SX = 3.493E+03				

2-162

Revision: 0



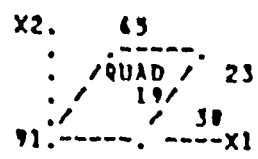
2-163



FY = 3.608E+01  
 FXY = -6.357E+02  
 MX = 5.896E+01  
 MY = 4.764E+00  
 MXY = -2.445E+01

SY = 2.26  
 SXY = -1.85  
 SX = 6.42  
 SY = -2.176  
 SXY = -6.846E+02

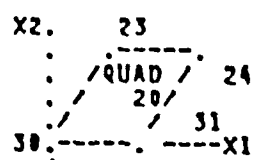
+ZFACE 4.333E+03 -6.143E+02 2.474E+03 -2'  
 VM 4.671E+03  
 -ZFACE 1.091E+03 -4.310E+02 7.610E+02 -32.059  
 VM 1.359E+03



FX = 1.538E+03  
 FY = 3.261E+03  
 FXY = -9.675E+02  
 MX = 1.464E+02  
 MY = -2.904E+01  
 MXY = -8.611E+01

+ZFACE SX = 6.572E+03  
 SY = 5.826E+03  
 SXY = -4.002E+03  
 -ZFACE SX = -4.537E+02  
 SY = 7.220E+03  
 SXY = 1.318E+02

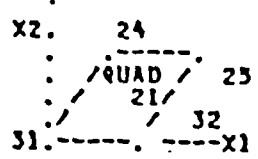
+ZFACE 1.022E+04 2.180E+03 4.019E+03 -42.337  
 VM 9.321E+03  
 -ZFACE 7.222E+03 -4.539E+02 3.839E+03 89.016  
 VM 7.460E+03



FX = 4.603E+02  
 FY = 8.732E+02  
 FXY = -7.866E+02  
 MX = 3.060E+01  
 MY = -4.653E+00  
 MXY = -1.468E+02

+ZFACE SX = 1.655E+03  
 SY = 1.635E+03  
 SXY = -5.096E+03  
 -ZFACE SX = 1.864E+02  
 SY = 1.858E+03  
 SXY = 1.950E+03

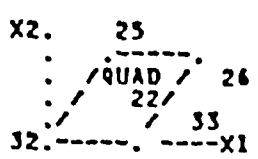
+ZFACE 6.741E+03 -3.451E+03 5.096E+03 -44.943  
 VM 8.979E+03  
 -ZFACE 3.143E+03 -1.099E+03 2.121E+03 56.603  
 VM 3.814E+03



FX = 1.194E+02  
 FY = -4.102E+02  
 FXY = -4.471E+02  
 MX = -3.881E+01  
 MY = -2.707E+01  
 MXY = -1.756E+02

+ZFACE SX = -6.926E+02  
 SY = -1.470E+03  
 SXY = -5.109E+03  
 -ZFACE SX = 1.170E+03  
 SY = -1.708E+02  
 SXY = 3.321E+03

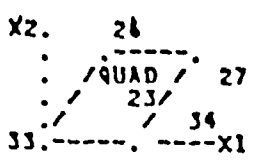
+ZFACE 4.043E+03 -6.206E+03 5.124E+03 -42.824  
 VM 8.941E+03  
 -ZFACE 3.888E+03 -2.888E+03 3.388E+03 39.292  
 VM 5.890E+03



FX = 2.912E+02  
 FY = -4.888E+02  
 FXY = -2.253E+02  
 MX = -4.368E+01  
 MY = 1.221E+01  
 MXY = -1.609E+02

+ZFACE SX = -4.659E+02  
 SY = -6.845E+02  
 SXY = -4.311E+03  
 -ZFACE SX = 1.631E+03  
 SY = -1.271E+03  
 SXY = 3.410E+03

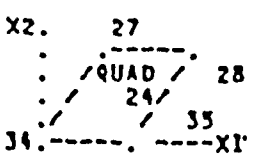
+ZFACE 3.738E+03 -4.888E+03 4.313E+03 -44.274  
 VM 7.492E+03  
 -ZFACE 3.886E+03 -3.526E+03 3.706E+03 33.478  
 VM 6.421E+03



FX = 5.575E+02  
 FY = -7.349E+01  
 FXY = -1.140E+02  
 MX = -5.275E+01  
 MY = 4.133E+01  
 MXY = -1.111E+02

+ZFACE SX = -1.510E+02  
 SY = 8.450E+02  
 SXY = -2.895E+03  
 -ZFACE SX = 2.381E+03  
 SY = -1.139E+03  
 SXY = 2.439E+03

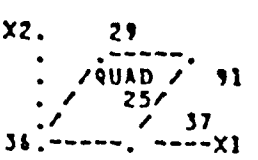
+ZFACE 3.285E+03 -2.591E+03 2.938E+03 -49.880  
 VM 5.100E+03  
 -ZFACE 3.629E+03 -2.387E+03 3.008E+03 27.092  
 VM 5.246E+03



FX = 7.215E+02  
 FY = 2.571E+02  
 FXY = -3.579E+01  
 MX = -6.161E+01  
 MY = 5.514E+01  
 MXY = -3.958E+01

+ZFACE SX = -3.570E+01  
 SY = 1.838E+03  
 SXY = -1.022E+03  
 -ZFACE SX = 2.922E+03  
 SY = -8.092E+02  
 SXY = 8.784E+02

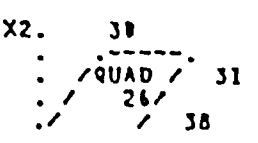
+ZFACE 2.287E+03 -4.850E+02 1.386E+03 -66.260  
 VM 2.564E+03  
 -ZFACE 3.118E+03 -1.006E+03 2.062E+03 12.607  
 VM 3.724E+03



FX = -2.180E+02  
 FY = 2.067E+03  
 FXY = 1.173E+00  
 MX = 4.540E+02  
 MY = 1.370E+02  
 MXY = -2.068E+01

+ZFACE SX = 1.046E+04  
 SY = 7.423E+03  
 SXY = -4.939E+02  
 -ZFACE SX = -1.133E+04  
 SY = 8.468E+02  
 SXY = 4.986E+02

+ZFACE 1.054E+04 7.344E+03 1.597E+03 -9.006  
 VM 9.360E+03  
 -ZFACE 8.672E+02 -1.135E+04 6.110E+03 87.660  
 VM 1.181E+04



FX = -9.230E+01  
 FY = 1.189E+03  
 FXY = -7.188E+02  
 MX = 2.187E+02  
 MY = 6.094E+01

+ZFACE SX = 5.064E+03  
 SY = 3.841E+03  
 SXY = -4.130E+03  
 -ZFACE SX = -5.433E+03  
 SY = 9.153E+02

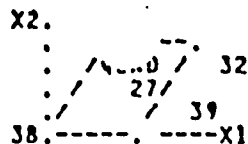
+ZFACE 8.628E+03 2.769E+02 4.176E+03 -40.787  
 VM 8.493E+03  
 -ZFACE 1.154E+03 -5.673E+03 3.413E+03 79.213

37. ---X1

MXY = -1.122E+02

SXY = 1.255E+02

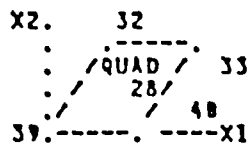
VH 6.329E+03



FX = 5.458E+01  
 FY = 1.619E+02  
 FXY = -5.074E+02  
 MX = 3.262E-01  
 MY = -1.190E+01  
 MXY = -1.577E+02

+ZFACE SX = 1.170E  
 SY = 3.835E  
 SXY = -4.848E+03  
 -ZFACE SX = 1.013E+02  
 SY = 6.094E+02  
 SXY = 2.818E+03

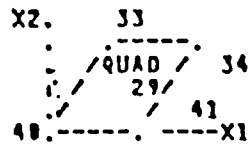
+ZFACE 4.925E+03 -4.770E+03 4.848E+03 -44.  
 VM 7.397E+03  
 -ZFACE 3.185E+03 -2.474E+03 2.829E+03 47.576  
 VM 4.914E+03



FX = -4.704E-01  
 FY = -1.433E+02  
 FXY = -1.996E+02  
 MX = -1.454E+02  
 MY = -6.550E+01  
 MXY = -1.561E+02

+ZFACE SX = -3.490E+03  
 SY = -1.858E+03  
 SXY = -4.145E+03  
 -ZFACE SX = 3.489E+03  
 SY = 1.285E+03  
 SXY = 3.346E+03

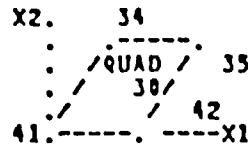
+ZFACE 1.550E+03 -6.899E+03 4.225E+03 -50.568  
 VM 7.791E+03  
 -ZFACE 5.910E+03 -1.136E+03 3.523E+03 35.890  
 VM 6.552E+03



FX = -6.363E+01  
 FY = 6.720E+01  
 FXY = -5.003E+01  
 MX = -2.411E+02  
 MY = -9.578E+01  
 MXY = -1.090E+02

+ZFACE SX = -5.914E+03  
 SY = -2.164E+03  
 SXY = -2.716E+03  
 -ZFACE SX = 5.659E+03  
 SY = 2.433E+03  
 SXY = 2.516E+03

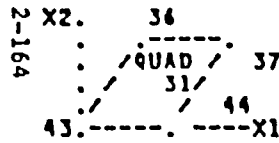
+ZFACE -7.385E+02 -7.339E+03 3.300E+03 -62.307  
 VM 6.999E+03  
 -ZFACE 7.035E+03 1.057E+03 2.989E+03 28.668  
 VM 6.570E+03



FX = -8.823E+01  
 FY = 3.323E+02  
 FXY = -7.304E+00  
 MX = -2.922E+02  
 MY = -1.106E+02  
 MXY = -3.872E+01

+ZFACE SX = -7.190E+03  
 SY = -1.989E+03  
 SXY = -9.440E+02  
 -ZFACE SX = 6.837E+03  
 SY = 3.318E+03  
 SXY = 9.148E+02

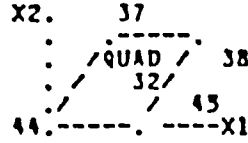
+ZFACE -1.823E+03 -7.356E+03 2.766E+03 -80.024  
 VM 6.635E+03  
 -ZFACE 7.060E+03 3.095E+03 1.983E+03 13.737  
 VM 6.130E+03



FX = -1.266E+02  
 FY = 1.311E+03  
 FXY = -2.930E+02  
 MX = 6.140E+02  
 MY = 1.830E+02  
 MXY = -3.734E+01

+ZFACE SX = 1.448E+04  
 SY = 7.013E+03  
 SXY = -1.482E+03  
 -ZFACE SX = -1.499E+04  
 SY = -1.771E+03  
 SXY = 3.103E+02

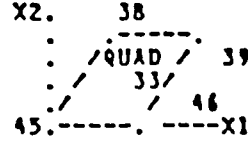
+ZFACE 1.477E+04 6.730E+03 4.018E+03 -10.823  
 VM 1.280E+04  
 -ZFACE -1.764E+03 -1.500E+04 6.616E+03 88.656  
 VM 1.420E+04



FX = -6.281E+01  
 FY = 8.476E+02  
 FXY = -3.641E+02  
 MX = 3.971E+02  
 MY = 1.249E+02  
 MXY = -1.073E+02

+ZFACE SX = 9.403E+03  
 SY = 4.692E+03  
 SXY = -3.307E+03  
 -ZFACE SX = -9.657E+03  
 SY = -1.301E+03  
 SXY = 1.843E+03

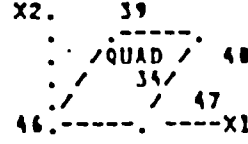
+ZFACE 1.111E+04 2.988E+03 4.061E+03 -27.262  
 VM 9.958E+03  
 -ZFACE -9.132E+02 -1.005E+04 4.566E+03 78.099  
 VM 9.621E+03



FX = 3.363E+01  
 FY = 5.506E+02  
 FXY = -4.360E+02  
 MX = 7.608E+01  
 MY = 2.345E+01  
 MXY = -1.532E+02

+ZFACE SX = 1.933E+03  
 SY = 1.664E+03  
 SXY = -4.548E+03  
 -ZFACE SX = -1.719E+03  
 SY = 5.385E+02  
 SXY = 2.804E+03

+ZFACE 6.348E+03 -2.751E+03 4.350E+03 -44.152  
 VM 8.083E+03  
 -ZFACE 2.432E+03 -3.613E+03 3.023E+03 55.962  
 VM 5.268E+03



FX = 7.975E+01  
 FY = 2.356E+02  
 FXY = -2.739E+02  
 MX = -2.027E+02  
 MY = -5.908E+01  
 MXY = -1.587E+02

+ZFACE SX = -4.786E+03  
 SY = -9.467E+02  
 SXY = -4.356E+03  
 -ZFACE SX = 5.025E+03  
 SY = 1.889E+03  
 SXY = 3.260E+03

+ZFACE 1.918E+03 -7.570E+03 4.744E+03 -56.670  
 VM 8.690E+03  
 -ZFACE 7.075E+03 -1.610E+02 3.618E+03 32.159  
 VM 7.157E+03



FX = 5.919E+01  
 FY = 2.542E+02

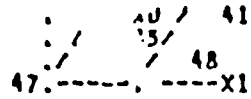
+ZFACE SX = -9.249E+03  
 SY = -2.088E+03

+ZFACE -9.937E+02 -1.034E+04 4.675E+03 -69.991

2-164



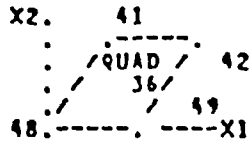
2-165



FX = -1.008E+02  
 FY = -3.903E+02  
 FXY = -1.082E+02  
 MX = -1.169E+02

+ZFACE SXY = -3.006  
 SX = 9.48  
 SY = 3.105  
 SXY = 2.603E+03

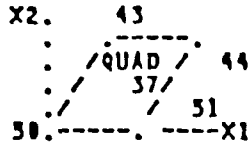
VH 9.885E+03  
 -ZFACE 1.041E+04 2.178E+03 4.118E+03 19.005  
 VH 9.513E+03



FX = 4.228E+01  
 FY = 3.882E+02  
 FXY = -1.865E+01  
 MX = -4.838E+02  
 MY = -1.295E+02  
 MXY = -4.257E+01

+ZFACE SX = -1.153E+04  
 SY = -2.331E+03  
 SXY = -1.059E+03  
 -ZFACE SX = 1.170E+04  
 SY = 3.884E+03  
 SXY = 9.845E+02

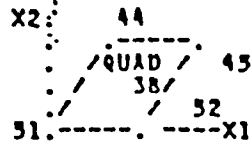
+ZFACE -2.218E+03 -1.165E+04 4.718E+03 -83.514  
 VH 1.071E+04  
 -ZFACE 1.182E+04 3.761E+03 4.028E+03 7.073  
 VH 1.046E+04



FX = -2.941E+02  
 FY = 7.912E+02  
 FXY = -8.724E+01  
 MX = 8.092E+02  
 MY = 2.693E+02  
 MXY = -3.666E+01

+ZFACE SX = 1.883E+04  
 SY = 8.046E+03  
 SXY = -1.054E+03  
 -ZFACE SX = -2.001E+04  
 SY = -4.881E+03  
 SXY = 7.054E+02

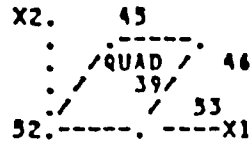
+ZFACE 1.893E+04 7.943E+03 5.495E+03 -5.531  
 VH 1.647E+04  
 -ZFACE -4.848E+03 -2.004E+04 7.597E+03 87.336  
 VH 1.811E+04



FX = -1.580E+02  
 FY = 7.347E+02  
 FXY = -2.794E+02  
 MX = 5.533E+02  
 MY = 1.833E+02  
 MXY = -1.042E+02

+ZFACE SX = 1.296E+04  
 SY = 5.869E+03  
 SXY = -3.060E+03  
 -ZFACE SX = -1.360E+04  
 SY = -2.930E+03  
 SXY = 1.942E+03

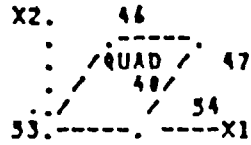
+ZFACE 1.410E+04 4.732E+03 4.684E+03 -20.389  
 VH 1.243E+04  
 -ZFACE -2.588E+03 -1.394E+04 5.675E+03 79.995  
 VH 1.284E+04



FX = -2.733E+01  
 FY = 5.874E+02  
 FXY = -3.026E+02  
 MX = 1.557E+02  
 MY = 5.329E+01  
 MXY = -1.492E+02

+ZFACE SX = 3.683E+03  
 SY = 2.456E+03  
 SXY = -4.186E+03  
 -ZFACE SX = -3.792E+03  
 SY = -1.043E+02  
 SXY = 2.975E+03

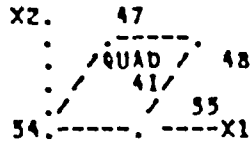
+ZFACE 7.299E+03 -1.162E+03 4.231E+03 -40.824  
 VH 7.944E+03  
 -ZFACE 1.552E+03 -5.449E+03 3.500E+03 60.894  
 VH 6.368E+03



FX = 1.102E+02  
 FY = 5.045E+02  
 FXY = -2.508E+02  
 MX = -2.498E+02  
 MY = -8.385E+01  
 MXY = -1.559E+02

+ZFACE SX = -5.774E+03  
 SY = -1.003E+03  
 SXY = -4.243E+03  
 -ZFACE SX = 6.215E+03  
 SY = 3.021E+03  
 SXY = 3.240E+03

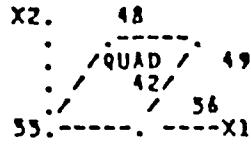
+ZFACE 1.479E+03 -8.257E+03 4.868E+03 -59.670  
 VH 9.087E+03  
 -ZFACE 8.230E+03 1.086E+03 3.612E+03 31.884  
 VH 7.776E+03



FX = 1.797E+02  
 FY = 4.700E+02  
 FXY = -1.341E+02  
 MX = -5.561E+02  
 MY = -1.897E+02  
 MXY = -1.177E+02

+ZFACE SX = -1.299E+04  
 SY = -3.588E+03  
 SXY = -3.093E+03  
 -ZFACE SX = 1.371E+04  
 SY = 5.468E+03  
 SXY = 2.556E+03

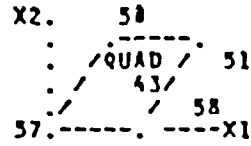
+ZFACE -2.662E+03 -1.391E+04 5.625E+03 -73.325  
 VH 1.279E+04  
 -ZFACE 1.443E+04 4.739E+03 4.847E+03 15.914  
 VH 1.274E+04



FX = 2.003E+02  
 FY = 4.989E+02  
 FXY = -3.675E+01  
 MX = -7.152E+02  
 MY = -2.428E+02  
 MXY = -4.368E+01

+ZFACE SX = -1.676E+04  
 SY = -4.829E+03  
 SXY = -1.122E+03  
 -ZFACE SX = 1.757E+04  
 SY = 6.823E+03  
 SXY = 9.748E+02

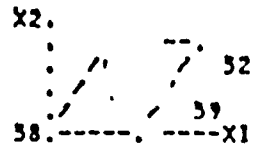
+ZFACE -4.724E+03 -1.687E+04 6.072E+03 -84.677  
 VH 1.507E+04  
 -ZFACE 1.765E+04 6.737E+03 5.458E+03 5.144  
 VH 1.543E+04



FX = -2.410E+02  
 FY = 6.092E+02  
 FXY = -8.901E+00  
 MX = 9.420E+02  
 MY = 1.695E+02  
 MXY = -4.070E+01

+ZFACE SX = 2.213E+04  
 SY = 5.286E+03  
 SXY = -9.946E+02  
 -ZFACE SX = -2.309E+04  
 SY = -2.850E+03  
 SXY = 9.590E+02

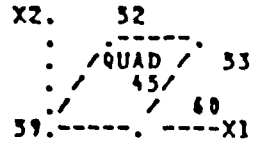
+ZFACE 2.219E+04 5.228E+03 8.479E+03 -3.368  
 VH 2.009E+04  
 -ZFACE -2.804E+03 -2.314E+04 1.017E+04 87.294  
 VH 2.187E+04



FX = -1.765E+02  
 FY = 6.109E+02  
 FXY = -2.148E+01  
 MX = 6.691E+02  
 MY = 1.210E+02  
 MXY = -1.137E+02

+ZFACE SX = 1.571E+04  
 SY = 4.125E+03  
 SXY = -2.771E+03  
 -ZFACE SX = -1.641E+04  
 SY = -1.682E+03  
 SXY = 2.685E+03

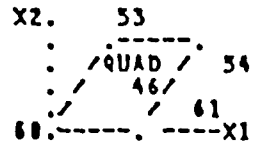
+ZFACE 1.634E+04 3.497E+03 6.419E+03 -12.7  
 VM 1.490E+04  
 -ZFACE -1.208E+03 -1.689E+04 7.839E+03 79.986  
 VM 1.632E+04



FX = -5.100E+01  
 FY = 6.064E+02  
 FXY = -3.988E+01  
 MX = 2.165E+02  
 MY = 3.831E+01  
 MXY = -1.606E+02

+ZFACE SX = 3.094E+03  
 SY = 2.132E+03  
 SXY = -3.934E+03  
 -ZFACE SX = -5.298E+03  
 SY = 2.934E+02  
 SXY = 3.775E+03

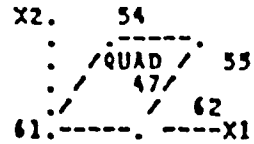
+ZFACE 7.817E+03 -5.909E+02 4.204E+03 -34.687  
 VM 8.128E+03  
 -ZFACE 2.195E+03 -7.199E+03 4.697E+03 63.262  
 VM 8.512E+03



FX = 7.265E+01  
 FY = 5.896E+02  
 FXY = -3.632E+01  
 MX = -2.733E+02  
 MY = -4.924E+01  
 MXY = -1.658E+02

+ZFACE SX = -6.414E+03  
 SY = -2.588E+00  
 SXY = -4.053E+03  
 -ZFACE SX = 6.704E+03  
 SY = 2.361E+03  
 SXY = 3.907E+03

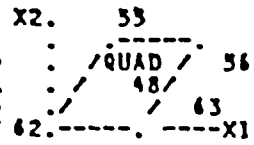
+ZFACE 1.959E+03 -8.375E+03 5.167E+03 -64.171  
 VM 9.507E+03  
 -ZFACE 9.803E+03 6.238E+01 4.470E+03 30.468  
 VM 8.972E+03



FX = 1.785E+02  
 FY = 5.867E+02  
 FXY = -2.508E+01  
 MX = -6.690E+02  
 MY = -1.196E+02  
 MXY = -1.244E+02

+ZFACE SX = -1.571E+04  
 SY = -1.696E+03  
 SXY = -3.036E+03  
 -ZFACE SX = 1.640E+04  
 SY = 4.043E+03  
 SXY = 2.935E+03

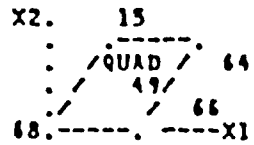
+ZFACE -1.067E+03 -1.634E+04 7.638E+03 -78.291  
 VM 1.584E+04  
 -ZFACE 1.706E+04 3.351E+03 6.838E+03 12.709  
 VM 1.564E+04



FX = 2.196E+02  
 FY = 5.839E+02  
 FXY = -8.317E+00  
 MX = -8.847E+02  
 MY = -1.576E+02  
 MXY = -4.614E+01

+ZFACE SX = -2.079E+04  
 SY = -2.614E+03  
 SXY = -1.124E+03  
 -ZFACE SX = 2.167E+04  
 SY = 4.950E+03  
 SXY = 1.091E+03

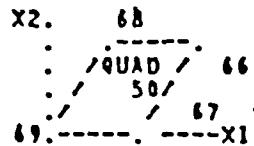
+ZFACE -2.545E+03 -2.086E+04 9.159E+03 -86.476  
 VM 1.971E+04  
 -ZFACE 2.174E+04 4.879E+03 8.432E+03 3.716  
 VM 1.976E+04



FX = -4.922E+03  
 FY = -4.319E+03  
 FXY = -3.334E+03  
 MX = -9.262E+03  
 MY = -3.117E+03  
 MXY = -2.903E+03

+ZFACE SX = -1.635E+04  
 SY = -6.834E+03  
 SXY = -6.021E+03  
 -ZFACE SX = 1.143E+04  
 SY = 2.516E+03  
 SXY = 2.688E+03

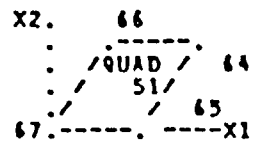
+ZFACE -3.919E+03 -1.927E+04 -7.674E+03 -64.165  
 VM 1.764E+04  
 -ZFACE 1.218E+04 1.768E+03 5.206E+03 15.542  
 VM 1.140E+04



FX = 3.120E+03  
 FY = 5.186E+03  
 FXY = 1.719E+02  
 MX = -2.882E+03  
 MY = 2.937E+03  
 MXY = -1.772E+03

+ZFACE SX = -1.563E+03  
 SY = 6.958E+03  
 SXY = -2.573E+03  
 -ZFACE SX = 4.683E+03  
 SY = -1.852E+03  
 SXY = 2.744E+03

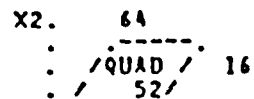
+ZFACE 7.675E+03 -2.280E+03 4.977E+03 -74.438  
 VM 9.033E+03  
 -ZFACE 5.683E+03 -2.852E+03 4.267E+03 20.013  
 VM 7.525E+03



FX = 4.449E+03  
 FY = 2.217E+03  
 FXY = -1.944E+03  
 MX = 4.382E+03  
 MY = -4.564E+03  
 MXY = 1.247E+03

+ZFACE SX = 8.797E+03  
 SY = -5.738E+03  
 SXY = 8.982E+02  
 -ZFACE SX = -4.349E+03  
 SY = 7.955E+03  
 SXY = -2.842E+03

+ZFACE 8.853E+03 -5.793E+03 7.323E+03 3.523  
 VM 1.278E+04  
 -ZFACE 8.579E+03 -4.974E+03 6.776E+03 -77.603  
 VM 1.187E+04

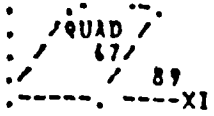


FX = -1.223E+03  
 FY = 8.804E+02  
 FXY = -2.351E+03  
 MX = -5.917E+01

+ZFACE SX = -3.866E+03  
 SY = 3.294E+03  
 SXY = -6.947E+03  
 -ZFACE SX = -1.025E+03

+ZFACE 7.530E+03 -8.101E+03 7.815E+03 -58.630  
 VM 1.354E+04

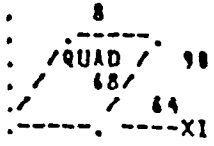
65. /	23	MY = 6.388E+01	SY = 2.277E	-ZFACE	2.136E+03	-2.934E+03	2.535E+03	-32.
---	---	MXY = -9.356E+01	SXY = -2.457E				VM 4.409E+03	
X2.	69	FX = 5.479E+03	+ZFACE SX = 1.127E+04	+ZFACE	1.791E+04	8.102E+03	4.903E+03	-55.383
.	.	FY = 6.121E+03	SY = 1.474E+04				VM 1.553E+04	
.	QUAD / 67	FXY = -3.832E+02	SXY = -4.585E+03					
.	53 /	MX = 5.685E+03	-ZFACE SX = -5.787E+03	-ZFACE	-2.770E+03	-1.164E+04	4.434E+03	35.680
22. /	65	MY = 7.788E+03	SY = -8.622E+03				VM 1.053E+04	
---	---	MXY = -2.929E+03	SXY = 4.202E+03					
X2.	72	FX = -4.815E+03	+ZFACE SX = -3.920E+03	+ZFACE	1.297E+03	-1.081E+04	6.853E+03	-41.820
.	.	FY = -3.803E+03	SY = -5.597E+03				VM 1.152E+04	
.	QUAD / 70	FXY = -3.457E+03	SXY = -5.997E+03					
.	54 /	MX = 1.584E+01	-ZFACE SX = -4.110E+03	-ZFACE	-1.663E+03	-4.454E+03	1.395E+03	-69.427
73. /	71	MY = -2.990E+02	SY = -2.009E+03				VM 3.893E+03	
---	---	MXY = -4.232E+02	SXY = -9.177E+02					
X2.	74	FX = -4.708E-09	+ZFACE SX = -4.708E-09	+ZFACE	5.627E+03	-2.778E+03	4.202E+03	-54.909
.	.	FY = 2.849E+03	SY = 2.849E+03				VM 7.417E+03	
.	QUAD / 72	FXY = -3.953E+03	SXY = -3.953E+03					
.	55 /	MX = 0.	-ZFACE SX = -4.708E-09	-ZFACE	5.627E+03	-2.778E+03	4.202E+03	-54.909
75. /	73	MY = 0.	SY = 2.849E+03				VM 7.417E+03	
---	---	MXY = 0.	SXY = -3.953E+03					
X2.	76	FX = 2.273E+03	+ZFACE SX = -7.373E+02	+ZFACE	2.107E+03	-1.472E+03	1.790E+03	-63.050
.	.	FY = -1.644E+03	SY = 1.372E+03				VM 3.116E+03	
.	QUAD / 77	FXY = 3.052E+03	SXY = -1.446E+03					
.	62 /	MX = -5.016E+02	-ZFACE SX = 5.282E+03	-ZFACE	9.350E+03	-8.727E+03	9.039E+03	28.319
83. /	84	MY = 5.026E+02	SY = -4.659E+03				VM 1.566E+04	
---	---	MXY = -7.496E+02	SXY = 7.549E+03					
X2.	77	FX = 1.576E+03	+ZFACE SX = -1.031E+03	+ZFACE	1.930E+03	-3.301E+03	2.616E+03	-49.021
.	.	FY = 2.356E+00	SY = -3.193E+02				VM 4.582E+03	
.	QUAD / 78	FXY = 3.966E+03	SXY = -2.590E+03					
.	63 /	MX = -4.378E+02	-ZFACE SX = 4.203E+03	-ZFACE	1.296E+04	-8.436E+03	1.870E+04	39.778
84. /	85	MY = -3.361E+01	SY = 3.240E+02				VM 1.867E+04	
---	---	MXY = -1.093E+03	SXY = 1.052E+04					
X2.	78	FX = 5.469E+02	+ZFACE SX = -1.971E+02	+ZFACE	2.542E+03	-2.520E+03	2.531E+03	-47.359
.	.	FY = 1.459E+02	SY = 2.192E+02				VM 4.383E+03	
.	QUAD / 79	FXY = 3.512E+03	SXY = -2.522E+03					
.	64 /	MX = -1.240E+02	-ZFACE SX = 1.291E+03	-ZFACE	1.025E+04	-8.884E+03	9.566E+03	43.175
85. /	86	MY = 1.220E+01	SY = 7.270E+01				VM 1.658E+04	
---	---	MXY = -1.006E+03	SXY = 9.547E+03					
X2.	79	FX = -6.571E+02	+ZFACE SX = 2.229E+02	+ZFACE	2.441E+03	-2.507E+03	2.474E+03	-42.032
.	.	FY = -9.351E+01	SY = -2.856E+02				VM 4.285E+03	
.	QUAD / 80	FXY = 2.526E+03	SXY = -2.461E+03					
.	65 /	MX = 1.467E+02	-ZFACE SX = -1.537E+03	-ZFACE	6.839E+03	-8.275E+03	7.557E+03	48.112
86. /	87	MY = -3.254E+01	SY = 1.817E+02				VM 1.311E+04	
---	---	MXY = -8.311E+02	SXY = 7.512E+03					
X2.	80	FX = -1.628E+03	+ZFACE SX = 5.871E+02	+ZFACE	2.059E+03	-1.557E+03	1.808E+03	-39.645
.	.	FY = -6.948E+01	SY = -8.490E+01				VM 3.142E+03	
.	QUAD / 81	FXY = 1.565E+03	SXY = -1.776E+03					
.	66 /	MX = 3.692E+02	-ZFACE SX = -3.843E+03	-ZFACE	3.310E+03	-7.207E+03	5.759E+03	55.557
87. /	88	MY = -2.571E+00	SY = -5.405E+01				VM 9.315E+03	
---	---	MXY = -5.568E+02	SXY = 4.906E+03					
X2.	81	FX = -2.136E+03	+ZFACE SX = 7.995E+02					



FY = -2.423E+01  
 FXY = 5.378E+02  
 MX = 4.925E+02  
 MY = 4.435E+01  
 MXY = -1.967E+02

SY = 2.418E+02  
 SXY = -6.426E+02  
 -ZFACE SX = -5.111E+03  
 SY = -2.903E+02  
 SXY = 1.718E+03

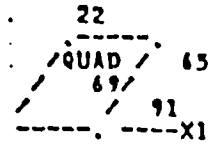
+ZF 1.221E+03 -1.798E+02 7.005E+02 -33.272  
 VM 1.320E+03  
 -ZFACE 2.595E+02 -5.660E+03 2.960E+03 72.257  
 VM 5.794E+03



FX = -1.067E+03  
 FY = -1.009E+03  
 FXY = 2.681E+02  
 MX = -3.488E+02  
 MY = -1.654E+02  
 MXY = -3.991E+01

+ZFACE SX = -1.051E+04  
 SY = -5.987E+03  
 SXY = -4.218E+02  
 -ZFACE SX = 6.237E+03  
 SY = 1.952E+03  
 SXY = 1.494E+03

+ZFACE -5.948E+03 -1.055E+04 2.299E+03 -84.714  
 VM 9.158E+03  
 -ZFACE 6.707E+03 1.483E+03 2.612E+03 17.445  
 VM 6.102E+03



FX = 4.513E+02  
 FY = 3.551E+03  
 FXY = -6.563E+02  
 MX = 2.418E+02  
 MY = 8.498E+01  
 MXY = -3.342E+01

+ZFACE SX = 6.707E+03  
 SY = 9.142E+03  
 SXY = -2.114E+03  
 -ZFACE SX = -4.902E+03  
 SY = 5.063E+03  
 SXY = -5.106E+02

+ZFACE 1.036E+04 5.484E+03 2.440E+03 -59.969  
 VM 8.981E+03  
 -ZFACE 5.089E+03 -4.928E+03 5.009E+03 -87.075  
 VM 8.676E+03

Quadrilateral Stresses and Forces for Output Vector

APPENDIX 2.10.3 TEST LOG ANALYSIS cont'd.

Revision 0

2.11 APPENDIX

ENGINEERING DROP TEST FOR 1-13C II  
SHIPPING PACKAGE

2.11.1 SCOPE

This appendix summarizes the plans for, conduct of, and results from the engineering drop test for the 1-13C II shipping package.

2.11.2 REFERENCES

Prior to performing the drop test, numerous planning documents were generated detailing data collection procedures and acceptance criteria. These reference documents are included in microfiche form in Section 2.11 on the microfiche entitled "2.11 Appendix: Drop Test Report Reference Documents 1-13C II Shipping Package." The documents include:

- 2.11.2.1 CNSI Procedure NE-TI-001, Rev. -, Drop Test Procedure for CNS-1600 Shipping Package 1-13C II: This document summarizes the planned sequence of events for the package drop test.
- 2.11.2.2 NuPac Procedure DT-01, Rev. 2. Drop Test Requirements Hypothetical Accident Conditions (Type "B") for the 1-13C Model 1600 Package: This document summarizes the drop test objectives, general strategy, and performance criteria. Included in this document are detailed procedures for obtaining bolt force measurements and dimensional survey data.
- 2.11.2.3 CNSI Procedure, 5-QP-004, Rev. -, "Liquid Penetrant Inspection Procedure: This inspection procedure, in conjunction with the Industrial NDT procedure QCP-401 reporting format, was used to perform dye penetrant pre- and post-tests.



- 2.11.2.4 NuPac Document CL-01, Rev. 0, Gamma Scan of CNSI Model 1600 Cask: This document, in conjunction with references 2.11.2.6 and 2.11.2.7, was used to perform the post-test gamma scan of the 1-13C II cask body.
- 2.11.2.5 X-Ray, Inc. Procedure No. VT-001 Visual Inspection of Weldments and Adjacent Materials.
- 2.11.2.6 NuPac Document GS-002, Rev. 0, General Procedure for Gamma Scan of Shielded Containers - Field Calibration Method.
- 2.11.2.7 Industrial NDT Procedure 601, Ultrasonic Testing for Metal Thickness and Soundness.

2.11.3 DETAILED PROCEDURE: CONDUCT OF DROP TEST2.11.3.1 Overview and Summary

The 1-13C II drop test was conducted in September, 1980, at the Chem-Nuclear site in Barnwell, South Carolina. Numerous pre-tests were performed to establish shielding integrity, and package dimensions of a 1-13C II cask. In the actual drop sequence, the cask was loaded with a dummy payload, sealed, and fitted in its transport overpack. The package was then lifted to a height of 30 feet and dropped vertically onto a concrete pad. After this bottom end flat drop, a new overpack pair was installed and the package was again dropped from a height of 30 feet, this time with the top (lid) end down and a package centerline orientation of approximately  $40^\circ$  with respect to horizontal. Following this top end oblique drop, post-test inspections were accomplished to document package changes and to verify post-drop shielding integrity. The package survived both drops, meeting all post-test shielding acceptance criteria. The overpacks, although deformed, did not fail. The cask itself was intact except for one cracked lid bolt boss which occurred because of interference between bolt force measurements transducers and the overpack tiedown plate. This interference allowed the overpack to load lid bolt heads in bending introducing a severe and unrealistic moment into the bolt boss. Furthermore, a dimensional review showed that if the maximum bolt head diameter (i.e., width across corners) was used, the edge of the 3 inch clearance hole in the overpack would contact the bolt head before the internal side wall of the overpack would contact the side of the cask. Modifications have since been made to the overpack to enlarge this 3 inch clearance hole to 3.548 inches. This dimensional change allows for sufficient clearance to eliminate interference between overpack tiedown plate and lid bolts. This modification is expected to have no effect on the energy absorbing capabilities of the overpacks. Also, a 1/8 inch thickness of neoprene has been added, as an option, to the inner vertical walls of both the upper and lower overpacks. This neoprene was added exclusively to minimize any chafing between the overpacks and cask,

and is not required to eliminate any previous tolerance problem in the area of the cask lid bolts. In addition, flat washers of 2 1/2 inches outside diameter have been added under each of the twelve lid bolts to eliminate any potential of galling between the bolt heads and the contact surface of the lid.

The remainder of this section provides a summary narrative of test procedures, with an emphasis on those areas which deviate from the planning documents (references 2.11.2.1 through 2.11.2.8).

#### 2.11.3.2 Pre-test Liquid Penetrant Inspection

On September 23, 1980, a certified inspector from Industrial NDT Company, Inc., performed a liquid penetrant inspection of all package weldments. The liquid penetrant inspection was observed by a CNSI Quality Assurance Representative to verify the integrity of the data and adherence to the written inspection procedures.

#### 2.11.3.3 Pre-test Gamma Scan

A pre-test gamma scan was performed on the 1-13C II cask on September 26, 1980, with the intention of comparing the results with post-drop data to determine shielding integrity. A Cobalt-60 (9 curies) source certified by Pittsburgh Testing Laboratory was used in the test. Unfortunately, following the conclusion of testing, the gamma scan technician discovered that the scintillator being used had a cracked crystal, thus invalidating all of the pre-test gamma scan data. The original strategy was therefore revised so that post-drop gamma scan data were compared with a calibration curve equal to nominal cask lead thicknesses. Acceptance criteria were also revised so that any obtained readings exceeding nominal lead thickness minus 10% were designated failure.

#### 2.11.3.4 Package Preparation

Following dimensional measurements of the package, the package was loaded and sealed. A 3,000 pound dummy payload of sand and lead shot was loaded into the cask. The lid gasket and lid were then put on the cask and the lid bolts torqued to 330 ft.-lbs. (lubricated). After installing bolt force measurement instrumentation, the cask was inserted in its upper and lower overpacks. Ratchet binders connecting the overpacks were torqued to 70 ft.-lbs. and the entire package weighed. Final package weight, verified by CNSI Quality Assurance representatives, was 26,500 pounds. Photo F1 shows the package being put into the lifting sling just prior to the flat end vertical drop.

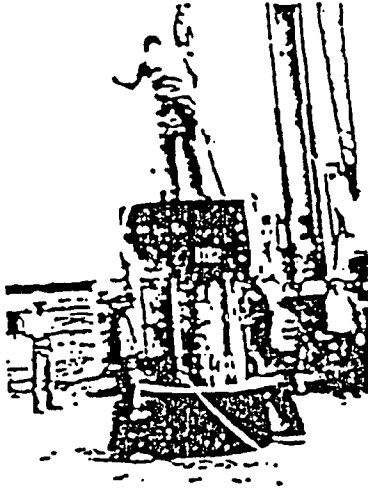
#### 2.11.3.5 Photographic Documentation

The drop test was documented in great detail photographically. Actual drop sequence (bottom end vertical and top end oblique) were recorded using a high speed 16mm movie camera shooting 500 frames per second on negative color film. The camera was placed so that it would record the package falling in front of a plywood backdrop with a 6 inch grid pattern. Drop sequences were also recorded at normal speed (24 frames per second) on 16mm negative color film. In addition to the movies, still pictures were taken of the drop sequences (35mm, ten frames per second). Finally, numerous 35mm color stills were obtained before and after each drop to provide detailed documentation of pre- and post-drop package condition.

#### 2.11.3.7 Bolt Force Measurement

Prior to installing the upper overpack, the instrumentation to measure bolt tension was implemented. Bolt tension was monitored by custom fabricated load cells. The cells were designed to fit under bolt heads as washers. They were compressed between the bolt head and lid top surface when the bolts were torqued down. Strain gage

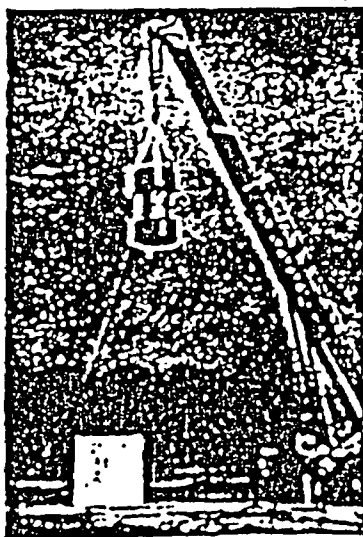
PREPARATION FOR BOTTOM END VERTICAL DROP



1 F1  
ATTACHING THE LIFTING SLING  
TO UPPER OVERPACK.



1 F2  
SLING HARDWARE BEING ATTACHED TO  
QUICK RELEASE HOOK ON CRANE.



1 F3  
FINAL CASK ORIENTATION AT 30°  
JUST PRIOR TO BOTTOM END VERTICAL DROP.

circuits inside the cells generated electrical signals proportional to the force between bolt head and container lid, thereby allowing bolt tension determination. In the original plan (see reference 2.11.2.2, Section 3.0), four force load cells were to be installed beneath the lid bolts, equally spaced at 90°. However, the General Electric technician conducting the bolt tension measurement alerted Chem-Nuclear personnel to the possibility of force washers being damaged during the first drop. Since only four of the custom force washers were available for the entire test, it was decided to install two of them during the first drop. All four could then be used for the second drop if no damage occurred during the first drop. Accordingly, force washers #1 and #2 were installed under two lid closure bolts 90° apart and electrically connected to a Vishay P-350A strain indicator. In Photo F1, cables connecting the force washers to the instrumentation are visible. Calibration resistors, supplied by the washer manufacturer, were shunted across each washer's bridge circuit, and the indication per simulated force level was noted. The sealing bolts were torqued to 200 ft.-lbs. and the force washer output levels recorded. While the cask was being prepared for the first drop and raised to the 30 foot drop height, the force washers were connected to the Accudata Signal Conditioners, which were in turn, tied into the instrumentation system. Immediately prior to the 10 second countdown, a calibration was recorded on the tape recorder and oscillograph. Pre-test force washer readings with 200 ft.-lbs. of torque on the bolts were 15,700 pounds on #1, and 9,600 pounds on #2.

#### 2.11.3.8 First Drop: Vertical Bottom End

The cask and overpacks were put in a lifting sling which was attached to a quick release hook on the crane (see photo F2). The entire package was then raised to a height of 30 feet above the concrete dop pad as shown in photo F3. Also shown are the instrumentation cables and tag lines. Photos F4 to F7 depict the package during the actual drop: the cask impacted on the target, rebounded to height of about 8 inches, then impacted again at a slightly oblique angle and came to rest.

Photos F8 to F19 illustrate in greater detail package behavior during the first drop. Under secondary impact, the package rotated slightly and impacted on the corner between quadrants I and IV, causing slight mushrooming confined to the lower five inches of the lower overpack (see photo F16). No general crush of the lower overpack was evident at this time. The upper surface of the lower overpack demonstrated ballooning due to the compressive forces of the foam (see photos F14 and F15). The impact in quadrants I and IV caused the ratchet binders on that side to deform and to buckle (see photo F17). On the opposite side (quadrants II and III), the ratchet binders were loaded with tensile forces, but there was little evidence of distress except in the attached clevis bolts, as seen in photo F18. The upper overpack showed corresponding compression and tensile loading, although there was no distress to ratchet binder lugs or to the overpack shell itself.

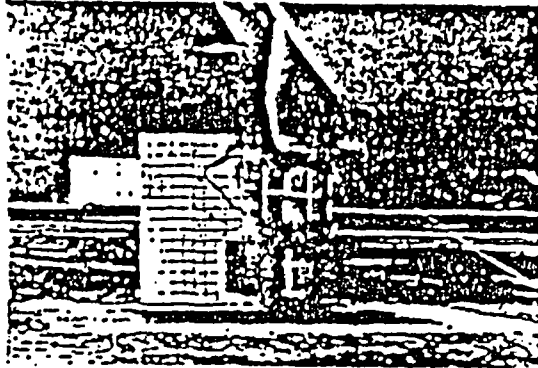
Although not evident in these photos, force washer #2 had its lead lines severed 80 milliseconds after impact and experienced undetermined internal damage. Bolt force measurement data showed that the pre-test load (15,700 pounds on force washer #1 and 9,600 pounds on #2, with 200 ft.-lbs. of torque on the bolts) were not permanently reduced by the impact of the drop. In fact, they were slightly increased. Temporary reduction of the initial clamping force by approximately 20% was seen for less than 4 milliseconds at impact. Otherwise, the clamping force was increased slightly and remained so after impact perturbations had ceased.

In summary, visual examination of the package indicated absolutely no damage to the 1-13C II cask body or lid. The overpacks and ratchet binders did not fail, although the lower overpack sustained moderate damage.

#### 2.11.3.9 Drop II: Top End Oblique Drop

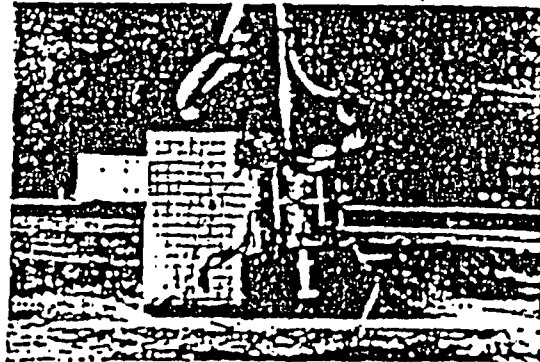
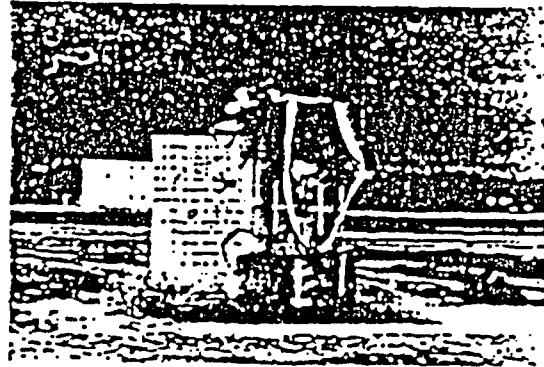
In preparation for this drop, the overpacks used in previous tests were removed and new ones installed. During this process, force

FIRST DROP: BOTTOM END VERTICAL DROP



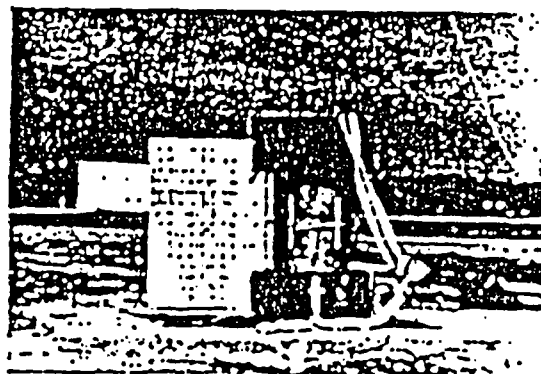
← F4 (LEFT)  
I-13C PACKAGE JUST PRIOR  
TO INITIAL IMPACT.

F5 (RIGHT) ←  
PACKAGE IN REBOUND  
AFTER INITIAL IMPACT.



← F6 (LEFT)  
SECONDARY IMPACT.

F7 (RIGHT) ←  
PACKAGE AT REST AFTER  
BOTTOM END VERTICAL DROP.





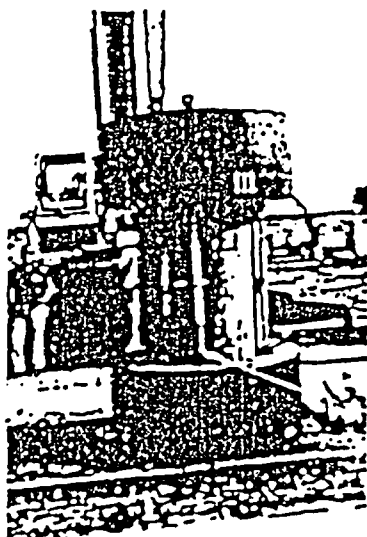
OVERALL PACKAGE CONDITION AFTER BOTTOM END VERTICAL DROP



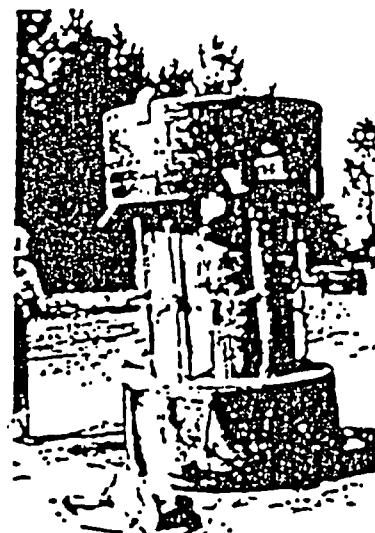
I F8  
COMPRESSIVE CRIPPLING OF OVERPACK  
PATCHET BINDERS IN QUADRANT I;  
NO DAMAGE TO CASK.



I F9  
COMPRESSIVE CRIPPLING OF PATCHET  
BINDERS IN QUADRANT IV;  
NO DAMAGE TO CASK.

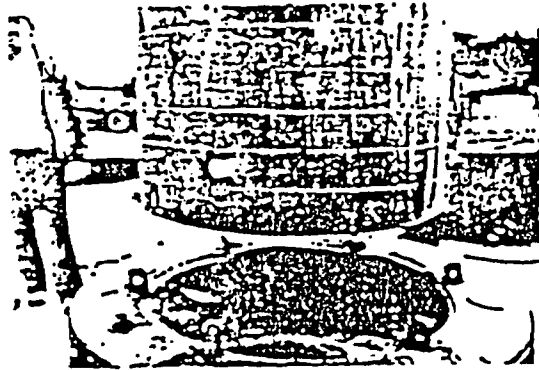


I F10  
TENSILE LOADING OF PATCHET BINDERS  
IN QUADRANT III;  
NO DAMAGE TO CASK.



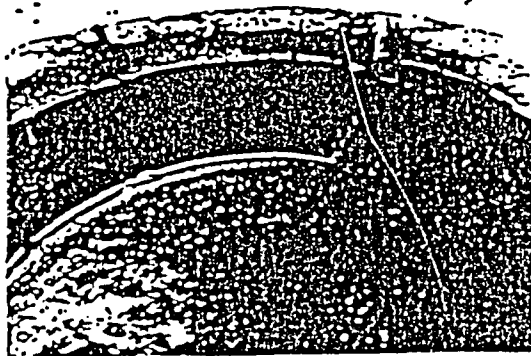
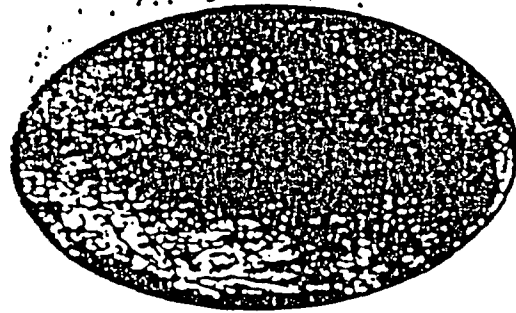
I F11  
TENSILE LOADING OF PATCHET BINDERS  
IN QUADRANT II;  
NO DAMAGE TO CASK.

VERTICAL DROP DAMAGE: DETAILED VIEWS



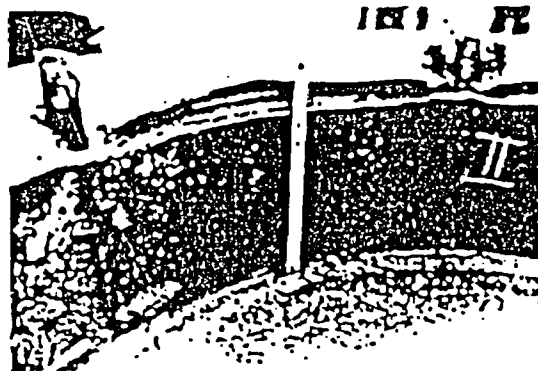
F12 (LEFT) —  
REMOVAL OF CASK FROM LOWER  
OVERPACK AFTER VERTICAL DROP.

F13 (RIGHT) —  
UNDAMAGED BOTTOM END OF L-13C CASK  
FOLLOWING 30' VERTICAL DROP.

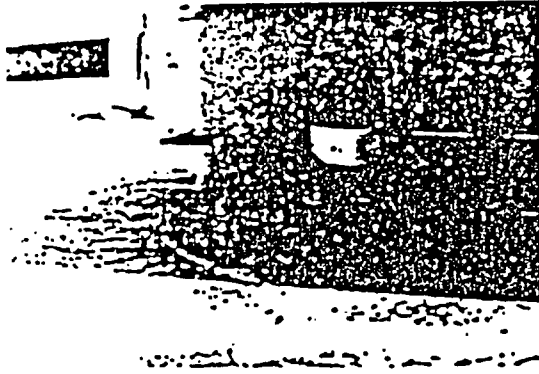


F14 (LEFT) —  
LOWER OVERPACK DAMAGE IN QUADRANT I:  
"COOKIE CUT" TEAR DUE TO COMPRESSION  
(LEFT), MUSHROOMING AND TEARING -  
(RIGHT) CAUSED BY TENSILE LOADS.

F15 (RIGHT) —  
MUSHROOM TEAR SHOWN IN F14, DETAILED  
VIEW: TEAR EXTENDS INTO QUADRANT II,  
AND INTERIOR FOAM IS VISIBLE.

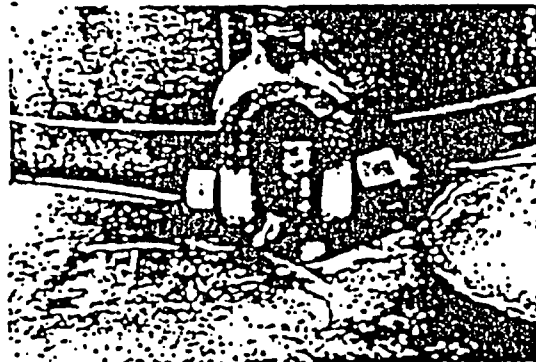
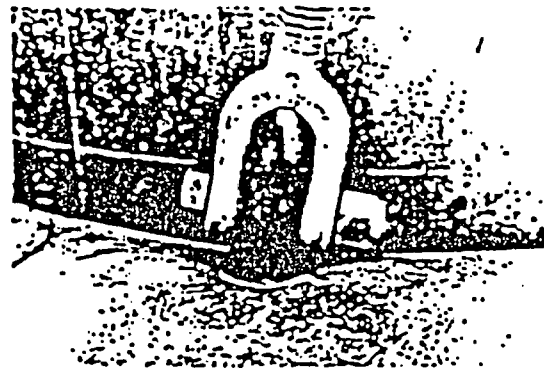


BOTTOM END VERTICAL DROP DAMAGE DETAILS (CONTINUED)



← F16 (LEFT)  
FINAL LOWER OVERPACK ORIENTATION  
FOLLOWING VERTICAL DROP, PAINT  
PATTERN ON DROP PAD SHOWS PACKAGE  
POSITION AT INITIAL IMPACT.

F17 (RIGHT) →  
RATCHET BINDER LUG (#2 BETWEEN  
QUADRANTS I AND IV) SHOWING  
CRIPPLING OF RATCHET BINDER; ALSO,  
DUCTILE TEAR OF LUG TO OVERPACK  
SHELL WELD; LUG REMAINS FIRMLY  
ATTACHED TO VERTICAL CYLINDRICAL  
WALL OF OVERPACK SHELL.



← F18 (LEFT)  
RATCHET BINDER (#3, IN QUADRANT  
II) SHOWING FLEXURAL YIELDING OF  
BOLT TO LUG UNDER RATCHET BINDER  
TENSILE LOADING; LUG REMAINS FIRMLY  
ATTACHED TO OVERPACK SHELL.

F19 (RIGHT) →  
UPPER OVERPACK LUG IN COMPRESSIVE  
REGION; NO DISTRESS TO LUG OR TO  
OVERPACK SHELL; NO DAMAGE TO UPPER  
OVERPACK OR CASK.

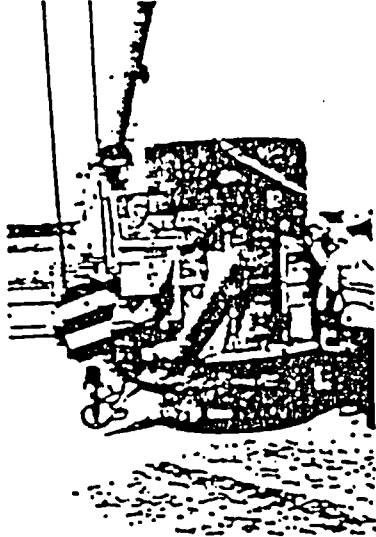


washers #3 and #4 were installed at  $90^{\circ}$  angle from force washers #1 and #2. Although the #2 force washer had been damaged during the first drop, an attempt was made to use it as well as force washer #1. The specially made top impact lift fixture, orienting the package of  $40^{\circ}$ , was installed and the force washer instrumentation cables were secured so that they would not be damaged or loosened during the cask drop. The package was lifted to a height of 30 feet and oriented at approximately  $40^{\circ}$  with respect to horizon. Photos T1 and T4 depict preparation for the oblique drop.

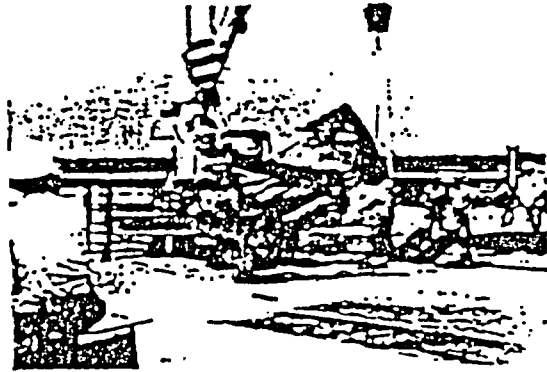
When the package was dropped, initial impact was on the Quadrant IV corner of the upper (lid end) overpack as shown in photo T5. It then rebounded, and the lower overpack experienced initial slapdown impact (see photo T6). The upper overpack impacted a second time while the lower overpack was still in rebound (photo T7).

The lower overpack experienced second and third slapdown impacts, and the package came to rest (see photo T8). At initial impact, all four force washers were destroyed and no significant data was transmitted. Visual inspection of the package (discussed at length in the next section) after the oblique drop revealed some crushing in both the top and bottom overpacks, but no bottom-out. Bottom-out was defined as a deformation of the overpacks exceeding 95% of the overpack foam thickness measured perpendicular to the crush plane. Had this occurred, a third (bottom end oblique) drop would have been necessary. The conditional third drop was waived and post-test inspections commenced.

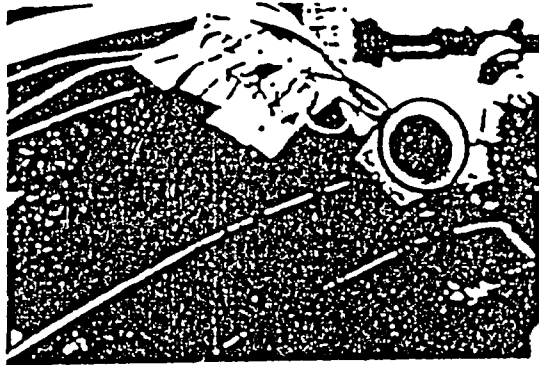
PREPARATION FOR TOP END OBLIQUE DROP



I T1  
CASK IN NEW OVERPACKS WITH  
SPECIAL LIFT FIXTURE ATTACHED.



I T2  
ROTATION OF PACKAGE TO OBLIQUE  
390° ORIENTATION.

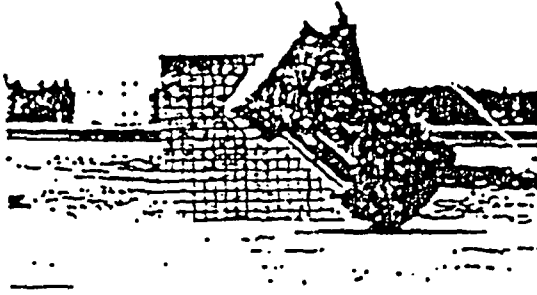


I T3  
ANGULAR MEASUREMENTS VERIFYING  
40° ORIENTATION.



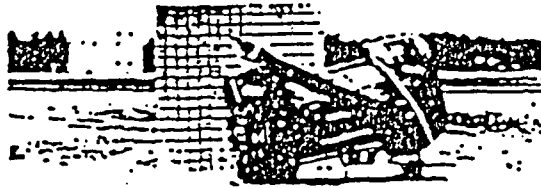
I T4  
PACKAGE BEING RAISED TO 33'  
HEIGHT PRIOR TO SECOND DROP.

SECOND DROP: TOP END OBLIQUE DROP

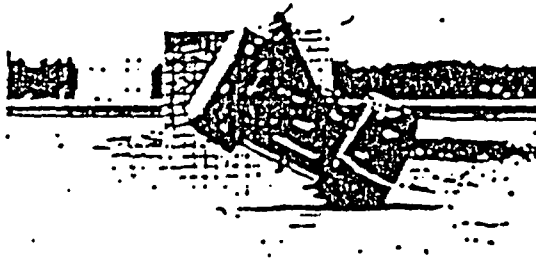


← T5 (LEFT)  
INITIAL IMPACT: CORNER OF  
UPPER OVERPACK.

T6 (RIGHT) ←  
INITIAL SLAPDOWN OF LOWER  
OVERPACK; UPPER OVERPACK  
IN REBOUND.



← T7 (LEFT)  
SECONDARY IMPACT OF UPPER  
OVERPACK; LOWER OVERPACK  
IN REBOUND AFTER SLAPDOWN  
IMPACT.



T8 (RIGHT) ←  
PACKAGE AT REST AFTER TOP END  
OBLIQUE DROP.



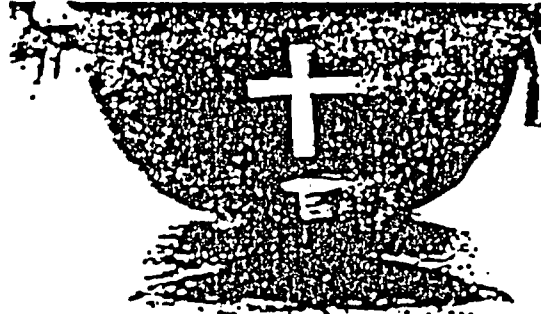
2.11.2.10 Post-test Visual Inspection

Photos T9 and T20 illustrate post-test visual examination findings. It should be noted that the drop orientation was selected to maximize potential damage to the cask lid and to the upper overpack shell. In spite of this "worst case" strategy, the upper overpack shell evidenced only moderate compression (photo T9). Furthermore, although the tiedown lugs deformed to conform to the overpack shell shape, there was only moderate distress in the vicinity of the tiedown lugs and to rupturing or tearing (photo T10).

The interior upper overpack shell likewise suffered little damage, although it caused problems with the force washer instrumentation. Photo T16 shows that bolt relief holes fashioned to accommodate the force washer instrumentation cables which had to be routed through the upper overpack. Unfortunately, inadequate clearances in the relief holes caused the vertical inner walls of the overpack to impact on the sides of the force washers. This lateral impact greatly increased the loads applied to the cask closure bolts. In the most extreme case, this resulted in a crack around 3/4 of the circumference of a lid bolt boss (photo T17). The boss was also raised 1/8 inch above the cask top surface. It should be noted that in service, no such loads would be used. In addition, the clearance holes in the overpack which receive the lid bolts have been enlarged from 3 inches to 3.548 inches, and a 1/8 inch thickness of neoprene has been added, as an option, to the inner vertical walls of both the upper and lower overpacks. Hence, the failure can be considered the result of an unrealistic over-test. The lateral impact also destroyed the force washers (see photo T18).

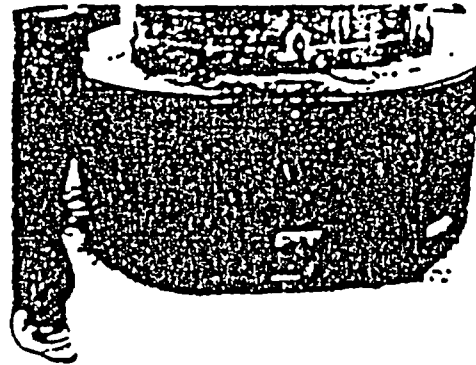
Visual inspection of the lower overpack, which experienced three slapdown impacts, showed only minor damage. In photo T14, the cask registry can be seen running along the circumference of the inside lower plate. There was no rupturing or tearing of the interior shell, however. Also shown is slight paint distress indicating some yielding along the vertical weld attaching ratchet binders in

OVERALL PACKAGE CONDITION AFTER TOP END OBLIQUE DROP



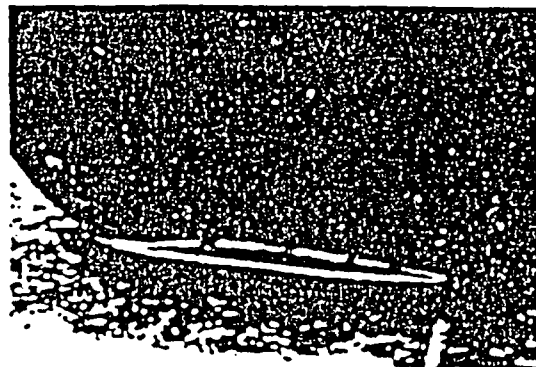
— T9 (LEFT)  
INITIAL IMPACT POSITION OF UPPER  
OVERPACK AS EVIDENCED BY PAINT  
ON DROP PAD.

T10 (RIGHT) —  
MODERATE CORNER AND SIDE  
COMPRESSION OF UPPER OVERPACK  
SHELL; ONLY MINOR DEFORMATION  
OF OUTER CYLINDRICAL WALL IN  
VICINITY OF TIE-DOWN LUGS.



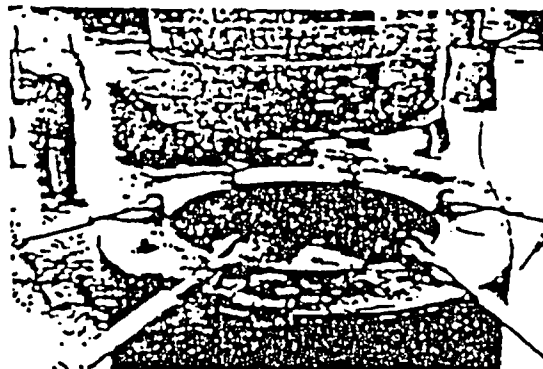
— T11 (LEFT)  
EFFECTS OF SLAPDOWN IMPACTS  
ON LOWER OVERPACK SHELL;  
SCALLOPED DEFORMATION CAUSED  
BY RETENTION CHAINS.

T12 (RIGHT) —  
EFFECTS OF LOWER OVERPACK SLAPDOWN  
IMPACT; FLATTENING IS LESS THAN  
2.5 INCHES.



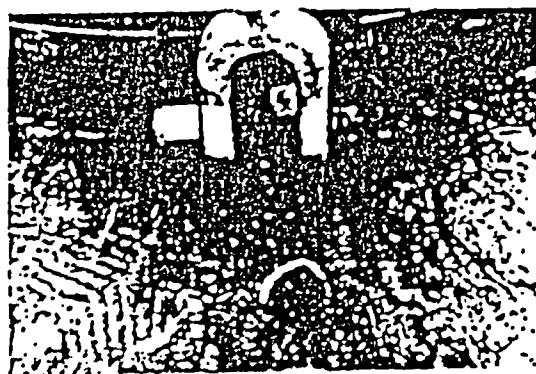
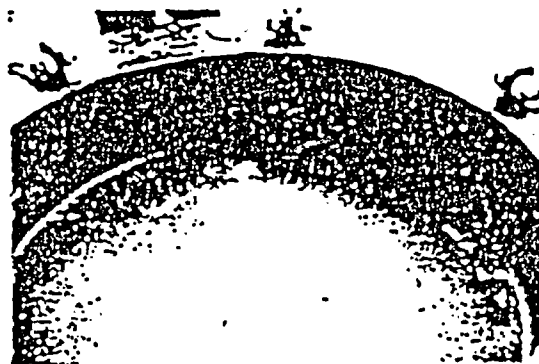


TOP END OBLIQUE DROP DAMAGE: DETAILED VIEWS



— T13 (LEFT)  
REMOVAL OF UNDAMAGED CASK FROM LOWER  
OVERPACK AFTER OBLIQUE DROP; UPPER  
OVERPACK USED IN SECOND DROP IS  
SHOWN IN BACKGROUND.

T14 (RIGHT) —  
LOWER OVERPACK, WHICH EXPERIENCED  
TWO SLAPDOWN IMPACTS, SHOWS NO  
TEARING OR DISTRESS; CASK IMPRINT  
RUNS ALONG CIRCUMFERENCE OF LOWER  
OVERPACK PLATE.

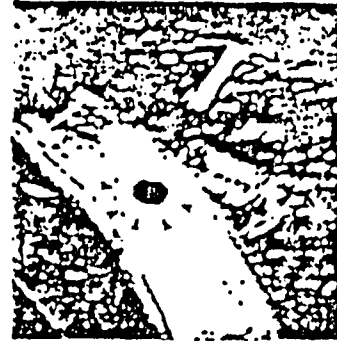


— T15 (LEFT)  
SLIGHT PAINT DISTRESS AT LOWER OVERPACK  
PATCHET BINDER LUG ATTACHMENT INDICATES  
MODEST STRAINS ABOVE MATERIAL ELASTIC  
LIMITS; NO RUPTURES OF OUTER OVERPACK  
SHELL OCCURRED.

TOP END OBLIQUE DROP DAMAGE DETAILS  
(CONTINUED)



I T15 (ABOVE)  
INTERIOR OF UPPER OVERPACK, WHICH EXPERIENCED INITIAL IMPACT; BURN MARKS ARE FROM TORCHING OF CASK LID BOLT RELIEF HOLES TO ACCOMMODATE FORCE WASHER INSTRUMENTATION CABLES.



I T17 (ABOVE)  
CIRCUMFERENTIAL CRACK ON CASK LID BOLT BOSS CAUSED BY LATERAL IMPACT OF OVERPACK LID BOLT RELIEF HOLE ON FORCE WASHER.



I T18 (LEFT)  
FORCE WASHER #3, DESTROYED BY LATERAL IMPACT OF OVERPACK BOLT RELIEF HOLES; INADEQUATE CLEARANCES IN BOLT RELIEF HOLES RESULTED IN OVERTEST OF CASK CLOSURE BOLTS.

T19 (BELOW)  
CASK LEAK CHECK AFTER OBLIQUE DROP; DESPITE DAMAGE TO FORCE WASHERS AND CASK LID BOLT BOSS, LEAK RATES DID NOT EXCEED ACCEPTANCE LIMITS.



I T20 (LEFT)  
CASK LID AND BODY FOLLOWING SECOND DROP; CASK REMAINS UNCHANGED EXCEPT FOR CRACKED LID BOLT BOSS AND OVERPACK PAINT REGISTRY MARKS.

Quadrants II and III to the overpack inner shell. Photo T15 shows additional paint distress on the upper surface of the lower overpack at the ratchet binder lug attachment. Although this indicates modest strains above material elastic limits, there were no ruptures or tears of the outer overpack shell.

#### 2.11.3.11 Post-test Dimensional Checks and Bolt Retorquing Values

The cask lid bolts were retorqued to their original values of 330 ft.-lbs. and the number of degrees required to obtain this value was documented. Not surprisingly, the two bolts requiring the most retorquing to obtain original values were those closest to the impact plane after the second drop. Lid bolts #5 and #9 required 25° and 15° respectively to obtain 330 ft.-lbs.; both were adjacent to the torn boss insert under Force Washer #2.

Post-drop cask diametrical measurements were also obtained. These measurements were identical to the pre-drop measurements within error tolerance (1/8 inch).

#### 2.11.3.12 Dye Penetrant Post-test

On October 2, 1980, the post-test liquid penetrant inspection was performed by Industrial NDT Company, Inc. Results were identical to pre-test findings with the exception of the cracked bolt hole boss discussed earlier.

#### 2.11.3.13 Post-test Gamma Scan

Due to equipment difficulties noted earlier, the post-test gamma scan was not concluded until February, 1981. The test was performed by the Quality Assurance Manager of Nuclear Packaging, Inc., of Tacoma, Washington. The following preliminary inspections were performed and verified:

- A. Exterior surface wipe test.
- B. Weld integrity of external heat shield welds.
- C. Cask dimensions

The cask surface was gridded in four inch squares, and the probe and source were calibrated in accordance with Gamma Scan Procedure No. GS-002, Rev. 0. The cask was first scanned without the 9 curie Cobalt 60 source, and all readings were recorded on a grid map corresponding to the cask surface. The source was then inserted into the cask, calibration rechecked, and a normal gamma scan completed. The "background" readings (no source in cask) for each grid were subtracted from readings obtained with the source in the cask. Obtain differences were the actual gamma readings in millirems per hour for each grid. Cask lead integrity was shown to be fully acceptable with no detectable lead settlement.

Gamma scan of the cask lid was not practical, so it was subjected to ultrasonic soundness inspection, performed by a certified Industrial NDT technician. No relevant indications were detected.

#### 2.11.4 TEST RESULTS/DATA

##### 2.11.4.1 Summary

Inspections and tests of the 1-13C II cask provided dramatic confirmation that the package is structurally adequate to survive accidental drops from 30 feet, in any orientation. The overpacks, although deformed, did not fail. The lid was not deformed. The cask itself was not deformed except in areas deformed by testing instrumentation. Post-drop package shielding capabilities, as measured by gamma scan data, were clearly acceptable. The damage which was sustained by the lid bolt boss noted previously is not expected to occur if the cask is subjected to hypothetical accident conditions in the future.

A potential interference problem existed between the bolt head (i.e., width across corners) and the edge of the 3 inch clearance hole in the overpack. The overpacks have since been modified to enlarge the lid bolt clearance holes from 3 inches to 3.548 inches. This eliminates any possibility of the overpack contacting the lid bolts when the package is subjected to hypothetical accident conditions.

Because of this design modification no damage is expected if the cask is again subjected to the hypothetical accident conditions. Therefore, the pre-accident cask condition is actually representative of the post-accident cask condition. Moreover, the pre-accident cask condition may be tested to demonstrate compliance with the post drop-test containment requirements of NUREG. 7.4 and ANSI N 14.5. This also affords the flexibility of making package design improvements without requiring additional testing. Additional package design improvements are noted as follows: An O-ring has been added to the lid to facilitate leak testing in accordance with NUREG. 7.4 and ANSI N 14.5 for assembly verification. There was no consideration given to this O-ring to enhance the sealing capabilities of the package. However, the addition of this O-ring does augment the existing sealing competence. The 3/8 inch thick silicone gasket has been reduced to a thickness of 1/4 inch to ensure metal to metal contact between the lid and the cask. This will result in more repeatable results when performing future leak tests.

#### 2.11.4.2 Dye Penetrant Inspections

Figures 2.11.4-1 and 2.11.4-2 show the pre-drop and post-drop dye penetrant inspections of the 1-13C II cask.

#### 2.11.4.3 Dimensional Checks

Figure 2.11.4-3 shows the pre- and post-test cask diametrical measurements. Pre-test figures are in the upper level and post-test measurements in the lower level. It was determined from a post-test dimensional survey completed at Barnwell, South Carolina, by CNSI Quality Assurance personnel that all pertinent areas of the cask lid which might have been affected by the drop test remained within fabrication tolerances.

Figure 2.11.4-4 is a sketch depicting the lower overpack after the bottom end vertical drop. Deformation of the upper overpack after top end oblique drop is shown in Figure 2.11.4-5.

#### 2.11.4.4 Gamma Scan Data

Figure 2.11.4-6 shows the calibration curve obtained prior to gamma scan of the 1-13C II cask. Also calculated in this figure are the gamma scan acceptance criteria derived by subtracting 10% from cask nominal lead thickness (which was 5.00 inches except at the lifting ear support band and in the tapered lid insertion area) and correlating these figures with calibration readings obtained with lead plates of the same thickness. The reader will note that the acceptance thresholds were 49.5 mR./hr. at lifting ear support band and 26.0 MR. for the rest of the cask. The 49.5 mR/hr. figure was projected, since no calibration lead plate with 3.82 inches thickness was available.

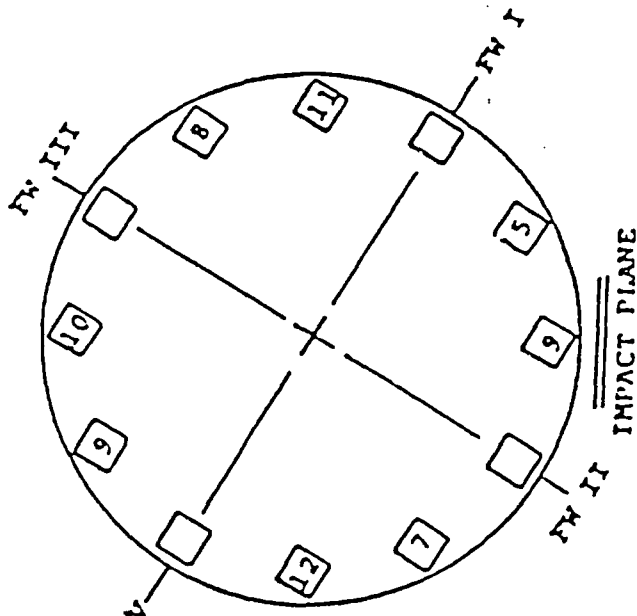
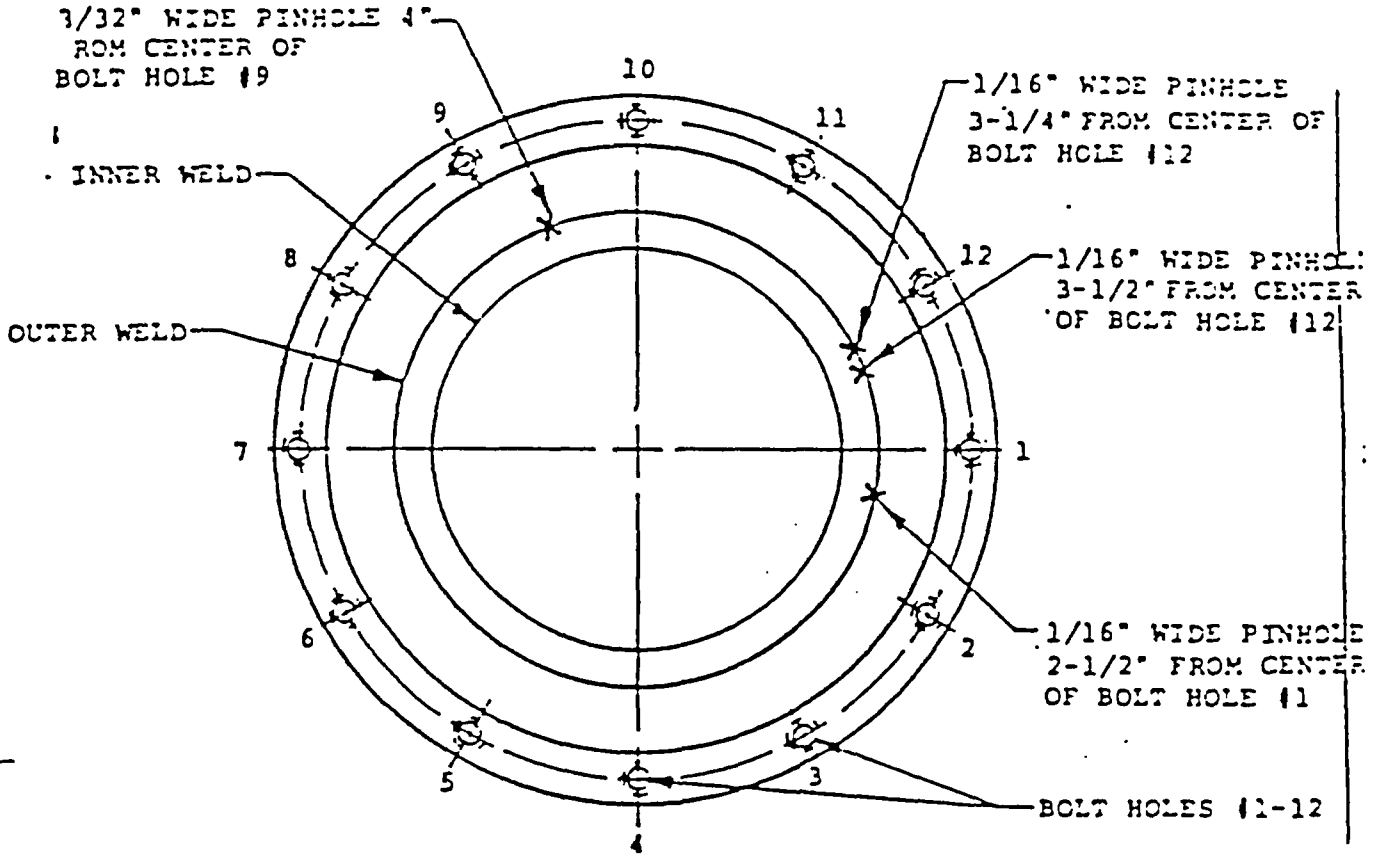
Figure 2.11.4-7 (3 pages) shows the post-test gamma scan with the 9 curie Cobalt 60 source inside the cask. No reading at lifting ear support band exceeds the maximum allowable limit of 49.5 mR./hr. No reading for the rest of the cask body exceeds the maximum allowable limit of 26.0 except in row 14. These higher readings are due to the taper present in the top area for insertion of the mating taper of the lid. At this taper, the cross section lead thickness is only about 50% of that in the main cask body.

#### 2.11.4.5 Bolt Force Measurement Data and Bolt Retorquing Data

Figure 2.11.4-8 shows a top down view of the cask lid bolts and force washers. Included in this sketch is the number of degrees to achieve original lid bolt torque values (330 ft.-lb.) after the two drops.

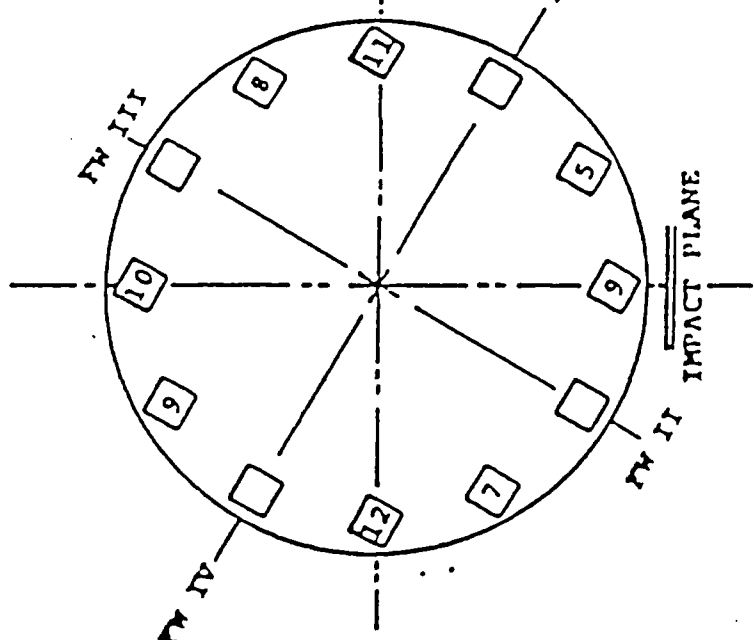
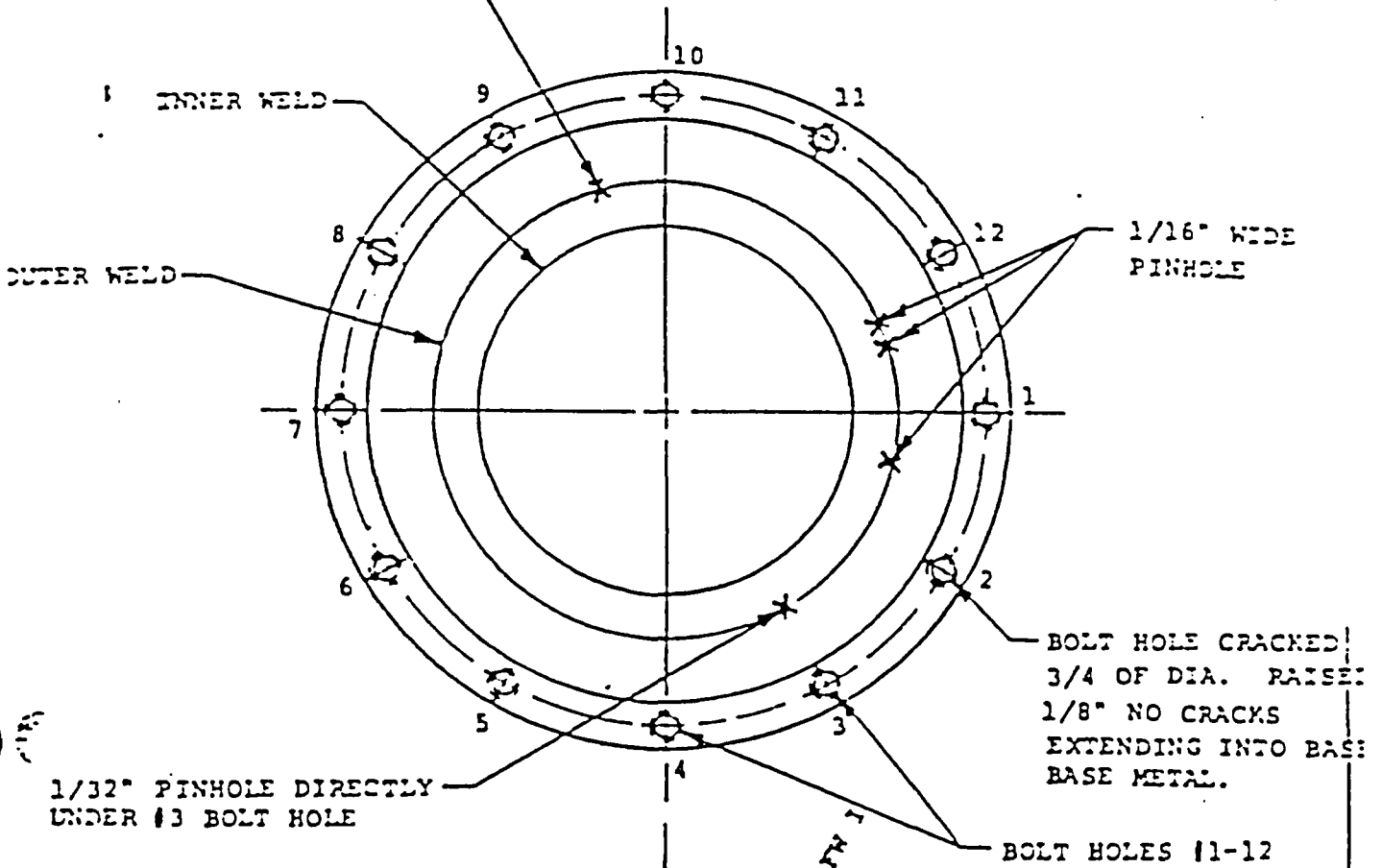
Bolt force time history for the first drop impact can be seen in Figure 2.11.4-9 (two pages).

FIGURE 2.11.4-1 PRE-TEST DYE PENETRANT RESULTS



CORRECTING ORIENTATION OF HOLE LOCATION NUMBERING SYSTEM USED ON ALL OTHER INSPECTIONS

FIGURE 2.11.4-2 POST TEST DYE PENETRANT FINDINGS  
3/32" WIDE PINHOLE



CORRESPONDING ORIENTATION OF HOLE LOCATION NUMBERING SYSTEM USED ON ALL OTHER INSPECTIONS



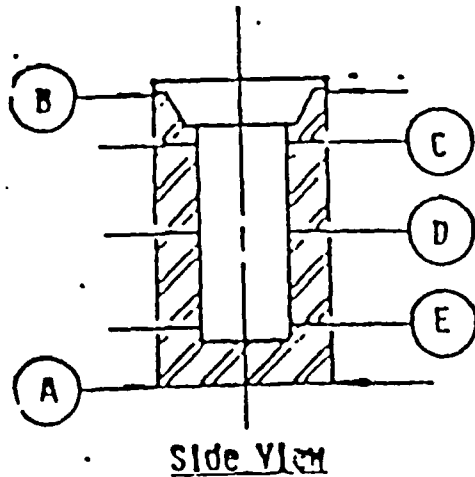
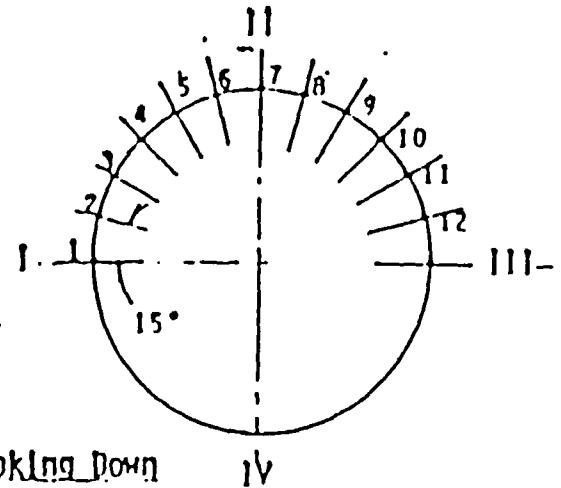


FIGURE 2.11.4-3  
 CASK DIAMETRICAL MEASUREMENTS  
 SUMMARY DATA SHEET

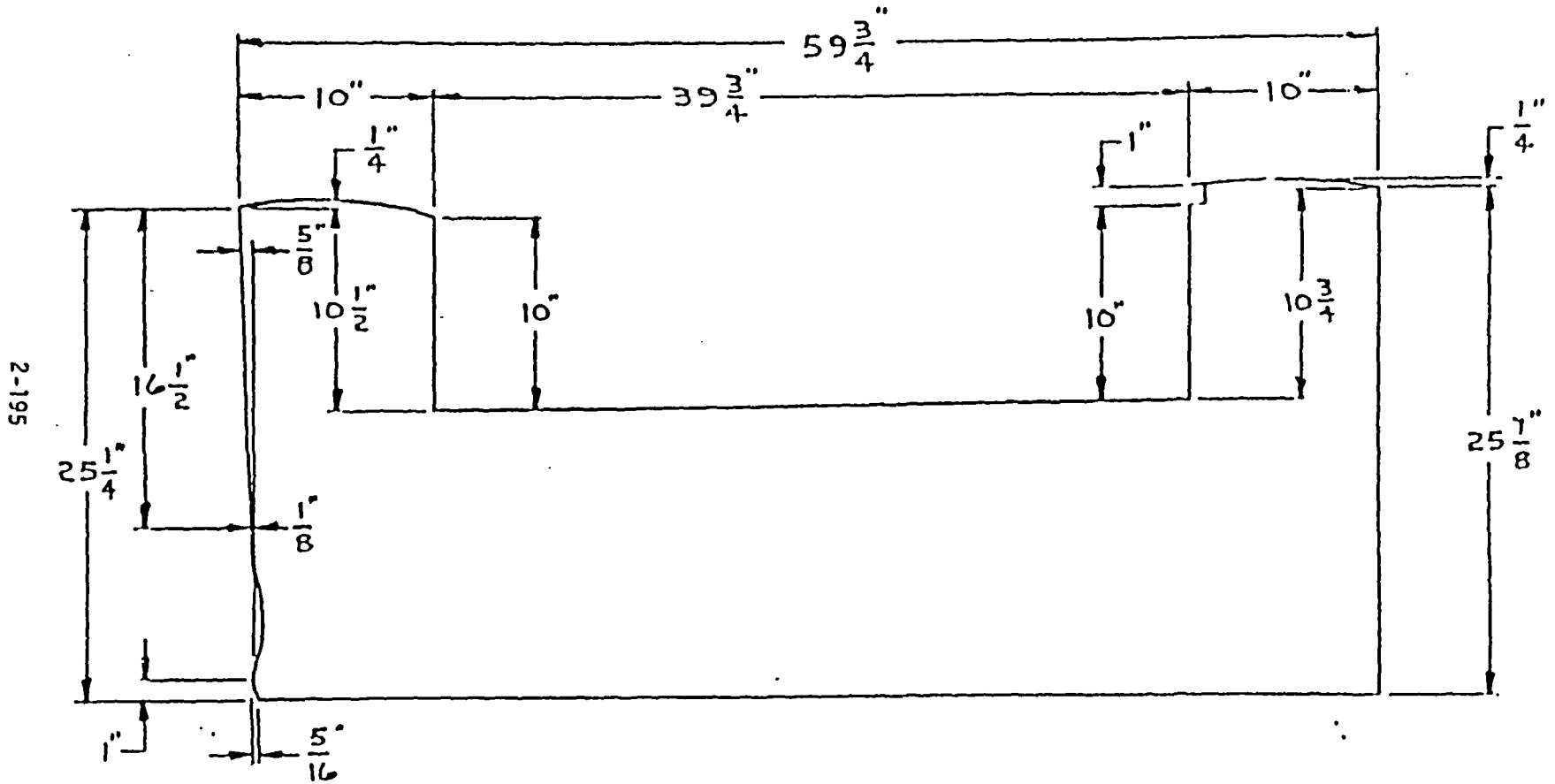


POL-2

		CIRCUMFERENTIAL POSITION - DIAMETER (IN. ± 1/8")											
		1	2	3	4	5	6	7	8	9	10	11	12
A	EXTERIOR	39-3/16"	39-3/16"	39-3/16"	39-3/16"	39-3/16"	39-3/16"	39-3/16"	39-7/32"	39-3/16"	39-3/16"	39-7/32"	39-9/32"
		39-1/16"	39-3/32"	39-1/16"	39-1/8"	39-1/8"	39-1/16"	39-1/16"	39-1/8"	39-5/32"	39-3/16"	39-1/4"	39-5/32"
B	EXTERIOR	39-1/4"	39-1/8"	39-1/8"	39-1/8"	39-1/8"	39-9/32"	39-7/32"	39-1/16"	39-1/8"	39-1/8"	39-1/8"	39-3/16"
		39-7/32"	39-1/8"	39-7/32"	39-3/16"	39-5/32"	39-1/4"	39-1/4"	39-3/16"	39-5/32"	39-1/16"	39-1/16"	39-1/16"
C	INTERIOR	26-7/16"	26-7/16"	26-11/32"	26-3/8"	26-3/8"	26-11/32"	26-11/32"	26-3/8"	26-11/32"	26-7/16"	26-7/16"	26-15/32"
		26-7/16"	26-3/8"	26-3/8"	26-3/8"	26-3/8"	26-5/16"	26-5/16"	26-11/32"	26-3/8"	26-7/16"	26-1/2"	26-15/32"
D	INTERIOR	26-11/32"	26-11/32"	26-7/16"	26-7/16"	26-15/32"	26-15/32"	26-15/32"	26-3/8"	26-3/8"	26-5/16"	26-9/32"	26-13/32"
		26-3/8"	26-3/8"	26-13/32"	26-7/16"	26-15/32"	26-15/32"	26-13/32"	26-3/8"	26-5/16"	26-5/16"	26-1/4"	26-3/8"
E	INTERIOR	26-7/16"	26-7/16"	26-7/16"	26-15/32"	26-7/16"	26-1/2"	26-1/2"	26-7/16"	26-3/8"	26-3/8"	26-3/8"	26-7/16"
		26-3/8"	26-7/16"	26-3/8"	26-7/16"	26-1/2"	26-1/2"	26-15/32"	26-3/8"	26-3/8"	26-3/8"	26-3/8"	26-1/2"

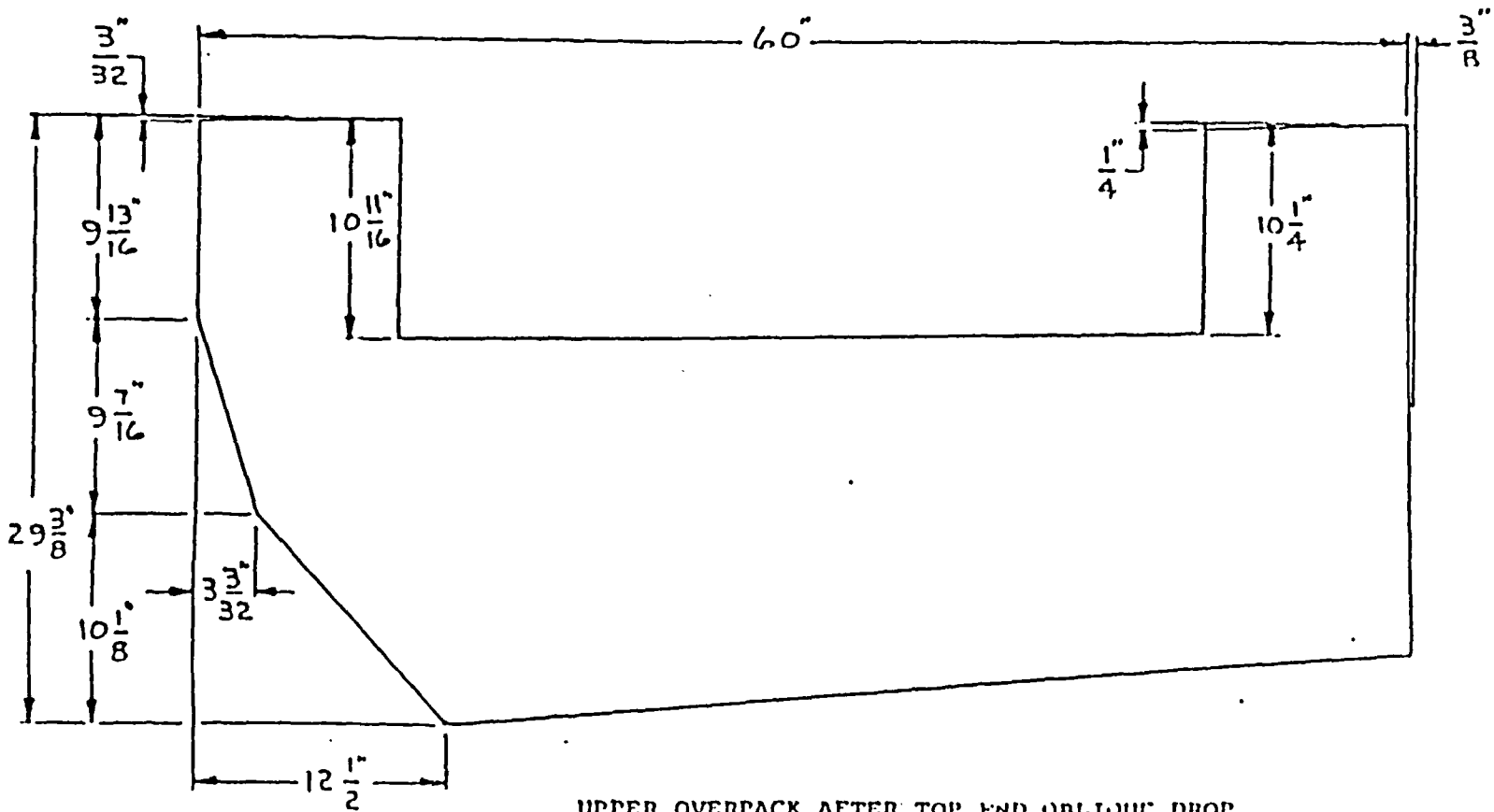
NOTE: FIGURES IN UPPER LEVEL ARE PRE-TEST MEASUREMENTS;  
 FIGURES IN LOWER LEVEL ARE POST-TEST MEASUREMENTS.

FIGURE 2.11.4-4



LOWER OVERPACK AFTER FLAT END DROP

FIGURE 2.11.4-5



UPPER OVERPACK AFTER TOP END OBLIQUE DROP

2-196

TIRE 2.11.4-6 CALIBRATION CURVE, 1-13 C II CASK

SCAN AT BARNWELL, 2/26/81

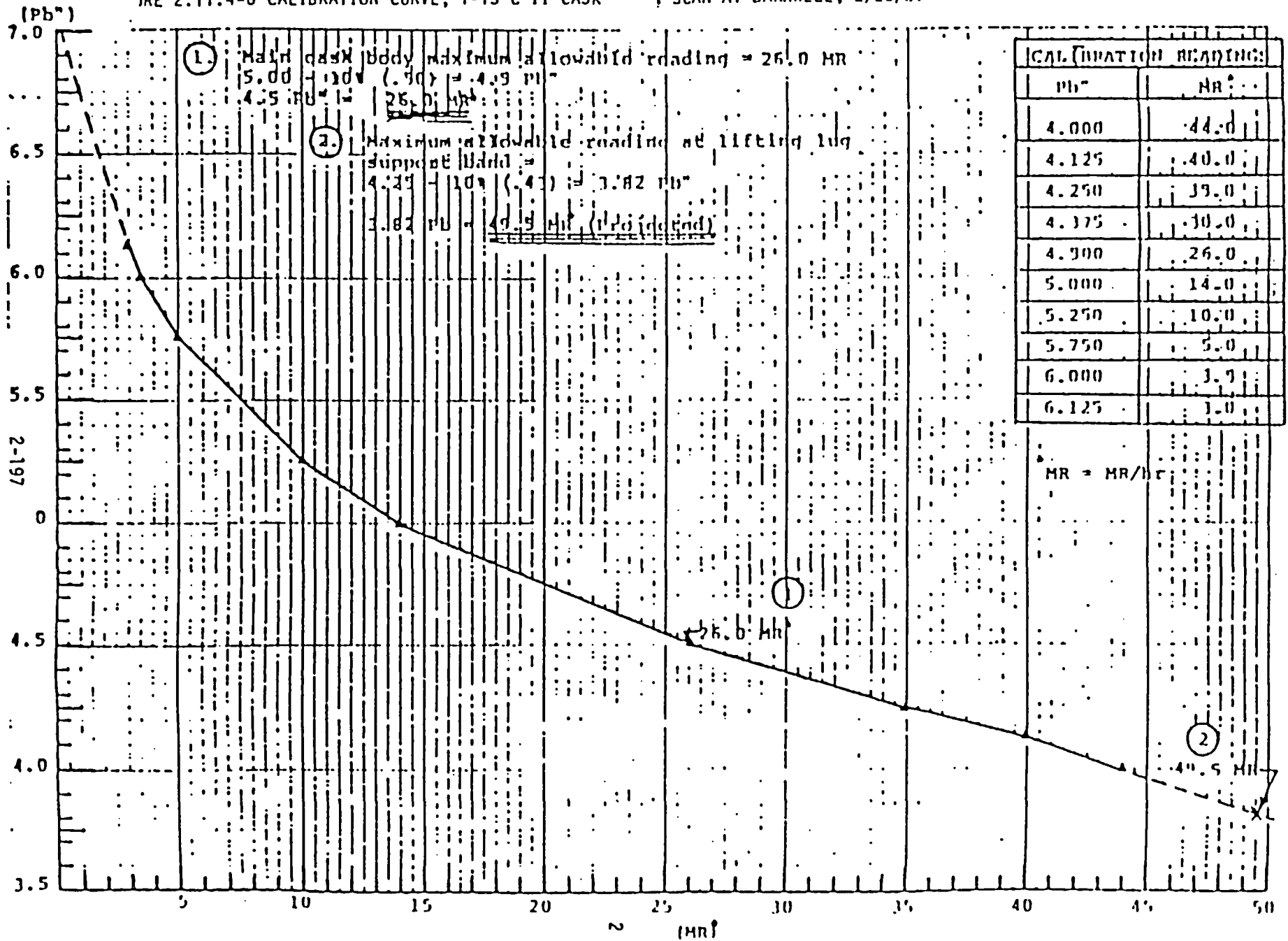


FIGURE 2.11.4-7  
 GAMMA SCAN READINGS IN MR OF 1-13C II CASK WITH 9 CURIES  
 COBALT 60 SOURCE

TOP										LEFT	NG	FAD				
14	27.0	25.0	25.0	25.0	25.0	25.0	25.0	21.0	21.0	21.0	21.0	21.0	21.0	21.0	21.0	21.0
13	16.0	16.0	15.0	15.0	16.0	16.0	16.0	17.0	17.0	17.0	17.0	17.0	17.0	17.0	17.0	19.0
12	18.0	19.0	17.0	18.0	17.0	18.0	19.0	19.0	21.0	21.0	21.0	21.0	20.0	19.0	19.0	21.0
	30.0	29.0	25.0	29.0	29.0	30.0	32.0	///	///	31.0	33.0	33.0	33.0	32.0	32.0	33.0
10	28.0	27.0	27.0	27.0	25.0	25.0	32.0	///	///	31.0	33.0	33.0	31.0	31.0	32.0	31.0
9	17.0	16.0	16.0	17.0	18.0	17.0	19.0	20.0	21.0	21.0	21.0	19.0	18.0	18.0	18.0	19.0
56" 8	17.0	16.0	16.0	16.0	17.0	17.0	18.0	19.0	20.0	21.0	21.0	20.0	19.0	18.0	17.0	19.0
7	17.0	16.0	16.0	17.0	17.0	18.0	19.0	20.0	20.0	21.0	20.0	19.0	18.0	17.0	18.0	18.0
6	18.0	17.0	17.0	17.0	17.0	18.0	19.0	20.0	21.0	20.0	20.0	19.0	19.0	18.0	17.0	18.0
5	18.0	16.0	17.0	17.0	18.0	19.0	20.0	20.0	20.0	20.0	20.0	19.0	19.0	17.0	17.0	18.0
4	18.0	17.0	16.0	17.0	18.0	19.0	20.0	21.0	21.0	21.0	21.0	20.0	19.0	19.0	18.0	17.0
3	19.0	18.0	17.0	19.0	20.0	20.0	21.0	22.0	22.0	22.0	22.0	21.0	20.0	19.0	18.0	18.0
2	18.0	17.0	17.0	18.0	19.0	20.0	21.0	22.0	22.0	22.0	21.0	20.0	19.0	19.0	19.0	18.0
1	15.0	15.0	15.0	15.0	16.0	17.0	17.0	17.0	17.0	16.0	15.0	12.0	12.0	14.0	15.0	15.0
	1	2	3	4	5	6	7	8	9	10	11	12	13	14	15	16

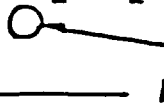

 DRAIN PLUG  
 BOTTOM

FIGURE 2.11.4-7  
 GAMMA SCAN READINGS IN MR OF 1-13C II CASK WITH 9 CURIES  
 COBALT 60 SOURCE (continued)

															:
									LIFTING PAD						
14	29.0	30.0	34.0	33.0	33.0	30.0	29.0	26.0	26.0	27.0	26.0	25.0	25.0	25.0	26.0
13	20.0	20.0	19.0	19.0	19.0	18.0	17.0	17.0	17.0	17.0	17.0	17.0	17.0	17.0	18.0
12	21.0	20.0	20.0	19.0	19.0	18.0	17.0	17.0	18.0	18.0	17.0	17.0	17.0	19.0	19.0
	34.0	35.0	34.0	33.0	32.0	32.0	23.0	23.0	32.0	32.0	31.0	31.0	30.0	30.0	31.0
10	31.0	31.0	31.0	32.0	32.0	32.0	23.0	22.0	31.0	31.0	31.0	31.0	30.0	30.0	30.0
9	18.0	18.0	18.0	17.0	17.0	17.0	17.0	17.0	17.0	17.0	17.0	17.0	17.0	17.0	18.0
8	19.0	18.0	17.0	17.0	17.0	16.0	16.0	16.0	16.0	17.0	17.0	16.0	17.0	17.0	17.0
7	19.0	17.0	17.0	17.0	16.0	16.0	15.0	15.0	16.0	17.0	17.0	17.0	17.0	18.0	18.0
6	17.0	17.0	16.0	16.0	15.0	15.0	14.0	14.0	15.0	16.0	17.0	17.0	17.0	15.0	15.0
5	17.0	17.0	16.0	15.0	15.0	15.0	15.0	15.0	15.0	16.0	17.0	16.0	17.0	18.0	19.0
4	17.0	16.0	15.0	15.0	14.0	14.0	14.0	14.0	15.0	15.0	15.0	16.0	16.0	17.0	19.0
3	17.0	16.0	15.0	15.0	13.0	14.0	15.0	14.0	14.0	14.0	15.0	15.0	16.0	17.0	19.0
2	17.0	16.0	15.0	14.0	14.0	14.0	14.0	14.0	13.0	14.0	14.0	15.0	16.0	17.0	18.0
	15.0	15.0	15.0	14.0	13.0	12.0	12.0	12.0	11.0	10.0	5.0	5.0	6.0	10.0	13.0
	17	18	19	20	21	22	23	24	25	26	27	28	29	30	31

FIGURE 2.11.4-7  
GAMMA SCAN READINGS IN MR OF 1-13C II CASK WITH 9 CURIES  
COBALT 60 SOURCE (continued)

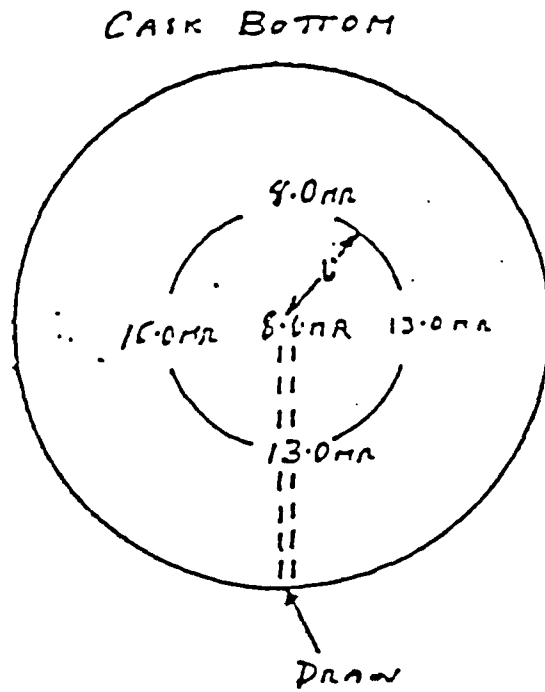
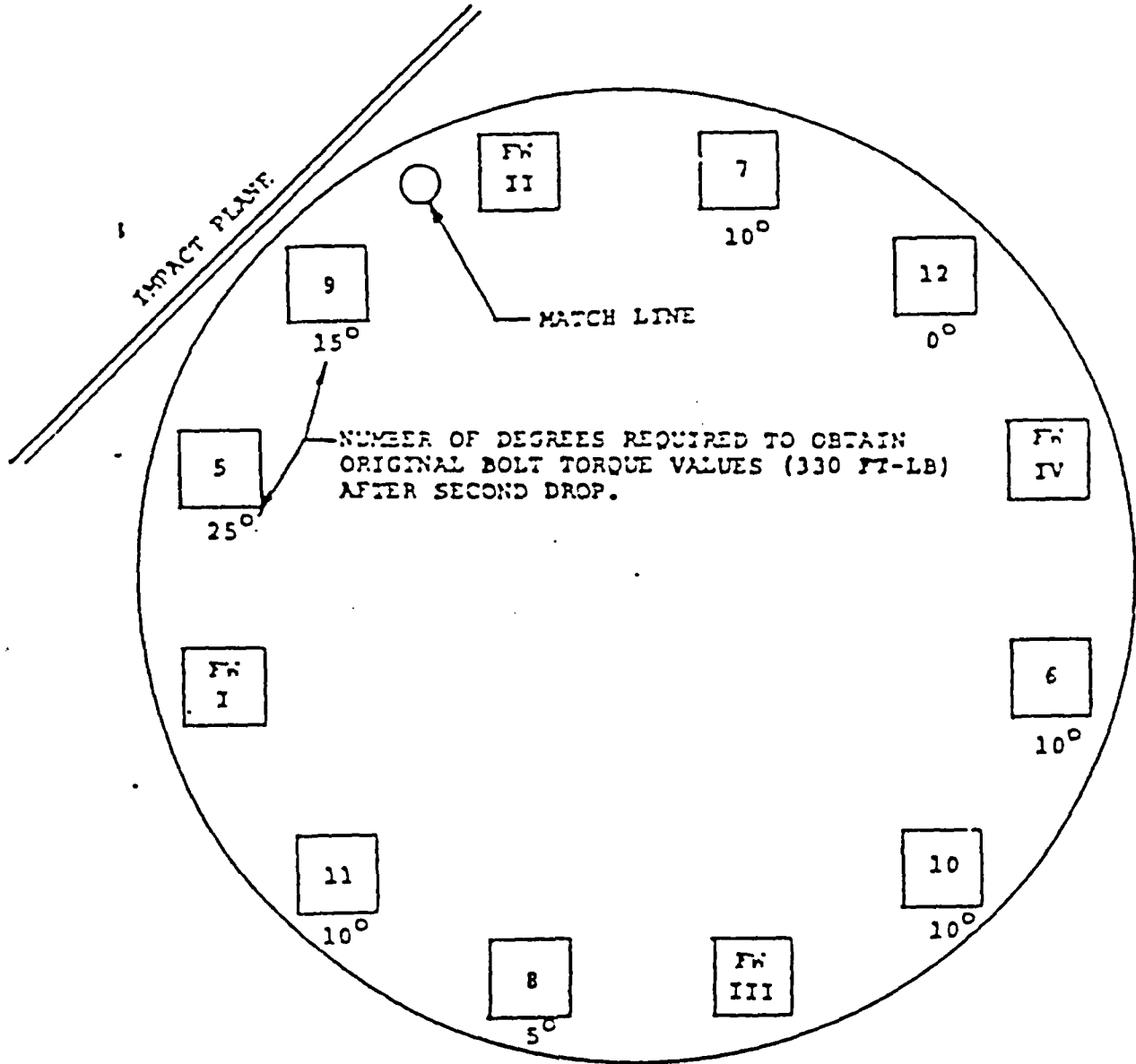


FIGURE 2.11.4-8



LID BOLT STATUS FOLLOWING  
OBLIQUE IMPACT

Degrees indicate turn required to restore bolt preload torque.



FIGURE 2.11.4-9

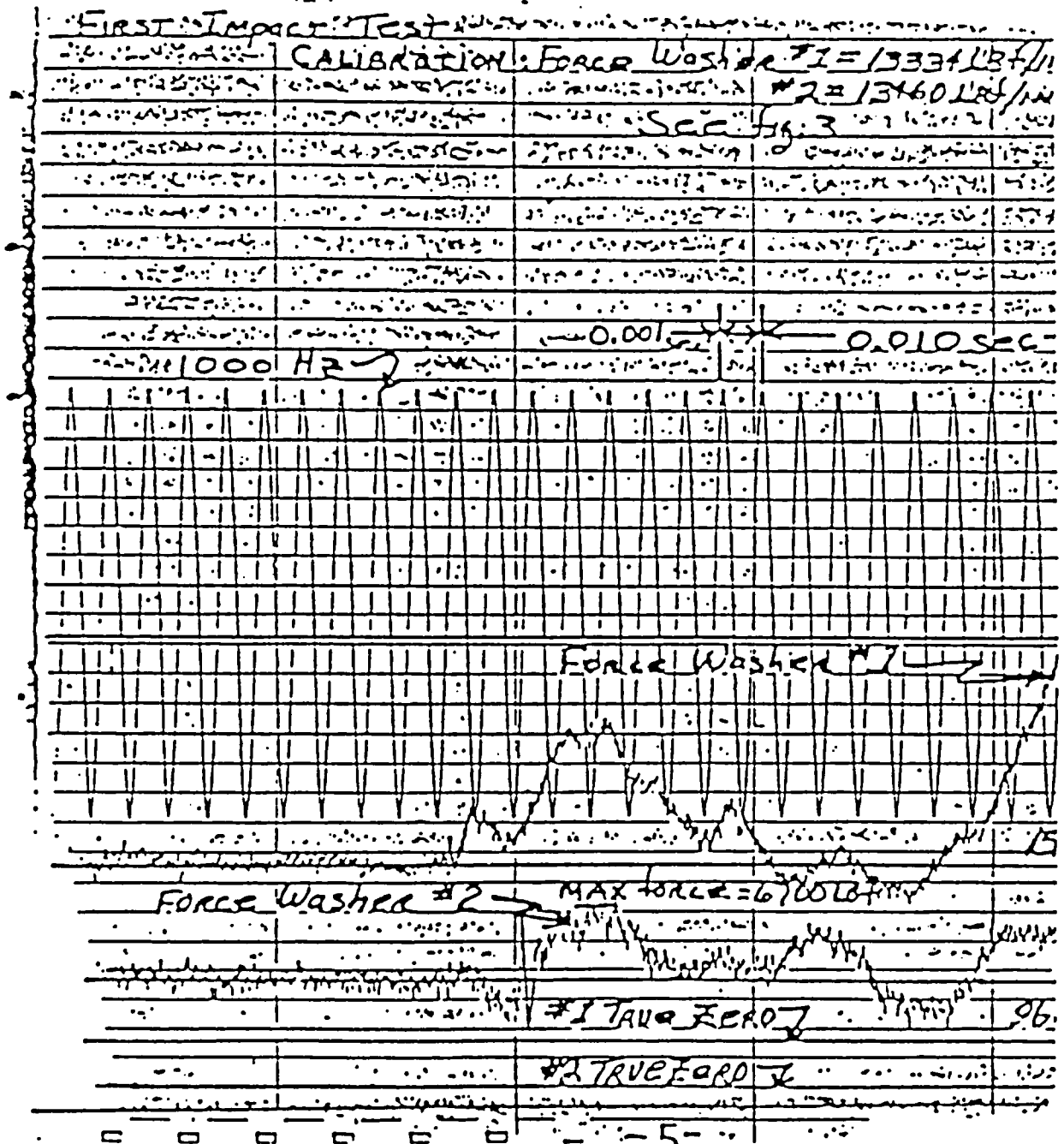
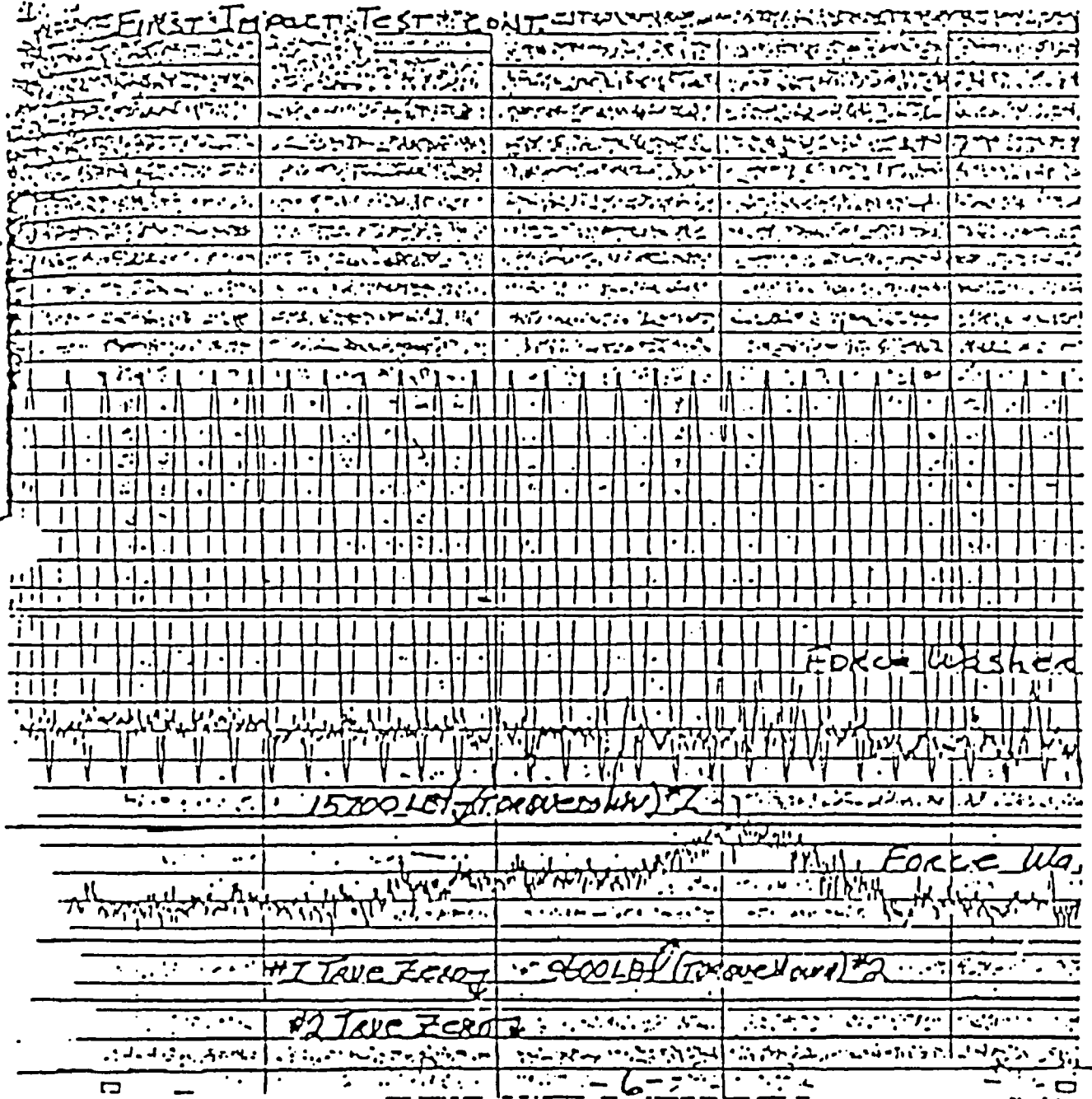


FIGURE 2.11.4-9 (continued)



## 2.11.5 INTERPRETATION, CORRELATION, AND CONCLUSIONS

This section briefly summarizes significant comments and conclusions. Where appropriate, correlations and meaningful interpretations are provided.

### 2.11.5.1 Cask Behavior

The drop tests conclusively demonstrated the capability of the 1-13C II cask to survive the 30 foot drop provisions of the hypothetical accident segments of CFR 71. Successful survival of two sequential 30 foot drops demonstrates the high degree of conservatism embodied in the 1-13C II design. Shield integrity was directly demonstrated by appropriate performance tests. Structural integrity was similarly demonstrated by the unchanged condition of the cask following these two drops, with the exception as previously noted.

#### 2.11.5.1.1 Shield Integrity

The post test gamma scan described in Section 2.11.4.4 demonstrates that the lead shield suffered no damage or change during two successive drop tests. There was no detectable lead settlement. All provisions of 10 CFR 71 relative to survival of shielding under hypothetical accident conditions are fully satisfied.

#### 2.11.5.1.2 Weld Integrity

Pre- and post-test dye penetration examinations fully demonstrated sufficient weld integrity to satisfy hypothetical accident conditions as defined in 10 CFR 71. However, there was one cracked lid bolt boss which occurred because of interference between bolt force measurement transducers and the overpack tiedown plate. Under normal shipping conditions, this interference situation would not prevail since force washers would not be present. Moreover, the diameter of the clearance area of the overpack has been increased from 3 inches to 3.548 inches.

### 2.11.3.1.3 Structural Integrity

Dimensional surveys before and after drop test show no change in cask geometry, see Paragraph 2.11.4.3. Diametrical measurements were taken at two outside locations (top and bottom) and three inside locations within the cask cavity or containment vessel (top, middle and bottom). None of these pre- and post-test measurements differed by more than the 1/8" measurement accuracy. Data fits, based on the very conservative assumption that any measurement differences were true physical changes, show that maximum possible strain cannot exceed:

Bending	.23%	Level 'A', Figure 2.11.4-4
Membrane	.19%	

This is well below the 40% ultimate strain of the stainless steel cask materials, and well below the permissible strains set for cask requalification following the test, see Paragraph 6.0 of reference 2.11.2.2. Thus, the cask meets the strain level requirements for return to service.

Closure bolt strains under two successive 30' drops were conservatively determined using a "turn of the bolt" method with "turn" values extracted from Figure 2.11.4-8, Maximum probable closure bolt strains are as follows:

<u>Bolt Nr.</u> <u>(Fig. 2.11.4-9)</u>	<u>Turn</u> <u>(°)</u>	<u>Strain*</u> <u>(%)</u>
5	25°	.44
10,7,11,6	10°	.18
8	5°	.09

$$* \text{Strain, } \epsilon = \Delta l / l ; 1\frac{1}{2}'' - 7\text{UNC} \times 2\frac{1}{2}''$$

$$\Delta l = \frac{(\text{°})}{360} \cdot \frac{1}{7} ; l = 2.25 (1'' + 1d)$$

With one exception, bolt #5, all closure bolts experienced strains less than the definition of engineering yield, 0.2% offset. The maximum possible strain in bolt #5 is just slightly more than this value. These predictions are very conservative since a major fraction of the retorque applied is probably related to the instantaneous release of friction forces upon impact.

Additional very useful data regarding closure bolt performance can be extracted from the end drop bolt force transducer #1 output, Figure 2.11.4-9. Essentially no high frequency response components may be observed. Additional frequency decomposition analyses of transducer data confirm this conclusion. Thus, for the 1-13C II package, bolt dynamic response effects due to wave propagation effects in the cask body, may be safely ignored. The primary reason for the absence of elastic body dynamic responses within the cask may be attributed to the decoupling of excitation and response afforded by the energy absorbing overpacks.

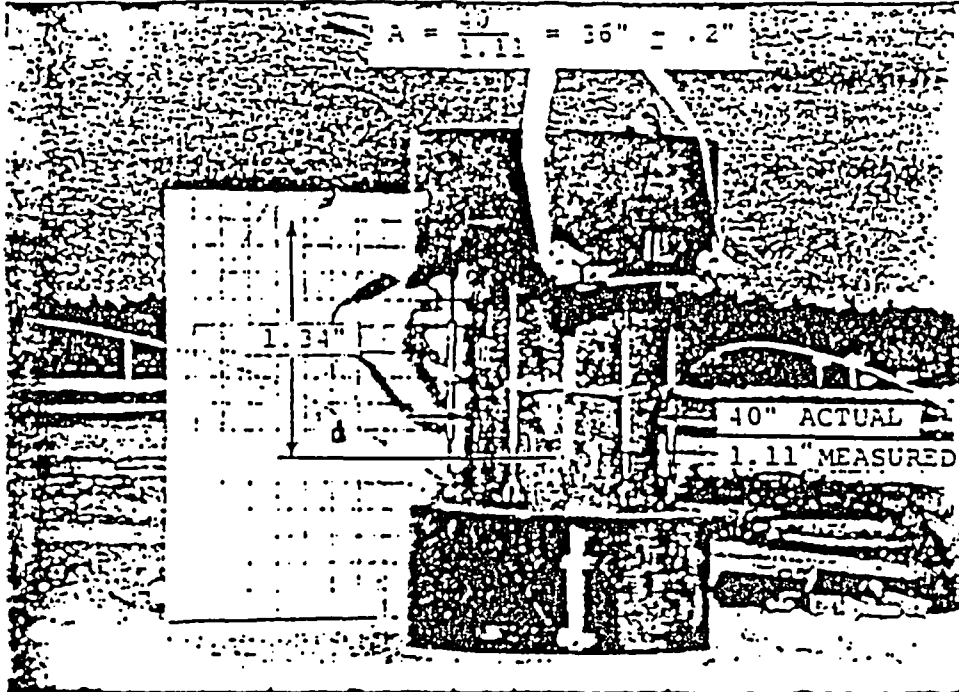
#### 2.11.5.2 Overpack Behavior

Where not directly measured or assessed by test, structural integrity of the package is demonstrated using stress values based upon analytic predictions of overpack performance. This section presents a comparison of test and analysis demonstrating a high degree of agreement.

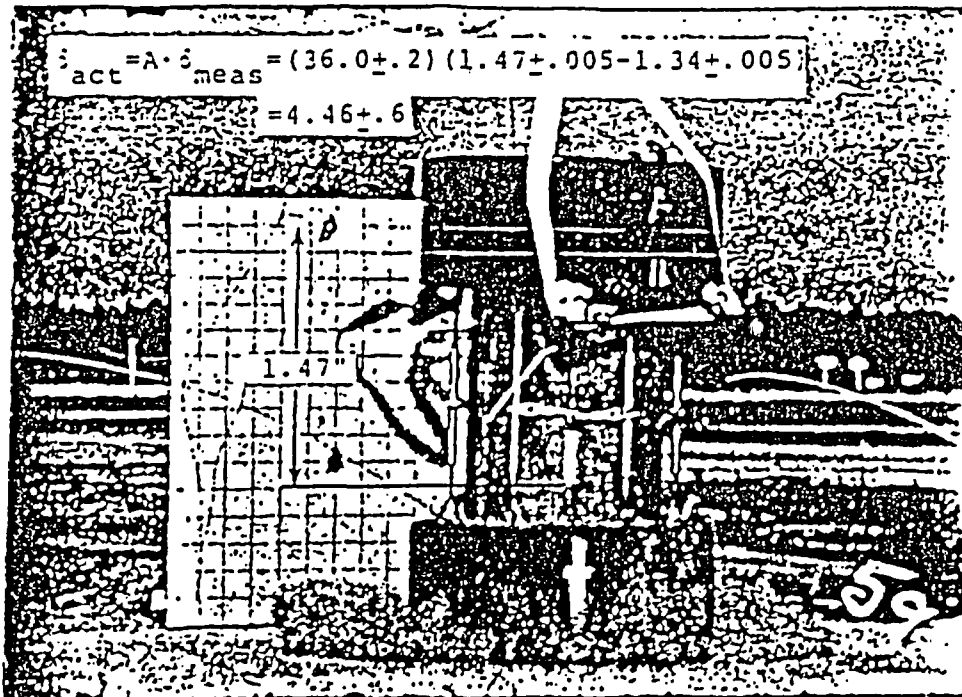
The end drop test provides an ideal vehicle to compare the prediction accuracy of overpack analyses since the geometry details are minimized as are complications arising from rotational motions during impact. Figure 2.11.5.2-1 represents a pair of high speed motion picture photos at the instant of initial impact and at maximum overpack deformation. Total test deformation, as measured from these photos is 4.46 inches. Corresponding analytic predictions, assuming a 50% effectiveness for unbacked foam, amounted to 5.5 inches. These values differ by approximately 23%.

Careful examination of data and comparison with probable causes leads to the conclusion that these modest differences relate to "effectiveness" assumptions for unbacked foam regions, i.e., that portion of the impact cross section that is not backed by the cask body. This unbacked "over-hang" clearly is capable of resisting loads up to some value where the foam fails in shear. Examinations of the post-test results for the impacted overpack show a shear failure of the foam along the bond surface of the inner overpack shell. This is matched by tensile ruptures of the overpack shell as shown in photos F14 and F15, Section 2.11.3. Thus, the unbacked foam generates a significant portion of the total impact force.

FIGURE 2.11.5.2-1



CASK AT INSTANT OF IMPACT



CASK AT INSTANT OF MAXIMUM DEFORMATION

To assess this effectiveness of unbacked regions, a series of end drop analysis (ZYDROP), see Section 2.10.2.1, were performed on varying effective impact areas. Results are as follows:

<u>Diameter</u> (in.)	<u>Area</u> (in <sup>2</sup> )	<u>Deflection</u> (in)
40.	1257	7.96
42.5	1419	7.29
45.	1590	6.68
47.5	1772	6.13
50.	1963	5.63
52.5	2165	5.19
55.	2376	4.79
57.5	2597	4.44
60.	2827	4.13
57.36"	2584	4.46 (See next sheet)

The total end area of the overpack is 2584 in<sup>2</sup> (60" O.D.). The end area backed by the cask body is 1257 in<sup>2</sup> (40" O.D.). Thus, the unbacked area of partial effectiveness is:

$$2827 - 1257 = 1570 \text{ in}^2$$



1-13C II OVERPACK END DROP ANALYSIS 16.5 PCF FOAM

1ETDKOP1ENB)

PACKAGE WEIGHT = 27000. (LBS)  
 PACKAGE DIAMETER = 57.36 (IN)  
 OVERPACK DEPTH = 15.00 (IN)  
 DROP HEIGHT = 30.10 (FT)

CRUSH DEPTH (IN)	STRAIN	*** IMPACT ***		***** ENERGY *****		
		FORCE (LBS)	ACCEL. (G)	KINETIC (IN-LB)	STRAIN (IN-LB)	RATIO (SE/KE)
.50	.033	1317568.	48.8	9733500.	329392.	.034
1.00	.067	2285806.	84.7	9747000.	1230236.	.126
1.50	.100	2454889.	90.9	9740500.	2415409.	.247
2.00	.133	2511278.	93.0	9774000.	3656951.	.374
2.50	.167	2508614.	92.9	9787500.	4911924.	.502
3.00	.200	2480729.	91.9	9801000.	6159260.	.628
3.50	.233	2500190.	92.6	9814500.	7404489.	.754
<u>.4c</u> 4.00	.267	2533049.	93.8	9828000.	8662799.	.881
4.50	.300	2584093.	95.7	9841500.	9942095.	1.010
5.00	.333	2644487.	98.7	9855000.	11254230.	1.142
5.50	.367	2767851.	102.5	9868500.	12612314.	1.278
6.00	.400	2894184.	107.2	9882000.	14027823.	1.420
6.50	.433	3037745.	112.5	9895500.	15510806.	1.567
7.00	.467	3232988.	119.7	9909000.	17078489.	1.724
7.50	.500	3498526.	129.2	9922500.	18758817.	1.891
8.00	.533	3798298.	140.7	9936000.	20580573.	2.071
8.50	.567	4171875.	154.5	9949500.	22573116.	2.269
9.00	.600	4651368.	172.3	9963000.	24778927.	2.487
9.50	.633	5309833.	196.7	9976500.	27269227.	2.733
10.00	.667	6252867.	231.4	9990000.	30159902.	3.019
10.50	.700	7545552.	279.5	10003500.	33609507.	3.360
11.00	.733	9147052.	338.8	10017000.	37782658.	3.772
11.50	.767	11510380.	426.3	10030500.	42947816.	4.282
12.00	.800	14987740.	555.1	10044000.	49571546.	4.935
12.50	.833	19723895.	730.5	10057500.	58249455.	5.792
13.00	.867	27145739.	1005.4	10071000.	69961813.	6.947
13.50	.900	37227760.	1397.3	10084500.	84185238.	8.546
14.00	.933	51056576.	1891.0	10098000.	108381322.	10.733
	.967	66634511.	2467.9	10111500.	13894.	13.628
	1.000	83983028.	3110.5	10125000.	4479.	17.329

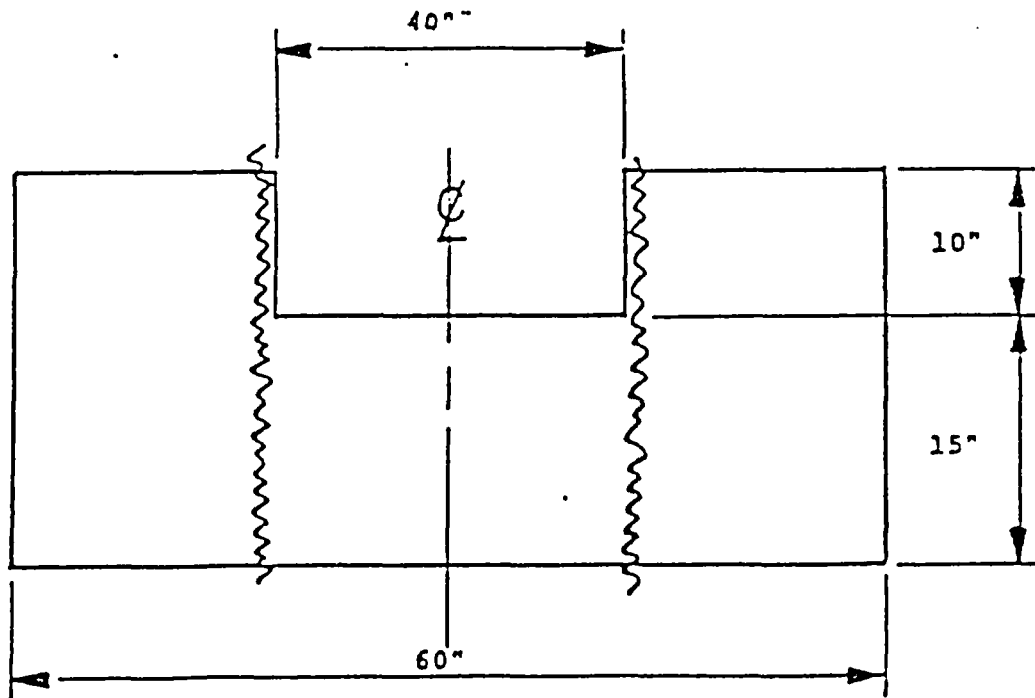
Test deformation are matched with an effective end area of 2584 in<sup>2</sup> (57.36" O.D.). The effective area of the unbacked region is thus calculated as:

$$2584 - 1257 = 1327 \text{ in}^2$$

The effectiveness ratio for this unbacked region is:

$$\text{Effective \%} = \frac{1327}{1570} = 84.5\%$$

An alternate approach is the assessment of unbacked foam effectiveness would assume that full section effective up to the point where shear failures of the foam no longer permits additional load transfer. For the 1-13C II cask overpack, the shear plane shown in Photos F14 and F15 is idealized as follows:



Allowable shear stresses for 16.5 lb/ft<sup>3</sup> foam, as provided by suppliers, are estimated as:

$$\tau = 13.27p^{1.2492} = 440 \text{ psi}$$

$$F_{\max} = (440)(25)(\pi)(40) = 1.383 \times 10^6 \text{ lbs.}$$

The area of unbacked impact cross section is

$$A_u = \frac{\pi}{4} (60^2 - 40^2) = 1570 \text{ in}^2$$

Maximum crush stress in unbacked regions is:

$$\sigma = \frac{F_{\max}}{A_u} = \frac{1.383 \times 10^6}{1570} = 880 \text{ psi}$$

The stress in backed regions at a deflection of 4.46 inches is found as approximately 1000 psi. Thus, the effectiveness of unbacked foam is estimated as:

$$\frac{880}{1000} = 88\%$$

The lesser of these two unbacked foam effectiveness values has been employed for all side, end and oblique orientation cask load analyses used in this report. This adjustment corrects the analytic "over prediction" of overpack deformations observed in test measurement.

2.12 ATTACHMENT

INFORMATION IN MICROFICHE FORM

2.10.3 Finite Element Stress Analysis  
(1-13C II Cask)

2.11 Appendix: Drop Test Report Reference Documents  
(1-13C II)

Appendix 2.10.4 Lift Lug Analysis - August 1981.

### 3.0 THERMAL EVALUATION

This chapter identifies and describes the principal thermal engineering design aspects of the 1-13C II package important to safety and to compliance with the performance requirements of 10 CFR 71.

#### 3.1 Discussion

The CNS 1-13C II package is designed with a totally passive thermal system. The principal physical characteristics of this thermal system consist of an external thermal fire shield surrounding a cylindrical stainless steel shell. The 1/2 inch cylindrical stainless steel shell surrounds a lead shield of approximately 5 inch thickness. The inner surface of the package consist of an 26-1/2 inch diameter stainless steel shell. The cylindrical package ends are similarly constructed of stainless steel and lead materials. These ends are enclosed in, and surrounded by, cylindrical foam impact absorbers (also called overpacks) that effectively serve as adiabatic boundaries for these end surfaces. The above components are identified on the drawings as noted in Appendix 2.10.1

The principal operating features of the 1-13C II package thermal system are as follows:

##### 1. Normal Transport Conditions

- a. The decay heat of the payload is transferred to the inner surface of the package by radial radial heat transfer means.
- b. This decay heat is transferred to the exterior of the cylindrical stainless steel shell by radial conductive heat transfer through the lead shield.
- c. Next, this decay heat is transferred to the exterior fire shield by radiant heat transfer.

- d. The fire shield dissipated this decay heat to the ambient environment by combined radiation and convection heat transfer.
- e. Essentially no heat is dissipated through package ends. The foam impact energy absorbers, enclosing these package ends, enforce adiabatic boundary conditions on all end surfaces.

2. Hypothetical Thermal Accident

- a. The heat of a hypothetical fire is imposed upon the exterior fire shield by radiant heat transfer means, as prescribed in 10 CFR 71.
- b. This fire heat is transferred to the stainless steel cylindrical shell by radiant heat transfer.
- c. Conductive heat transfer conveys this heat to the lead shield.
- d. Both the lead shielding material and the steel end assemblies store heat during the period of the fire.
- e. Subsequent to the fire, the stored fire heat is dissipated to the ambient environment as described, above, for normal transport conditions.
- f. During fire exposure portions of the foam end impact absorbers char but retain a cellular structure to trap a dead air void of equivalent dimensions.

The important maximum temperatures of the 1-13C II package for both normal transport and hypothetical thermal accident conditions are summarized below.

o Normal Transport Conditions

TEMPERATURE °F

	<u>Cask Body</u>	<u>Fire Shield</u>
100°F Ambient Air*	190.6°F	156.3°F
130°F Ambient Air*	214.4°F	182.1°F
-40°F Ambient Air/	81.5°F	37.3°F

o Hypothetical Fire Accident

	<u>Node</u>	<u>Temperature °F</u>
Fire Shield	9	1174.0°F
Lift Lug	2	508.7°F
Side Outer Shell	10	434.5°F
Top Outer Shell	3	363.4°F
Bottom Outer Shell	16	365.1°F
Case Cavity	22	371.4°F

\*Includes heating due to solar insolation.

√With maximum decay heat load = 800 watts.

The important conclusions derived from the above results include:

The lead shield does not melt under hypothetical thermal accident conditions (maximum lead temperature = 508.7°F at lift lug; melt = 621°F).

The components of the closure systems (bolts, seals) at both ends are exposed to temperatures not in excess of 363.4°F. Silicon seals retain excellent sealing properties up to 400°F.\* The maximum predicted temperature of the pressurized containment cavity is 371.4°F. This temperature is used to derive maximum containment vessel pressure magnitudes.

The package has been evaluated for payload decay heats ranging up to 800 watts. Maximum temperatures reported above correspond to the 800 watt case. Specific steady state (at 100°F ambient air) and hypothetical accident transient analyses have been performed for decay heat values of: 150, 200, 300, 400, 500, 600, 700, and 800 watts.

---

\*Shappert, L.B., Cask Designers Guide, Oak Ridge National Laboratory, ORNL-NSIC-68, 1968, Table 2.3, Page 32.



### 3.2 Summary of Thermal Properties of Materials

Metallic thermal material properties used for analyses were taken directly from Shappert, "Cask Designer's Guide - A Guide for the Design, Fabrication and Operation of Shipping Casks for Nuclear Applications", ORNL-NSIC-68, page 166. These properties are as follows:

<u>Property</u>	<u>Symbol</u>	<u>Stainless Steel</u>	<u>Solid Lead</u>
Thermal Conductivity (Btu/hr-ft - F)	k	11.	18.6
Specific Heat Capacity	C <sub>p</sub>	.125	.0325
Density (lb/ft <sup>3</sup> )	ρ	485	687

Surface emissivities and absorptivities, used in radiant heat transfer calculations, were taken from a variety of sources, as later defined. The specific analysis assumptions are tabulated below:

#### o Source Model and Fire Shield Exterior

Properties for the external surface of the cask and the source are taken directly from requirements defined in 10 CFR 71 such that the heat input to the package is not less than that which would result from exposure of the whole package to a radiation environment of 1,475°F for 30 minutes with an emissivity coefficient of 0.9 assuming the surfaces of the package have an absorption coefficient of 0.8. Thus, the exterior surface of the package fire shield is assumed to possess an emissivity and absorptivity of 0.8. The emissive power of the hypothetical accident source is assumed equivalent to a grey body with emissivity of 0.9 at a temperature of 1475°F. This is equivalent to a black body source with a temperature of 1424.71°F as shown in the following calculations:

$$T_o = \left[ \epsilon_o (T_o)^4 \right]^{1/4}$$

$$T_o = \left[ (.9) (1475 + 459.69)^4 \right]^{1/4} - 459.69$$

$$T_o = 1424.71^\circ\text{F}$$

o Fire Shield Interior and Cask Exterior

Both bodies are 304 stainless steel and possess emissivity properties varying with temperature. An empirical equation of the form:

$$\epsilon = A + BT^C$$

was fitted to available data from three sources. This fit found coefficients of:

$$A = .430$$

$$B = 3.1359 \times 10^{-5}$$

$$C = 1.2850$$

Numerical evaluation at varying temperatures gives values used in the analyses:

<u>Temperature</u>	<u>Emissivity <math>\epsilon</math></u>
50	.43
200	.46
400	.50
600	.54
800	.60
1000	.65
1200	.71
1300	.74
1400	.78
1475	.80

The data sources used for this empirical fit were as follows:

- (1) Kreith, Frank, Radiation Heat Transfer.

International Textbook Co., 1962, Table 2-5.

	<u><math>^{\circ}</math>F</u>	<u><math>\epsilon</math></u>
Type 301	96	.44
	638	.50
	1213	.86
	1710	.90
Type 316	98	.49
	665	.52
	1193	.61
	1575	.89

- (2) Holman, J.P., Heat Transfer, McGraw-Hill Book Company, 1963, Table A-10.

	$^{\circ}\text{F}$	$\epsilon$
Type 301	450	.54
	1725	.63

- (3) Baumeister, Theodore, Mark's Standard Handbook for Mechanical Engineers, McGraw-Hill Book Co. Eighth Edition, 1978, Table 2, Page 4-73.

	$^{\circ}\text{F}$	$\epsilon$
Type 304	428	.62
	986	.73

### 3.3 Technical Specifications of Components

Not Applicable.

### 3.4 Thermal Evaluation for Normal Conditions of Transport

The thermal evaluation of the 1-13C II package to the Normal Conditions of Transport, defined in 10 CFR 71, has been performed by analytic means. Eight alternate payload decay heat configurations have been considered, as described in Section 3.1.

#### 3.4.1 Thermal Model

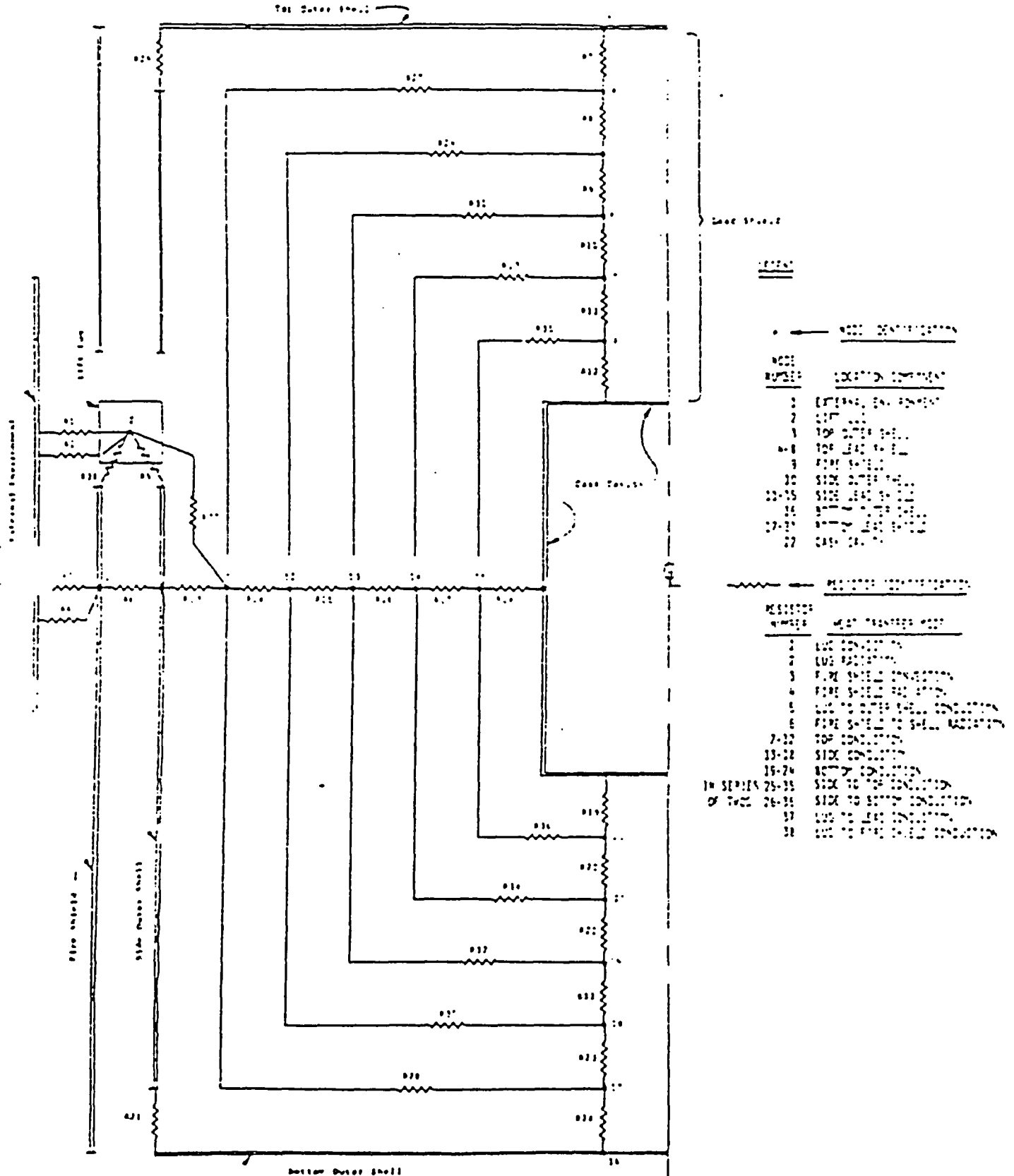
A common thermal analysis model was used for both steady state evaluation of the normal conditions of transport and transient evaluation of the

hypothetical thermal accident. The common thermal model consists of a 22 node lumped parameter axisymmetric idealization. Heat transfer is represented by 38 resistor elements of both linear (conduction) and non-linear (radiation and convection) form. Figure 3.4.1-1 depicts this thermal idealization.

The general characteristics of this model may be summarized as:

- o The model consists of three zones - two end zones and one mid-body zone.
- o Each zone is comprised of 5 lead shield nodes and two stainless steel nodes representing inner and outer shells. Within a zone these nodes are connected by 6 conduction resistors ( $R_7$  to  $R_{24}$ ).
- o Coupling between each zone is achieved by a total of twelve conduction resistors ( $R_{25}$  to  $R_{36}$ ).
- o The outer shell is enclosed by a fire shield comprised of a 1/4" stainless steel plate offset from the cask outer shell by a 16 gauge (.065") wire spacer at 6" centers. This fire shield is thermally linked to the cask outer shell by a radiation resistor ( $R_6$ ).
- o The fire shield is penetrated by a pair of lug pads attaching to the lifting ring integrally on the cask outer shell. Conductive resistors coupling this lug pad to the fire shield ( $R_{38}$ ), outer shell ( $R_5$ ), and lead ( $R_{37}$ ) are provided.

Figure 3.4.1-1 THERMAL ANALYSIS - MODEL 1-13C II



- o The ambient external environment is represented by a single node held at constant temperature, or at programmed temperatures versus time for the hypothetical thermal accident. Every external node of the 1-13C II package is linked to this external environment node by a pair of resistors - one for radiation, one for free convection ( $R_1$  to  $R_4$ ). During the hypothetical thermal accident, the convection resistors are "switched off".
  
- o Solutions are achieved by using a conventional thermal analyzer program, THAN, based on the well-known Lockheed Thermal Analyzer.

The separate steady-state conditions were evaluated: eight to establish initial conditions for the hypothetical thermal accident analyses per NRC Regulatory Guide 7.8, paragraph C.1.a (all run at an ambient environmental temperature of  $100^{\circ}\text{F}$ ): one at the "hot" conditions specified by 10 CFR 71 ( $130^{\circ}\text{F}$ ) for Normal Transport and one at the "cold" conditions ( $-40^{\circ}\text{F}$ ) specified for Normal Transport.

The derivation of model properties follows:

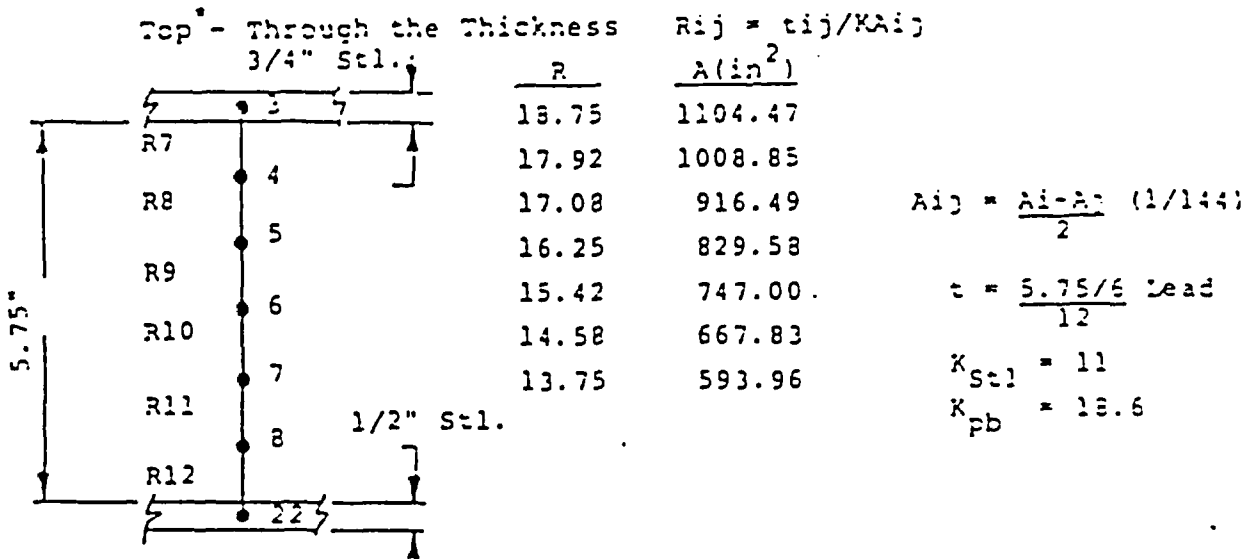
1. THERMAL CAPACITANCE

$$C_i = \rho V C_p$$

NODE (i)	MATERIAL	VOLUME (in <sup>3</sup> )	C <sub>i</sub>
2	Steel ↓	$(5.5)(8)(2)(2) = 176 \text{ in}^3$	6.17
3		$\pi(3/4)(19.25)^2 = 873.1 \text{ in}^3$	30.63
9		$2\pi(19.565)(1/4)(68.63) = 2109.2 \text{ in}^3$	74.00
10		$2\pi(1/2)(19)(68.6) = 4094.8 \text{ in}^3$	143.66
16		$\pi(1/2)(19.25)^2 = 582.1 \text{ in}^3$	20.42
22		$2\pi(1/2)(13.25)^2 + 2\pi(55)(13.5)(1/2)$	101.19
4	Solid Lead ↓	$V = \pi R_j^2 t; t = 5.75/5$	$\frac{(\text{in}^3)}{683.1}$ 8.83
5		$R_j = 13.75 + t(j-1)$	802.1 10.36
6		$j = i-3$	930.7 12.03
7			1068.8 13.81
8			1216.5 15.72
11	↓	$V_j = \pi(R_{j+1}^2 - R_j^2) l_i$	5103.5 65.94
12		$l_j = 55 + 2(j-1)t$	5653.3 73.05
13		$t = 5"/5$	6228.2 80.47
14		$R_j = 13.75 + (j-1)t$	6828.3 88.23
15		$j = i-10$	7453.4 96.31
17	↓	$V_j = \pi R_j^2 t; t = 6/5$	712.75 9.21
18		$R_j = 13.75 + t(j-1)$	842.6 10.89
19		$j = i-16$	983.3 12.70
20			1134.8 14.66
21			1297.2 16.76



2. END CONDUCTION RESISTORS (R7 - R12 and R19 - R24)

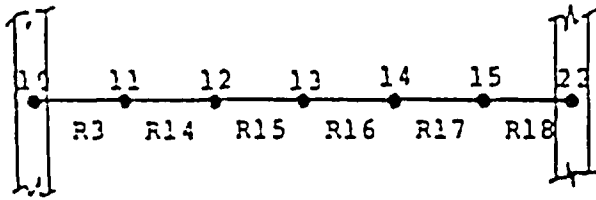


RESISTOR	NODE	A <sub>i</sub> (in)	LEAD RESISTOR	STEEL RESISTOR	TOTAL RESISTOR
7, 19	3, 16	1104.47	585.13-6	740.79-6	1.3259-3
8, 20	4, 17	1008.85	642.25-6		
9, 21	5, 18	916.49	708.20-6		
10, 22	6, 19	829.58	784.33-6		
11, 23	7, 20	747.	874.00-6		
12, 24	8, 21	667.83	980.00-6	918.34-6	1.8923-3
	22	593.96			

\*Assume Bottom Identical

3. MODEL PROPERTIES - SIDE CONDUCTION RESISTORS (R13-R18)

Side - Through the thickness -

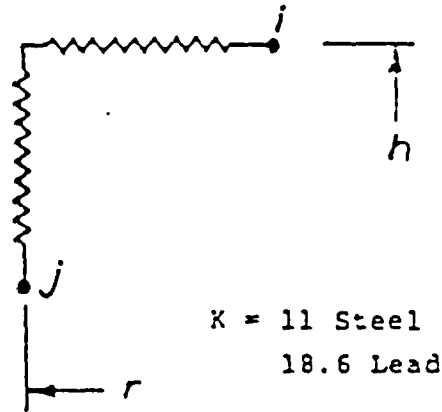


$$R_{ij} = \frac{\ln(r_j/r_i)}{2\pi K t}$$

r:	19.00	18.00	17.17	16.25	15.33	14.42	13.50
r:	67.38	65.32	63.25	61.19	59.13	57.06	55.00

RESISTOR	NODE	RADIUS (in.)	LENGTH (in.)	LEAD RESISTORS	STEEL RESISTORS	TOTAL RESISTORS
13	10	19.00	67.38	76.809-6	67.814-6	144.62-6
14	11	18.08	65.32	82.487-6		
15	12	17.17	63.25	90.882-6		
16	13	16.25	61.19	99.474-6		
17	14	15.33	59.13	108.16-6		
18	15	14.42	57.06	120.82-6	116.93-6	237.75-6
	22	13.50	55.00			

(4) COUPLING CONDUCTION RESISTORS - (R25-R36)



Lateral Resistors  
 $R = \frac{L}{KA} + \ln \frac{(r_o/r_i)}{2\pi K h}$

$r_i = 6; r_o = 4$

$L = h$

$\lambda = .75$  for R25, 26  
 1.15 for others

K = 11 Steel  
 18.6 Lead

RESISTOR	NODES		RADIUS r	HALF HT. h	MATERIAL	RESISTOR
	i	j				
25, 26	3	10	19.00	33.69	Steel	$574.71 \times 10^{-3}$
27, 28	4	11	18.08	32.66	Lead	$283.97 \times 10^{-3}$
29, 30	5	12	17.17	31.63	↓	283.03-3
31, 32	6	13	16.25	30.60		282.32-3
33, 34	7	14	15.33	29.57		281.82-3
35, 36	8	15	14.42	28.53		281.45-3

5. EXTERNAL RADIATION TO SIDES (R2 and R4)

$$K_1 = \sigma E; \quad \sigma = .1714 \times 10^{-8}$$

$$E = .8 \text{ (10 CFR 71)}$$

The exposed gross area of the shield is:

$$A_4 = 2 Rl \quad R = 19.565 \text{ in.}^2$$

$$l = 68.63 = 2(10) = 48.63 \text{ in.}$$

$$A_4 = (2)(19.565)(48.63)(144) = 41.515 \text{ ft.}^2$$

The exposed area of the pad is:

$$A_2 = \frac{(5.5)(8)(2)}{144} = 0.611 \text{ Ft.}^2$$

The net area of the fire shield is:

$$A_{4 \text{ net}} = 41.515 - 0.611 = 40.904 \text{ in.}^2$$

The external radiation coefficients are:

$$K_4 = (.1714 \times 10^{-8})(.8)(41.515 - .611) = 56.088 \times 10^{-9}$$

$$K_2 = (.1714 \times 10^{-8})(.8)(.611) = 837.80 \times 10^{-12}$$

6. FIRE SHIELD TO OUTER SHELL RADIATION (R6)

$$K_{ij} = \frac{c A_i}{\left(\frac{1}{\epsilon_i} - 1\right) + \frac{1}{F_{ij}} + \frac{A_i}{A_j} \left(\frac{1}{\epsilon_j} - 1\right)}; \quad \begin{array}{l} i = \text{Node 10} \\ j = \text{Node 9} \end{array}$$

$$A_i = 2\pi(19.315)(68.63)/144 = 57.418 \text{ ft.}^2$$

$$A_j = 2\pi(19.565)(68.63)/144 = 58.528 \text{ ft.}^2$$

$$\epsilon_i = .52; \quad \epsilon_j = .71 \text{ (interpolated from Section 3.2)}$$

$$\text{Therefore: } K_{ij} = 42.334 \times 10^{-9}$$

7. CONVECTION RESISTORS (R1 and R3)

The film coefficient,  $h$ , depends upon  $(Gr \ Pr.)$

$$\text{Assume } T_{\infty} = 130^{\circ}\text{F}$$

$$T_{\text{avg}} = 150^{\circ}\text{F}$$

$$T_w = 170^{\circ}\text{F}$$

$$\begin{aligned} Gr &= \left(\frac{\rho^2 g \beta \Delta T}{\mu^2}\right) (T_w - T_{\infty}) L^3 \\ &= (1.305)(40) \left(\frac{68.63}{12}\right)^3 \times 10^6 = 9.7649 \times 10^9 \end{aligned}$$

$$Pr = .72, \text{ see Kreith } \underline{\text{Principals of Heat Transfer, 3rd Edition}}$$

$$(GrPr) = \underline{\underline{7 \times 10^9}}$$

Therefore; the flow turbulent and we may use McAdams recommendations:

$$\text{Vert Cyl: } h = .19 \Delta T^{1/3} \quad (\text{sides})$$

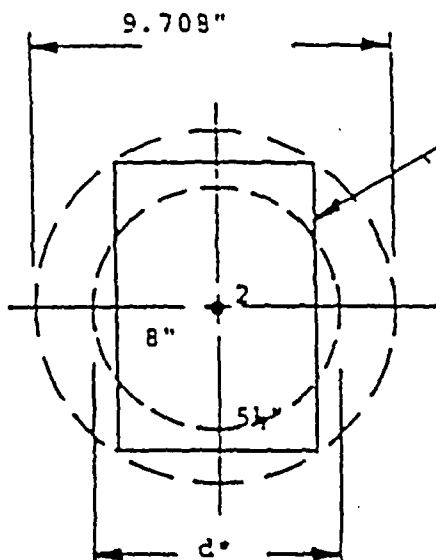
The effective convection areas are:

Node	Area (ft <sup>2</sup> )
2	0.611
9	40.904

3. CONDUCTION RESISTANCE TERMS FOR THE LUG PAD

R5 - Link to Outer Shell

$$t = (1/2)(2) = 1''$$



Lug Pad

$$A = \frac{\pi}{4} d^{*2} = (8.)(5.5)$$

$$d^* = 7.485$$

$$R5 = \frac{\ln(ro/ri)}{2\pi K l} = \frac{\ln(9.708/7.485)}{(2\pi)(11)(1/12)} = \underline{\underline{45.151 \times 10^{-3}}}$$

$$R38 = (1/4'' \text{ Fire Shield}) = \underline{\underline{22.576 \times 10^{-3}}}$$

R37 - Link to Lead

$$R = \frac{t}{KA} \quad t = (1/12)(19.00-1808-.5) = .035$$

$$K = 18.6$$

$$A = .611$$

$$R37 = \frac{.035}{(18.6)(.611)} = \underline{\underline{3.0797 \times 10^{-3}}}$$

9. SOLAR INSOLATION LOADS (Nodes 2 and 9)

Per NRC Regulatory Guide 7.8, Table #1, the solar insolation load applied to vertical curved surfaces is  $1475 \text{ Btu/ft}^2$  per 12 hour period.

The projected gross exposed area of the thermal shield is:

$$\begin{aligned} A_{g\text{gross}} &= (68.63-20)(2)(19.565)/144 \\ &= 13.215 \text{ ft.}^2 \end{aligned}$$

The projected area of the lug pad is:

$$A_2 = .611/2 = 0.306 \text{ ft.}^2$$

The net projected area of the fire shield is:

$$A_{g\text{net}} = 13.215 - .306 = 12.910 \text{ ft.}^2$$

The solar loads are:

$$q_2 = (.306)(1475/12)/3.41 = 11.01 \text{ watts}$$


$$q_9 = (12.910)(1475/12)/3.41 = 465.20 \text{ watts}$$

3.4.2 Maximum Temperatures

Maximum steady state temperatures, under normal conditions of transport, for selected locations in the package are shown in Table 3.4.2-1. Essentially all locations within the package, excepting the fire shield, exhibit near constant temperatures, for a given condition. It can also be observed that the predicted temperatures are a nearly linear function of applied decay heat. Detailed analysis results are found in Tables 3.4.2-2 to 3.4.2-10.



TABLE 3.4.2-1: Selected Maximum Temperatures for Normal Conditions of Transport, 1-13 C 11

CASE #	DECAY HEAT (WATTS)	AMBIENT AIR TEMP. (°F.) (NODE 1)	MAXIMUM TEMPERATURES (°F)					DETAIL. TABLE #
			FIRE SHIELD (NODE 9)	LIFT LUG (NODE 2)	SIDE OUTER SHELL (NODE 10)	TOP OUTER SHELL (NODE 3)	CAVITY (NODE 22)	
1	150	100	131.20	137.26	138.00	138.33	138.35	3.4.2-2
2	200		133.28	141.24	142.23	142.67	142.70	-3
3	300		137.35	149.03	150.49	151.16	151.20	-4
4	400		141.32	156.60	158.53	159.42	159.47	-5
5	500		145.17	163.96	166.35	167.46	167.51	-6
6	600		148.96	171.16	173.98	175.32	175.39	-7
7	700	152.66	178.16	181.42	182.97	183.06	-8	
8	800	100	156.27	185.00	188.67	190.45	190.55	-9
9	800	130	182.09	209.11	212.55	214.34	214.43	-10

3-21

\*Includes Solar Insolation per NRC Regulatory Guide 7.8.

TABLE 3.4.2-2 : 1-13 C II NORMAL TRANSPORT TEMPERATURES  
 150 WATT DECAY HEAT, 100 ° F AMBIENT AIR

STEADY STATE PROBLEM

TOTAL NUMBER OF NEWTON ITERATIONS = 8  
 NUMBER OF TEMPERATURE DEPENDENT INTERPOLATIONS = 4  
 NO. OF NEWTON ITERATIONS FOR FINAL UPDATE = 1

CLASS 2 - TEMPERATURE, T

ID	DEGREES F	ID	DEGREES F	ID	DEGREES F	ID	DEGREES F
1	100.000000	2	137.2511193	3	138.3357349	4	138.3365007
5	138.3372426	6	138.3371297	7	138.3415724	8	138.3452509
9	138.1006703	10	138.0037330	11	138.0410248	12	138.0824492
13	138.1237768	14	138.1712077	15	138.2337003	16	138.3357349
17	138.3350007	18	138.3375424	19	138.3393297	20	138.3416924
21	138.3435317	22	138.3537648				

TABLE 3.4.2-3 : 1-13 C II NORMAL TRANSPORT TEMPERATURES  
 200 WATT DECAY HEAT, 100 °F AMBIENT AIR

STEADY STATE PROBLEM

Total Number of Newton Iterations = 8  
 Number of Temperature Dependent Interpolations = 4  
 No. of Newton Iterations for Final Update = 1

CLASS 2 - Temperature, T

ID	DEGREES F	ID	DEGREES F	ID	DEGREES F	ID	DEGREES F
1	100.0029000	2	141.217444	3	142.6739202	4	142.6749494
5	142.5761140	6	142.5767217	7	142.6821307	8	142.6866169
9	133.2695512	10	142.2112441	11	142.2509326	12	142.3368616
13	142.3482518	14	142.4552263	15	142.5378431	16	142.5739282
17	142.5742474	18	142.6701140	19	142.6707217	20	142.6671367
21	142.5765164	22	142.673421				

TABLE 3.4.2-4 : 1-13 C11 NORMAL TRANSPORT TEMPERATURES  
 300 WATT DECAY HEAT, 100 °F AMBIENT AIR

STEADY STATE PROBLEM

TOTAL NUMBER OF NEWTON ITERATIONS = 8  
 NUMBER OF TEMPERATURE DEPENDENT INTERPOLATIONS = 4  
 NO. OF NEWTON ITERATIONS FOR FINAL UPDATE = 1

CLASS 2 - TEMPERATURE, T

ID	DEGREES F	ID	DEGREES F	ID	DEGREES F	ID	DEGREES F
1	100.0000000	2	149.0310249	3	151.1630035	4	151.1645269
5	151.1662225	6	151.1731264	7	151.1753230	8	151.1720412
9	137.7524714	10	150.6984189	11	150.5735431	12	150.6574416
13	150.7574964	14	150.6445580	15	150.4184429	16	151.1630035
17	151.1541360	18	151.1666220	19	151.1701260	20	151.1753230
21	151.1720412	22	151.1721305				

TABLE 3.4.2-5 : 1-13 C II NORMAL TRANSPORT TEMPERATURES  
 400 WATT DECAY HEAT, 100 °F AMBIENT AIR

STEADY STATE PROBLEM

TOTAL NUMBER OF NEWTON ITERATIONS = 8  
 NUMBER OF TEMPERATURE DEPENDENT INTERPOLATIONS = 4  
 NO. OF NEWTON ITERATIONS FOR FINAL UPDATE = 1

CLASS 2 - TEMPERATURE, T

ID	DEGREES F	ID	DEGREES F	ID	DEGREES F	ID	DEGREES F
1	159.0000000	2	156.6000963	3	159.4202341	4	159.4227808
5	157.4279222	6	159.4278248	7	157.4366662	8	157.4456252
9	141.1155473	10	155.5330786	11	157.6343664	12	158.7461642
13	151.7457936	14	157.0029521	15	157.1481047	16	157.4272341
17	157.4272808	18	157.4250622	19	159.4296248	20	157.4365462
21	157.4479252	22	157.4570814				

TAL 3.4.2-6: 1-13 C II NORMAL TRANSPORT TEMPERATURE  
 500 WATT DECAY HEAT, 100° F AMBIENT AIR

STEADY STATE PROBLEM

TOTAL NUMBER OF NEWTON ITERATIONS = 5  
 NUMBER OF TEMPERATURE DEPENDENT INTERPOLATIONS = 3  
 NO. OF NEWTON ITERATIONS FOR FINAL UPDATE = 1

CLASS 2 - TEMPERATURE, T

ID	DEGREES F	ID	DEGREES F	ID	DEGREES F	ID	DEGREES F
1	177.000000	2	163.4533043	3	167.4553214	4	167.4524434
5	167.4614516	6	167.4573226	7	167.4764700	8	167.4676700
9	167.4714103	10	167.4735002	11	167.4730042	12	167.46133511
13	167.4647746	14	167.4742100	15	167.4750000	16	167.4559218
17	167.4524434	18	167.4517610	19	167.4673223	20	167.4764700
21	167.4476703	22	167.454412				

TABLE 3.4.2-7 : 1-13 C II NORMAL TRANSPORT TEMPERATURES  
 600 WATT DECAY HEAT, 100° F AMBIENT AIR

STEADY STATE PROBLEM

TOTAL NUMBER OF NEWTON ITERATIONS = 4  
 NUMBER OF TEMPERATURE DEPENDENT INTERPOLATIONS = 2  
 NO. OF NEWTON ITERATIONS FOR FINAL UPDATE = 1

CLASS 2 - TEMPERATURE, T

3-27

ID	DEGREES F	ID	DEGREES F	ID	DEGREES F	ID	DEGREES F
1	100.0000000	7	171.1540155	3	175.3168582	4	175.3194359
5	175.3241116	8	175.3212870	7	175.3415258	8	175.3549691
9	174.0245516	10	173.0824145	11	174.1390275	12	174.3057034
13	176.4406015	14	174.8308231	15	174.9047012	16	175.3168582
17	175.3197359	19	175.3241116	19	175.3312670	20	175.3415258
21	175.3549691	22	175.3471616				

TABLE 3.4.2-8 : 1-13 CII NORMAL TRANSPORT TEMPER. .ES

700 WATT DECAY HEAT, 100 °F AMBIENT AIR

STEADY STATE PROBLEM

TOTAL NUMBER OF NEWTON ITERATIONS = 6

NUMBER OF TEMPERATURE DEPENDENT INTERPOLATIONS = 3

NO. OF NEWTON ITERATIONS FOR FINAL UPDATE = 1

CLASS 2 - TEMPERATURE, T

3-28

ID	DEGREES F	ID	DEGREES F	ID	DEGREES F	ID	DEGREES F
1	100.000000	7	179.1631416	3	182.9737595	4	182.9773546
5	182.9972283	4	182.9705745	7	183.0025496	8	183.0182362
0	157.6543126	10	181.4154732	11	191.5485426	12	191.7742072
13	182.0019096	14	182.2476073	15	182.4077727	16	182.9737595
17	182.9773546	18	182.0422293	19	182.9905785	20	183.0125496
21	182.0132362	22	183.0454021				



TABLE 3.4.2-9 : 1-13CII NORMAL T<sub>1</sub> PORT TEMPERATURES  
 800 WATT DECAY HEAT, 100 °F AMBIENT AIR

STEADY STATE PROBLEM

TOTAL NUMBER OF NEWTON ITERATIONS = 8

NUMBER OF TEMPERATURE DEPENDENT INTERPOLATIONS = 4

NO. OF NEWTON ITERATIONS FOR FINAL UPDATE = 1

CLASS 2 - TEMPERATURE, T

ID	DEGREES F	ID	DEGREES F	ID	DEGREES F	ID	DEGREES F
1	100.0000000	2	135.0015911	3	170.4530011	4	170.4571140
5	170.4526571	6	170.4722328	7	190.4859168	8	190.5036474
9	154.7675180	10	150.6629394	11	148.6813742	12	169.1049674
13	170.4504435	14	150.6123376	15	109.9089852	16	170.4530011
17	170.4571148	18	170.4526571	19	170.4722328	20	170.4859168
21	170.5036474	22	170.5057569				

TABLE 3.4.2-10 : 1-13 CII NORMAL TRANSPORT TEMPERATURES

800 WATT DECAY HEAT, 130 °F AMBIENT AIR

STEADY STATE PROBLEM

TOTAL NUMBER OF NEWTON ITERATIONS = 8  
 NUMBER OF TEMPERATURE DEPENDENT INTERPOLATIONS = 4  
 NO. OF NEWTON ITERATIONS FOR FINAL UPDATE = 1

CLASS 2 - TEMPERATURE, T

ID	DEGREES F	ID	DEGREES F	ID	DEGREES F	ID	DEGREES F
1	130.000000	2	209.1090136	3	214.3410132	4	214.3451503
5	214.3507337	6	214.3602914	7	214.3739886	8	214.3919336
9	182.0957505	10	212.5477853	11	212.7695123	12	212.9931026
13	213.2345757	14	213.5064664	15	213.7970954	16	214.3410132
17	214.3451503	18	214.3507337	19	214.3602914	20	214.3739886
21	214.3919336	22	214.4349039				

### 3.4.3 Minimum Temperatures

The minimum temperatures of the 1-13C II package approach  $-40^{\circ}\text{F}$  since several of the planned payloads possess very low decay heats. The stainless steel and lead materials of construction for the packaging are not significantly affected by an ambient temperature of  $-40^{\circ}\text{F}$ . For higher decay heats, these minimum temperatures do not exceed  $82^{\circ}\text{F}$ . Table 3.4.3-1 summarizes predicted temperatures for an 300 watt decay heat payload.

### 3.4.4 Maximum Internal Pressures

Internal pressure in the cask activity is calculated assuming:

- o The cask is loaded at a temperature of  $70^{\circ}\text{F}$  and is unpressurized.
- o A small but sufficient quantity of free water is always present. This conservatively permits pressure calculations to be based on tabulated thermodynamic properties of saturated water and steam.

LE 3.4.3-1 : 1-13 C II NORMAL TRANSPORT TEMPER. ES

800 WATT DECAY HEAT, -40<sup>D</sup> AMBIENT AIR

STEADY STATE PROBLEM

TOTAL NUMBER OF NEWTON ITERATIONS = 12  
 NUMBER OF TEMPERATURE DEPENDENT INTERPOLATIONS = 5  
 NO. OF NEWTON ITERATIONS FOR FINAL UPDATE = 1

CLASS 2 - TEMPERATURE, T

ID	DEGREES F	ID	DEGREES F	ID	DEGREES F	ID	DEGREES F
1	-40.000000	2	74.4113738	3	81.3793387	4	81.3839329
5	81.3894488	4	81.3894329	7	81.4125500	4	81.4104069
9	37.3391247	10	79.6485305	11	79.8975699	12	80.0312776
13	80.2747835	14	80.5446205	15	80.8353213	16	81.3793387
17	81.3894329	14	81.3894488	19	81.3894329	20	81.4125500
21	81.4125500	22	81.4731874				

3-32

- o The cask cavity serves as the pressure boundary of the system; conservatively no pressure retention capability is assumed for the payload container (liner, drum, etc.)

Pressure calculations are based upon the appropriate partial pressures of air and water. At the time of loading, the total pressure is the sum of partial pressures for air and water and is equal to atmospheric pressure:

$$T_F = P_{AF} + P_{WF} \quad (1)$$

Where:  $T_F$  = Total Pressure

$P_{AF}$  = Partial pressure of air, at temperature, F

$P_{WF}$  = Partial pressure of water, at temperature, F

The partial pressure of air, at time of loading, is found as:

$$P_{AF} = T_F - P_{WF} \quad (2)$$

Once steady state equilibrium temperatures are established, the total and gauge pressures in the package are found as:

$$T_X = P_{AX} + P_{WX} \quad (3)$$

$$G_X = T_X - T_F \quad (4)$$

Where: x = the steady state equilibrium temperature of the coolest portion of cask cavity; i.e., the condensation surface.

$G_X$  = Gauge pressure of cask at temperature, x

The partial pressure of air at temperature,  $x$ , is calculated assuming adiabatic constant volume relations:

$$\frac{PV}{T} = \text{constant}$$

$$P_{AX} = P_{AF} \cdot \frac{(460 + X)}{(460 + F)} \quad (5)$$

The partial pressures of water,  $P_{AF}$  and  $P_{AX}$ , are taken directly from the thermodynamic properties of saturated water and steam. The tabulated values developed by Joseph H. Keenan and Frederick G. Keyes, "Thermodynamic Properties of Steam", John Wiley & Sons, 1936, are reproduced below:

Temp. °F	Abs. Press. Lb Sq In.	Temp. °F	Abs. Press. Lb Sq In.
70	0.00454	300	97.012
80	0.00663	310	77.64
90	0.00970	320	69.64
100	0.01433	330	100.00
110	0.02111	340	118.01
120	0.0303	350	134.83
130	0.0431	360	151.04
140	0.0596	370	167.37
150	0.0803	380	183.77
160	0.1063	390	200.37
170	1.3748	400	217.21
180	1.816	410	234.25
190	2.375	420	251.51
200	3.064	430	268.97
210	3.918	440	286.64
220	4.971	450	304.52
230	6.26	460	322.6
240	7.81	470	340.8
250	9.56	480	359.1
260	11.55	490	377.4
270	13.81	500	395.8
280	16.27	510	414.3
290	19.96	520	432.8
300	24.91	530	451.4
310	30.17	540	470.0
320	36.78	550	488.7
330	44.78	560	507.4
340	54.20	570	526.1
350	65.18	580	544.8
360	77.77	590	563.5
370	92.03	600	582.2
380	108.03	610	600.8
390	125.83	620	619.4
400	145.48	630	637.9
410	167.03	640	656.4
420	190.53	650	674.8
430	216.03	660	693.2
440	243.58	670	711.5
450	273.23	680	729.8
460	305.03	690	748.0
470	339.03	700	766.2
480	375.28	710	784.4
490	413.83	720	802.5
500	454.73	730	820.6
510	498.03	740	838.6
520	543.78	750	856.6
530	592.03	760	874.5
540	642.83	770	892.4
550	696.13	780	910.2
560	752.98	790	927.9
570	812.33	800	945.5
580	874.23	810	963.1
590	938.63	820	980.6
600	1005.58	830	998.0
610	1075.03	840	1015.3
620	1147.03	850	1032.5
630	1221.53	860	1049.6
640	1298.58	870	1066.6
650	1378.13	880	1083.5
660	1460.23	890	1100.3
670	1544.83	900	1117.0
680	1631.98	910	1133.6
690	1721.63	920	1150.1
700	1813.83	930	1166.5
710	1908.53	940	1182.8
720	2005.78	950	1199.0
730	2105.53	960	1215.1
740	2207.83	970	1231.1
750	2312.63	980	1247.0
760	2419.98	990	1262.8
770	2529.83	1000	1278.5
780	2642.23		
790	2757.13		
800	2874.58		

Substitution of equations (3), (5) and (2) into equation (1) gives a final expression for gauge pressures,  $G_X$ , in the package:

$$G_X = \frac{(T_F - P_{WF})(460 + X)}{(460 + F)} + P_{WX} - T_F \quad (6)$$







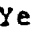
For this evaluation the following values are constant:

$$F = 70^\circ\text{F, temperature at fill}$$

$$P_{WF} = 0.3631 \text{ psi, partial pressure of water at loading temperature}$$

$$T_F = 14.7 \text{ psi, at atmospheric pressure}$$

Normal transport pressure results are summarized for the 1-13C II package, as follows:

Case No.	Decay Heat (Watts)	Air Temp. ( $^\circ\text{F}$ )	Solar Insol. Present	Cavity Temp. ( $^\circ\text{F}$ )	Internal Pressure (psic)
1	150	100	Yes	138.35	4.27
2	200	  	  	142.70	4.72
3	300			151.20	5.68
4	400			159.47	6.75
5	500			167.51	7.96
6	600			175.39	9.30
7	700	183.06	10.77		
8	800	100		190.55	12.36
9	800	130		Yes	214.43
10	800	-40	No	81.47	0.48

#### 3.4.5 Maximum Thermal Stresses

Table 3.4.2-1 demonstrates that the cask body possesses less than a two degree gradient through the walls, under a maximum decay heat payload of 200 watts; thus, stresses due to differential radial thermal expansions are negligible. Comprehensive evaluation of pressure and axial differential thermal expansions are completely evaluated in Section 2.6.1 utilizing two axisymmetric finite element models for the cask body and lid. All stresses are found to be well within established limits for the materials of construction.

#### 3.4.6 Evaluation of Package Performance for Normal Conditions of Transport

The thermal behavior of the 1-13C II package is completely consistent with the allowables for all materials of construction. In particular, the maximum predicted temperature of the payload cavity, 214.43°F, is well below the established service limit of 400°F for silicon seals.

Key findings used elsewhere in this report for detail stress analyses are summarized in Table 3.4.2-1.



### 3.5 Hypothetical Thermal Accident Evaluation

The thermal evaluation of the 1-13C II package for the hypothetical thermal accident defined in 10 CFR 71, has been performed analytically using essentially the same model as described in Section 3.4 for normal transport conditions. The eight payload decay heats, discussed in Section 3.4.2, have been thoroughly evaluated versus the requirements of 10 CFR 71.

#### 3.5.1 Thermal Model

The common thermal model, described in Section 3.4.1, has been used for the transient analyses associated with the Hypothetical Thermal Accident. Salient differences are as follows:

The ambient environment, node 1, is described by a tabular definition of temperature versus time. Up to a time of 0.5 hours this environment is 1475° F. Subsequent to this time, the ambient environment drops to 70° F.

Initial conditions correspond to the eight decay heats examined in Section 3.4.2 and defined in Table 3.4.2-1.

The external convection heat transfer modes became effective only at the termination of the 0.5 hour accident event. Three hours following the termination of the thermal accident, artificial cooling is introduced by increasing the free convection film coefficient by one hundred fold.

#### 3.5.2 Package Conditions and Environment

Free drop and puncture test damage do not measurably alter the thermal behavior of the 1-13C II package. Specifically, free drop damage only affects the geometry of the overpack. This fact has been demonstrated conclusively by test, see Section 2.11. Since the net affect of the

overpack is to enforce near adiabatic thermal boundary conditions on the package ends, any change to the thermal characteristics of the overpack is of modest second order proportions. Similarly, since puncture deformations imposed upon the thermal shield can, at worst, change its thermal behavior less than one-half percent, the resultant changes may be dismissed as trivial.

### 3.5.3 Package Temperatures

Particularly important component temperatures are summarized in Section 3.1. Table 3.5.3-1 summarizes extreme temperatures encountered for all decay heats examined. Figures 3.5.3-1 to -16 plot the temperature versus time response of key locations in the package.

Table 3.5.3-1 Selected Maximum Temperatures for  
Hypothetical Accident Conditions, 1-13 C II

Case #	Decay Heat (Watts)	MAXIMUM FIRE TEMPERATURES (°F)					Transient Results Figure #
		Fire Shield (Node 9)	Left Lug (Node 2)	Side Outer Shell (Node 10)	Top Outer Shell (Node 7)	Cavity (Node 22)	
1	150	1170	463.60	384.23	313.48	320.42	3.5.3-1 to -2
2	200	1170	467.37	388.44	317.63	324.67	-3 to -4
3	300	1171	474.73	396.66	325.76	332.98	-5 to -6
4	400	1171	481.89	404.64	333.66	341.06	-7 to -8
5	500	1172	488.85	412.40	341.35	348.93	-9 to -10
6	600	1173	495.65	419.99	348.88	356.62	-11 to -12
7	700	1173	502.27	427.37	356.20	364.11	-13 to -14
8	800	1174	508.73	434.56	363.35	371.43	-15 to -16

FIGURE 3.5.3-1

HYPOTHETICAL FIRE ACCIDENT

CNS 1-13C W/ OVERPACK. TRANSIENT. 100 DEG-F AIR. 150 WATTS

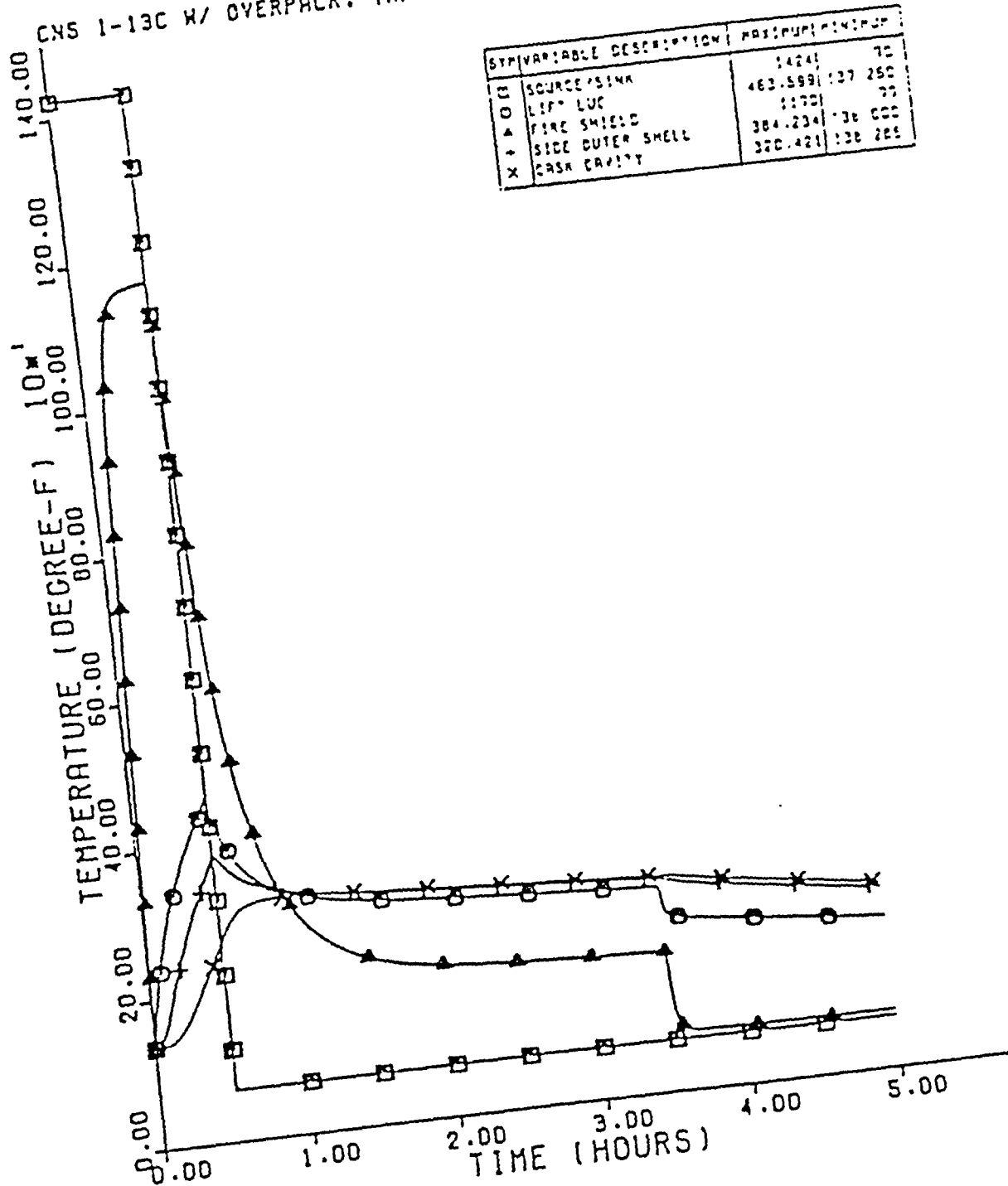


FIGURE 3.5.3-2

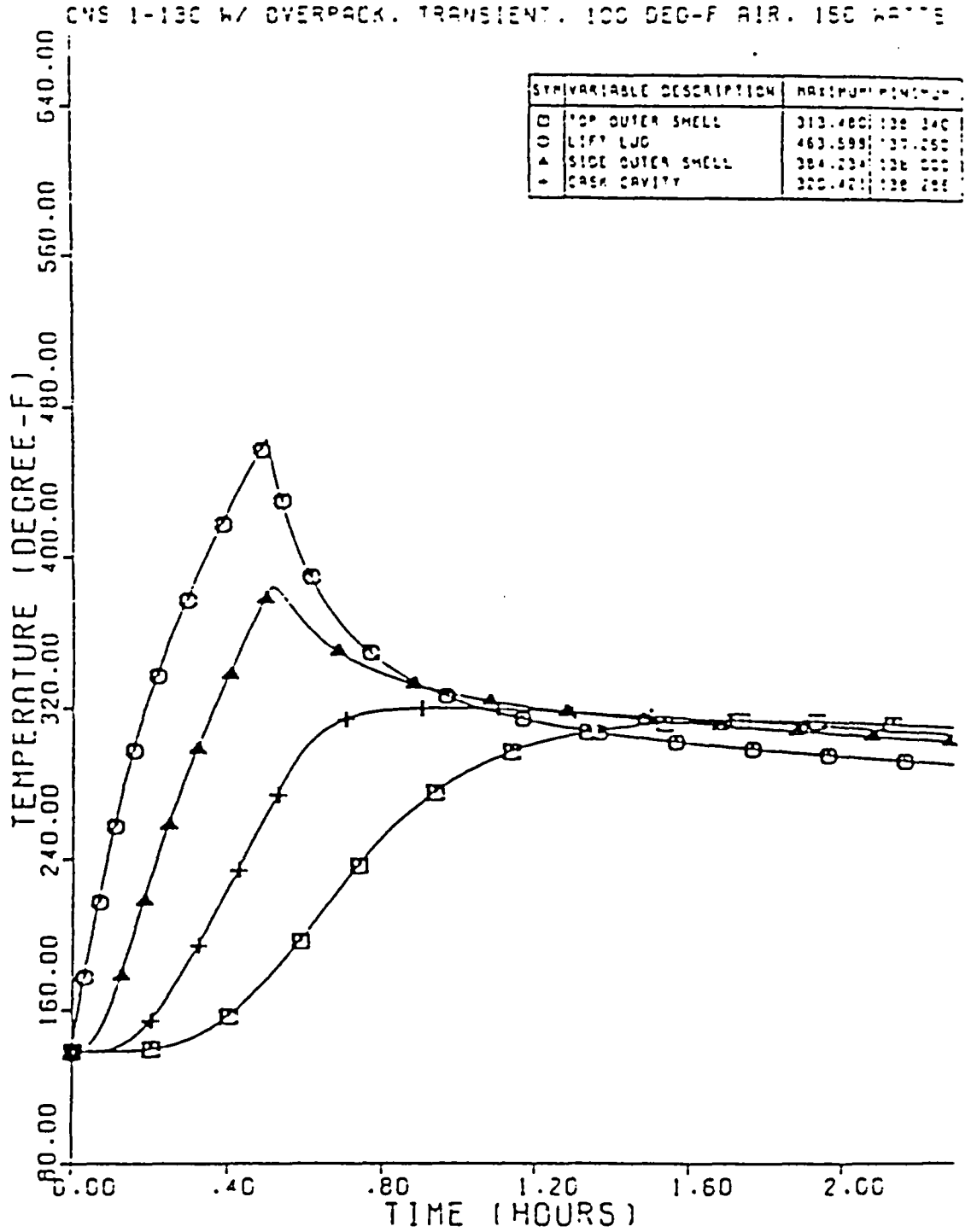


FIGURE 3.5.3-3

HYPOTHETICAL FIRE ACCIDENT

CNS 1-130 W/ OVERPACK. TRANSIENT. 100 DEG-F AIR. 200 WATTS

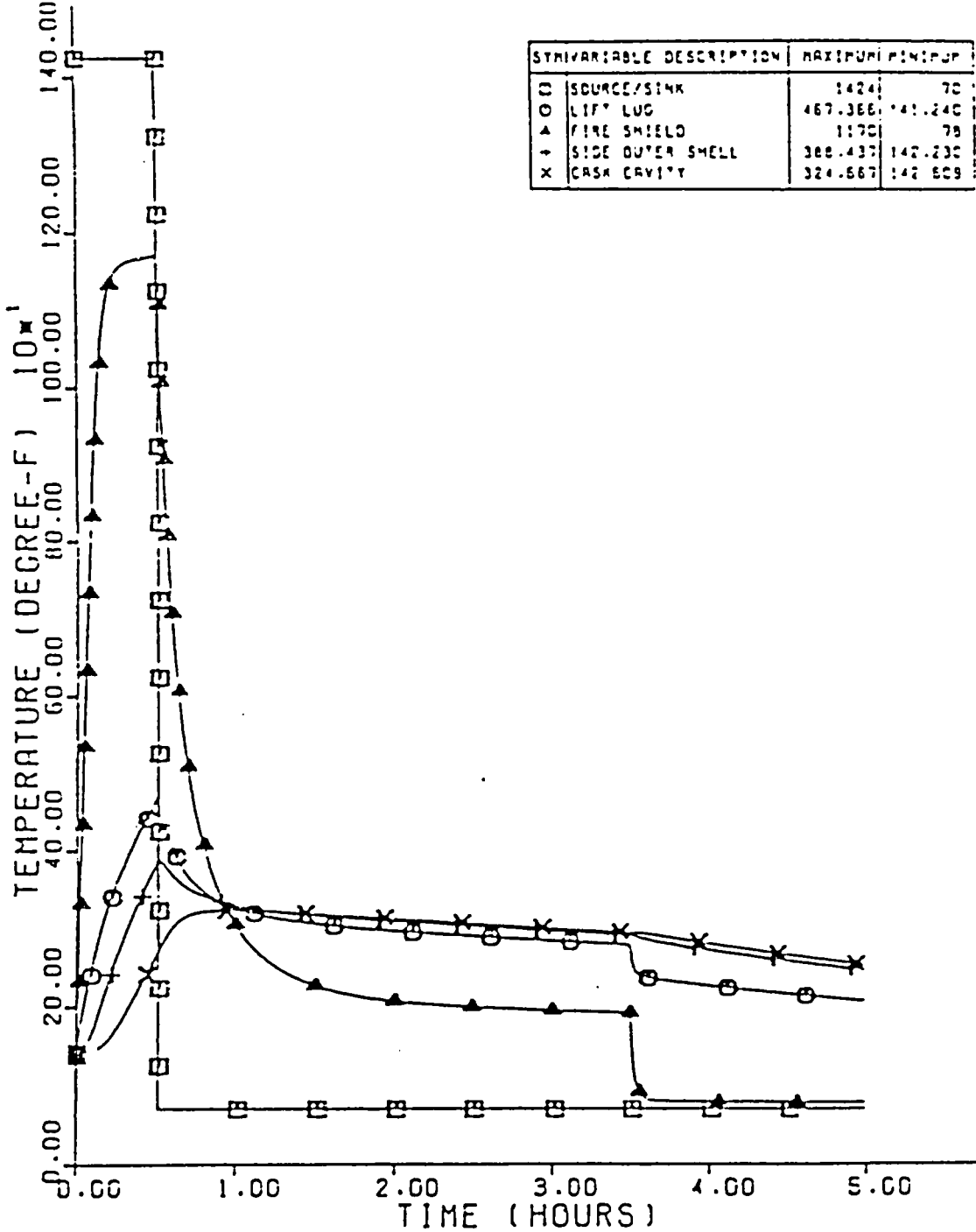


FIGURE 3.5.3-4

HYPOTHETICAL FIRE ACCIDENT

CNS 1-130 W/ OVERPACK. TRANSIENT. 100 DEG-F AIR. 200 WATTS

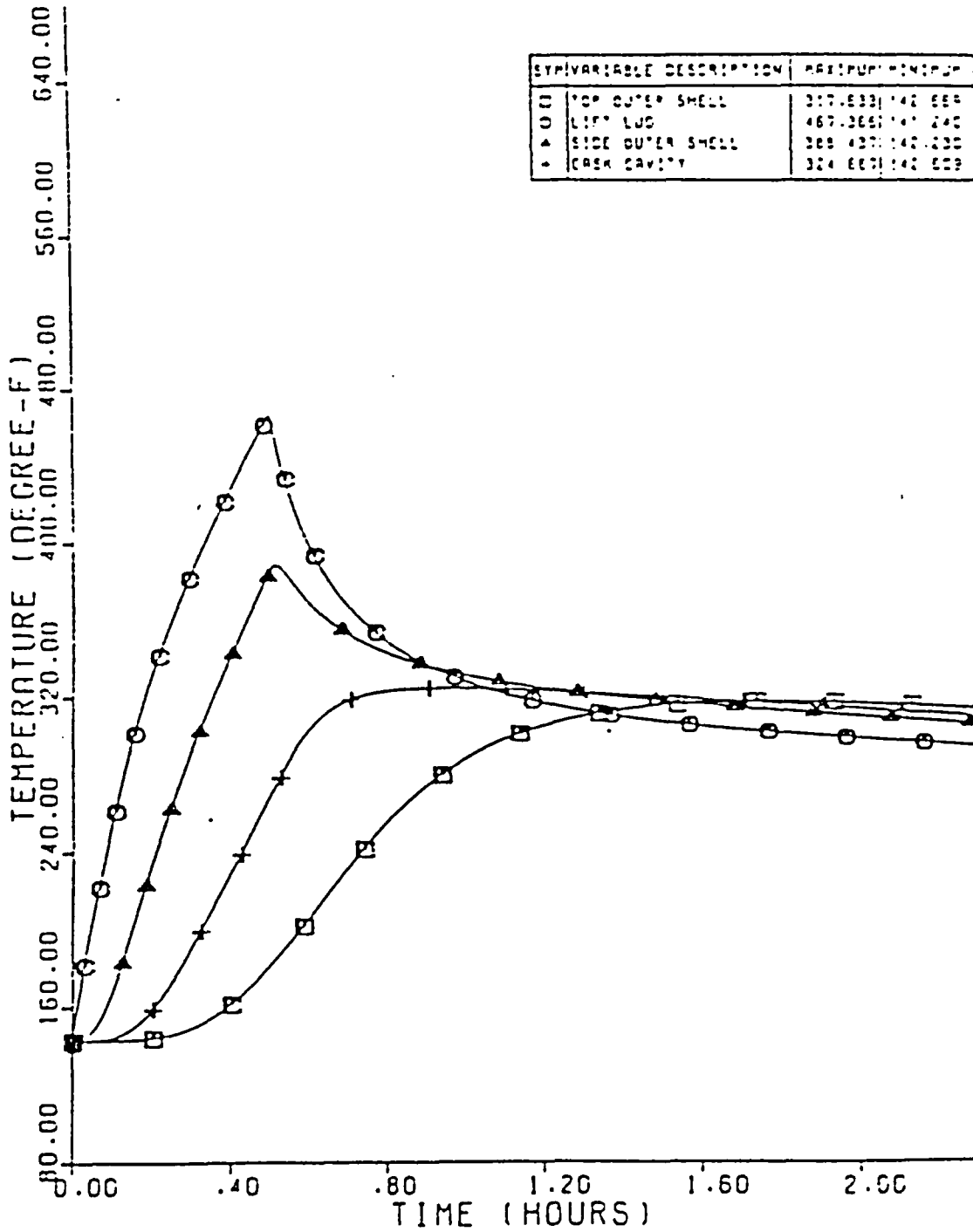


FIGURE 3.5.3-5

HYPOTHETICAL FIRE ACCIDENT

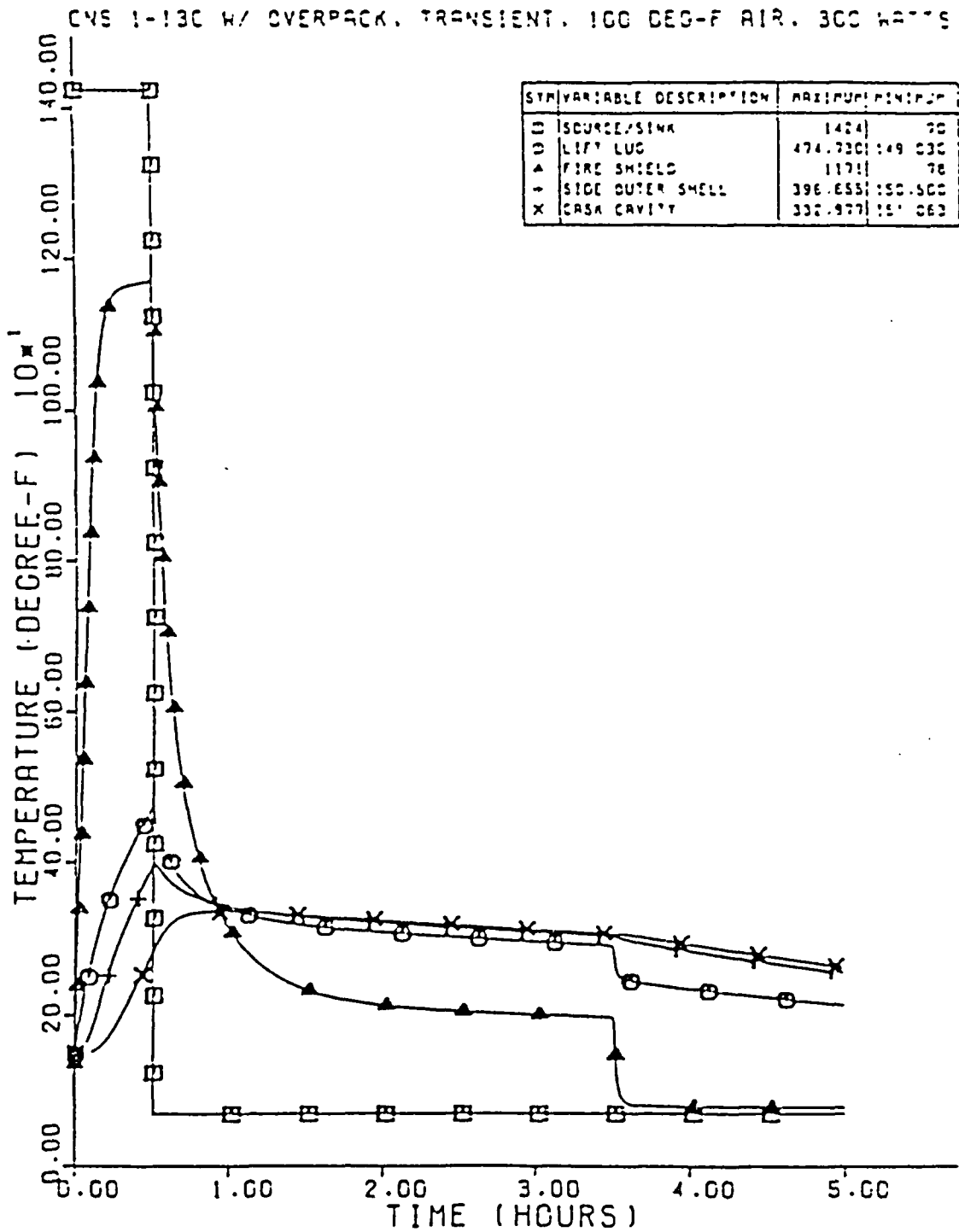




FIGURE 3.5.3-6

HYPOTHETICAL FIRE ACCIDENT

CNS 1-130 W/ OVERPACK. TRANSIENT. 100 DEG-F AIR. 300 WATTS

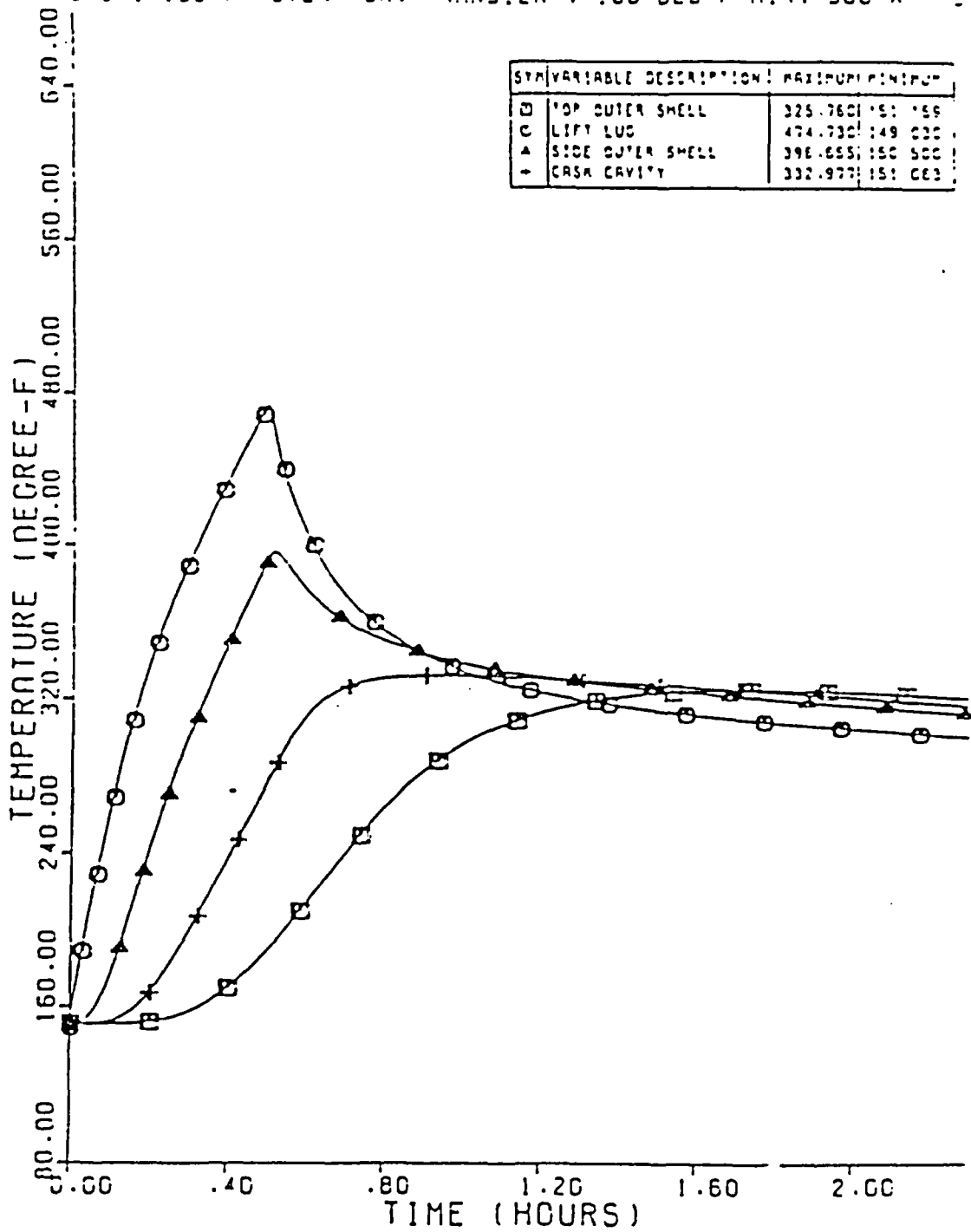


FIGURE 3.5.3-7

HYPOTHETICAL FIRE ACCIDENT

CNS 1-13C W/ OVERPACK. TRANSIENT. 100 DEG-F AIR. 400 WATTS

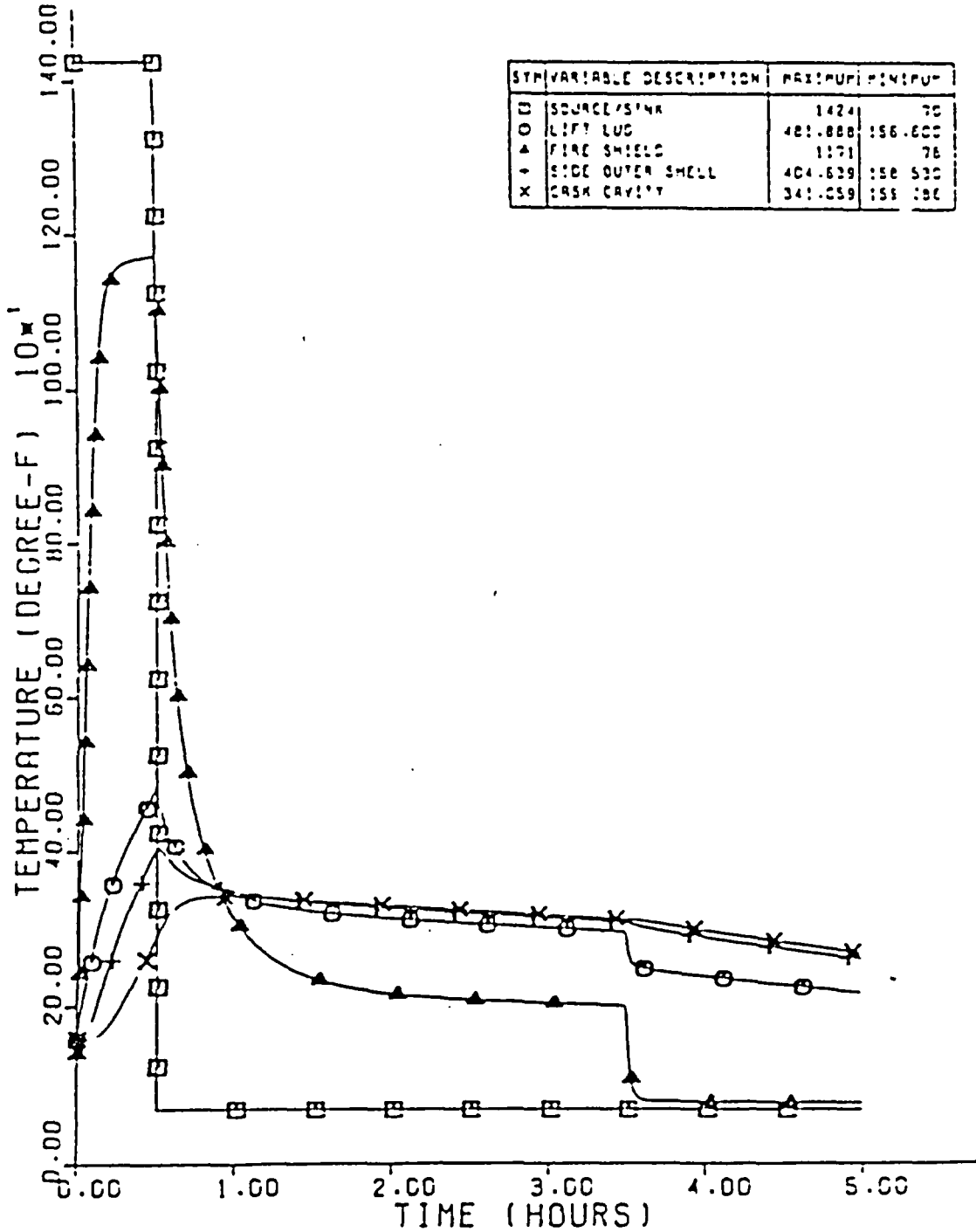


FIGURE 3.5.3-8

HYPOTHETICAL FIRE ACCIDENT

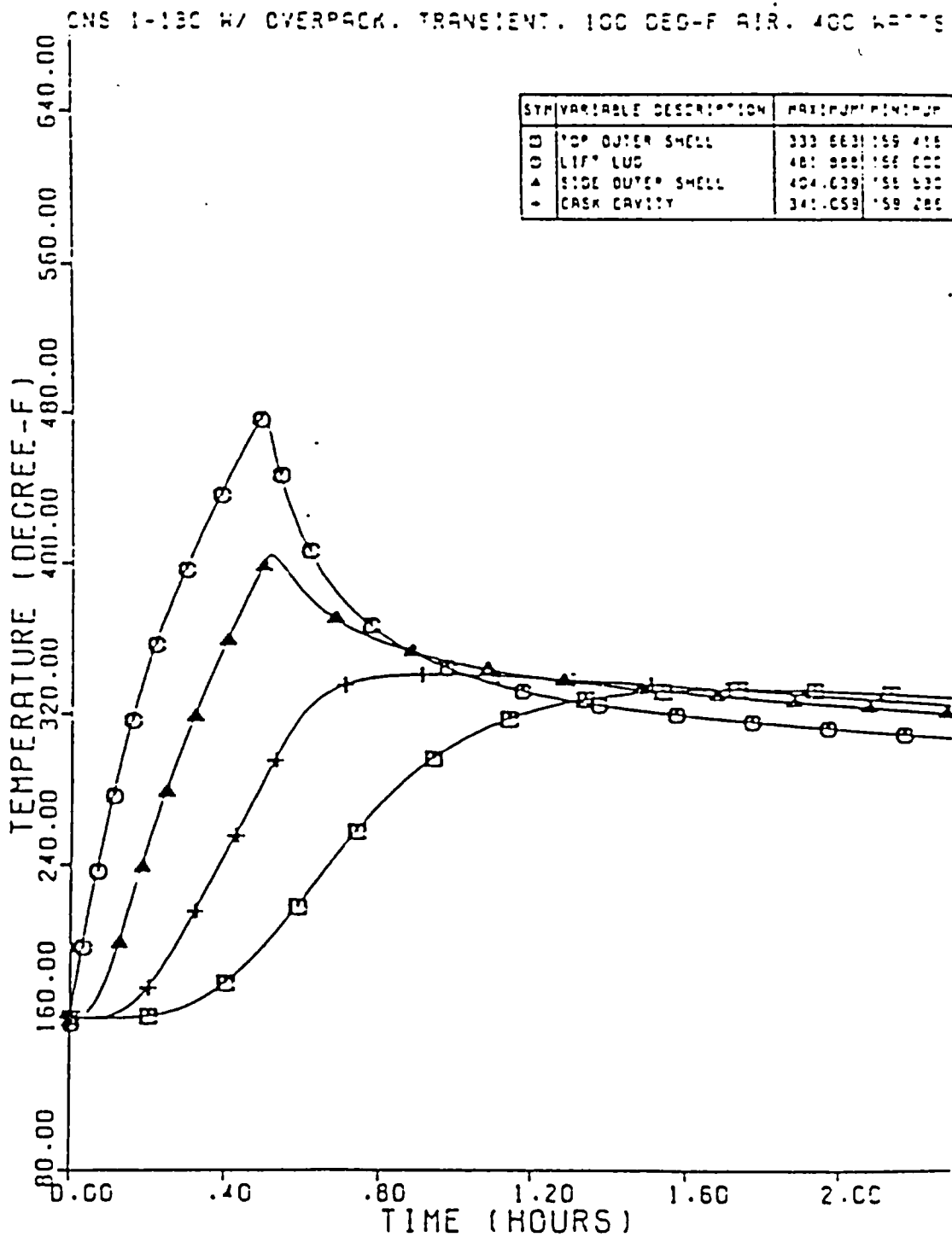


FIGURE 3.5.3-9

HYPOTHETICAL FIRE ACCIDENT

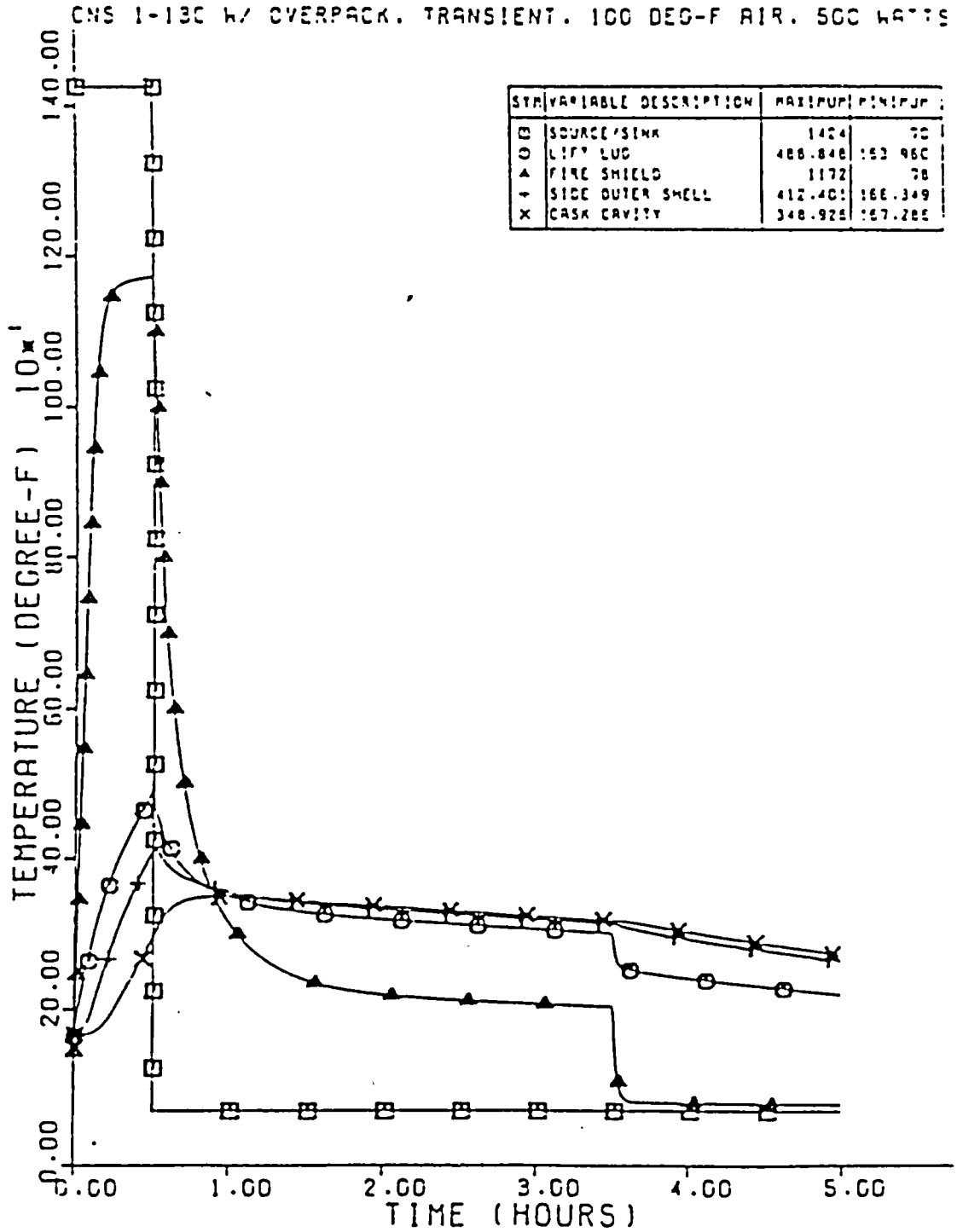


FIGURE 3.5.3-10

HYPOTHETICAL FIRE ACCIDENT

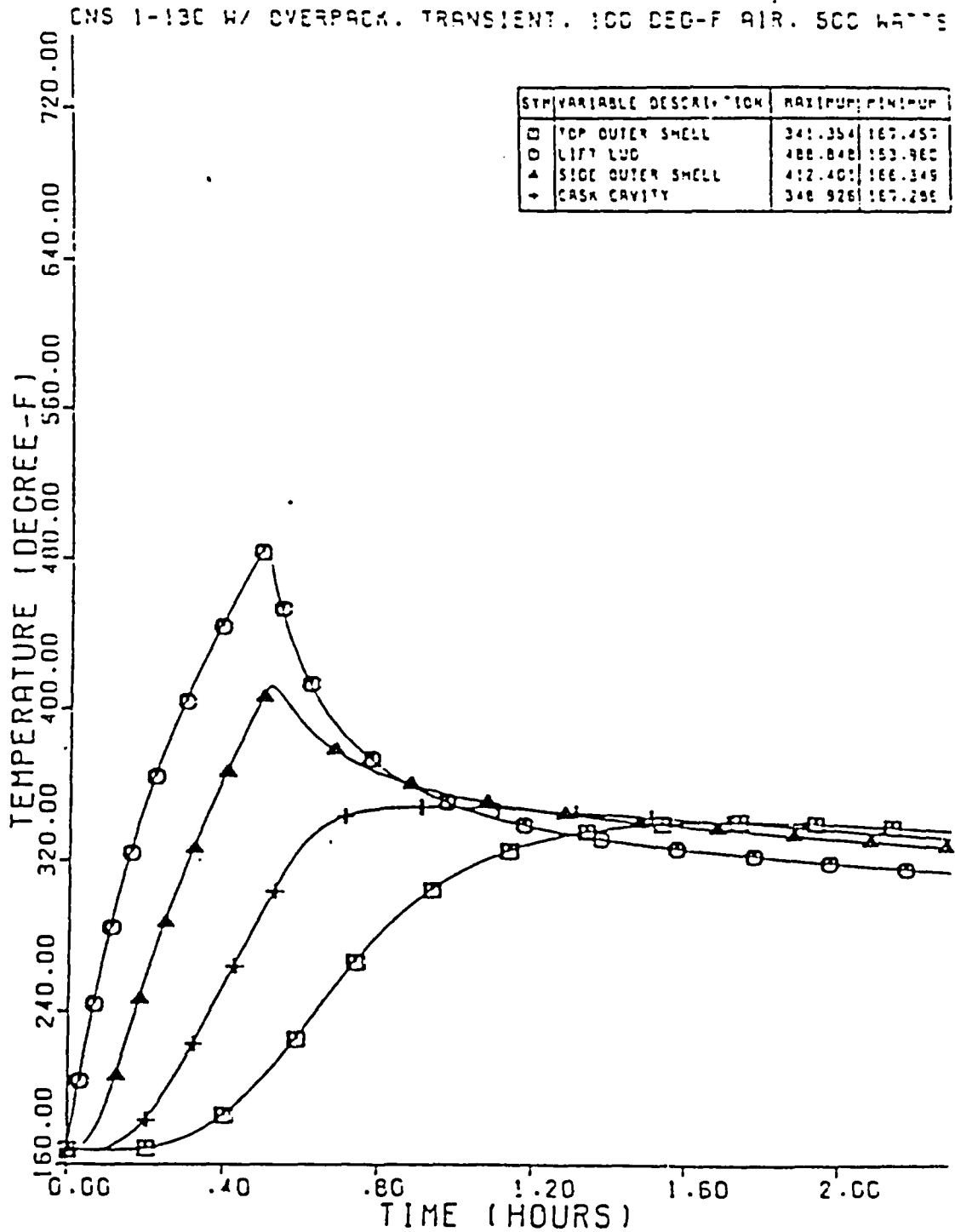


FIGURE 3.5.3-11

HYPOTHETICAL FIRE ACCIDENT

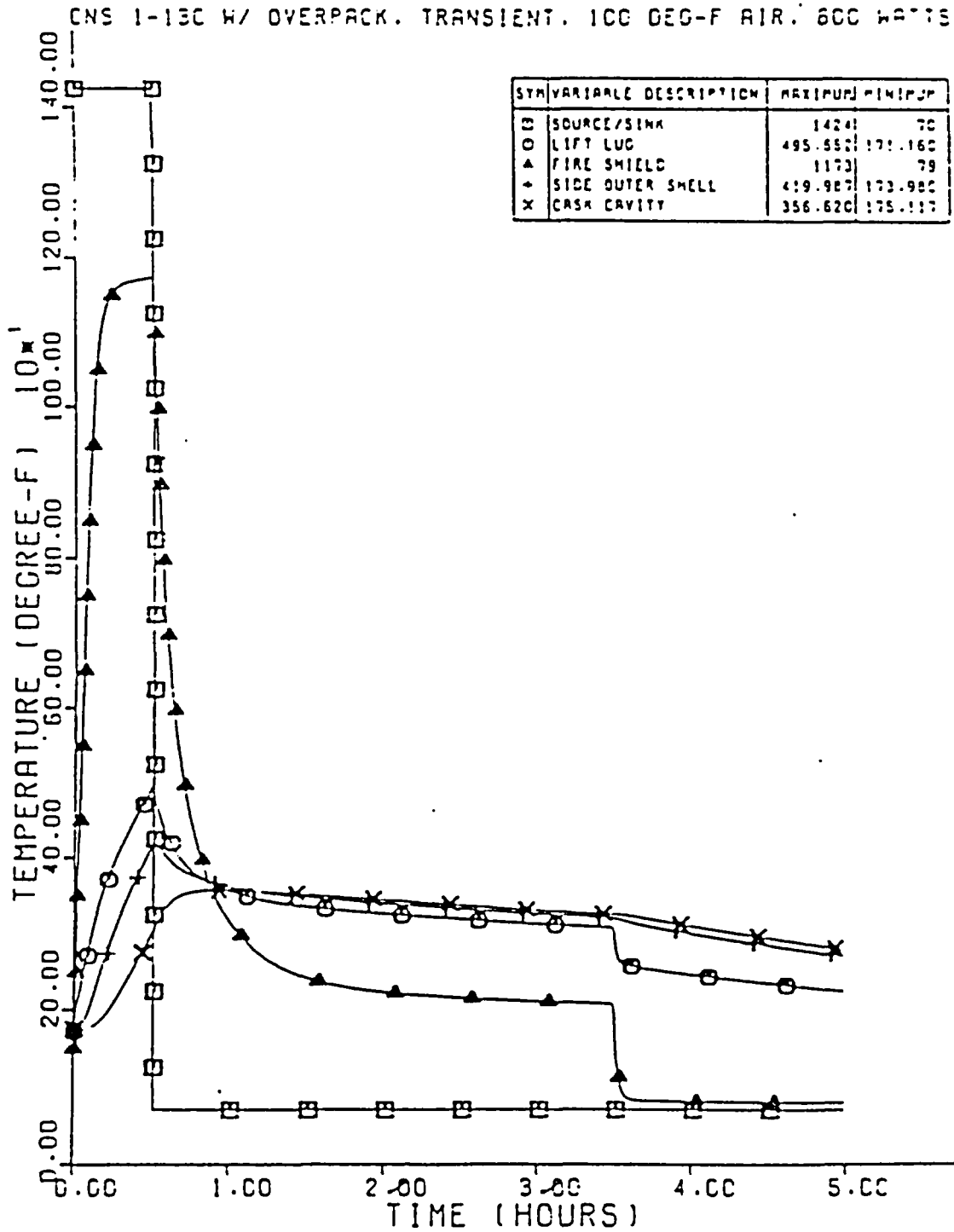


FIGURE 3.5.3-12

HYPOTHETICAL FIRE ACCIDENT

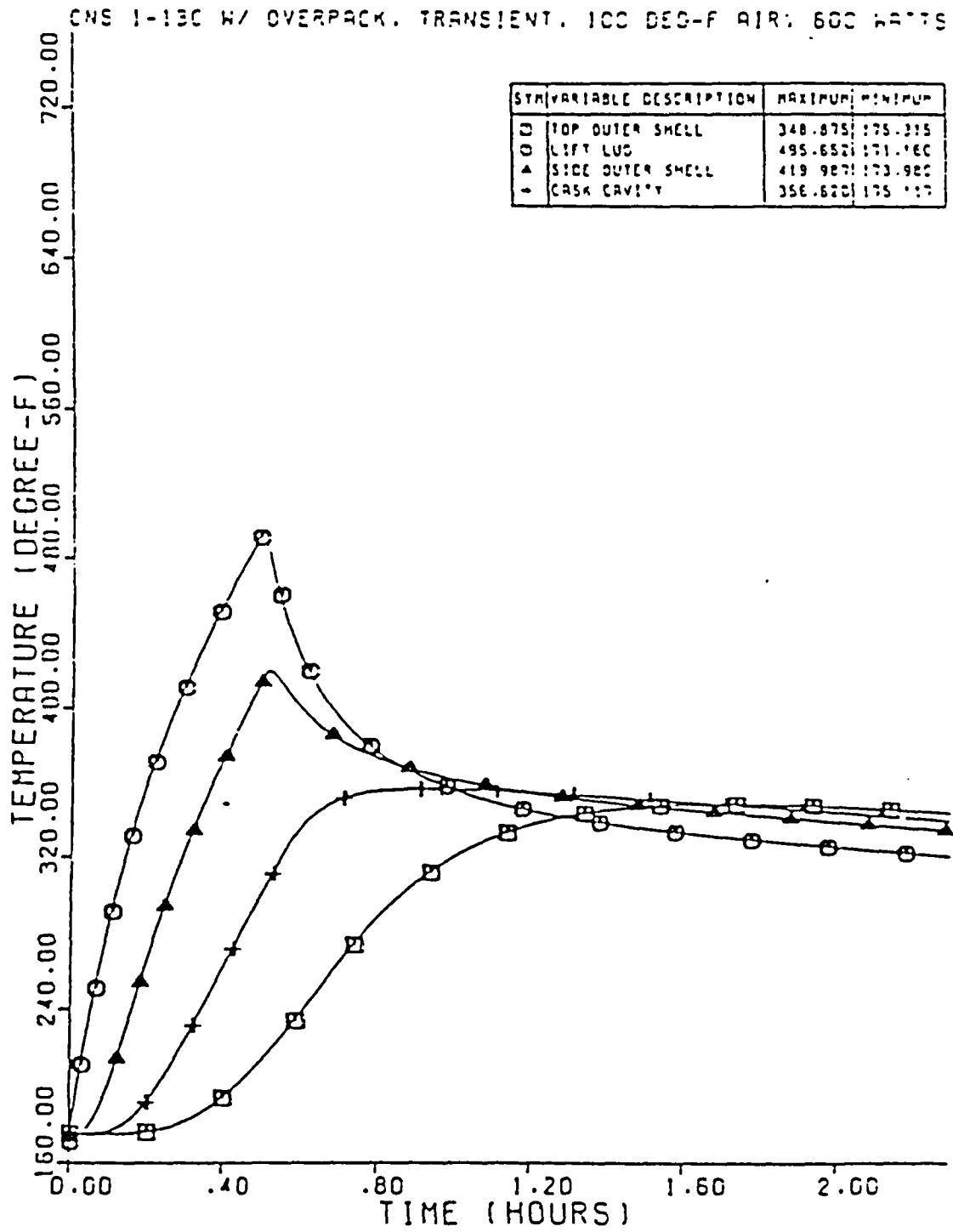


FIGURE 3.5.3-13

HYPOTHETICAL FIRE ACCIDENT

CNS 1-13C W/ OVERPACK. TRANSIENT. 100 DEG-F AIR. 700 WATTS

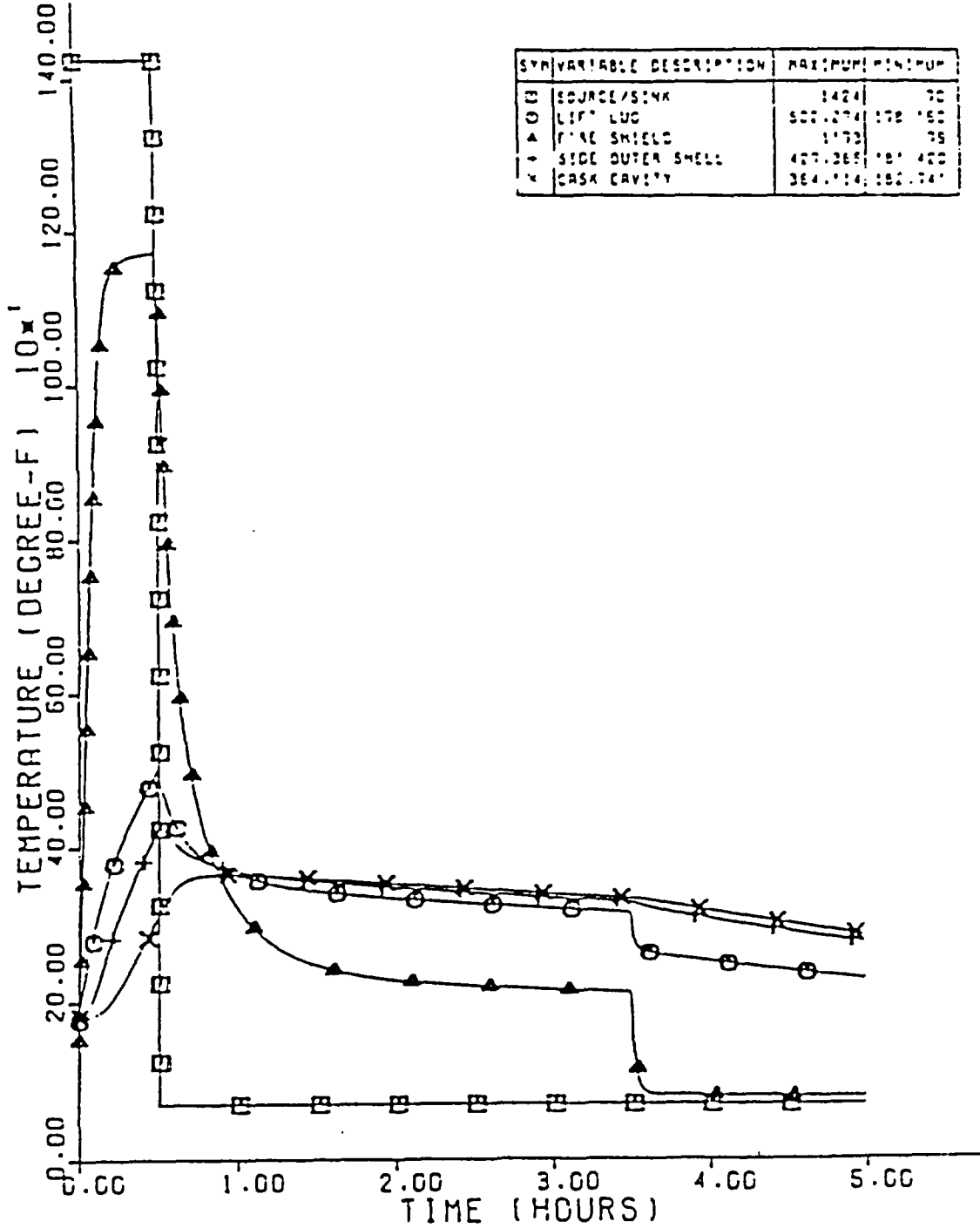




FIGURE 3.5.3-14

HYPOTHETICAL FIRE ACCIDENT

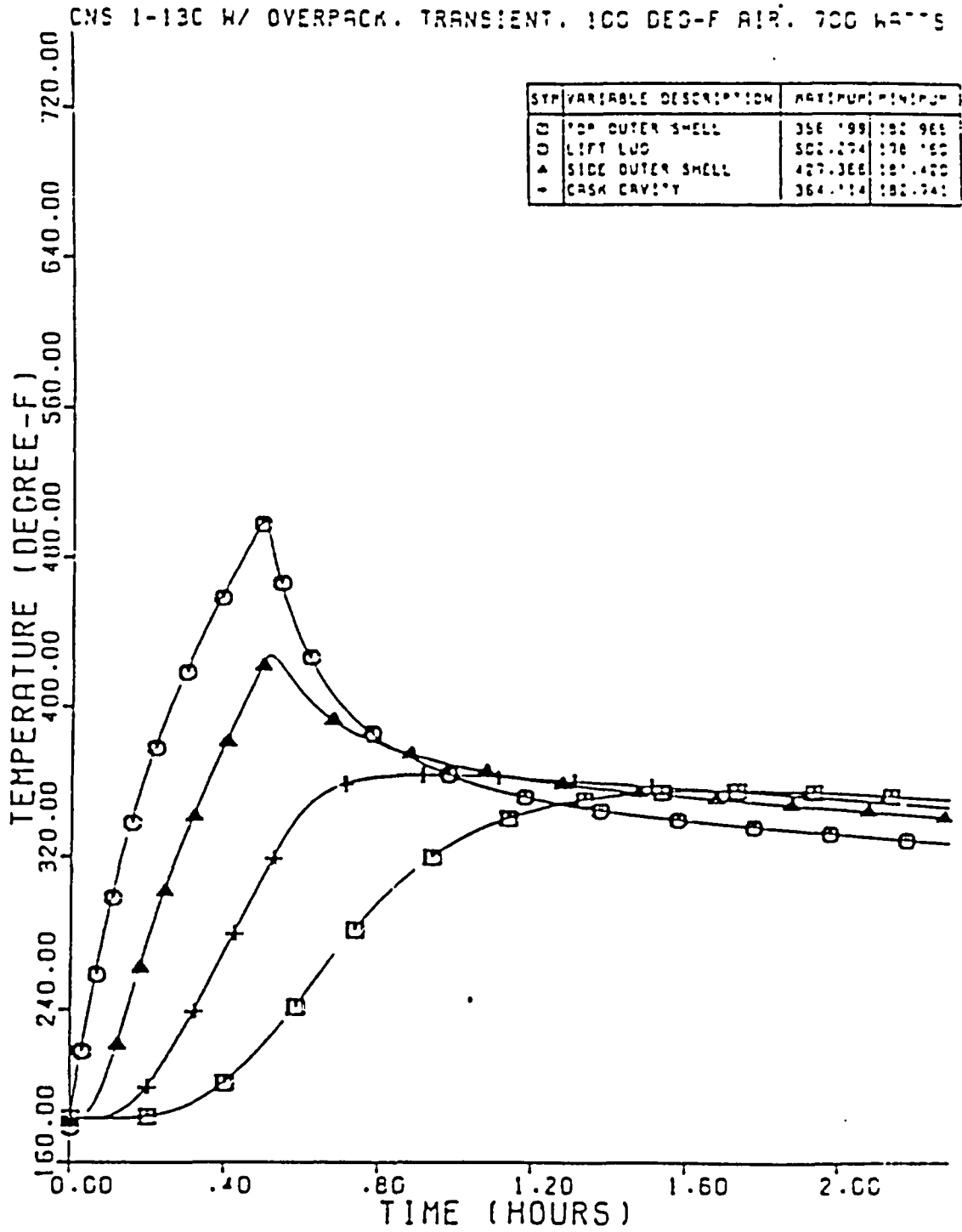


FIGURE 3.5.3-15

HYPOTHETICAL FIRE ACCIDENT

CNS 1-130 W/ OVERPACK. TRANSIENT. 100 DEG-F AIR. 800 WATTS

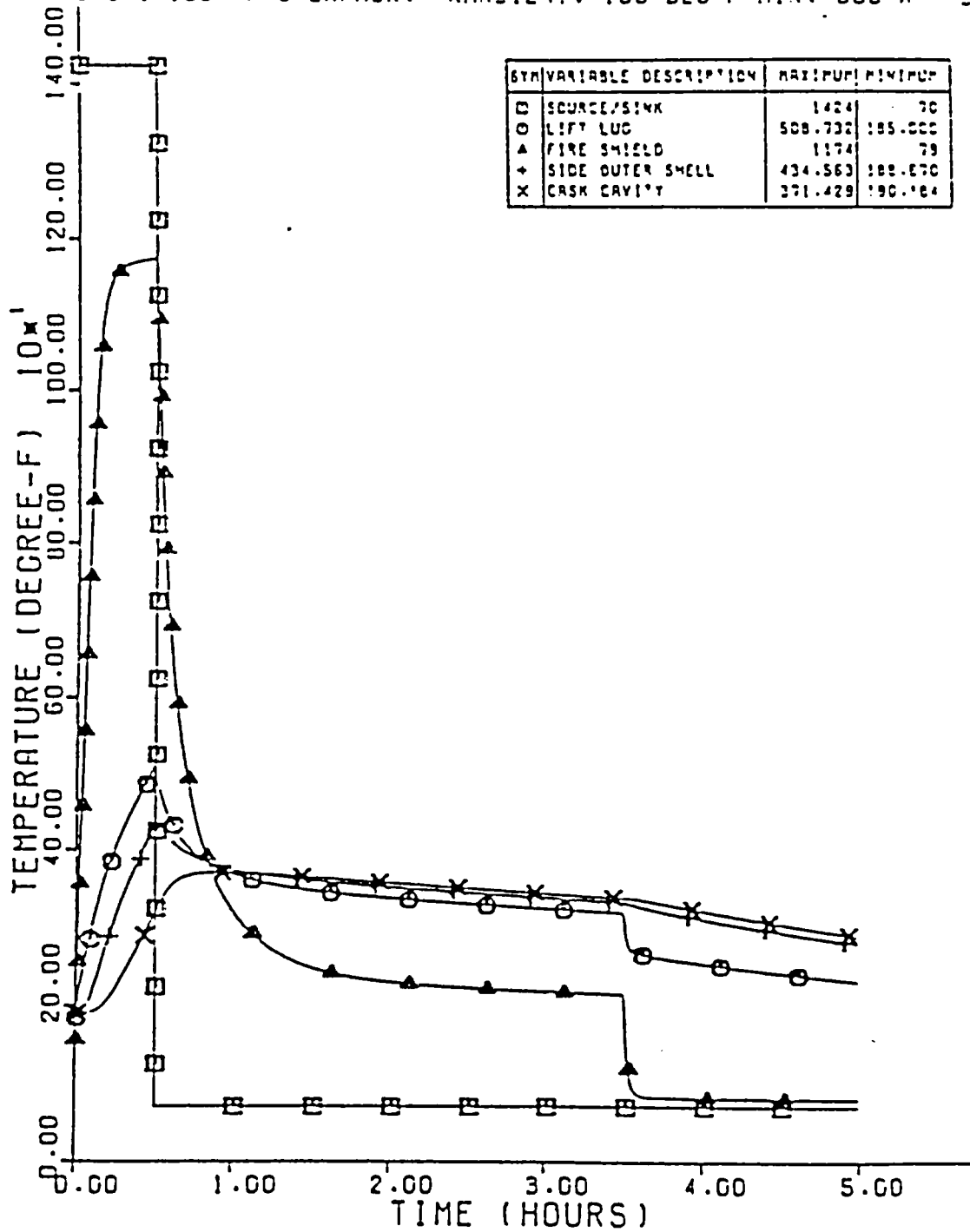
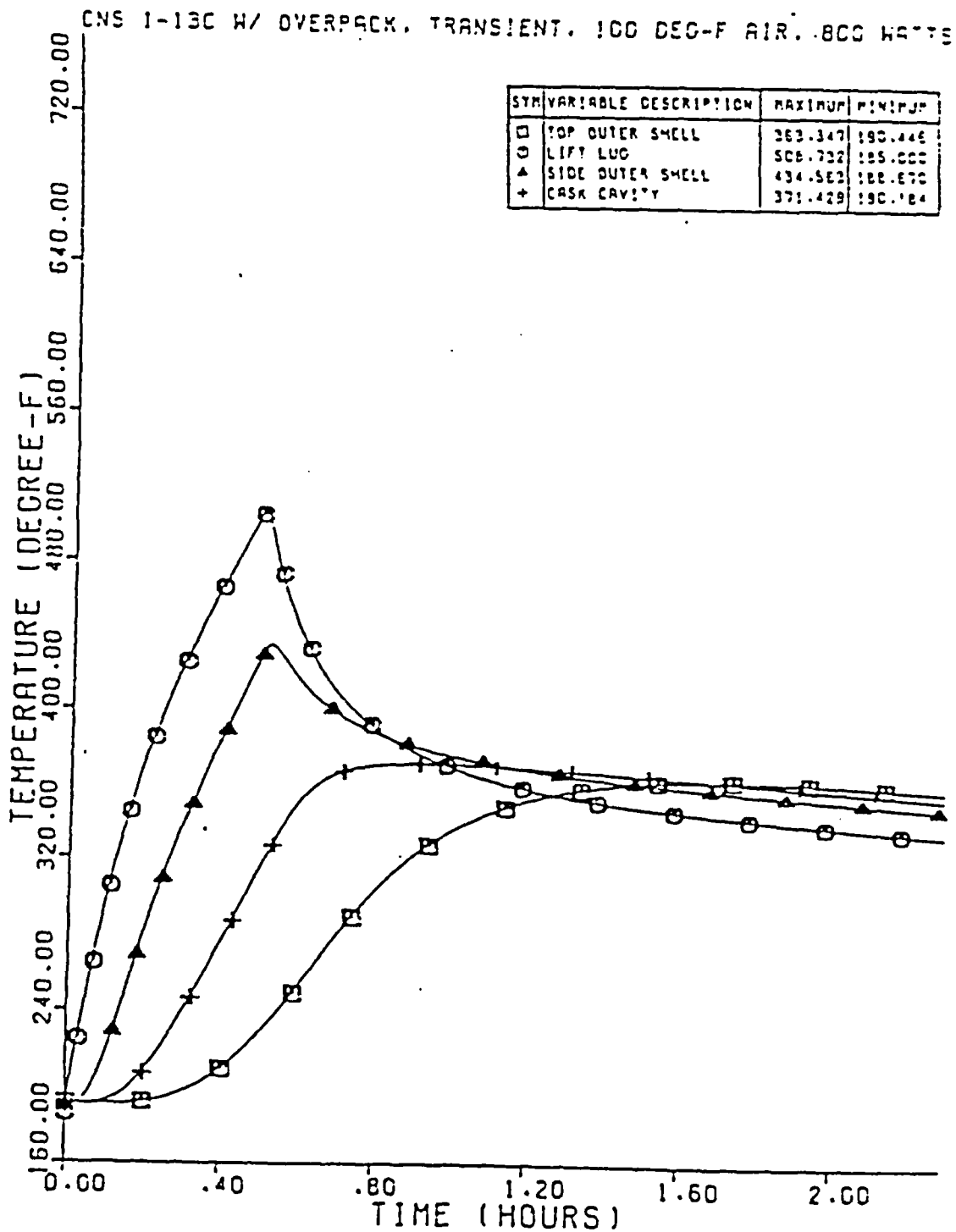


FIGURE 3.5.3-16

HYPOTHETICAL FIRE ACCIDENT



### 3.5.4 Maximum Internal Pressures

The maximum internal pressures under hypothetical accident conditions are found using the methodology and assumptions discussed in Section 3.4.4. Accident pressure results are summarized for the 1-i3C II package as follows:

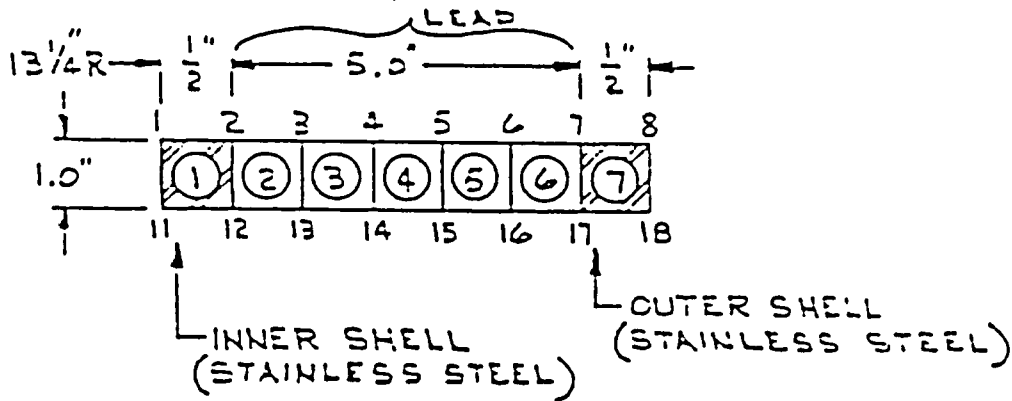
Case Number	Decay Heat (Watts)	Cavity Temp. ( $^{\circ}$ F)	Internal Pressure (psig)
1	150	320.42	96.64
2	200	324.67	102.45
3	300	332.98	114.27
4	400	341.06	126.75
5	500	348.93	140.04
6	600	556.62	154.21
7	700	364.11	168.99
8	800	371.43	184.37

### 3.5.5 Maximum Thermal Stresses

Comprehensive evaluation of pressure and axial differential thermal expansions are completely evaluated in Section 2.7.3 utilizing two axisymmetric finite element models for the cask body and lid. All stresses are found to be well within established limits for the materials of construction.

To illustrate the relatively low magnitude of resultant stresses, a simple ANSYS axisymmetric finite element solution was performed for the eight decay heats of the payload. A quasi-plane-strain solution was employed maintaining a common axial deformation. By "quasi", we mean

axial distortion of the body was allowed but the "plane-section remained plane" assumption was invoked at every cut. The analysis conservatively utilizes maximum pressures as derived in Section 3.5.4 and maximum thermal gradients (about  $112-114^{\circ}$ ) as shown in Figures 3.5.3-1 to -16, although these do not occur at the same point in time. The model used was as follows:



- Notes:
- Nodes 1-8 and 11-18 are coupled in the vertical direction
  - Node 1 is supported vertically
  - Therefore, vertical displacement of nodes 1-8 is always zero, and vertical displacements of nodes 11-18 are always equal to each other.

Tables 3.5.3-1 to -8 present stress results for the eight decay heat cases. Note that the highest stress anywhere, 14,756 psi tension, occurs in the inner shell in the axial direction for the 800 watt load case.

NEW TITLE= FIRE TRANSDUCER 150 WATTS  
 \*\*\*\*\* ELEMENT STRESSES \*\*\*\*\* TIME = 0.  
 EL= 1 NODES= 1 11 12 2 MAT= 1 ISYM= 1 MODE= 0  
 XC, YC= 13.50 -.5000 TEMP= 276.8 SX, SY, SZ= 137.45  
 EL= 2 NODES= 2 12 13 3 MAT= 2 ISYM= 1 MODE= 0  
 XC, YC= 14.25 -.5000 TEMP= 296.9 SX, SY, SZ= 330.00  
 EL= 3 NODES= 3 13 14 4 MAT= 2 ISYM= 1 MODE= 0  
 XC, YC= 15.25 -.5000 TEMP= 315.5 SX, SY, SZ= 531.26  
 EL= 4 NODES= 4 14 15 5 MAT= 2 ISYM= 1 MODE= 0  
 XC, YC= 16.25 -.5000 TEMP= 332.8 SX, SY, SZ= 320.10  
 EL= 5 NODES= 5 15 16 6 MAT= 2 ISYM= 1 MODE= 0  
 XC, YC= 17.25 -.5000 TEMP= 349.2 SX, SY, SZ= 271.57  
 EL= 6 NODES= 6 16 17 7 MAT= 2 ISYM= 1 MODE= 0  
 XC, YC= 18.25 -.5000 TEMP= 364.6 SX, SY, SZ= 210.60  
 EL= 7 NODES= 7 17 18 8 MAT= 1 ISYM= 1 MODE= 0  
 XC, YC= 19.00 -.5000 TEMP= 378.2 SX, SY, SZ= 12.842

ITERATION=	1	2	3	4	5	6	7	8
CONV. FLAG=	1							
		.71737E-08	1.2423.					
		.42112E-09	497.72					
		.42112E-09	5.5743					
		.49707E-09	-307.38					
		.66710E-07	-703.20					
		.28567E-10	-1004.11					
		-.14347E-07	-6644.2					

TABLE 3.5.5-1 Pressure and Thermal Induced Stresses, 150 Watts, I-13C II



NEW TITLE=		FIRE TRANSIENT 200 WATTS				LOAD STEP= 2		ITERATION= 1		CUR. STEP= 2		
***** ELEMENT STRESSES ***** TIME = 0.												
EL=	1	MODES=	1	11	12	2	MAT=	1	ISYM=	1	MODE=	0
XL, YC=	13.50		-0.0000		TEMP=	283.0		SX, SY, IX, SZ=	133.37	14298.	.77716E-08	12515.
EL=	2	MODES=	2	12	13	3	MAT=	2	ISYM=	1	MODE=	0
XL, YC=	14.25		-0.5000		TEMP=	301.1		SX, SY, IX, SZ=	355.70	559.43	.42112E-09	425.13
EL=	3	MODES=	3	13	14	4	MAT=	2	ISYM=	1	MODE=	0
XL, YC=	15.25		-0.5000		TEMP=	317.7		SX, SY, IX, SZ=	348.80	123.83	.49769E-09	.93569
EL=	4	MODES=	4	14	15	5	MAT=	2	ISYM=	1	MODE=	0
XL, YC=	16.25		-0.0000		TEMP=	337.1		SX, SY, IX, SZ=	317.00	-209.72	.57425E-09	-373.119
EL=	5	MODES=	5	15	16	6	MAT=	2	ISYM=	1	MODE=	0
XL, YC=	17.25		-0.0000		TEMP=	355.4		SX, SY, IX, SZ=	288.87	-687.21	.65082E-09	-708.11
EL=	6	MODES=	6	16	17	7	MAT=	2	ISYM=	1	MODE=	0
XL, YC=	18.25		-0.5000		TEMP=	368.8		SX, SY, IX, SZ=	207.87	-1032.5	.52207E-09	-1000.1
EL=	7	MODES=	7	17	18	8	MAT=	1	ISYM=	1	MODE=	0
XL, YC=	19.00		-0.5000		TEMP=	382.4		SX, SY, IX, SZ=	114.17	-2512.6	-.14347E-09	-6013.5

3-59

TABLE 3.5.5-2 Pressure and Thermal Induced Stresses, 200 Watts, 1-13C II

3-60

NEW TITLE=		FIRE TRANSIENT 300 WATTS				LOAD STEP=		ITERATION=	CUM. THER.=	3		
***** ELEMENT STRESSES ***** TIME = 0.												
EL=	1	NODES=	1	11	12	2	MAT=	1	ISIN=	1	MOPE=	0
XC, YL=	13.50		-0.5000		TEMP=	271.2		SX, SY, IXI, SZ=	128.49	14370.	.77716E-08	12647.
EL=	2	NODES=	2	12	13	3	MAT=	2	ISYM=	1	MOPE=	0
XC, YC=	14.25		-0.5000		TEMP=	307.4		SX, SY, IXI, SZ=	353.04	545.40	.38284E-09	414.04
EL=	3	NODES=	3	13	14	4	MAT=	2	ISIN=	1	MOPE=	0
XC, YC=	15.25		-0.5000		TEMP=	327.9		SX, SY, IXI, SZ=	345.55	107.80	.38284E-09	-10.564
EL=	4	NODES=	4	14	15	5	MAT=	2	ISYM=	1	MOPE=	0
XC, YL=	16.25		-0.5000		TEMP=	345.3		SX, SY, IXI, SZ=	315.74	-300.76	.55577E-09	-3114.7
EL=	5	NODES=	5	15	16	6	MAT=	2	ISIN=	1	MOPE=	0
XC, YC=	17.25		-0.5000		TEMP=	361.6		SX, SY, IXI, SZ=	264.67	-685.34	.65062E-07	-718.73
EL=	6	NODES=	6	16	17	7	MAT=	2	ISIN=	1	MOPE=	0
XC, YC=	18.25		-0.5000		TEMP=	377.0		SX, SY, IXI, SZ=	203.34	-1048.5	0.	-1817.4
EL=	7	NODES=	7	17	18	8	MAT=	1	ISYM=	1	MOPE=	0
XC, YL=	19.00		-0.5000		TEMP=	390.6		SX, SY, IXI, SZ=	89.053	-7426.2	-.17434E-07	-4361.6

TABLE 3.5.5-3 Pressure and Thermal Induced Stresses, 300 Watts, 1-130 II

Revision 0



3-61

NEW TITLE	FIRE TRANSIENT 400 WATTS				LOAD STEP	ITERATION	TIME	TEMP
***** ELEMENT STRESSES ***** TIME = 0.								
EL= 1	NODES= 1 11 12 2	MAI= 1	ISYM= 1	MODE= 0	1	1	116.65	1290.2
IC, IC=	13.50	-.5000	TEMP=	299.2				
EL= 2	NODES= 2 12 13 3	MAI= 2	ISYM= 1	MODE= 0	2	2	146.27	1418.27
IC, IC=	14.25	-.5000	TEMP=	317.3				
EL= 3	NODES= 3 13 14 4	MAI= 2	ISYM= 1	MODE= 0	2	3	138.86	116.447
IC, IC=	15.25	-.5000	TEMP=	333.9				
EL= 4	NODES= 4 14 15 5	MAI= 2	ISYM= 1	MODE= 0	2	4	107.13	-317.11
IC, IC=	16.25	-.5000	TEMP=	353.3				
EL= 5	NODES= 5 15 16 6	MAI= 2	ISYM= 1	MODE= 0	2	5	238.14	-701.69
IC, IC=	17.25	-.5000	TEMP=	369.6				
EL= 6	NODES= 6 16 17 7	MAI= 2	ISYM= 1	MODE= 0	2	6	196.84	-1064.9
IC, IC=	18.25	-.5000	TEMP=	385.0				
EL= 7	NODES= 7 17 18 8	MAI= 1	ISYM= 1	MODE= 0	1	7	85.393	-1118.1
IC, IC=	19.00	-.5000	TEMP=	390.6				

TABLE 3.5.5-4 Pressure and Thermal Induced Stresses, 400 Watts, 2-13C II

Revision 0

TABLE 3.5.5-5 Pressure and Thermal Induced  
Stresses, 500 WATTS, 1-13C II

NEW FILE#	FIXE TRANSIENT 500 WATTS				LOAD STEP#	ITERATION#	CUR. ITER#	
***** ELEMENT STRESSES ***** TIME = 0.					5	1	5	
EL= 1	NODES= 1 11 12 2	MAT= 1	ISTH= 1	MODE= 0				
XC, YC=	13.50	-0.5000	TEMP= 307.0	SX, SY, TX, SZ=	107.51	1938.	.75000E-01	13123.
EL= 2	NODES= 2 12 13 3	MAT= 2	ISTH= 1	MODE= 0				
XC, YC=	14.25	-0.5000	TEMP= 320.1	SX, SY, TX, SZ=	341.31	512.07	.49269E-09	401.115
EL= 3	NODES= 3 13 14 4	MAT= 2	ISTH= 1	MODE= 0				
XC, YC=	15.25	-0.5000	TEMP= 343.7	SX, SY, TX, SZ=	555.25	26.157	.45740E-09	-71.220
EL= 4	NODES= 4 14 15 5	MAT= 2	ISTH= 1	MODE= 0				
XC, YC=	16.25	-0.5000	TEMP= 361.1	SX, SY, TX, SZ=	701.71	-332.69	.52425E-09	-392.61
EL= 5	NODES= 5 15 16 6	MAT= 2	ISTH= 1	MODE= 0				
XC, YC=	17.25	-0.5000	TEMP= 377.4	SX, SY, TX, SZ=	252.80	-717.54	.80372E-09	-751.85
EL= 6	NODES= 6 16 17 7	MAT= 2	ISTH= 1	MODE= 0				
XC, YC=	18.25	-0.5000	TEMP= 392.8	SX, SY, TX, SZ=	191.39	-1041.0	.76562E-10	-1032.5
EL= 7	NODES= 7 17 18 8	MAT= 1	ISTH= 1	MODE= 0				
XC, YC=	19.00	-0.5000	TEMP= 406.4	SX, SY, TX, SZ=	83.026	-2222.4	-.17434E-07	-2222.4

3-63

NEW TITLE=		FINE TRANSIENT 600 WATTS				***** ELEMENT STRESSES *****		TIME = 0.	LOAD STEP = 0	ITERATION = 1	LOAD INCR. = 0	
EL=	1	NODES=	1	11	12	2	MAT=	1	ISYM=	1	MODE=	0
XC, YC=	15.50		-0.5000				TEMP=	314.5	SX, SY, IXY, SZ=	97.457		14698.
EL=	2	NODES=	2	12	13	3	MAT=	2	ISYM=	1	MODE=	0
XC, YC=	14.25		-0.5000				TEMP=	332.7	SX, SY, IXY, SZ=	335.40		476.01
EL=	3	NODES=	3	13	14	4	MAT=	2	ISYM=	1	MODE=	0
XC, YC=	15.25		-0.5000				TEMP=	351.2	SX, SY, IXY, SZ=	327.79		60.544
EL=	4	NODES=	4	14	15	5	MAT=	2	ISYM=	1	MODE=	0
XC, YC=	16.25		-0.5000				TEMP=	366.6	SX, SY, IXY, SZ=	295.92		-318.17
EL=	5	NODES=	5	15	16	6	MAT=	2	ISYM=	1	MODE=	0
XC, YC=	17.25		-0.5000				TEMP=	384.9	SX, SY, IXY, SZ=	248.80		-732.75
EL=	6	NODES=	6	16	17	7	MAT=	2	ISYM=	1	MODE=	0
XC, YC=	18.25		-0.5000				TEMP=	400.3	SX, SY, IXY, SZ=	185.37		-1075.9
EL=	7	NODES=	7	17	18	8	MAT=	1	ISYM=	1	MODE=	0
XC, YC=	19.00		-0.5000				TEMP=	413.9	SX, SY, IXY, SZ=	80.011		-7184.1

TABLE 3.5.5-6 Pressure and Thermal Induced Stresses, 600 Watts, I-13C II

Revision C

3-64

NEW TITLE=		FIRE TRANSIENT 700 WATTS				***** ELEMENT STRESSES *****		TIME = 0.	LOAD STEP= 7	ITERATION= 1	CUM. DECK= 7
EL= 1	MOSES= 1	11	12	2	MAT= 1	ISIN= 1	NUME= 0				
IC, IC=	13.50	-.5000	TEMP=	321.9	SX, SY, IX, SZ=	87.078		14881.	.95650E-08	13565.	
EL= 2	MOSES= 2	12	13	3	MAT= 2	ISIN= 1	NUME= 0				
IC, IC=	14.25	-.5000	TEMP=	340.1	SX, SY, IX, SZ=	327.49		480.95	.49787E-09	507.38	
EL= 3	MOSES= 3	13	14	4	MAT= 2	ISIN= 1	NUME= 0				
IC, IC=	15.25	-.5000	TEMP=	358.6	SX, SY, IX, SZ=	321.90		45.337	.42112E-09	-35.171	
EL= 4	MOSES= 4	14	15	5	MAT= 2	ISIN= 1	NUME= 0				
IC, IC=	16.25	-.5000	TEMP=	376.0	SX, SY, IX, SZ=	290.04		-383.23	.38284E-09	-404.47	
EL= 5	MOSES= 5	15	16	6	MAT= 2	ISIN= 1	NUME= 0				
IC, IC=	17.25	-.5000	TEMP=	392.3	SX, SY, IX, SZ=	240.94		-747.81	.68910E-09	-743.24	
EL= 6	MOSES= 6	16	17	7	MAT= 2	ISIN= 1	NUME= 0				
IC, IC=	18.25	-.5000	TEMP=	407.7	SX, SY, IX, SZ=	177.55		-1111.0	0.	-1043.8	
EL= 7	MOSES= 7	17	18	8	MAT= 1	ISIN= 1	NUME= 0				
IC, IC=	19.00	-.5000	TEMP=	421.3	SX, SY, IX, SZ=	77.075		-7113.1	-.19130E-07	-5467.9	

TABLE 3.5.5-7 Pressure and Thermal Induced Stresses, 700 WATTS, 1-13C II

Revision 0

3-55

NEW TITLE=	FIRE TRANSIENT: 600 WATTS				LOAD STEP=	ITERATION=	CON. THER.-	
***** ELEMENT STRESSES *****				TIME = 0.				
EL= 1	MODES= 1	11	12	2	MAT= 1	ISYM= 1	MODE= 0	
IC,TC= 13.50	-.5000		TEMP= 329.1		SX,SY,IXY,SZ= 76.253	14756.	.8364E-08	131109.
EL= 2	MODES= 2	12	13	3	MAT= 2	ISYM= 1	MODE= 0	
IC,TC= 14.25	-.5000		TEMP= 347.5		SX,SY,IXY,SZ= 123.31	466.20	.42112E-09	304.07
EL= 3	MODES= 3	13	14	4	MAT= 2	ISYM= 1	MODE= 0	
IC,TC= 15.25	-.5000		TEMP= 365.8		SX,SY,IXY,SZ= 315.81	30.500	.53597E-09	-40.019
EL= 4	MODES= 4	14	15	5	MAT= 2	ISYM= 1	MODE= 0	
IC,TC= 16.25	-.5000		TEMP= 383.2		SX,SY,IXY,SZ= 284.03	-377.90	.04224E-00	-414.41
EL= 5	MODES= 5	15	16	5	MAT= 2	ISYM= 1	MODE= 0	
IC,TC= 17.25	-.5000		TEMP= 374.5		SX,SY,IXY,SZ= 234.98	-762.50	.64224E-09	-7411.24
EL= 6	MODES= 6	16	17	7	MAT= 2	ISYM= 1	MODE= 0	
IC,TC= 18.25	-.5000		TEMP= 414.9		SX,SY,IXY,SZ= 173.64	-1125.7	.76587E-10	-1646.7
EL= 7	MODES= 7	17	18	8	MAT= 1	ISYM= 1	MODE= 0	
IC,TC= 19.00	-.5000		TEMP= 424.5		SX,SY,IXY,SZ= 74.117	-7040.2	-.16737E-07	-5247.5

TABLE 3.5.5-d Pressure and Thermal Induced Stresses, 800 watts, 1-13C II

Revision 0

Both values are well below accepted allowables for the stainless steel inner and outer shells.

3.5.6 Evaluation of Package Performance for Hypothetical Accident Thermal Conditions

The thermal behavior of the 1-13C II package is completely consistent with the allowables for all materials of construction. In particular, the maximum predicted temperature of the payload cavity, 363.4°F, is well below the established service limit of 400°F for silicon seals.

Key findings used elsewhere in this report for detailed stress analysis are summarized in Tables 3.5.3-1 and in Section 3.5.4.

3.5 Appendix

The thermal analysis presented in Section 3.0 shows the adequacy of the cask to meet a heat load of 800 W. This will not be exceeded by using the general debris containers or the shielded debris containers. Since the shielded debris containers can contain a greater quantity of fissile material than the general debris containers, the shielded debris containers will be used in the calculation of an average heat load. The following calculation show that expected heat loads are far less than this value.

- o Total TMI - II core  
decay heat load  $\leq 15,000$  W
- o Total fuel loading  
177 assembly  $\times \frac{463 \text{ Kg}}{\text{assembly}} = 81,951 \text{ KgU}$
- o Maximum container fuel content 60KgU  
Average heat load  $= 15,000 \text{ W} \times \frac{60 \text{ KgU}}{81,951} = 10.98 \text{ W} \ll 800 \text{ W}$

## 4.0 CONTAINMENT

This chapter delineates the containment configuration of the 1-13C II package for normal transport and hypothetical accident conditions.

### 4.1 CONTAINMENT BOUNDARY

#### 4.1.1 Containment Vessel

The package containment vessel is defined as the inner shell of the shielded transport cask, together with the associated lid seals and lid closure bolts. The inner shell of the cask, or containment vessel, consists of a right circular cylinder of 26-1/2 inches inner diameter and 54 inches inside height. The shell is fabricated of 1/2 inch thick stainless steel plate, Type 304 (ASTM A-240). At the base, the cylindrical shell is attached to a circular end plate with full penetration welds. At the top, similar construction techniques are used for the removable lid. The lid is attached to the cask body with twelve equally spaced 1-1/4 inch bolts in a 35.38 inches diameter bolt circle. See Section 4.1.4 for closure details.

#### 4.1.2 Containment Penetration

There are two penetrations of the containment vessel, a drain line and a vent line. At the base, the drain line consists of a 1/2 inch O.D. by 0.065 inch wall stainless steel tube gravity line from the center of cavity bottom to the side of the outer shell near the cask bottom. At the top, a comparable vent/test line exists to the base of the recessed lid step. Both penetrations are sealed with silicone, one piece molded in place seals with the rubber sealing element mechanically locked to a stainless steel retainer. Both seals are protected from fire exposure by the "adiabatic" end overpacks. The fasteners installed in both lines are provided with pressure relief features.



#### 4.1.3 Welds and Seals

The containment vessel is fabricated using full penetration groove welds. All weld configurations are designed and fabricated to the intent of Section III of the ASME Boiler and Pressure Vessel Code. Seals are described in Sections 4.1.2 and 4.1.4.

#### 4.1.4 Closure

The top closure consists of a shielded lid, with tapered sidewalls to assist in positioning and sealing. The lid is supported on the outermost top circular plate by a circumferential step. This step confines a flat solid high temperature silicone seal. A solid silicone O-ring also exists near the edge of the bottom of the lid. The step prevents overcompression of the flat gasket and O-ring by the closure bolt preload forces and hypothetical accident impact forces. The lid is attached to the cask body by twelve (12) equally spaced 1-1/4 inch - 7 UNC x 2-1/4 inch long bolts. These bolts are fabricated of ASTM A-354, Grade BD material. These bolts are torqued to 270 ft-lbs.  $\pm$  10% (lubricated) or 360 ft-lbs.  $\pm$  10% (dry). The lid bolt torque calculations are found in Appendix 4.4.3, p. 4-25.

The vent and drain penetrations are sealed with Parker Stat-O-Seals (applicable catalogue excerpts may be found in Appendix 4.4.4, p. 4-30) which are used beneath the heads of the S.S. 3/8 - 16 UNC Hex H.D. cap screws at both locations. Overcompression of the silicone is prevented because the silicone rubber sealing element is molded and mechanically locked into a stainless steel retainer. The vent and drain screws are torqued to 12 ft-lbs. lubricated (i.e. 144 in.-lbs.) which is well above the 80 in.-lbs. minimum torque requirements for sealing and well below the 220 in.-lbs. maximum torque for crushing the retainer.

4.2 Requirements for Normal Conditions of Transport4.2.1 Containment of Radioactive Material

The 1-13C II cask is designed to assure no release of radioactive material in excess of limits prescribed in N.R.C. Regulatory Guide 7.4, "Leakage Tests on Packages for the Shipment of Radioactive Materials", under normal conditions of transport.

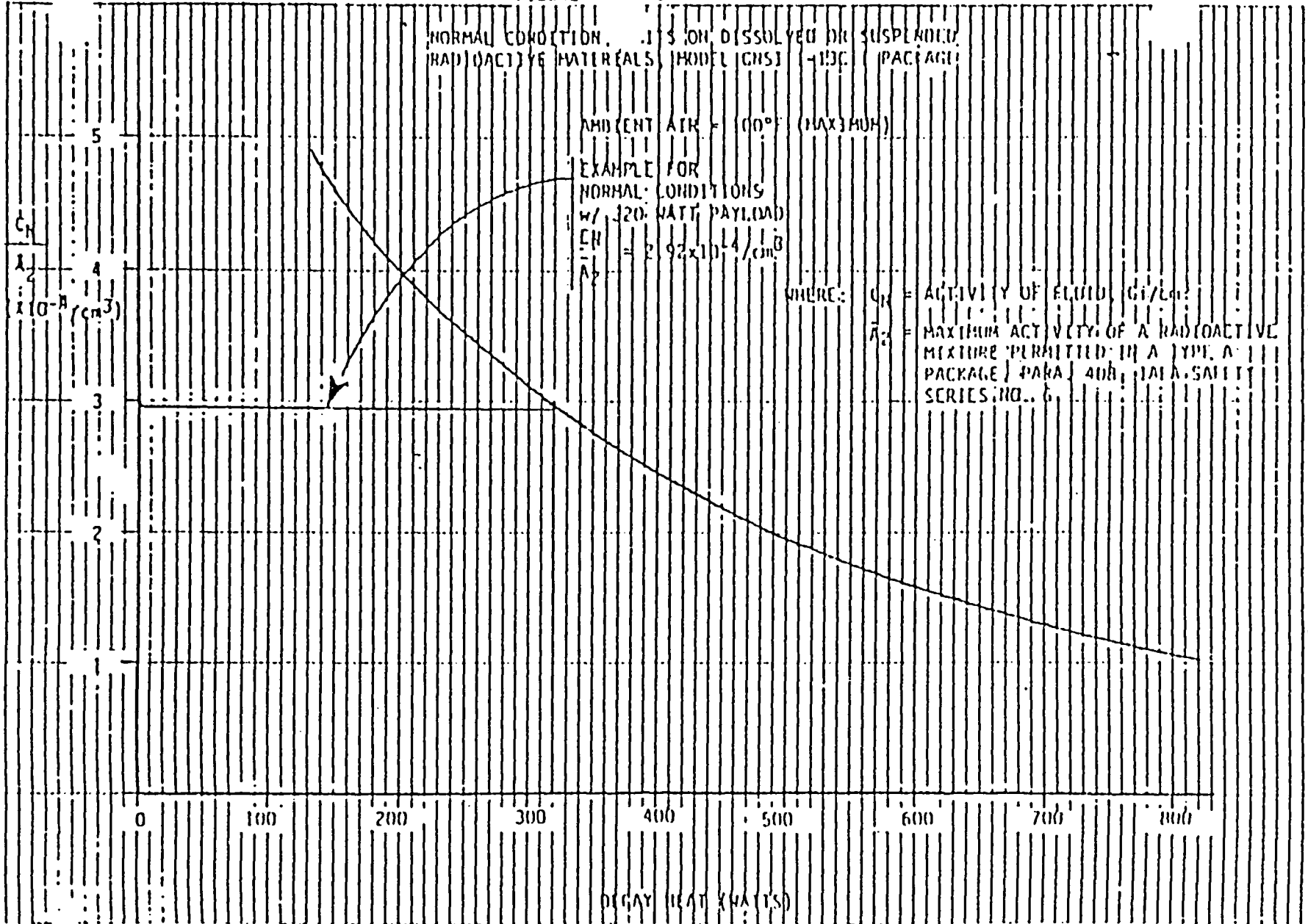
The 1-13C II package is designed to accommodate a variety of payloads with differing contents possessing a range of normal condition temperatures and pressures, each associated with a differing decay heat value.

Figure 4.2.1-1 defines limitations on dissolved or suspended radioactive materials in residual fluids which may be present in the package containment cavity for dewatered resins. These limitations are defined as a function of payload decay heat. Appendix 4.5 summarizes the derivation and application of this limit relation for normal conditions. Provided these limits are not exceeded, compliance of the 1-13C II package with the requirements of N.R.C. Regulatory Guide 7.4 is assured. In accordance with the Regulatory Position, Paragraph C of this guide, compliance of the 1-13C II package with the requirements of Section 71.51 of 10 CFR 71, for "no loss or dispersal of radioactive contents, as demonstrated to a sensitivity of  $10^{-6} \text{A}_2$  per hour", Paragraph 71.51 (a)(1), is demonstrated.

4.2.2 Pressurization of Containment Vessel

Section 3.4.4 summarizes normal condition temperatures and pressures within the containment vessel. The predicted pressure values conservatively assume a sufficient quantity of free water is present; thus all pressure predictions are based upon the properties of saturated water and steam. These conservative predictions of pressure and associated temperatures are used to evaluate integrity of the 1-13C II package. None of these conditions reduce the effectiveness of the package containment.

FIGURE 4



#### 4.2.3 Containment Criterion

The containment criteria of section 4.2.1 are satisfied through the use of leak test procedures for fabrication verification, periodic, annual and seal replacement for 1-13C II Transport Cask. Procedures are based on ANSI N14.5-1977, American National Standard for leak tests on packages for shipment of radioactive materials.

#### 4.3 CONTAINMENT REQUIREMENTS FOR THE HYPOTHETICAL ACCIDENT CONDITIONS

The following is an assessment of the packaging containment under hypothetical accident conditions as a result of the analyses performed in Chapters 2.0 and 3.0 above. In summary, the containment vessel was not affected by these tests (refer to Section 2.7).

##### 4.3.1 Fission Gas Products

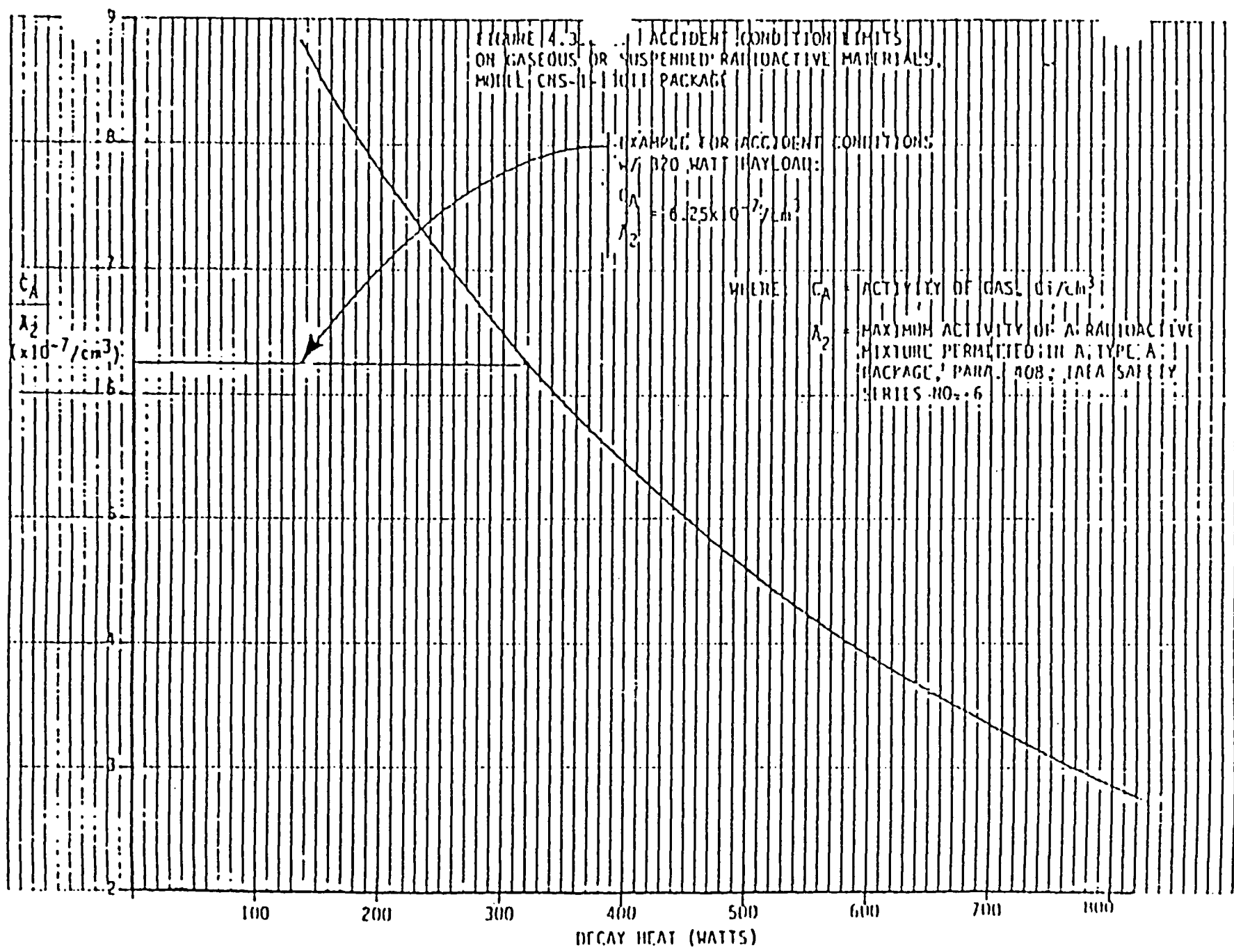
There are no fission gas products present. Any fission products contained in the fissile debris has previously been released.

##### 4.3.2 Containment of Radioactive Materials

The 1-13C II cask is designed to assure no release of radioactive material in excess of limits prescribed in N.R.C. Regulatory Guide 7.4, "Leakage Tests on Packages for Shipment of Radioactive Materials", under hypothetical accident conditions.

The 1-13C II package is designed to accommodate a variety of payloads with differing contents possessing a range of accident condition temperatures and pressures, each associated with a differing decay heat value.

Figure 4.3.2-1 defines limitations on suspended radioactive materials in residual steam which may be present in the package containment cavity. These limitations are defined as a function of payload decay heat. Appendix 4.5 summarizes the derivation and application of this limit relation for accident conditions. Provided these limits are not exceeded, compliance of the 1-13C II package with the requirements of N.R.C. Regulatory Guide 7.4 is assured. In accordance with the Regulatory Position, Paragraph C of this guide, compliance of the 1-13C II package with the requirements of Section 71.51 (a)(2) of 10 CFR 71, for no release of radioactive material from the containment vessel exceeding specified limits is demonstrated.



A-7

#### 4.3.3 Containment Criterion

A design verification leak test was performed according to Section 7.4.1. No leakage was detected at a temperature of 59°F and cask charge pressure of 12.0 psig, using a leak detector calibrated for detecting leaks in excess of 0.21 oz/yr of dichlorodifluoromethane (Freon-12) at 25°C and 1 ATM pressure.

The result of the design verification leak test serves two purposes;

- (1) it provides a means to determine permissible activity concentrations of the leakable medias for normal and accident conditions of transport.

(i.e.,  $\frac{C_N}{A_2}$  and  $\frac{C_A}{A_2}$ ; Re: Section 4.4)

- (2) it established acceptance criteria for verifying leaktightness upon fabrication of new packages, after the third use of the package, annually thereafter, and any time that the flat gasket O-ring or seals may need to be replaced.

##### 4.3.3.1 Problem Description

Typically halogen detectors are designed to identify the presence of leaks in excess of some threshold value. These thresholds are generally calibrated for detecting leakage of dichlorodifluoromethane (Freon-12) gas in terms of oz/yr.

For the 1-13C II cask, permissible leak rate limits are specified for normal and accident conditions in atm-cm<sup>3</sup>/sec, standard conditions per ANSI 14.5. These conditions imply the presence of a 1 atmosphere pressure differential at a temperature of 25°C.

To test the adequacy of containment, the threshold values of the sensor must be equated to the prescribed leak rate limits for normal and accident conditions. This may be achieved by proper selection of the Freon (R-12) charge pressure applied to the cask cavity.

Solution Method

The threshold sensitivity of the sensor is given in (oz/yr), a weight per unit time. This must be converted to a volumetric flow (equivalent to the sensor threshold) becomes a variable expressed in terms of both pressure and temperature.

The prescribed leakage limits for the cask are stated in terms of standard conditions. This, in effect, defines the permissible size of the leak orifice. If pressure and temperature vary, during test, from standard conditions, the acceptable test leak limit differs from the standard condition value. Thus the permissible leak rate is also a variable of both test pressure and temperature.

If sensor threshold, expressed in volumetric terms, is equated to test leak rate limits, an equation is formed in terms of pressure and temperature. For each value of temperature, a charge pressure value can be found that sets this detector threshold at the prescribed leakage limits.

Detector Threshold

In fps units, the detector threshold may be expressed as:

$$l_H = C_1 i_H$$

Where:  $l_H$  = detector threshold in lbs/sec

$i_H$  = detector threshold in oz/year

$$C_1 = \frac{1 \text{ lb.}}{16 \text{ oz.}} \frac{1 \text{ year}}{(3600)(24)(365) \text{ sec}} = 1.9819 \times 10^{-9} \text{ lb-yr/sec-oz}$$



The volumetric equivalent of this threshold is:

$$L_v = \frac{1_H}{(M_R/V)}$$

Where:  $L_v$  = detector threshold in  $\text{ft}^3/\text{sec}$

$(M_R/V)$  = specific concentration of R-12 per unit cavity volume in  $\text{lbs}/\text{ft}^3$

The specific concentration of trace gas,  $(M_R/V)$  is obtained by use of the perfect gas law considering the partial pressures of trace gas and air within the cask cavity. The total pressure in the cask cavity is:

$$P_T = P_R + P_A \quad (\text{lbs}/\text{ft}^2)$$

Where:  $P_T$  = total pressure,  $\text{lbs}/\text{ft}^2$  (absolute)

$P_R$  = partial pressure of R-12

$P_A$  = partial pressure of air

$$= (14.7) (144) = 2116.8 \text{ lb}/\text{ft}^2$$

From the perfect gas law<sup>1</sup>:

$$P_R = \left(\frac{M_R}{V}\right) \cdot R_R T_R$$

Where:  $T_R$  = temperature,  $^{\circ}\text{R}$

$R_R$  = gas constant =  $1545.32^{(1)} = 12.78$

$M_R$  = lb molecular wt. of R-12 =  $120.93^{(2)}$

Thus:  $P_T = \left(\frac{M_R}{V}\right) R_R T + P_A$

and, the specific concentration of trace gas is found as:

$$\frac{M_R}{V} = \frac{P_A (P_T - 1)}{R_R T_R}$$

Where:  $P_T = \frac{P_T}{P_A}$  the total pressure expressed in atm.

Now, in fps units the volumetric equivalent of detector sensitivity is:

$$L_V = i_H = \frac{C_1 i_H R_R T_R}{(M_R/V) P_A (P_T - 1)} \quad \text{ft}^3/\text{sec}$$

This can be expressed in S. I. units as:

$$L_H = C_2 \cdot L_V \quad \text{cm}^3/\text{sec}$$

$$\text{Where: } C_2 = (1728 \text{ in}^3/\text{ft}^3) (2.54 \text{ cm/in})^3 = 28316.85 \text{ cm}^3/\text{ft}^3$$

Finally, the detector sensitivity may be expressed as:

$$L_H = \frac{C_3 \cdot i_H T_K}{(P_T - 1)} \quad \text{cm}^3/\text{sec} \quad \text{Eq. (A)}$$

$$\begin{aligned} \text{Where: } C_3 &= \frac{C_1 \cdot C_2 \cdot R_R \cdot (9/5)}{P_A} \\ &= \frac{(1.9819 \times 10^{-9}) (28316.85) (12.78) (9/5)}{2116.8} \\ &= 6.0988 \times 10^{-7} \end{aligned}$$

$$\begin{aligned} T_K &= \text{temperature, } ^\circ\text{K} \\ (T_R &= 9/5 \cdot T_K) \end{aligned}$$

As a check, standard conditions are inserted:

$$\begin{aligned} (P_T - 1) &= 1 \text{ atm} \\ T_K &= 25^\circ\text{C} + 273 = 298^\circ\text{K} \end{aligned}$$

$$\text{Then, } L_H = \frac{(6.0988 \times 10^{-7})(298)}{1} \times i_H = 1.8 \times 10^{-4} i_H \text{ cm}^3/\text{sec}$$

This compares precisely with the value shown on page 40 of the G.E. Leak Detector Manual, ID-48163

References:

- (1) C.L. Brown, "Basic Thermodynamics", McGraw Hill, 1951, p. 80
- (2) ASHRAE Handbook of Fundamentals, Table 2, Chapter 15, 1967

Permissible Leak Rates at Test Pressures

Equation B5 of ANSI 14.5 provides a means to translate test conditions to Standard conditions:

$$L_t = L_s n_s \frac{(P_u^2 - P_d^2)_t}{n_t (P_u^2 - P_d^2)_s}$$

Where: subscripts s and t refer to "standard" and "test", respectively.  
 subscripts u and d refer to "upstream" and "downstream" respectively.

n = viscosity of gas at temperature, in centipoises  
 P = pressure in atmospheres  
 $L_t$  = leak rates in  $\text{cm}^3/\text{sec.}$  @ test conditions  
 $(L_s)$  = standard permissible leak rate

For standard conditions:

$$\begin{aligned} n_s &= .0185 \text{ cP (air at } 25^\circ\text{C)} \\ P_{us} &= 1 \text{ atm} \\ P_{ds} &= 1 \times 10^{-2} \text{ atm} \end{aligned}$$

For test conditions:

$$\begin{aligned} n_t &= .0126 \text{ cP}^{(3)} \text{ (R-12 at } 80^\circ\text{F)} \\ P_{ut} &= P_t, \text{ atm.} \\ P_{dt} &= 1, \text{ atm} \end{aligned}$$

Substituting, the permissible leak rate at test conditions is found as:

$$L_T = C_4 L_S (P_T^2 - 1) \quad \text{Eq. (3)}$$

Where:  $C_4 = \frac{.0185}{0.0126 (1 - 1 \times 10^{-4})} = 1.4684$

---

Reference:

(3) ASHRAE Handbook of Fundamentals, Table 4, Chapter 15, 1967.

Equations (A) and (3) represent the detector threshold flow rate and permissible cask test leak rate, respectively. Equating these two gives:

$$L_H = L_T$$

$$\frac{C_3 i_H T_K}{(P_T - 1)} = C_4 L_S (P_T^2 - 1)$$

The expression for charge pressure is found as:

$$P_T^3 - P_T^2 - P_T + 1 = \left( \frac{C_3}{C_4} \right) \frac{i_H T_K}{L_S} = 0 \quad \text{Eq. (C)}$$

A leak test was performed for design leaktightness verification. No leakage was detected at a temperature of 59°F (288°K) and a charge pressure of 12 psig (1.816 atm) using a leak detector calibrated for detecting leaks in excess of 0.21 oz/yr. Solving equation (c) for the equivalent leak rate of air at Standard conditions:

$$L_S = \left( \frac{C_3}{C_4} \right) \frac{i_H T_K}{(P_T^3 - P_T^2 - P_T + 1)}$$

Where:

$$\frac{C_3}{C_4} = 4.1534 \times 10^{-7}$$

$$i_H = 0.21 \text{ oz/yr}$$

$$T_K = 288^\circ\text{K}$$

$$p_T = (1 + 12/14.7) = 1.816 \text{ ATM}$$

$$L_S = \frac{(4.1534 \times 10^{-7})(0.21)(288)}{(1.816^3 - 1.816^2 - 1.816 + 1)}$$

$L_S = 1.34 \times 10^{-5} \text{ ATM} \cdot \text{cc/sec.}$  (Standard conditions, air at 25°C and 1 ATM pressure).

4.4 APPENDIX A - NORMAL AND ACCIDENT RADIOACTIVE MATERIAL LIMITS  
FOR THE 1-13C II CASK

Figures 4.2.1-1 and 4.3.2-1 define limits for activity of the medium within the containment vessel as defined in Paragraph 5.3.1 of ANSI Standard N14.5-1977. For the 1-13C II package, the medium is assumed to be a small quantity of residual water or steam, as appropriate.

Paragraph 4.4.1 outlines the method employed to establish these activity limit relations. Paragraph 4.4.2 outlines an example application of the method to a particular payload.

4.4.1 Derivation of Limit Relations

A leak test for design leaktightness verification (Re: P. 4-13) demonstrated that a new 1-13C II package did not leak at a rate of:

$$L_s = 1.34 \times 10^{-5} \text{ atm-cm}^3/\text{sec}$$

This rate is at Standard Conditions per Paragraph 3.3 of ANSI N14.5 (. . . dry air at 25°C for a pressure differential at 1 atm. against a vacuum of 10<sup>-2</sup> atm. or less.)

Because of the procedure sensitivity requirements of ANSI N14.5, the cask may only be considered not to leak at a rate of two times the demonstrated leaktightness value or:

$$L = 2L_s = 2(1.34 \times 10^{-5}) \text{ atm-cm}^3/\text{sec}$$

(Standard Conditions)

Additional testing, for information only, showed that the package did not leak at a rate considerably less than  $1.34 \times 10^{-5}$  atm-cm<sup>3</sup>/sec. For discussion purposes and because of the procedure sensitivity requirements of ANSI N14.5 it will be conservatively assumed that the leak rate after normal and accident conditions was: (See Discussion, Section 2.11, Paragraph 2.11.4.1, P. 2-233 showing that the pre-accident cask condition is actually representative of the post-accident cask condition).

$$L = 2.58 \times 10^{-5} \text{ atm-cm}^3/\text{sec} \quad (\text{Standard Conditions})$$

respectively. These rates are at standard conditions per Paragraph 3.3 of ANSI Standard N14.5 (. . . dry air at 25°C for a pressure differential at 1 atm against a vacuum of  $10^{-2}$  atm or less.)

For normal conditions, the permissible leak rate is given as:

$$L_N = \frac{R_N}{C_N} \text{ cm}^3/\text{sec}$$

Where:  $R_N = 2.78 \times 10^{-10} A_2/\text{sec}$  (Table 1, ANSI N14.5)

$C_N$  = Permissible activity of medium, Ci/cm<sup>3</sup>

$\bar{A}_2$  = Maximum Activity for Type A Mixtures

$$= \frac{\sum Ci}{\sum Ci/A_2}$$

$A_2$  = Maximum Activity for Type A (para. 3.2, ANSI N14.5)

$$\text{or: } L_N = 2.78 \times 10^{-10} \frac{\bar{A}_2}{C_N}$$

$$\frac{C_N}{A_2} = \frac{2.78 \times 10^{-10}}{L_N}$$

The quantity,  $L_N$ , represents the permissible leak rate of the medium (water) at temperatures and pressures associated with normal transport conditions. Correlation of this quantity with the demonstrated leak rate at standard conditions,  $L_N$ , is achieved via use of Equation (3.9) of ANSI N14.5:

$$L_N = \frac{2L_n \eta_n (P_u - P_d)H}{\eta_N (P_u^2 - P_d^2)H}$$

Where:  $L_n = 2.58 \times 10^{-5}$  atm-cm<sup>3</sup>/sec  
 $\eta_n = .0185$  cP, air viscosity  
 $P_{un} = 1$  atm  
 $P_{dn} = 1 \times 10^{-2}$  atm.  
 $\eta_N =$  water viscosity, cP  
 $P_{uN} =$  vessel pressure, atm  
 $= 1 + (\text{psig}/14.7)$   
 $P_{dN} = 1$  atm

{ "Standard  
Conditions",  
ANSI N14.5  
at "normal"  
temperature  
and pressure  
conditions.

The calculations for normal conditions are found in the table below:

Case No.	Decay Heat (Watts)	Cavity Temp. (°F)	Internal Pressure (psig)	Water Viscosity (cP)	$(C_N/\eta_N)_3$ (cm <sup>3</sup> )
1	150	138.35	4.27	.4759	$4.592 \times 10^{-4}$
2	200	142.70	4.72	.4584	$4.002 \times 10^{-4}$
3	300	151.20	5.68	.4290	$3.112 \times 10^{-4}$
4	400	159.47	6.75	.4010	$2.448 \times 10^{-4}$
5	500	167.51	7.96	.3790	$1.962 \times 10^{-4}$
6	600	175.39	9.30	.3590	$1.591 \times 10^{-4}$
7	700	183.06	10.77	.3395	$1.299 \times 10^{-4}$
8	800	190.55	12.36	.3239	$1.080 \times 10^{-4}$

## NOTE:

- (1) Handbook of Chemistry & Physics, Chemical Rubber Company, New York  
Page 2181: Viscosity & Fluidity of Water, 0°-100°C.



For accident conditions, the permissible leak rate is given as:

$$L_A = \frac{R_A}{C_A} \text{ cm}^3/\text{sec}$$

Where:  $R_A = 1.65 \times 10^{-9} \lambda_2 / \text{sec}$  (Table 1, ANSI N14.5)

$C_A =$  Permissible Activity of Medium, Ci/cm<sup>3</sup>

$\lambda_2 =$  Maximum Activity for Type A Mixtures

$$= \frac{I C_1}{I(C_1/\lambda_2)}$$

$\lambda_2 =$  Maximum Activity for Type A  
(Para. 3.2, ANSI N14.5)

Or:  $L_A = 1.65 \times 10^{-9} \frac{\lambda_2}{C_A}$

$$\frac{C_A}{\lambda_2} = \frac{1.65 \times 10^{-9}}{L_A}, \text{ 1/cm}^3$$

The quantity,  $L_A$ , represents the permissible leak rate of the medium (steam) at temperatures and pressures associated with accident conditions. Correlation of this quantity with the demonstrated leak rates at standard conditions,  $L_a$ , is achieved via use of Equation (B.5) of ANSI N14.5:

$$L_A = \frac{L_a n_a (P_u^2 - P_d^2)_A}{\eta_A (P_u^2 - P_d^2)_a}$$

Where:  $L_a = 2.68 \times 10^{-5} \text{ atm-cm}^3/\text{sec}$

$n_a = .0185 \text{ cP}$ , air viscosity { "Standard"

$P_{ua} = 1 \text{ atm}$  { Conditions,

$P_{da} = 1 \times 10^{-2} \text{ atm}$  { ANSI N14.5

$n_A =$  steam viscosity, cP { at "accident"

$P_{uA} =$  vessel pressure, atm { temperature

$= 1 + (\text{psig}/14.7)$  { and pressure

$P_{dA} = 1 \text{ atm}$  { conditions.

The calculations for accident conditions are found in the table below:

Case Number	Decay Heat (Watts)	Cavity Temp. (°F)	Internal Pressure (psig)	Steam(i) Viscosity (cP)	(CA/2) (1/cm <sup>3</sup> )
1	150	320.42	96.62	.01454	8.585x10 <sup>-7</sup>
2	200	324.67	102.45	.01463	7.789x10 <sup>-7</sup>
3	300	332.98	114.27	.01483	6.496x10 <sup>-7</sup>
4	400	341.06	126.75	.01501	5.454x10 <sup>-7</sup>
5	500	348.93	140.04	.01519	4.604x10 <sup>-7</sup>
6	600	356.62	154.21	.01537	3.904x10 <sup>-7</sup>
7	700	364.11	168.99	.01554	3.333x10 <sup>-7</sup>
8	800	371.43	184.37	.01571	2.866x10 <sup>-7</sup>

- (1) Doolittle, Jesse S., "Thermodynamics for Engineers", International Textbook Company, 1964, Figure A-1: Viscosity of Gases, pp. 632.

At the temperatures and pressures associated with accident conditions for different payload decay heats the actual activity concentrations of the vapor inside the cask will vary. In order to determine the activity concentration of the vapor concentration (ml water/cm<sup>3</sup> vapor) must first be determined as related to payload decay heats.

$$\text{Vapor Concentration} = \frac{1}{\text{Specific Vol.}} \times \frac{(\text{Density Water})}{1} =$$

$$\frac{1}{\text{Specific Vol.}} \times \frac{1 \text{ lbm}}{\text{ft}^3} \times \frac{1 \text{ in}^3}{16.39 \text{ cm}^3} \times$$

$$\frac{\text{ft}^3}{1728 \text{ in}^3} \times \frac{2.832 \times 10^4 \text{ ml}}{\text{ft}^3} \times \frac{\text{ft}^3}{62.4 \text{ lbm}}$$

The results of the calculations are given in the following table and depicted graphically on Fig. 4.4.1-1.

WATTS	CAVITY TEMP. °F	PARTIAL VAPOR PRES. psia*	SPEC. VOL. OF VAPOR* Ft /lbm	VAP. CONC. ml WATER/ cm VAPOR
150	320.42	90.25	4.886	$3.280 \times 10^{-3}$
200	324.67	95.92	4.614	$3.473 \times 10^{-3}$
300	332.98	107.52	4.146	$3.865 \times 10^{-3}$
400	341.06	119.77	3.737	$4.286 \times 10^{-3}$
500	348.93	132.85	3.390	$4.727 \times 10^{-3}$
600	356.92	147.37	3.070	$5.220 \times 10^{-3}$
700	364.11	161.40	2.814	$5.695 \times 10^{-3}$
800	371.43	176.57	2.582	$6.207 \times 10^{-3}$

\* Interpolated from The Saturated Steam: Temperature Table;

\*Fundamentals of Classical Thermodynamics, 2nd Edition; Van Wylen and Sonntag, 1973.

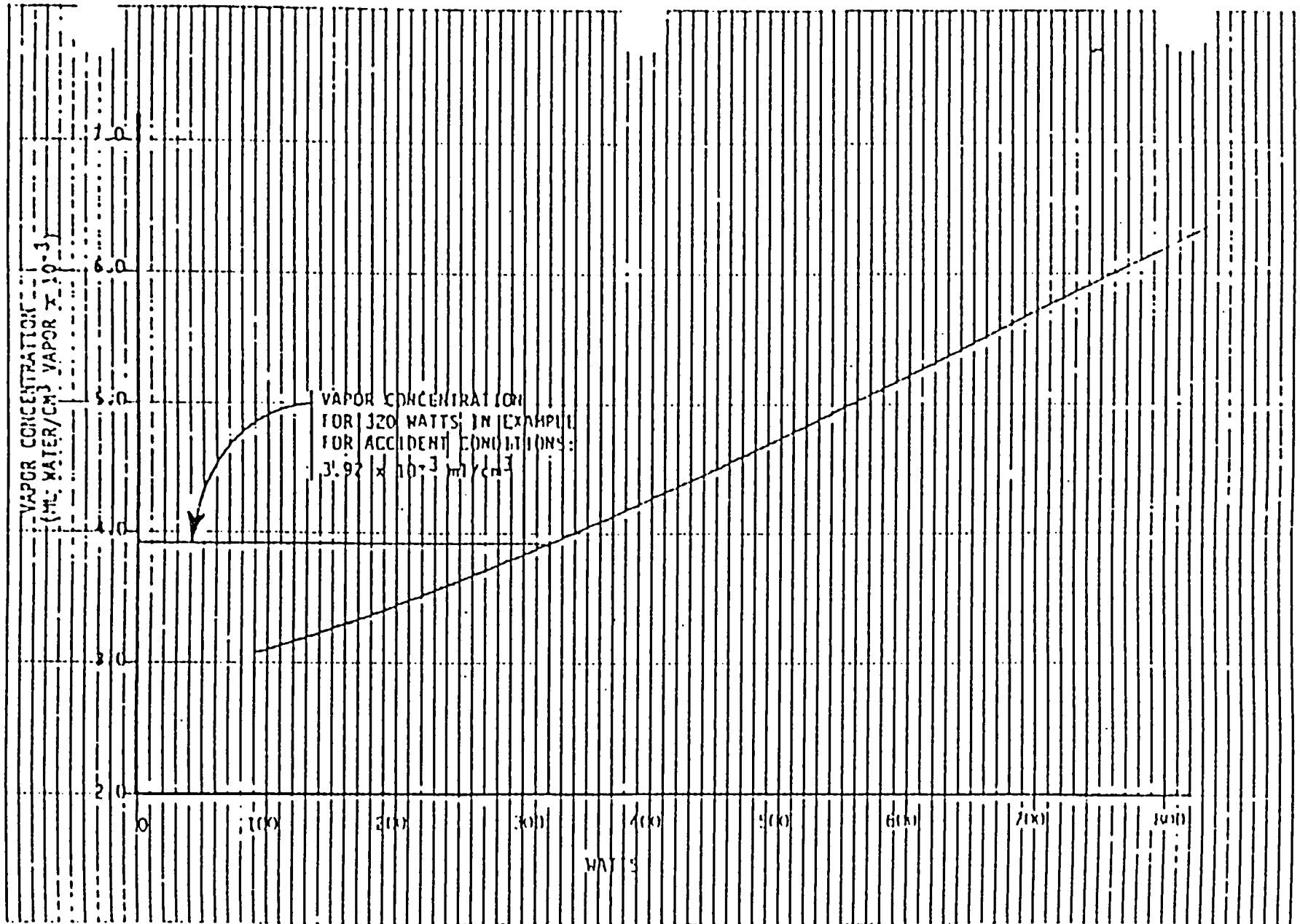


FIGURE 4.4.1-1 VAPOR CONCENTRATIONS - ACCIDENT CONDITIONS

4.4.1 Example Use of Activity Limits

The activity limits derived in Section 4.4.1 are strictly applicable only to those payloads possessing some potentially leakable portion, such as residual water existing in dewatered resins. Clearly, solid materials, such as neutron activated reactor components, possess no leakable fraction. As a result, these solid materials comply with containment requirements so long as there is "no ejection of contents."

To assess the containment requirements for materials such as dewatered resins, the specific activities of isotopes within the leakable fraction results from residual fluid present in dewatered resins.

As an example, consider a vessel containing approximately 8 cu. ft. of ion exchange resins where the only leakable portion of this payload is a small quantity of residual process fluid. There are no gaseous radioactive decay products present.

Example: Normal Conditions

Assume the radionuclide distribution and maximum concentration for the residual water in the resin are as given in Table 4.4.2-1.

TABLE 4.4.2-1

ISOTOPE	ACTIVITY OF WATER Ci/ml	$\lambda_2$ VALUE	$(Ci/ml)/\lambda_2$
Cesium 134	2.770E-005	10.00	2.770E-006
Cesium 137	1.720E-004	20.00	8.600E-006
Strontium 90	1.900E-005	0.40	4.750E-005
Tritium	1.000E-006	1000.00	1.000E-009
Niobium 95	1.000E-009	20.00	5.000E-011
Zirconium 95	1.100E-009	20.00	5.500E-011
Ruthenium 106	7.300E-008	7.00	1.043E-008
Antimony 125	1.500E-008	30.00	5.000E-010
Iodine 129	5.700E-012	2.00	2.850E-012
Tellurium 125M	1.200E-009	100.00	1.200E-011
Tellurium 127M	2.200E-008	40.00	5.500E-010
Tellurium 129M	4.400E-011	30.00	1.467E-012
Cobalt 60	1.400E-009	7.00	2.000E-010
Manganese 54	1.200E-009	20.00	6.000E-011
Cerium 144	1.000E-007	7.00	1.429E-008
Uranium 234	1.560E-012	0.10	1.560E-011
Uranium 235	1.670E-010	0.20	8.350E-010
Uranium 236	4.620E-012	0.20	2.310E-011
Uranium 238	6.930E-009	unlimited	---
Plutonium 239	1.290E-011	0.002	6.400E-009
Plutonium 240	1.050E-012	0.002	5.250E-010
Plutonium 241	1.540E-013	0.10	1.540E-012
Americium 241	8.110E-014	0.01	1.014E-011

$$\sum Ci/ml = 2.199E-004$$

$$\sum (Ci/ml)/\lambda_2 = 5.890E-005$$

$$\text{Composite } \bar{\lambda}_2 = \frac{\sum (Ci/ml)}{\sum (Ci/ml)/\lambda_2} = \frac{2.199E-004}{5.890E-005} = 3.733 \text{ Ci}$$

$$C_n = \sum Ci/ml = 2.199E-004$$

From Figure 4.2.1-1 the permissible activity of the water for a 320 watt payload decay heat is found to be:

$$\frac{C_N}{\lambda_2} = 2.92 \times 10^{-4} \text{ l/cm}^3$$

$$\lambda_2 = 3.733 \text{ Ci as determined previously}$$

Therefore the permissible activity of the water is:

$$C_H = (2.92 \times 10^{-4}) \times 3.733 = 1.09 \times 10^{-3} \text{ Ci/cm}^3$$

The Containment Factor of Safety is:

$$F.S. = \frac{C_H}{C_N} = 1.09 \times 10^{-3} / 2.199 \times 10^{-4} = \text{a number larger than 1.0}$$

If the factor of safety had been less than 1.0 the wattage was too high. A lower value would then need to be assumed and the calculations revised until a positive F.S. is obtained.

Example: Accident Conditions

To determine the containment safety factor for accident conditions the vapor concentration is determined from Figure 4.4.1-1 given an actual payload decay heat. The actual activity concentration of the vapor ( $C_a$ ) is then determined knowing the radionuclide distribution and residual fluid activity concentrations. The actual activity concentrations of the vapor are then compared to the permissible vapor activity ( $C_A$ ) found from Figure 4.3.2-1 for the given payload decay heat and the composite  $\lambda_2$  value determined previously.

Using the same radionuclide distribution and residual fluid activity concentrations as the example for normal conditions and an actual payload decay heat for accident conditions of 320 watts, the vapor concentration is found to be  $0.00392 \text{ ml/cm}^3$ , from Figure 4.4.1-1.

The vapor activity is therefore determined from knowing the residual fluid activity (determined in the example for normal conditions) and the vapor concentration.

$$\begin{aligned} C_A = \text{Vapor Activity} &= 2.199 \times 10^{-4} \text{ Ci/ml} \times 0.00392 \text{ ml/cm}^3 \\ &= 8.62 \times 10^{-7} \text{ Ci/cm}^3 \end{aligned}$$

From Figure 4.3.2-1 the permissible activity of the vapor is computed for a 320 watt payload decay heat as follows:

$$\frac{C_A}{\lambda_2} = 6.25 \times 10^{-7} \text{ 1/cm}^3$$

$$\lambda_2 = 3.733 \text{ Ci as determined previously.}$$

Therefore the permissible vapor activity  $C_A$  is found to be:

$$C_A = (6.25 \times 10^{-7}) \times 3.733 = 2.333 \times 10^{-6} \text{ Ci/cm}^3$$

The containment factor of safety is:

$$\text{F.S.} = \frac{C_A}{C_B} = \frac{2.333 \times 10^{-6}}{8.62 \times 10^{-7}} = 2.71$$

If the factor of safety had been less than 1.0 the assumed maximum wattage was too high. A lower value would then need to be assumed and the calculations revised until a positive F.S. is obtained.

For radionuclides and actual residual fluid activity concentrations different from those assumed in this example, the package operator may demonstrate compliance to the containment requirements by appropriate modifications of the methods outlined herein.



2-5.3 Gasket Size and Bolt Torque Calculations:

Determination of Required Gasket thickness and Bolting Torque for the  
1-13C II Cask.

Gasket: Duro 50

.114" x 1.3", 32.90" I.D.

Maximum internal pressure = 184 psi

Using the ASME Code & Section VIII, Division 1, Appendix 2, Part A-Flanges  
with ring type gaskets.

Two design conditions must be considered.

- 1) Operation conditions determine bolt load resulting from the hydrostatic end force and the clamping force necessary to maintain a seal.
- 2) An initial seating load must be applied to the joint to assure a complete seating of the gasket.

- 1) From Paragraph 2-5(c) the operating bolt load is determined from:

$$W_{ml} = H + H_p = 0.785 G^2 p + (2b \times 3.14 GmP)$$

Where

H is the load due to hydrostatic pressure and  $H_p$  is the reaction of the compressive load on the gasket required to maintain a tight joint.

$H_p$  must be provided by the torquing of the bolts. From Formula (1) of the above paragraph:

Where

b = gasket seating width determined from Table 2-5.2

$$b = \sqrt{b_o}/2, \quad b_o = N/2$$

For the 1-13C II,  $H = 1.3''$

$$b = \sqrt{1.3/2/2} = .403''$$

$$G = \text{gasket OD} - 2b = 35.5 - 2(0.403) = 34.694$$

$m = .5$  for gasket with <75A Shore Durometer

$P =$  Internal pressure.

$$H_p = 2(.403) 3.14 (34.694)(.5) 184 = \underline{8872 \text{ lb.}}$$

- 2) Check also minimum initial seating load which is determined using Formula (2) of Paragraph 2-5(c)(2).

$$W_{m2} = 3.14bGy \quad (2)$$

Where

$y =$  minimum design seating stress = 0

Table 2-5(1)

$$W_{m2} = 0$$

Also from Formula (1) of the previous page:

$$H = 0.785G^2P = 0.785 (34.694)^2(184) = 173859 \text{ lbs.}$$

Total initial bolt load required:

$$W_{m1} = H + H_p = 173859 + 8141 = 182,000 \text{ lbs.}$$

$$\text{Load per bolt} = F_b = 182,000/12 = 15167 \text{ lbs.}$$

Finally, the minimum bolt load for fully seating the lid standoff against the top of the cask body will be determined by following the method of Harris & Crede on page 35-15 of "Shock & Vibration Handbook". Eqn. 35.8 is:

$$E = \frac{F}{S} \left( \frac{h_1}{h - h_1} \right)$$

Where

$E$  = elastic compression modulus  
(use 375 psi for Duro 50 rubber)

Gasket area  $S = \frac{\pi}{4} (35.5^2 - 32.9^2) = 139.7 \text{ in}^2$

$F$  = compressive force in lbs.

$h$  = unstrained gasket thickness

$h_1$  = standoff height (i.e. gasket thickness when fully compressed)

For a 1/4" gasket of Duro 50 material

$E = 375 \text{ psi}$

$h_1 = .216$

$h = .250$

$$F = \frac{E(h - h_1) S}{h_1}$$

$$= \frac{375 (.250 - .216) 139.7}{.216} = 8246 \text{ lbs.}$$

The minimum load per bolt required to fully compress the gasket initially is therefore:

$$F_b' = 8246/12 = 687 \text{ lbs/bolt}$$

The bolt load required for maintaining the gasket sealing capabilities at the maximum expected pressures for accident conditions was shown to be:

$$F_b = 15167 \text{ lbs.}$$

Since  $F_b > F_b'$  the lid will be fully seated against the cask body when torqued initially.

Torque required:

$$T = kF_b d$$

Where

$k = .20$  (dry)

$= .15$  (lubricated)

$$\begin{aligned}
 d &= \text{nominal diameter of bolt} = 1.25'' \\
 T_{\text{dry}} &= .20 (15167) (1.25) = 3792 \text{ in-lbs.} \\
 &= \underline{316 \text{ ft-lbs.}}
 \end{aligned}$$

$$\begin{aligned}
 T_{\text{lubr.}} &= .15 (15167) (1.25) = 2844 \text{ in-lbs.} \\
 &= \underline{237 \text{ ft-lbs.}}
 \end{aligned}$$

For a 10% tolerance in a torque wrench the lid bolt torque requirements for the 1/4 gasket are as follows:

$$\text{Lubricated: } T_L = \frac{237}{0.9} = 263 \text{ ft-lbs.}$$

$$\text{Dry: } T_D = \frac{316}{0.9} = 351$$

Use: 270 ft-lbs  $\pm$  10% lubricated  
 360 ft-lbs.  $\pm$  10% dry.

4.5 APPENDIX B

PARKER STAT-O-SEAL INFORMATION

--Applicable Catalogue Excerpts--

# Stat-O-Seal features

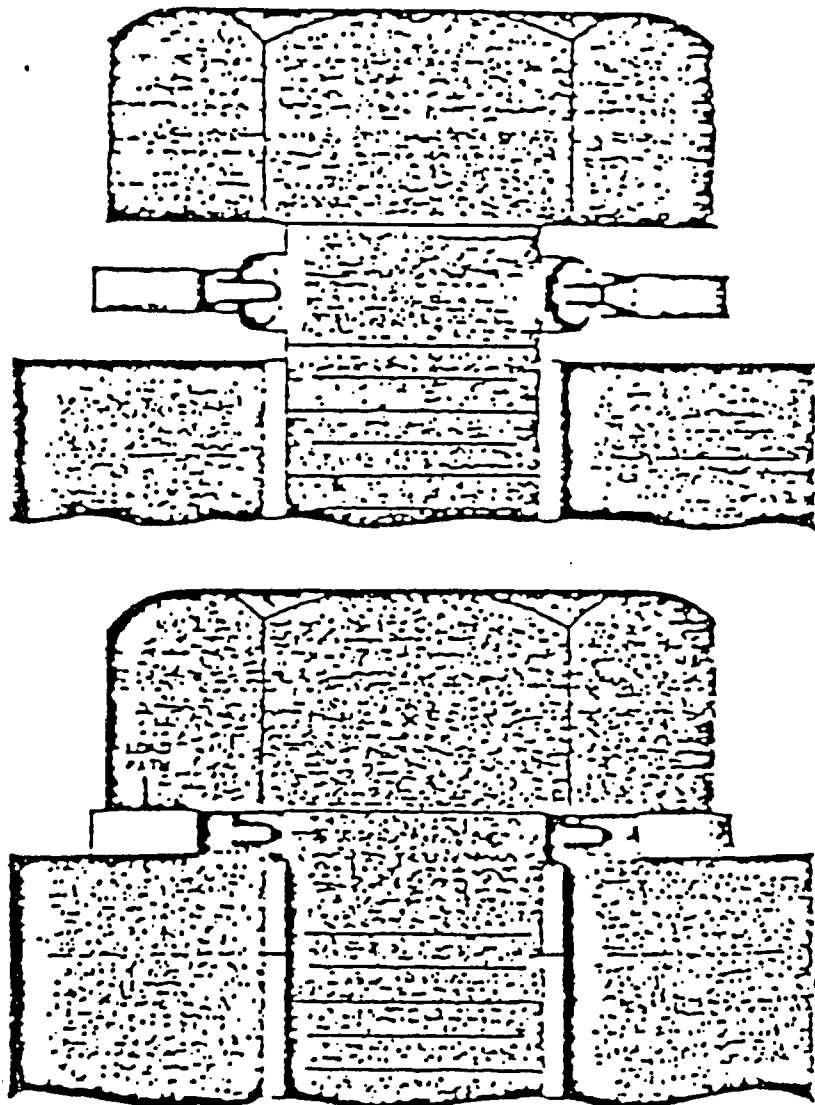
Revision 0

Parker STAT-O-SEALS are one-piece, molded-in-place seals with the rubber sealing element mechanically locked to the metal retainer. STAT-O-SEALS are designed to seal beneath the head of the fastener as shown for both INTERNAL and EXTERNAL pressure systems.

The principle of controlled confinement is utilized in the Stat-O-Seal. As the fastener is tightened the rubber seal is compressed, forcing the sealing surfaces securely around the fastener shank — but without squeezing the rubber beyond its elastic limit, or destroying its inherent "memory." With the Stat-O-Seal there is full metal-to-metal contact of faying surfaces. The unique Stat-O-Seal design provides:

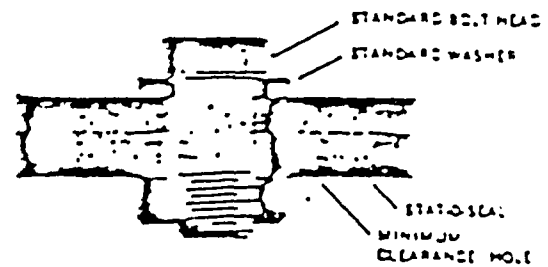
- SELF-CENTERING OF SEAL
- VACUUM SEALING TO POSITIVE HIGH PRESSURE SEALING (SEE PAGE 2)
- HIGH RE-USABILITY FACTOR
- LONG, RELIABLE SERVICE
- POOL-PROOF INSTALLATION
- MODERATE TORQUING
- NO RETORQUING
- QUICK VISUAL INSPECTION

Stat-O-Seals are available for immediate delivery in standard sizes for bolts and screws, from the number 6 size thru one inch, and will seal against fluids and gases at temperatures from  $-80^{\circ}\text{F}$ . to  $450^{\circ}\text{F}$ . The following information on the following pages will assist you in ordering.



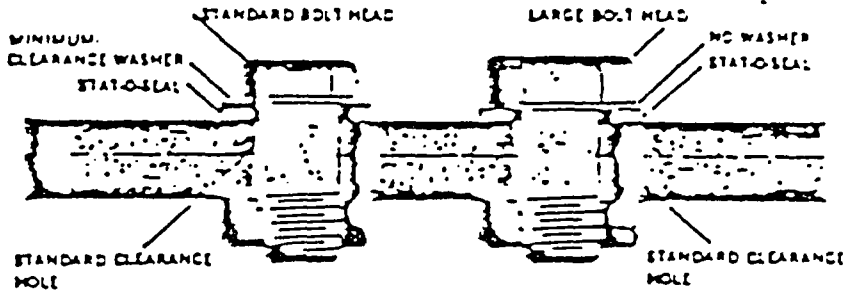
# high pressure considerations for series 600 Stat-O-Seals

DESIGN FOR EXTERNAL PRESSURE APPLICATIONS



**MAXIMUM SAFE OPERATING PRESSURES** The operating pressure of a Stat-O-Seal must be kept well below the pressure at which the retainer metal would rupture. The following table gives the maximum recommended operating pressure for 600 series Stat-O-Seals as determined from Lamé hoop stress calculations. A safety factor of 3 was applied to the tensile strength of the metal.

ALTERNATE DESIGNS FOR INTERNAL PRESSURE APPLICATIONS



MAXIMUM SAFE OPERATING PRESSURE, P.S.I.

FASTENER	RETAINER METAL			
	ALUMINUM	1818/1850 STEEL	STAINLESS STEEL	CHROME MOLY STEEL
-6	8,900	10,100	11,100	18,600
-8	7,100	8,100	8,900	14,800
-10	6,000	6,800	7,500	12,600
-10 OS	4,200	4,800	5,300	8,800
-1/4	4,900	5,600	6,100	10,200
-1/4 OS	4,000	4,500	4,900	8,300
-1/2	3,500	4,000	4,400	7,300
-1/2 OS	3,300	3,800	4,100	6,900
-3/4	3,600	4,100	4,500	7,500
-1	4,400	5,000	5,500	9,100
-1 1/4	6,400	7,200	8,000	13,300
-1 1/2	7,000	8,000	8,800	14,700
-2	8,900	9,700	10,600	17,800
-2 1/2	6,100	7,000	7,600	12,800
-3	7,000	8,000	8,800	14,600

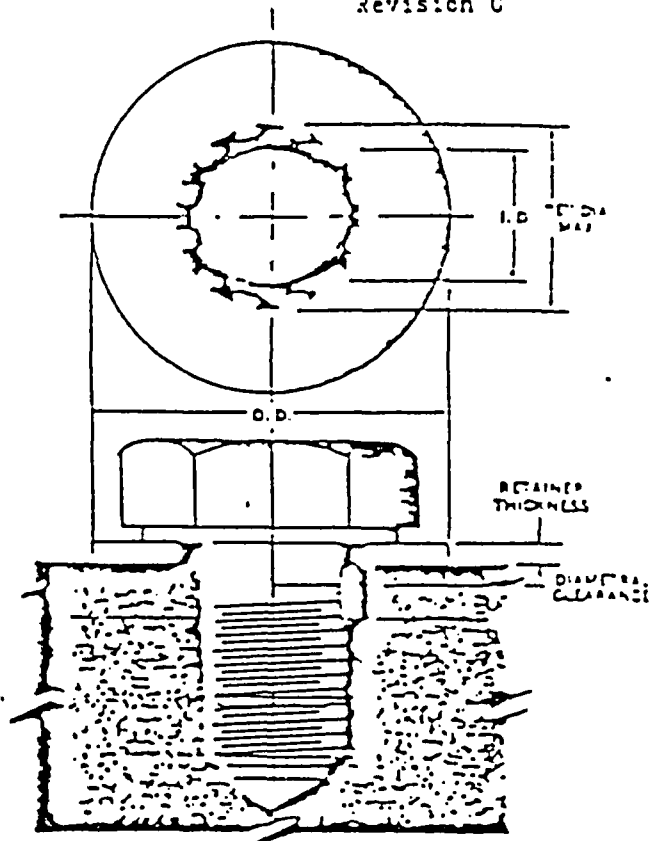
**BOLT TORQUE** High pressure fluids acting under the head of a bolt tend to stretch it, lifting the bolt head off its seat. When this happens, the space exposed under the bolt head can permit the Stat-O-Seal elastomer to extrude and fail. It is, therefore, important in high pressure applications to torque the bolt well at assembly, providing enough prestress in the bolt

to prevent stretching.  
**CLEARANCE FOR EXTRA RUBBER** Most Stat-O-Seals have some excess rubber, and, as noted on page 5, clearance must be provided to receive it. In low pressure applications, this clearance may be either in the mounting surface or in a washer between the bolt head and the Stat-O-Seal. In high pressure applications,

however, the normal clearance must be on the high pressure side of the Stat-O-Seal, with little or no clearance on the low pressure side. Otherwise, the fluid pressure will extrude too much rubber into the clearance gap, resulting in a leak.

# Lock-O-Seal® 600 series

Revision C



VISIONS

SIZE DASH NUMBER	THREAD MAJOR DIAMETER (IN.)	I.D. ± .010	O.D. MAXIMUM	O.D. ± .010	RETAINED THICKNESS	PURSED THICKNESS	DIAMETRAL CLEARANCE (REF.)
-6	.138	.130	.229	.385	.040 ± .004	.050 ± .003	½ MAX.
-8	.164	.156	.255	.385	.040 ± .004	.050 ± .003	½ MAX.
-10	.190	.180	.317	.443	.050 ± .005	.072 ± .005	½ MAX.
-10 O.S.	.190	.186	.365	.468	1	1	½ TO ¾
-¼	.250	.240	.381	.505			½ MAX.
-¼ O.S.	.250	.245	.422	.531			½ TO ¾
-½	.312	.301	.488	.603			
-¾	.375	.364	.546	.666			
-1	.438	.427	.618	.760			
-1½	.500	.490	.696	.880			
-2	.562	.552	.759	1.067	1	1	
-2½	.625	.615	.818	1.193	.050 ± .005	.072 ± .005	
-3	.750	.740	.982	1.322	.064 ± .005	.096 ± .005	
-3½	.875	.864	1.105	1.510	.064 ± .005	.096 ± .005	1
-4	1.000	.988	1.234	1.760	.064 ± .005	.096 ± .005	½ TO ¾

NOTES:

- [1] Color code provided only when specified by customer.
- [2] A washer may be required under the bolt head to distribute torque pressure (see page 4).  
Fastener size dash number to complete the call-out.  
Ex. 600-001-¼.
- [4] For uses not listed here, see Parker Seal Gask-O-Seal Handbook, or contact your local Parker Seal representative.
- [5] Chrome Molybdenum retainers are heat treated to 125,000 psi minimum tensile strength.

- [6] Stainless steel retainers are annealed to half hard.
- [7] A slight parting line projection, similar to that found on O-Rings, will often be observable around the inside of the sealing element.
- [8] Trademarks: Viton — duPont, Fluorel — Minnesota Mining
- [9] This material combination is not available in sizes -6 & -8. See 800 Series Lock-O-Seals.
- [10] Other material combinations available on special order.



## CALL OUTS

PART NO. NUMBER	MATERIAL (SPECIFICATION)	FINISH (SPECIFICATION)	RESIST. COMPOUND (SPECIFICATION)	USAGE (A)
<b>STOCK STANDARD PARTS</b>				
600-010	Steel (No Specification)	Cadmium Plate (No Specification)	Nitrile (Buna-N) (No Specification) N406-60	Industrial for weather and petroleum fluids -65°F to +225°F (-54°C to +107°C). Water and many other fluids suitable with lower maximum temperature
600-001	1020/1030 Steel (QQ-S-695)	Cadmium Plate (QQ-P-416 Cl. 2 Type II)	Nitrile (Buna-N) (MIL-R-6255 Class 1 & 2 Grade 60) N406-60	Air, petroleum fluids, (fuel's oils, gases), silicone lubricants and diester base lubricants -65° to +225°F (-54° to +107°C).
600-015	7075-T6 Aluminum (QQ-A-250/12)	Anodize (MIL-A-8625, Type II)		
<b>NON STOCK STANDARD PARTS (MADE TO ORDER) (18)</b>				
600-042	4130 Chrome Moly Steel [5] (MIL-S-18729)	Cad. Plate Dye Black (QQ-P-416 Cl. 2, Type II)	Nitrile (Buna-N) (MIL-R-6255 Class 1 & 2, Grade 60) N406-60	Air petroleum fluids, (fuel's oils, gases) silicone lubricants and diester base lubricants -65° to +225°F (-54° to +107°C)
600-430	302/304 Stainless Steel [6] (MIL-S-5059)	Passivate (QQ-P-35)	Nitrile (Buna-N) (MIL-R-7362 Type II) 47-071	MIL-L-7828 Synthetic engine oil -65° to +275°F (-54° to +135°C).
600-442	4130 Chrome Moly Steel [5] (MIL-S-18729)	Cad. Plate Dye Black (QQ-P-416 Cl. 2 Type II)		
600-701	1020/1030 Steel (QQ-S-695)	Cadmium Plate (QQ-P-416 Cl. 2 Type II)	Neprene (No Specification) C406-70	Silicate Ester -65° to +275°F (-54° to +135°C).
600-742	4130 Chrome Moly Steel [5] (MIL-S-18729)	Cad. Plate Dye Black (QQ-P-416 Cl. 2 Type II)		
600-3130	302/304 Stainless Steel [6, 19] (MIL-S-5059)	Passivate (QQ-P-35)	Fluorocarbon [8, 9] (MIL-R-83248, Type I Class 1) V1854-75	Air, Petroleum fluids, silicone fluids, many acids and phosphate esters -20° to +400°F (-29° to +204°C).
600-3142	4130 Chrome Moly Steel [5] (MIL-S-18729)	Cadmium Plate Dye Black (QQ-P-416 Cl. 2 Type II)		
600-6015	7075-T6 Aluminum (QQ-A-250/12)	Anodize (MIL-A-8625 Type II)	Fluorosilicone (MIL-R-25988) Type II Cl. I GR 60 L1830-65	Petroleum fluids, silicone fluids, silicate esters -65° to +350°F (-54° to +177°C)
600-6030	302/304 Stainless Steel [6] (MIL-S-5059)	Passivate (QQ-A-35)		
600-6042	4130 Chrome Moly Steel [5] (MIL-S-18729)	Cad. Plate Dye Black (QQ-P-416 Cl. 2 Type II)		
600-6230	302/304 Stainless Steel [6] (MIL-S-5059)	Passivate (QQ-A-35)	Silicone (AMS 3304) S604-7C	Air and gases -80° to +450°F (-62° to +232°C)
600-6242	4130 Chrome Moly Steel [5] (MIL-S-18729)	Cadmium Plate Dye Black (QQ-P-416 Cl. 2 Type II)		
-6230	302/304 Stainless Steel [6] (MIL-S-5059)	Passivate (QQ-A-35)	Buryl (AMS 3238) B318-70	Hydrol, phosphate esters, water, steam and air -65° to +225°F (-54° to +107°C)

## recommended torque

## RECOMMENDED BOLT TORQUE VALUES FOR STAT-O-SEALS—POUND INCHES

Retainer Metal	Steel		Aluminum		Inconel Steel		Chrome-plated	
Part Numbers	BOC-0101 BOC-0201 BOC-0301 BOC-0401 BOC-0501 BOC-0601		BOC-0111 BOC-0211		BOC-0110 BOC-0210 BOC-0310 BOC-0410 BOC-0510		BOC-0412 BOC-0512 BOC-0612 BOC-0712 BOC-0812	
SIZE	Min.	Max.	Min.	Max.	Min.	Max.	Min.	Max.
6	5	33	5	25	—	—	5	45
8	10	60	10	50	—	—	10	75
10	13	60	13	70	13	60	13	90
10 OS.	13	60	13	80	13	60	13	95
1/4	40	100	40	110	40	100	40	145
1/4 OS.	40	100	45	110	40	100	75	145
1/2	60	180	70	85	60	140	75	180
3/4	80	220	80	160	80	220	80	230
1 1/2	110	280	110	260	110	300	110	400
2	130	540	130	360	130	420	130	600
3	450	800	400	500	250	1000	400	1000
4	650	1100	650	1040	350	1100	650	1700
5/8	650	2900	550	1550	500	2900	650	3800
3/4	650	3900	650	1900	570	3900	650	6400
1	720	5900	850	2840	700	5900	700	8000

The values in this table exceed permissible torques for many bolt materials.

Data is for fine thread, lubricated, SAE Grade 8 Bolts.

Torque values may be increased 20% if the bearing surface under the head of the bolt completely covers the Stat-O-Seal.

## fastening torques

Whenever fastening torques are discussed by engineers, there is always controversy. There are many variables such as wrenching methods and thread friction influenced by lubrication, plating, surface finishes, length of grip, class of thread, etc. Often torque wrenches are not even used. Machines do a fairly consistent job, but if the seating surface is not flat, using pure torque values can cause difficulty.

Parker STAT-O-SEALS provide a certain amount of latitude in torque requirements. Actually, STAT-O-SEALS are often capable of sealing when only "finger tight" so that extra high fastening torques may not be necessary. If extra firm seating is required, STAT-O-SEALS should be torqued within the limits shown to avoid crushing the metal retainer itself.

## SUGGESTED MAXIMUM TORQUE VALUES FOR FASTENERS OF DIFFERENT MATERIALS

DOWEL SIZE	LOW CARBON STEEL	11% ST. ST.	BRASS	SILICON BRONZE	ALUMINUM METS.	316 ST. ST.	MONEL
	IN.	IN.	IN.	IN.	IN.	IN.	IN.
6-32	8.7	9.6	7.9	8.9	5.3	10.1	9.8
6-40	10.9	12.1	9.8	11.2	6.6	12.7	12.3
8-32	17.8	19.8	16.2	18.4	10.8	20.7	20.2
8-36	19.8	21.0	18.0	20.4	12.0	23.0	22.4
10-24	20.8	22.8	18.6	21.2	13.8	23.8	23.9
10-32	29.7	31.7	25.9	29.3	19.2	33.1	34.9
1/4"-20	65.0	75.2	61.5	68.8	45.6	78.8	81.3
1/4"-28	90.0	94.0	77.0	87.0	57.0	99.0	106.0
1/2"-18	129	132	107	123	80	138	149
1/2"-24	139	142	116	131	86	147	160
5/8"-16	212	236	192	219	143	247	261
5/8"-24	232	259	212	240	157	271	294
3/4"-14	338	376	317	349	228	393	427
3/4"-20	361	400	327	371	242	418	451
1"-13	485	517	422	480	313	542	584
1"-20	487	541	443	502	328	565	613
1 1/8"-12	613	682	558	632	413	713	774
1 1/8"-18	668	752	615	697	456	787	855
1 1/2"-11	1000	1110	907	1030	715	1160	1330
1 1/2"-18	1140	1244	1016	1154	798	1301	1482
1 3/4"-10	1259	1530	1249	1416	980	1582	1832
1 3/4"-16	1230	1490	1220	1382	958	1558	1790
2"-9	1919	2328	1905	2140	1495	2430	2775
2"-14	1911	2313	1895	2130	1490	2420	2755
2 1/2"-8	2832	3440	2815	3185	2205	3595	4130
2 1/2"-14	2562	3110	2545	2885	1995	3250	3730

NOTE: Table is intended as a guide, obtained from Machine Design's Reference Issue, "Fastening and Joining," June 15, 1967

4.2.5 Combustible Gas Generation Safety Assurance

Assurance of safe shipment of vessels which may generate combustible gas is based on meeting the following criteria over the shipment period.

- (i) The quantity of hydrogen generated must be limited to a molar quantity that would be no more than 5% by volume at STP (or equivalent limits for other inflammable gases) of the secondary container gas void (i.e., no more than 0.063 g-moles/ft<sup>3</sup>); or
- (ii) The secondary container and the cask cavity (if required) must be inerted with a diluent to assure the oxygen, including that radiolytically generated, shall be limited to 5% by volume in those portions of the package which could have hydrogen greater than 5%.

The following discussion establishes the safety assurance of the above criteria and describes how vessels will be prepared such that the above criteria will be met while the vessels are in shipment.

Criterion (i) essentially stipulates that the quantity of hydrogen shall be limited to 5% of the secondary container gas void at STP. This 5% hydrogen gas volume at standard conditions is equivalent to a hydrogen partial pressure of 0.735 psi or 0.063 gram moles/cubic foot. By actual experiment\*, the ignition of a 5% (H<sub>2</sub>) gas volume has been demonstrated to produce an approximate 2.3 psi incremental pressure increase above an initial pressure of approximately atmospheric. The reason this is so is that the 0.063 gram moles of hydrogen per cubic foot provides such a small source that the peak pressure rise resulting from ignition of this source is slight. It is felt that 1-13C II is able to sustain an incremental 3 psi internal pressure rise from atmospheric pressure without failure. This pressure increase is not considered in Section 2.6 and Chapter 3 and 4 calculations as it is considered to be insignificant.

Criteria (ii) is invoked to ensure that when a secondary container's hydrogen concentration potentially exceeds 5% volume, release of that hydrogen to the then existing total volume (secondary container void plus cask void) will not result in a total mixture of greater than 5% volume hydrogen in a greater than 5% oxygen atmosphere. Maintaining the oxygen lower than five (5) volume % assures a non-flammable mixture.\*\*

- \* Carlson, L.W., et al., "Flame and Detonation Initiation area Propagation in Various Hydrogen - Air Mixtures With and Without Water Spray", Atomic International Division of Rockwell International, Canoga Park, California, May 11, 1973. (The incremental pressure rise is basically independent of the total volume under test--i.e.,--that the 0.063 gram moles per cubic foot relationship to 2.3 per rise is valid for one or many cubic foot of specimen volume.)

- \*\* Lewis, B. and von Elbe, G., "Combustion, Flames and Explosions of Gases", Academic Press, New York, 1961, Second Edition, Appendix B.

## 5.0 SHIELDING

### 5.1 Discussion and Results

This cask will be operated such that the radioactive inventory within the cask will not result in dose rates exceeding 200 mRem/hr on the cask surface, or 10 mRem/hr at six feet from the surface of the cask.

The package shielding must be sufficient to satisfy the conditions on 10 CFR 71, Paragraph 71.73 for the hypothetical accident conditions. It is shown that shielding loss resulting from either the 30-foot drop or the fire transient will not increase the external radiation dose rate to more than 1,000 mRems/hr at 3 feet from the external surface of the cask.

The fissile material to be loaded into the debris containers has experienced small burnup levels of only 3165 MWD/MTU. This results in a very small neutron dose rate relative to the fuel gamma levels. Hence, the effect on shielding is insignificant.

### 5.2 Source Specification

The equivalent point source, assuming  $\text{Co}^{60}$  energy, is determined for the normal geometry. This equivalent source is then used to evaluate the effects of the hypothetical accidents.

$$\phi_{\gamma} = \frac{BS_0 e^{-b_1}}{4\pi z^2} \quad (1)$$

$$\phi_{\gamma} = \text{Photon Flux, } \frac{\gamma}{\text{cm}^2\text{-s}}$$

$$S_0 = \text{Equivalent Source} = \frac{\gamma}{\text{s}}$$

$$b_1 = \sum_i \mu_i t_i \text{ for shielding}$$

B = Buildup Factor

r = Distance from source to dose point

$$D = K \frac{C}{r^2}$$

$$K = 2.3 \times 10^{-6} \frac{R/hr}{\frac{cm^2}{gm}} \text{ for } Co^{60} \quad (2)$$

Through the side of the cask, the following values are used: (3)

$$\text{Lead: } t = 5'' = 12.7 \text{ cm, } \nu/\rho = .0600 \frac{cm^2}{gm}$$

$$\text{Steel: } t = 1\frac{1}{2}'' = 3.175 \text{ cm, } \nu/\rho = .0515 \frac{cm^2}{gm}$$

For these values:

$$b_1 = 10.0$$

$$B = 4.0 \quad (4)$$

For the two dose conditions:

$$D_1 = 10 \text{ mRem/hr. } r = 6.31 + 36 = 42.31 \text{ inch}$$

$$D_2 = 200 \text{ mRem/hr. } r = 6.31 \text{ inches - Distance to surface of cavity.}$$

$$S_o = \frac{4\pi r^2 D}{BKe^{-b_1}}$$

Substituting into the above expression:

$$(1) \quad D = 10 \text{ mRem/hr @ 3 feet}$$

$$S_o = 3.475 \times 10^{12} \quad \gamma/s$$

$$(2) \quad D = 200 \text{ mRem/hr on Surface}$$

$$S_o = 1.546 \times 10^{12} \quad \gamma/s$$

The dose rate on the surface governs and will be used in the accident analysis.

### 5.3 Model Specification

Hypothetical accident drop tests described in Section 2.11 demonstrate conclusively that the cask and its shield are not altered in any fashion by the hypothetical accident conditions. Nonetheless, shielding analyses for accident conditions, are carried out assuming a damaged geometry presuming no overpack exists. These very conservative analyses are taken directly from the Safety Analysis Report supporting the 1-13C II Packaging, USA/9081/B( ). In all instances, both impact and thermal damage assumptions due to hypothetical accident events are more severe than found by test, for drop events, (see Section 2.11) and analyses, for thermal events (see Section 3.0).

Shield displacements are assumed to result from either the 30 ft drop or from the lead melt in the fire transient. The maximum displacement for the drop will occur using the minimum dynamic flow pressure for lead given. This value is:

$$k = 5000 \text{ psi}$$

The shielding deformation resulting from the 30 ft drop will be developed for each impact mode using this value.

The lead volume displacement for the fire transient is assumed as:

$$V_F = 1305 \text{ in}^3$$

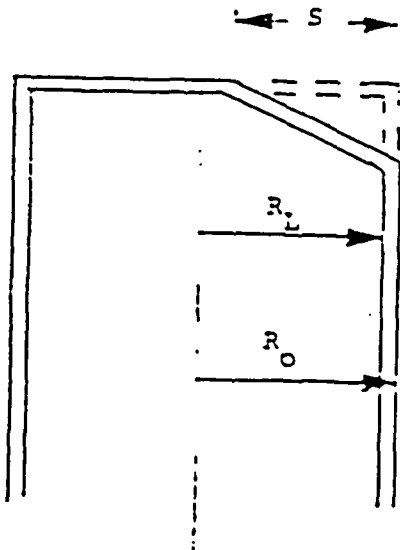
#### 5.3.1 Damage Predictions - Corner

The shielding displacement for the 30 ft corner drop will be determined for the combined displacement of the lead shield and the steel shell and fire shield.



The volume of the ungula of a cylinder is:

$$V = R^3 \tan \alpha \{f(\theta)\}$$



Lead Displacement:

$$V_L = R_L^3 \tan \alpha \{f(\theta_L)\}$$

Total Displacement:

$$V_T = R_O^3 \tan \alpha \{f(\theta_T)\}$$

For:  $\theta_L = \theta_T$ ,

The steel displaced volume is:

$$V_S = V_T - V_L = (R_O^3 - R_L^3) \tan \alpha \{f(\theta)\}$$

The total displaced volume from kinetic energy considerations is:

$$V_T = \frac{hW}{\bar{k}}$$

Where:  $\bar{k}$  is the effective dynamic flow stress of the combined lead and steel.

$$\text{Assume: } \bar{k} = \frac{k_s V_s + k_L V_L}{V_s + V_L}$$

$$\text{Then: } V_T = \frac{hW(V_s + V_L)}{k_s V_s + k_L V_L} = \frac{k_s V_T}{k_s V_s + k_L V_L}$$

$$\begin{aligned} hW &= k_s V_s + k_L V_L \\ &= k_s (R_o^3 - R_L^3) \tan^2 \{f(\theta)\} + k_L R_L^3 \tan^2 \{f(\theta)\} \\ &= (k_s R_o^3 + R_L^3 (k_L - k_s)) \tan^2 \{f(\theta)\} \end{aligned}$$

$$f(\theta) = \frac{hW}{(k_s R_o^3 - R_L^3 (k_s - k_L)) \tan^2 \theta}$$

Let:  $R_L$  = Lead Outer Radius = 18.75 inch

$R_o$  = Cask Outer Radius = 19.50 inch (with fire shield)

$k_s$  = Steel Dynamic Flow Stress = 45,000 psi

$k_L$  = Lead Dynamic Flow Stress = 5,000 psi

$\alpha = 23.3^\circ$

$h = 360$  inch

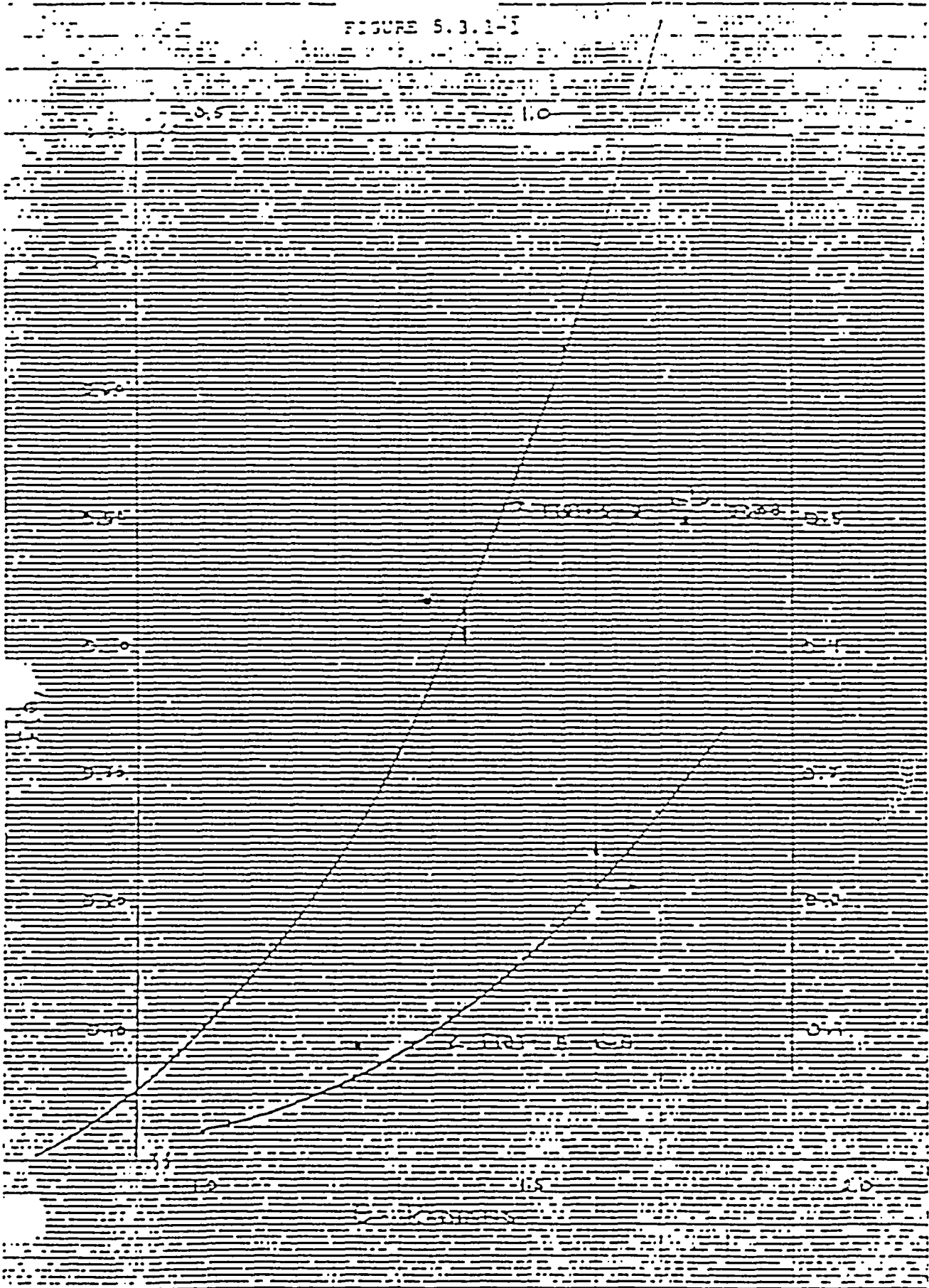
$W = 25,950$  lbs.

$$\begin{aligned} F(\theta) &= \frac{(360) \text{ in } (25950) \text{ lbs-in}^2}{(0.533) \{ (45000)(19.50)^2 - (5000)(18.75)^3 \}; \text{ lbs-in}^3} \\ &= \frac{1.73 \times 10^7}{(3.337 - 2.637) 10^8} \\ &= .248 \end{aligned}$$

From Figure 5.3.1-1:  $\theta = 1.225$  Radians

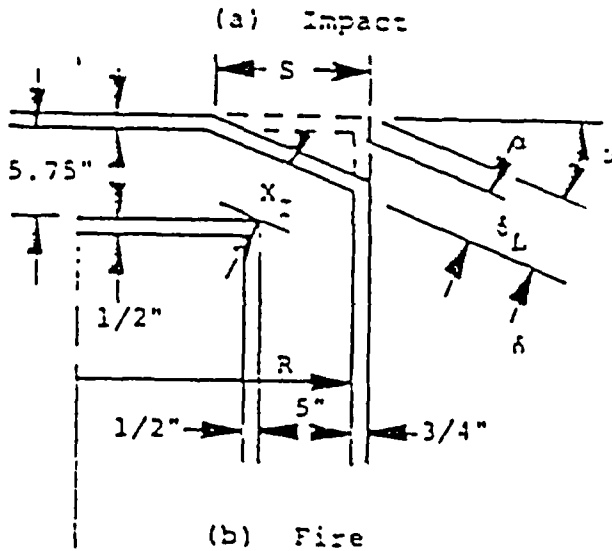
$= 70.2^\circ$

FIGURE 5.3.1-1



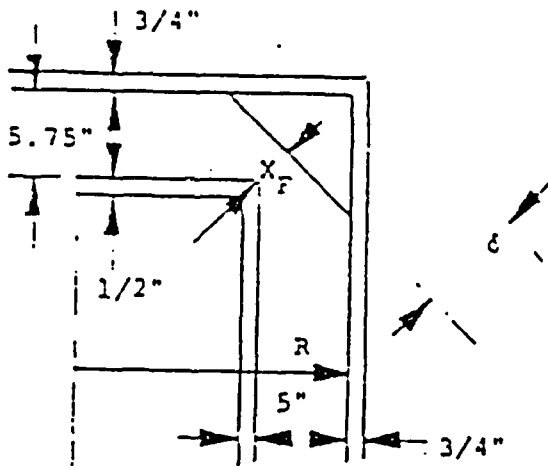
The shielding geometry for lead displacement in the corner for the two cases is as shown:

CASE 1



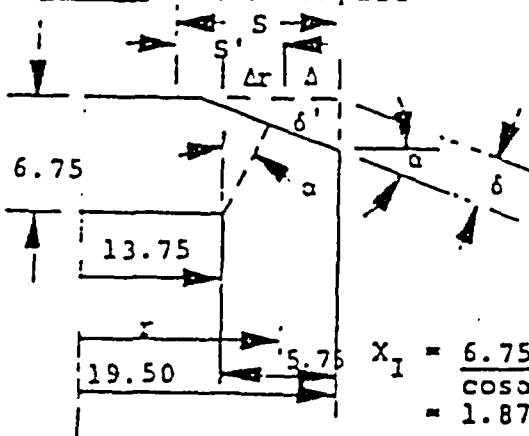
$$\begin{aligned} \theta &= 70.2^\circ \text{ (Figure 5.3.1-1)} \\ \alpha &= 28.3^\circ \\ R &= 19.50'' \end{aligned}$$

$$\begin{aligned} \delta &= (1 - \cos \theta) R = 12.89 \text{ in.} \\ \delta &= S \tan \alpha = 6.94 \text{ in.} \\ t_S &= 1.0 + \frac{.50}{\cos \alpha} = 1.57 \text{ in.} \end{aligned}$$



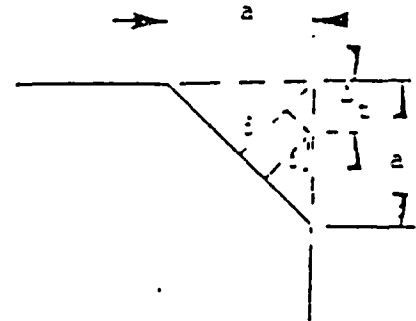
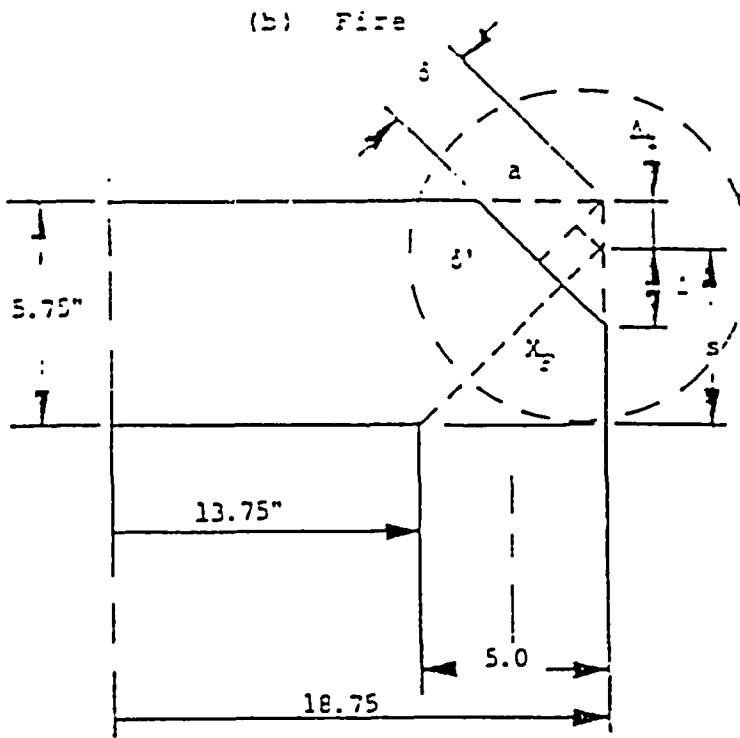
$$\begin{aligned} R &= 18.75'' \\ \epsilon &= 3.45 \text{ in.} \end{aligned}$$

CASE 2 (a) Impact



$$\begin{aligned} \Delta r &= (6.75) \tan \alpha = 3.63'' \\ T &= 13.75 + \Delta T = 17.38'' \\ \Delta &= 19.50 - r = 2.19'' \\ S' &= S - \Delta = 10.77'' \\ \delta' &= \delta \left( \frac{S'}{S} \right) = (6.94) \left( \frac{10.77}{12.89} \right) \\ \delta' &= 5.80 \text{ in.} \end{aligned}$$

$$\begin{aligned} X_I &= \frac{6.75}{\cos \alpha} - \delta' = \frac{(6.75)}{.880} - 5.80 \\ &= 1.87 \text{ in.} \end{aligned}$$



$$\delta' = \delta - \frac{z}{\sqrt{2}}$$

$$z = 5.75 - 5.00 = .75 \text{ in.}$$

$$X_f = \sqrt{2} z - \delta'$$

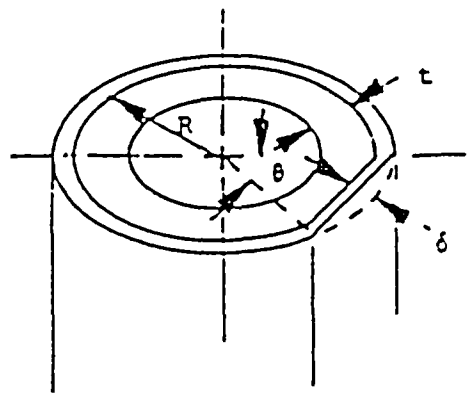
$$= \sqrt{2} (5.00) - 3.45 - \frac{.75}{\sqrt{2}}$$

$$= 4.15 \text{ in.}$$

5.3.2 Damage Prediction - Side

The lead displacement for the geometries along the side of the cask are shown below. The displacement for the fire analysis assumes all the lead melt opposite the reinforcing ring.

(a) Impact



$$\theta = 59.9^\circ \text{ (Figure 5.3.1-1)}$$

$$R = 18.75''$$

$$\delta = (1 - \cos \frac{\theta}{2}) R$$

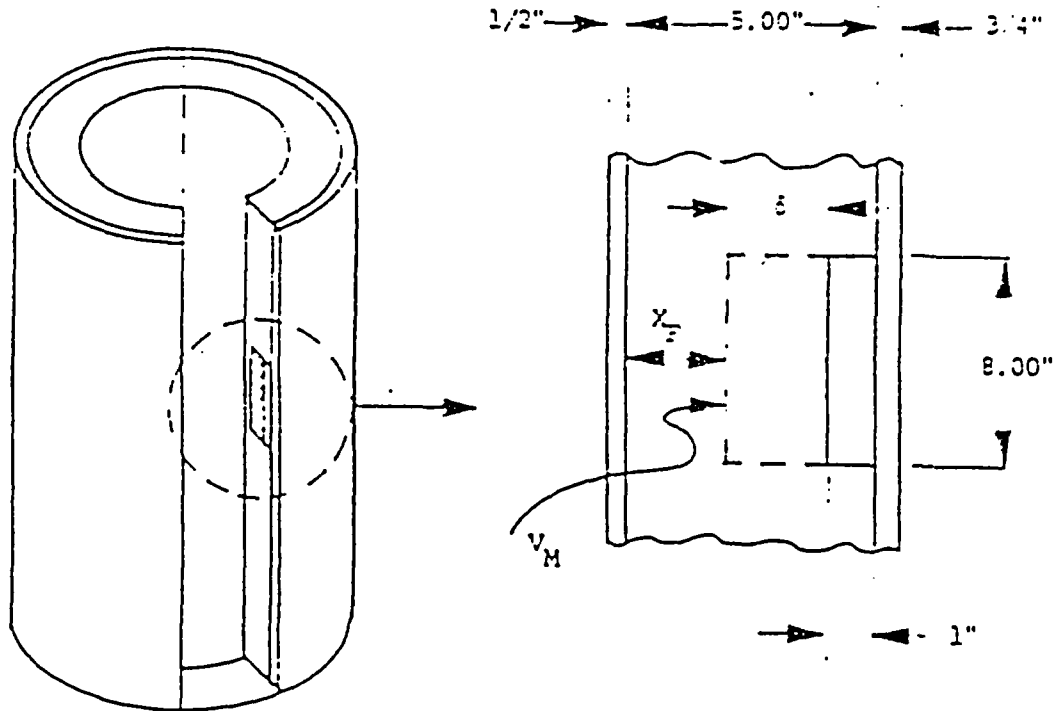
$$\delta = 2.50 \text{ inch}$$

$$t = 5.00 \text{ inch}$$

$$X_I = t - \delta = 2.50 \text{ inch}$$

(b) Fire

$$V_M = 1303 \text{ in}^3$$



$$V_M = 2\pi R_F^2 H_R$$

$$H_R = 8.00 \text{ inch}$$

$$R_F = 17.75" - \delta$$

$$\delta^2 - 17.75\delta + \frac{V_M}{2\pi H_R} = 0$$

$$\delta = 1.61 \text{ inch}$$

$$x_F = 4.00 - 1.61$$

$$x_F = 2.39 \text{ inch}$$

### 5.3.3 Damage Prediction - Ends

Consider the amount of lead displacement for the 30 foot free drop on both the top and the bottom of the cask. The displacement will be determined as follows.

$$\Delta H = \frac{R W H}{\pi (R^2 - r^2) (\tau_s c_s + R c_{pb})}$$

Where: R - Outer Radius of Lead = 18.75 in.

r - Inner radius of lead = 13.75 in.

W - Cask Weight = 25,950 lbs.

H - Drop Height = 360 in.

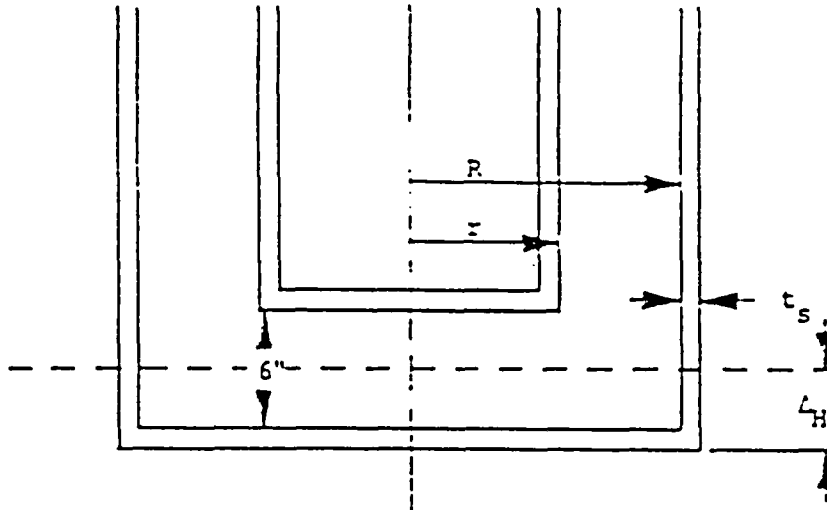
$c_s$  - Steel Dynamic Flow Stress = 45,000 psi

$c_{pb}$  - Lead Dynamic Flow Stress = 5,000 psi

$t_s$  - Steel Shell Thickness = 0.50 in.

The thickness of the steel shell has been taken as the thickness of the cask outer shell. The displacement of the 0.25 inch thick fire shield has been neglected for conservatism.

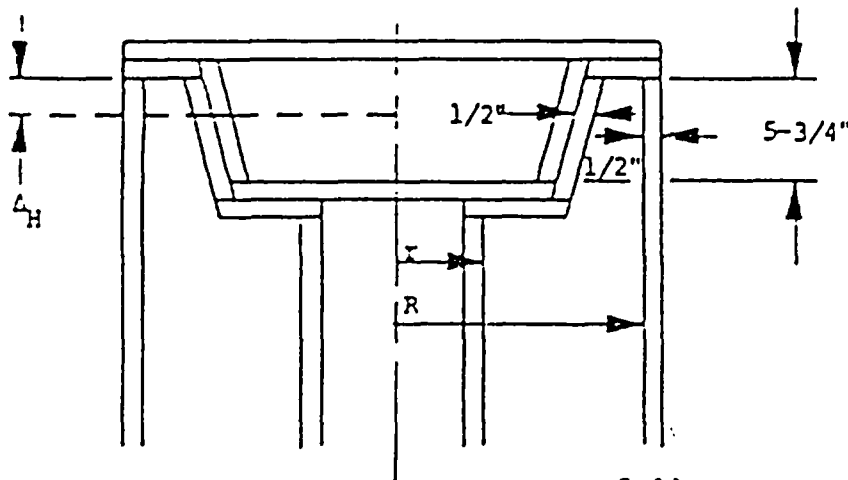
(a) Bottom Displacement



$$\begin{aligned} \Delta H &= \frac{(18.75) \text{ in.} (25950) \text{ lbs.} (260) \text{ in-in}^2}{\pi \{ (18.75)^2 - (13.75)^2 \} (0.5) (45000) + (18.75) (5000)} \\ &= \frac{(1.75 \times 10^8) \text{ in.}}{\pi (162.5) (1.16 \times 10^5)} \\ &= 2.96 \text{ in.} \end{aligned}$$

$$\begin{aligned} X_{IB} &= t_{pb} - \Delta H \\ &= 3.04 \text{ inch} \end{aligned}$$

(b) Top Displacement



$$r = 13.75 \text{ in.}$$

$$R = 18.75 \text{ in.}$$

Assume only the lid does not deform and all deformation occurs in the cask body.



$$\Delta H = \frac{(13.75) \text{ in} (25950) \text{ lbs} (360) \text{ in-in}^2}{-((13.75)^2 - (13.75)^2) \text{ in}^2 ((1.0) (45000) - (5.00) (3000)) \text{ lbs-in}}$$

$$= \frac{(1.75 \times 10^8) \text{ in}}{(162.5) (7.0 \times 10^7)}$$

$$= 4.90 \text{ in.}$$

$$X_{IT} = t_{pb} - \Delta H$$

$$= 0.85 \text{ inch}$$

The deformation stops short of the cask cavity lid for this case. If the lid also deforms, the deformation model will be the same as for the bottom end drop.

$$\Delta H = 2.96 \text{ in.}$$

$$X_{IT} = t_{pb} - \Delta H$$

$$= 2.79 \text{ inch}$$

#### 5.4 Shielding Evaluation

To determine the lead displacement having the greatest effect on dose rate, compare the attenuation for each case as follows:

$$A = \frac{3e^{-b_1}}{4\pi r^2} \quad \text{Where: } b_1 = \sum_{i=1}^n \mu_i t_i$$

$r$  - Distance from inside surface of cask cavity to a dose point 3 feet from the outside surface of the cask.

A summary of the pertinent data is presented in the following table.

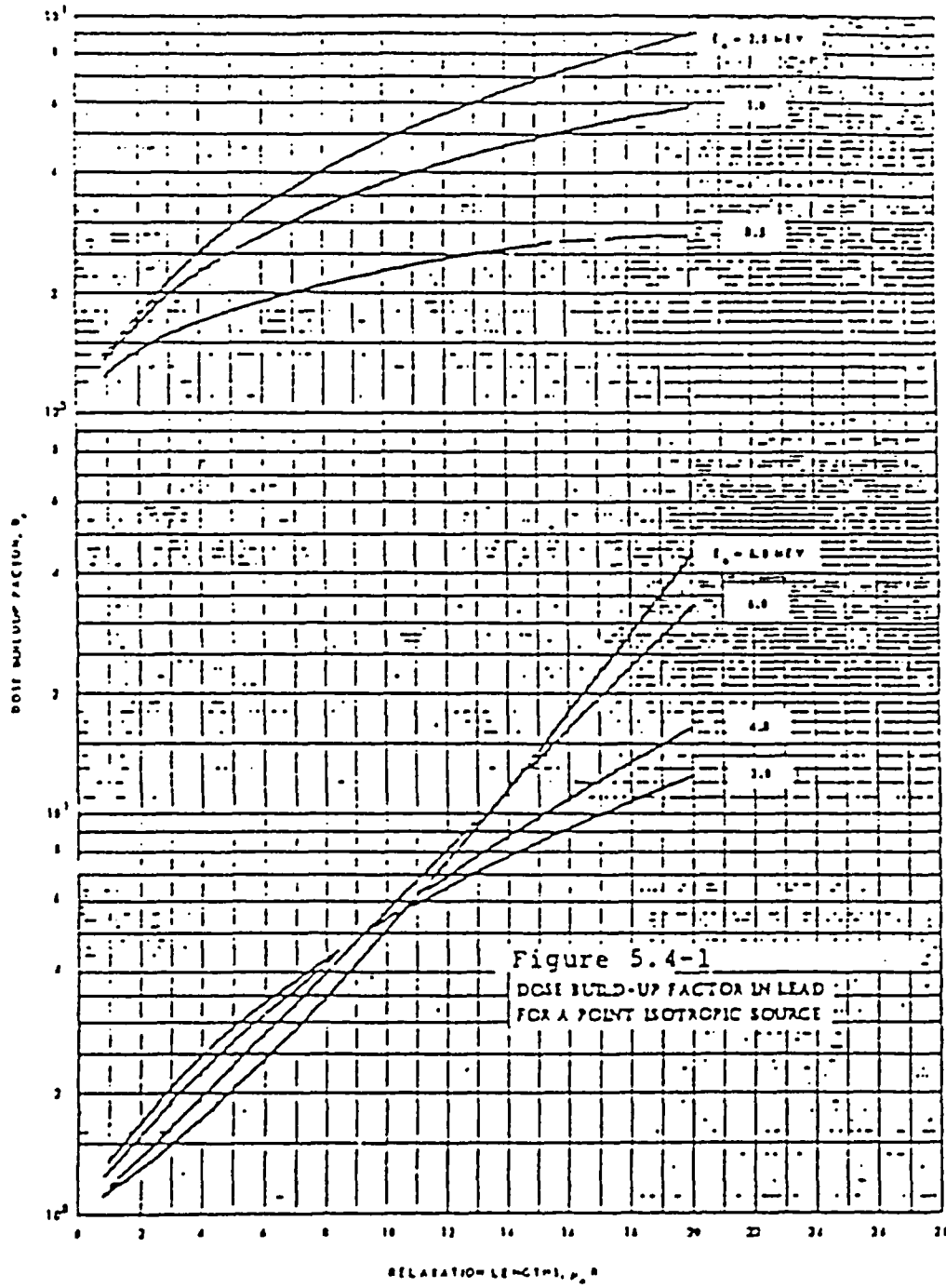
TABLE 5.4.1

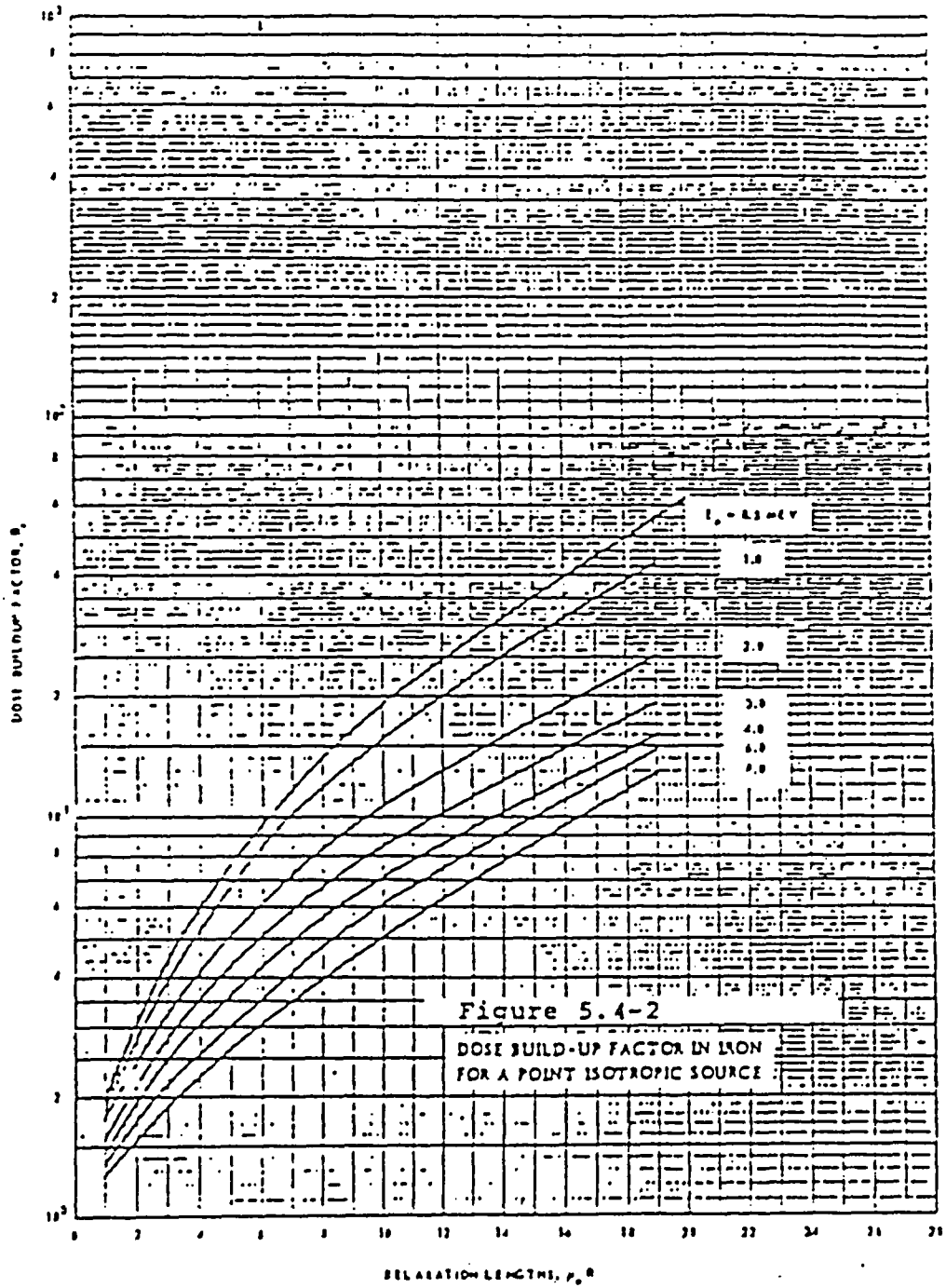
CASE	$\bar{x}$ (cm)	$\bar{x}$ -steel (cm)	$\bar{x}$ -lead (cm)	$b_1$	$e^{-b_1}$	$\beta(4,5)$	$\lambda$
CORNER-IMPACT	100.17	3.93	4.75	4.89	7.531-3	2.5*	$1.493 \times 10^{-7}$
CORNER-FIRE	112.73	3.18	10.54	3.52	1.995-4	3.6*	$4.497 \times 10^{-8}$
SIDE-IMPACT	100.97	3.18	6.35	5.65	3.505-3	2.8*	$7.660 \times 10^{-8}$
SIDE-FIRE	107.47	5.72	6.07	6.509	1.491-3	9.0**	$9.246 \times 10^{-3}$
TOP-IMPACT	102.34	3.81	7.09	6.419	1.630-3	3.0*	$3.715 \times 10^{-3}$
BOTTOM-IMPACT	102.34	3.175	7.72	6.59	1.376-3	3.0*	$3.136 \times 10^{-3}$

\*Use Buildup for Lead, Figure 5.4-1

\*\*Use Buildup for Iron, Figure 5.4-2

BASIC DATA





The case of 30 foot impact on the corner will be limiting:

$$D = K A \delta_0$$

$$K = 2.3 \times 10^{-5} \text{ R/hr}$$

$$S_0 = 1.546 \times 10^{12} \text{ } \overset{\phi}{\gamma/S}$$

$$D = 0.530 \text{ R/hr} < 1.0 \text{ R/hr}$$

Therefore, the dose rate following hypothetical accident events, assuming very conservative damage estimates, is less than the maximum permissible rates defined in 10 CFR 71. The Model 1-13C II package fully complies with all shielding requirements of 10 CFR 71.

5.5 References

1. Reactor Shielding Design Manual, Theodore Rockwell III, D. Van Nostrand Co., Inc., Princeton, N. J. 1956 - page 247
2. IBID, page 19
3. IBID, page 447
4. IBID, page 430
5. IBID, page 432

## 6.0 CRITICALITY EVALUATION

### 6.1 Discussion and Results

The general debris container configuration can be shown to be safe since the maximum quantity of material shipped is significantly less than the critical mass limited to (15.4 kg - UO<sub>2</sub>/400 gm &-235).

### 6.2 Package Fuel Loading

Fissile material is shipped in the general debris containers with a limit of 400 grams as U-235 in a solid form. the shipment meets the requirements of 10 CFT 71.22.

### 6.3 Model Specification

Not applicable

### 6.4 Criticality Calculation

- A criticality evaluation on a shipment with the general debris containers considers the effect of the shipment of 400 grams of U-235 with the fuel debris. It is conservatively assumed that the maximum fuel enrichment in the TMI-2 core (prior to burnup) of 3% comprises the sample. The configuration is shown to be safe since the maximum quantity of material shipped is significantly less than the critical mass.

The original TMI-2 UO<sub>2</sub> fuel pellets has a maximum of 3% U-235 (uranium dioxide with the uranium content enriched to 3% U-235 by weight). It is impossible to achieve a critical configuration of pure UO<sub>2</sub> enriched to 3% with a mass of less than 75 kg assuming optimal moderation and full neutron reflection. Hence no arrangement of the TMI-2 core debris samples contained in the shielded debris canisters can result in a critical configuration under any normal or accident



conditions with the total mass limited by 29 kg by the volume restriction. The actual mass of approximately 15 kg will provide a safety factor of five.

Isotopes of plutonium generated by neutron activation can be ignored in the criticality evaluation since the calculated total core inventory of 161 kg of Pu isotopes in the total core mass of approximately 125,000 kg represents a negligible percent compared to the U-235 content.

#### 6.5 Critical Benchmark Experiments

Not applicable.

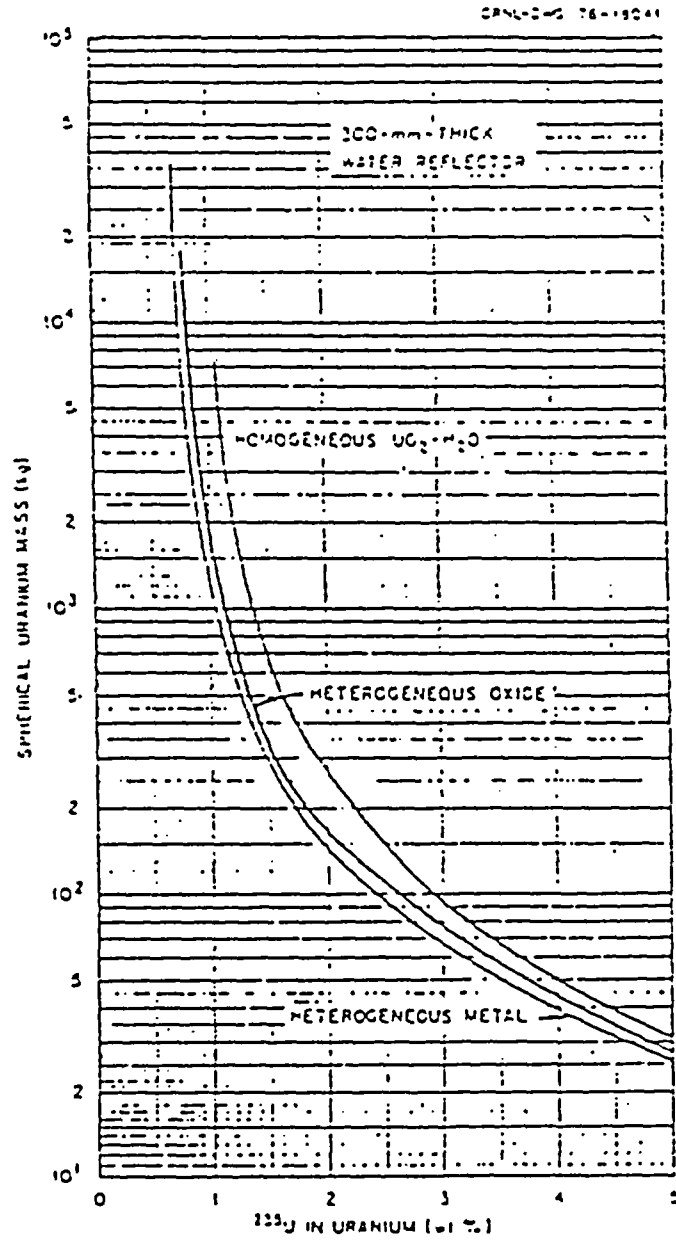


FIGURE 6.4.1

SUBCRITICAL MASS LIMITS FOR INDIVIDUAL SPHERES  
OF WATER REFLECTED AND MODERATED U ( $\leq 5$ )

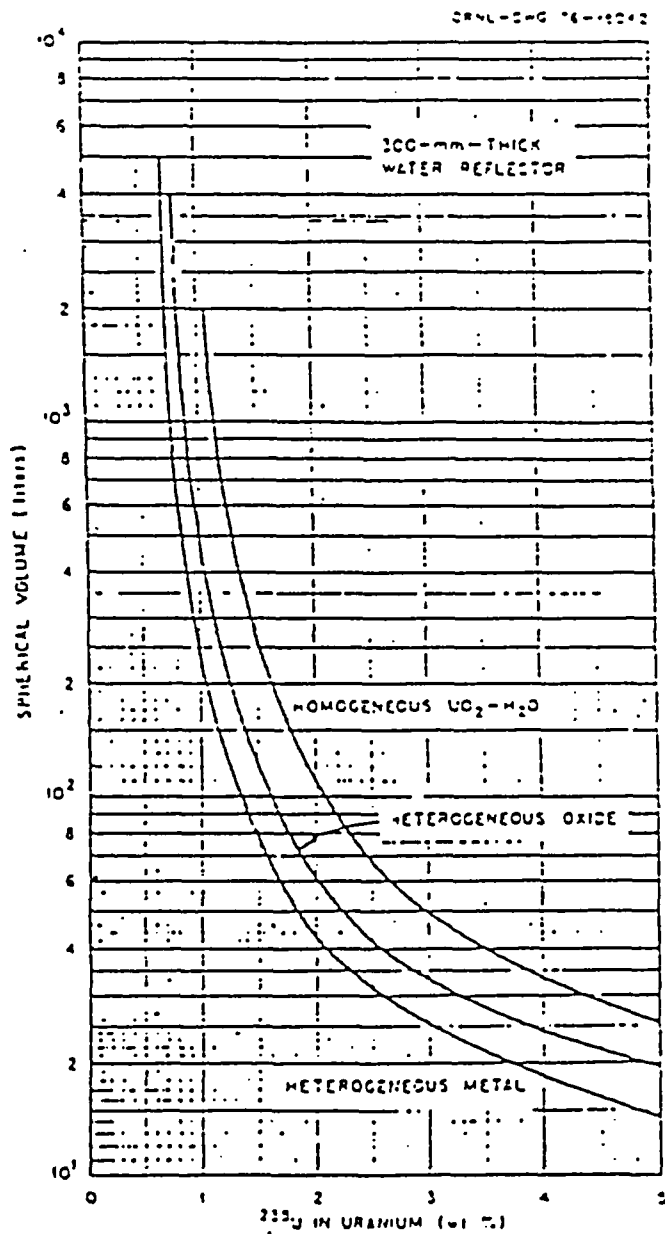


FIGURE 6.4.2

SUBCRITICAL VOLUME LIMITS FOR INDIVIDUAL SPHERES  
OF WATER REFLECTED AND MODERATED U ( $\leq 5$ )

CRNL-DWG 75-18C-3

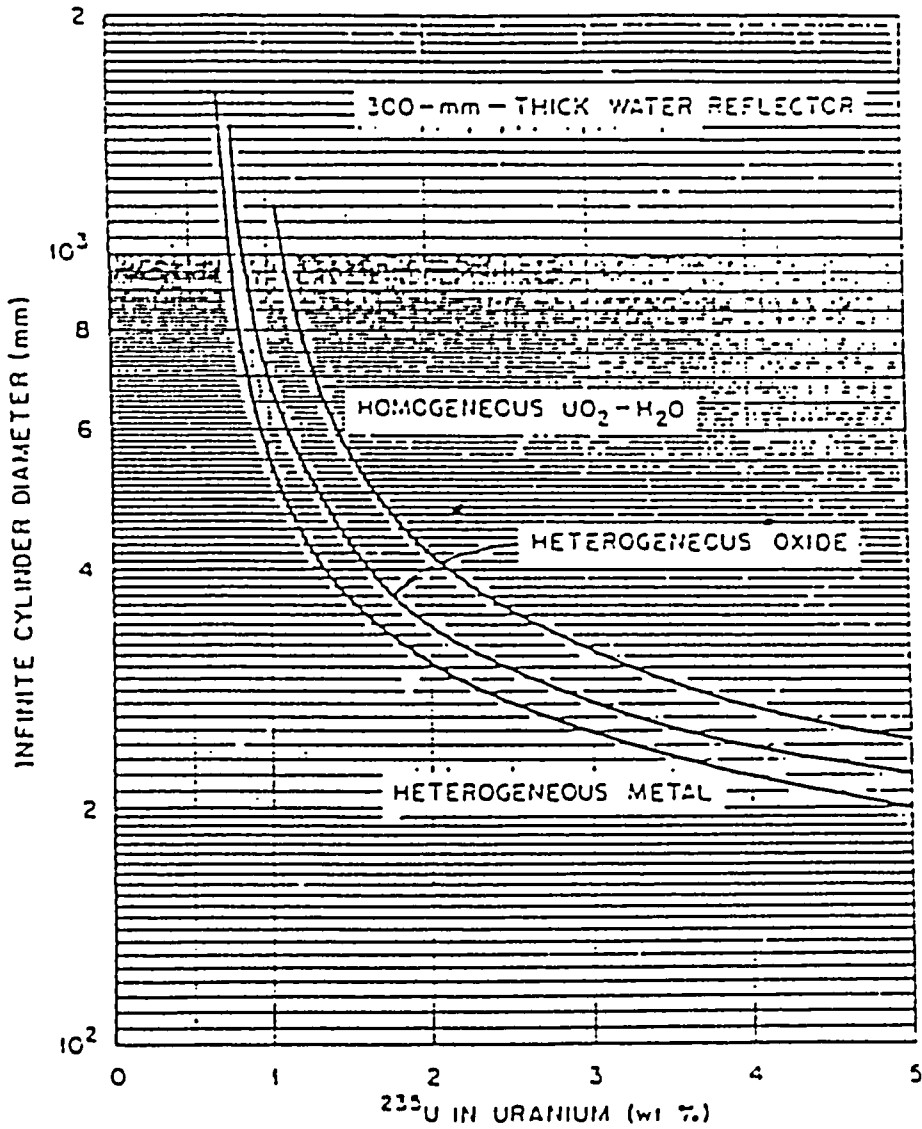


FIGURE 6.4.3

SUBCRITICAL DIAMETER LIMITS FOR INDIVIDUAL CYLINDERS  
OF WATER REFLECTED AND MODERATED U ( $\leq 5$ )

5.6 Appendix - References

1. J. T. Thomas, Ed. Nuclear Safety Guide, Tfd - 7015, Rev. 2, June 1978.
2. L. K. Poppe's letter Charles E. MacDonald, "Amendment to Certificate of Compliance USA/9152/B to Handle Fissile Material", July 15, 1985.

## 7.0 OPERATING PROCEDURES

This chapter describes the general procedures for loading and unloading the Model 1-13C II Shipping Package.

### 7.1 Procedures for Loading Package

- 7.1.1 Loosen and release ratchet binders securing upper overpack to lower overpack.
- 7.1.2 Remove upper overpack by attaching suitable hooks to lifting lugs. Care should be taken during this operation so that the overpack is not damaged while setting it down.
- 7.1.3 Determine if cask must be removed from lower overpack in order to load. If so, attach two lifting ears to cask walls and torque lifting ear bolts to 200 ft.-lbs. ( $\pm$  10% lubricated or dry). Cask may then be lifted vertically from lower overpack and carefully placed in position for loading.
- 7.1.4 Using proper radiological precautions, loosen vent plugs to relieve potential internal cask pressure prior to loosening and removal of the 12 bolts which secure the cask lid to the cask body.
- 7.1.5 Remove the lid by attaching a suitable hook to the lid lifting lug. Care should be taken during this operation so that the lid gasket and O-ring are not damaged.
- 7.1.6 Inspect the cask interior to ensure that there are no loose articles.
- 7.1.7 Inspect and clean lid gasket, O-ring, drain seal, and vent seal and gasketed surfaces. Replace any gasket if it shows sign of wear or deterioration.

7.1.3 Load cask

7.1.8.1 Payload weight shall not exceed 3,000 pounds. When loaded in a submerged fashion, both vent and drain plugs should be removed. Plugs should be reinstalled after cask cavity is drained. When positioning the lid onto the cask while loading in a submerged fashion, the lid shall be shimmed open to allow venting and drainage from the area between the O-ring and flat lid gasket.

7.1.8.2 Special Options for Loading Fissile Material

For guidelines formulated for the detailed procedure for collecting nuclear core assembly debris from the reactor vessel in the shielded container of 2R Vessel see section 7.1.8.2.1. For guidelines formulated for a detailed procedure of collecting fissile material or surface contaminated material from the reactor vessel by special buckets see section 7.1.8.2.2.

7.1.8.2.1 Shielded Container with 2R Vessel Option7.1.8.2.1.1 Sample Collection

- a. Weigh the debris shielded container with debris bucket or fuel pin sample cell prior to loading with core assembly debris. (See Section 1.3.1.2).
- b. Place an open debris shielded container on a platform with either the debris bucket or the fuel pin sample cell in the bottom of the debris shielded container. Lower the container into the reactor vessel.

7.1.8.2.1.2 Sample Collection from the Reactor Vessel

- a. Samples will be collected from the reactor vessel.
- b. Samples will be individual chunks of debris and/or small gravel/fines whose volume will not exceed the volume of the cavity of the debris bucket in the debris shielded container. (See Section 1.3.1.2)
- c. Other samples will be short sections of fuel rod pins whose volume will not exceed the volume of the fuel pin sample cells. (See Section 1.3.1.2.)

7.1.8.2.1.3 Placement of Samples in Debris Shielded Container

Place the sample in the appropriate debris bucket or fuel pin sample cell within the shielded container.

7.1.8.2.1.4 Closure of Container

Close the lid on the debris shielded container.

7.1.8.2.1.5 Drainer Container and Sample

- a. Raise the platform with the debris shielded container(s) above the surface of the water.



- b. Allow the debris shielded container(s) to drain and drip-dry until no water is discharged from the container(s).
- c. Tighten the lid locking bolt and jam nut on the container(s).

7.1.8.2.1.5 Placement of Loaded Debris Shielded Containers in 2R Vessels

- a. Weigh the loaded shielded debris container(s) after draining.
- b. After a debris shielded container is thoroughly drained and weighed, transfer the container to a 2R vessel. Shore up the debris container in the 2R vessel as shown. (See Section 1.3.1.3.)

7.1.8.2.1.7 Close 2R vessel per prescribed procedures

Loading Cask with 2R Vessels

Verify that the total net weight of the samples to be placed in the shipping cask is less than 15.4 kg.

- a. Place shoring for the first 2R vessel in the 1-13C II cask. (See Section 1.3.1.3.)
- b. Transfer the first 2R vessel to the 1-13C II cask, being sure that vessel is aligned per shoring drawing.

- c. Place additional shoring over the first vessel and repeat the transfer and shoring procedure for the second and third vessels.

- 7.1.9 Remove the lid shims and secure the lid to the cask body by torquing the 12 lid bolts to 270 ft-lbs  $\pm$  10% lubricated (360 ft-lbs  $\pm$  10% dry).
- 7.1.10 Verify the leaktightness of the assembled package prior to each shipment according to Section 8.1.3.
- 7.1.11 If cask has been removed from lower overpack for loading, use lifting ears to place it back in lower overpack on transport vehicle. Remove lifting ears.

NOTE: UPPER OVERPACK WILL NOT FIT ON CASK TOP AND RATCHET BINDERS CANNOT BE TIGHTENED IF LIFTING EARS ARE LEFT ON CASK.

- 7.1.12 Verify that package is oriented on transport vehicle per Figure 7.1.1-1. Verify that distance from cask centerline to transport vehicle tiedown lug is 76 inches.
- 7.1.13 Install the overpack, verifying that tiedown lugs are oriented to trailer tiedown assemblies and that ratchet binder lugs are aligned vertically.
- 7.1.14 Attach and tighten ratchet binders attaching upper overpack to lower overpack.
- 7.1.15 Inspect the package for proper labeling required to meet applicable regulations.

7.1.16 Secure package to transport vehicle using appropriate tiedowns.

7.2 Procedures for Unloading the Package

7.2.1 Move transport vehicle to unloading site.

7.2.2 Perform a visual inspection of unopened package exterior. Record any significant observations.

7.2.3 Repeat steps 7.1.1 to 7.1.3 above.

7.2.4 Loosen drain and vent plugs six (6) turns to vent pressure generated by decay heat.

7.2.5 Repeat steps 7.1.4 to 7.1.5.

7.2.6 Unload case.

7.3 Preparation of Empty Packages for Transport

The 1-13C II shipping package requires no special transport preparation when empty. Standard loading and unloading procedures outlined above shall be followed.

7.4. Procedures for Shipment of Packages Which  
Generate Combustible Gases

Procedures for preparing packages for shipment which radiolytically generate combustible gases are outlined below. These procedures are divided into two categories:

- a. Combustible gas control by inerting, and
- b. Combustible gas suppression.

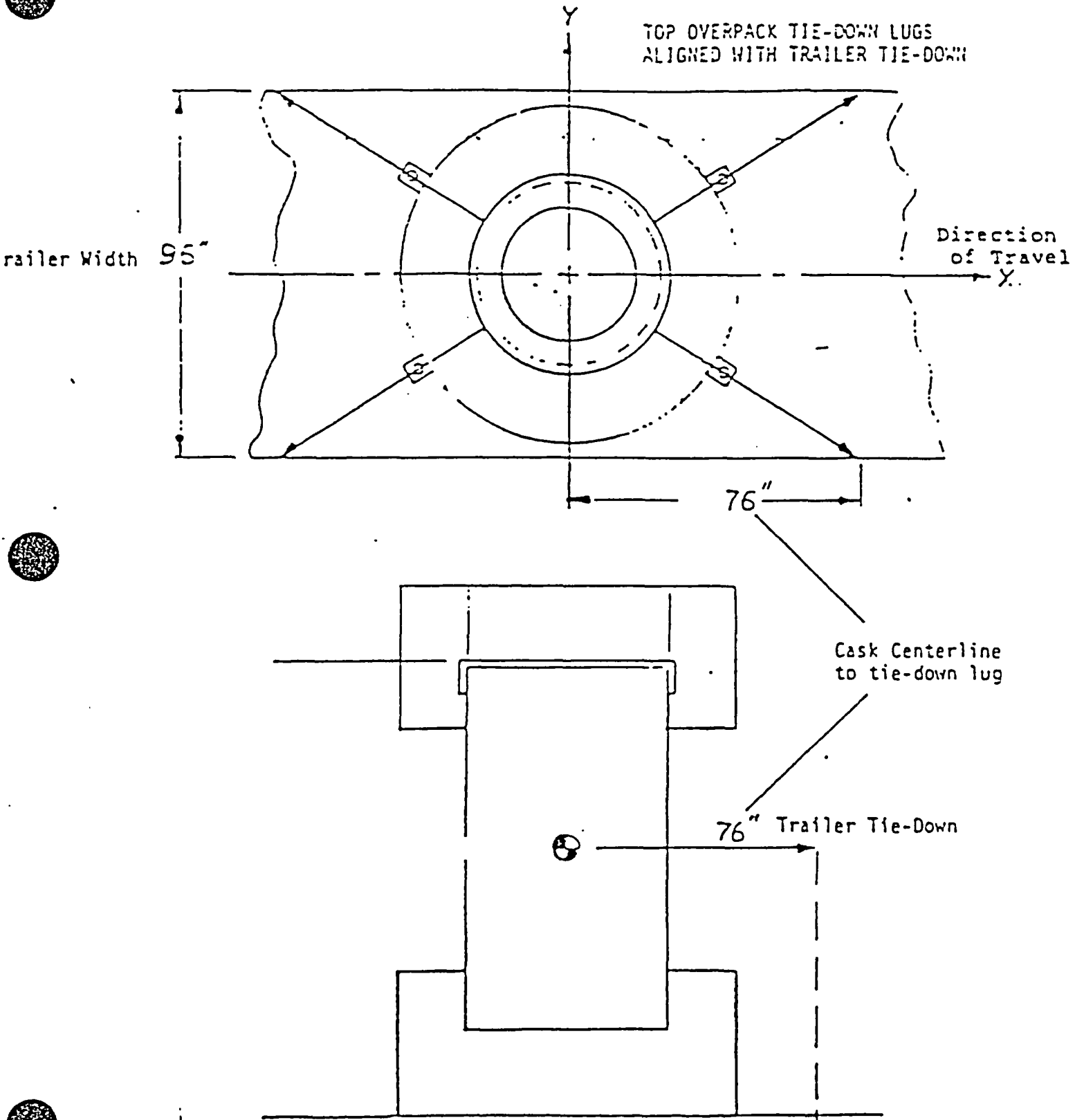
7.4.1 Combustible gas control by inerting

- a. Dewater the secondary container. The bulk of the free water is removed from the secondary container by displacing the water with nitrogen gas.
- b. Inert the secondary container (and, if necessary, the cask). The inerting operation is done at the dewatering station just before the cask is loaded. Inerting is performed if the hydrogen generated will be greater than 5% in any portion of the package. Inerting is intended to limit the oxygen that is radiolytically generated. If a leak path can develop between the secondary container and the cask, the cask will also be inerted. (The inerting of the cask shall be performed according to a special procedure.)
- c. Sample the gas in the package (and cask, if inerted).
- d. Load the secondary container.

7.4.2 Combustible gas suppression

- a. Dewater the secondary container.
- b. Install the combustible gas suppression system (e.g., a vapor pressure catalytic recombiner).
- c. Sample the gas in the secondary container and measure static pressure. This will assure that the combustible gas control method is working properly.
- d. Load the secondary container.

FIGURE 7.1.1-1  
ORIENTATION OF 1-13C II PACKAGE ON TRANSPORTER



### 3. ACCEPTANCE TESTS AND MAINTENANCE PROGRAM

#### 3.1 Acceptance Tests

The following discussion includes details of those tests which must be performed on the I-13C II package.

##### 3.1.1 Visual Inspection

The entire package, both inside and out, shall be visually inspected prior to loading, noting any significant damage (cracks, punctures, broken welds, etc.). Exterior stencils and nameplates must be in place and legible. Seals and bolts must be in place and in good condition.

##### 3.1.2 Structural and Pressure Tests

No structural or pressure testing is required.

##### 3.1.3 Leak Tests

The package shall be leak tested before first use in accordance with the requirements of ANSI N 14.5, Paragraph 6.3.1 for Containment System Fabrication Verification. The package will be leak tested every twelve months thereafter in accordance with the requirements of ANSI 14.5, Paragraph 6.3.1 for periodic testing. After the third use of the package and whenever any gasket or seal is replaced, it will again be tested to the same levels as the fabrication verification test. All the above tests will be per the leak test procedure of Appendix 8.3.

The flat lid seal will be leak tested after each loading with radioactive material prior to shipment in accordance with the assembly verification test procedure (Appendix 8.3).

3.1.4 Component Tests

There are no valves or other penetrations into the containment boundary, excepting the vent/test ports noted in Section 3.1.2, and, therefore, no additional component testing will be performed. The various foam properties of the impact limiters will be checked and verified during fabrication.

8.1.5 Test for Shield Integrity

A gamma scan or equivalent test shall be performed on the 1-13C II package prior to initial use to detect any shielding deficiencies from lead voids equal to or greater than 10% of shielding thickness.

8.1.6 Thermal Acceptance Tests

No thermal acceptance test will be performed on the 1-13C II package. Please refer to Section 3.0 for thermal evaluation.

8.2 Maintenance Program

The owner (US DOE) is committed to an ongoing preventative maintenance program for all shipping packages. The 1-13C II package will be subjected to routine and periodic inspections and tests as outlined in this section and DOE approved procedures.

3.2.1 Structural and Pressure Tests

Routine visual examinations will be performed to detect damage or defects significant to package condition. Exterior stencils, nameplates, seals and bolts will be verified in place.

8.2.2 Leak Test

Leak test procedures are discussed in Appendix 8.3.

8.2.3 Subsystem Maintenance

The cask does not have any subsystems.

3.2.4 Valves and Gaskets on Containment Vessel

Annual replacement will be made of all seals and gaskets.

3.2.5 Shielding

No tests are required for shielding performance other than normal transportation compliance surveys.

3.2.6 Thermal

No thermal tests are required.



APPENDIX 8.3

APPENDIX 2A  
LEAK TEST PROCEDURE

1.0 SCOPE

1.1 Purpose

This procedure will be used in performance of Halogen Gas Leak Testing of the 1-13C II Transport Cask.

1.2 Applicability

This procedure establishes the method for fabrication verification, third use, annual and/or seal replacement leak testing.

NOTE: THIS PROCEDURE IS NOT TO BE USED FOR ASSEMBLY VERIFICATION OF A LOADED CASK.

2.0 REFERENCES

- 2.1 ANSI N14.5 - 1977, American National Standard for leak test on packages for shipment of radioactive materials.
- 2.2 General Electric Operating Instructions "The Ferret Leak Detector" Type H-25, No. 198-4540K15-001F, Dated 1/81.
- 2.3 CNSI Drawing 1-436-111, Rev. D, sheets 1 and 2.
- 2.4 1-13C II Cask Handling Procedure, TR-OP-026.

3.0 RESPONSIBILITIES

3.1 Test Technicians - Performs leak testing in accordance with this procedure.

4.0 DESCRIPTION

Leak testing is performed to verify the integrity and proper sealing of the cask. A R-12 Freon source is connected to the cask drain port, the cask is pressurized and after 10 minutes the potential areas of leakage are checked. If leakage in excess of the specified acceptance criteria is detected, the cask must be disassembled to repair the leaks.

5.0 REQUIREMENTS

5.1 Prerequisites

5.1.1 Interior and exterior cask surfaces shall be clean and free of contaminants which could affect leak test sensitivity.

5.2 Equipment

5.2.1 Leak Detector - General Electric Type H-25 "The Ferret Leak Detector" or equivalent equipment.

5.2.2 Pressure Gauge - A gauge capable of indicating required pressure with a calibrated accuracy of  $\pm .25^{\circ}$  of gauge reading.

5.2.3 Temperature recording equipment capable of reading within  $\pm 2^{\circ}\text{F}$ .

5.2.4 Halogen Gas Source (dichlorodifluoromethane, Freon R-12) shall be the halogen gas.

5.2.5 Test Rig Adaptor

6.0 ENVIRONMENTAL CONDITIONS

Ambient conditions

7.0 SPECIAL PRECAUTIONS

Proper radiological precautions should be used to prevent the spread of contamination which may be present.

8.0 PROCEDURE

8.1 Leak Detector Preparation

- (1) Leak detector is to be calibrated and operated in accordance with Reference 2.2.
- (2) Temperature measuring equipment shall be attached to cask with the temperature reading recorded.
- (3) Calibration of the leak detector shall be established at .21 ounces/year for Freon R-12. ( $3.86 \times 10^{-5}$  ATM - cc/sec)

8.2 Discussion of allowable leak rates derived from containment Section 4.0 of 1-13C II Safety Analysis Report.

The following calculations are shown for the determination of cask charge pressure based on the ambient temperature at time of test.

NOTE: THE GRAPH, FIGURE 1, DEPICTS THE RESULTS OF THESE CALCULATIONS AND WILL BE USED FOR ALL NORMAL CONDITIONS AT TIME OF LEAK TEST.

$$P_t^3 - P_t^2 - P_t - 1 - (4.1534 \times 10^{-7}) \frac{I_h T_K}{L_s} = 0$$

Where:

$T_K$  = Cask Temperature, °K

$P_t$  = Required Charge Pressure, ATM

$L_s$  = Permissible Standard Leak Rate (Dry air at 25°C and ATM)

$$1.34 \times 10^{-5} \text{ ATM} - \text{cc/sec}$$

$I_h$  = Detector Sensitivity = 0.21 oz/yr ( $3.26 \times 10^{-5}$  atm - cc/sec)

### 2.3 Leak Testing

- (1) Check all surfaces with detector to determine cask is free of residual halides which could affect test.
- (2) Clean any surfaces found to have halide levels above background indications.
- (3) Examine flat gasket and O-ring for damage or deterioration and replace as applicable.
- (4) Install lid in cask in accordance with Reference 2.4.

- (5) Record temperature measurement of cask.
- (6) Connect R-12 Freon source to the cask drain port using test rig adaptor
- (7) Pressurize cask to the proper level as determined by value from Figure 1 and record pressure
- (8) Allow 10 minutes dwell time after pressurization of cask.
- (9) Using leak detector check area around vent and test rig adaptor assembly for halides and record results.
- (10) Remove vent seal plug and check orifice for halides and record results.
- (11) If results of leak checks are acceptable, proceed to next step.  
If leakage in excess of acceptance level is detected, disassemble cask and inspect for damage to the seals, cask, and test rig.  
Return to 8.3 (1) and repeat test and record results.
- (12) Close off pressure line to cask drain port leaving cask pressurized and remove Freon R-12 source.

NOTE: RELEASE OF PRESSURIZED R-12 IN CASK TO THE  
ATMOSPHERE WILL CONTAMINATE TEST AREA.

- (13) Reconnect Freon R-12 source at vent port.
- (14) Pressurize (area between gasket and O-ring) to the established pressure from Figure 1. Record pressure.
- (15) Allow 10 minutes dwell time after pressurization of cask.
- (16) Using leak detector check area around contact surface between lid and cask, bolt connection areas, vent port and test rig adaptor assembly. Record Results
- (17) If results of leak check are acceptable, proceed to next step. If leakage rate in excess of acceptance criteria is detected, disassemble cask and inspect for damage to seals and casks surfaces. Repeat test as required. Record Results
- (18) Record Temperature
- (19) Verify the following leak checks have been completed:
  - (a) Vent and drain ports
  - (b) O-ring seal
  - (c) Flat gasket seal.

- (20) Turn off and remove leak testing equipment from test area. (Release of R-12 directly to test equipment may cause damage.)
- (21) Remove Freon R-12 source and open vent and drain ports to release pressure.
- (22) Remove lid and clean cask as necessary to remove residual halogen.
- (23) Reassemble and prepare cask for shipment in accordance with Reference 2.4.

5.0 RECORDS, REPORTS AND NOTIFICATIONS

5.1 Reports

Each leak test performed shall be documented by a report which shall include as a minimum:

- (a) Type of test - annual, gasket replacement,
- (b) Equipment and calibration data,
- (c) Temperature of cask surface prior to and after test
- (d) Charge pressure of Freon R-12,
- (e) Results of all leak checks performed, and
- (f) Date and signature of test operator.

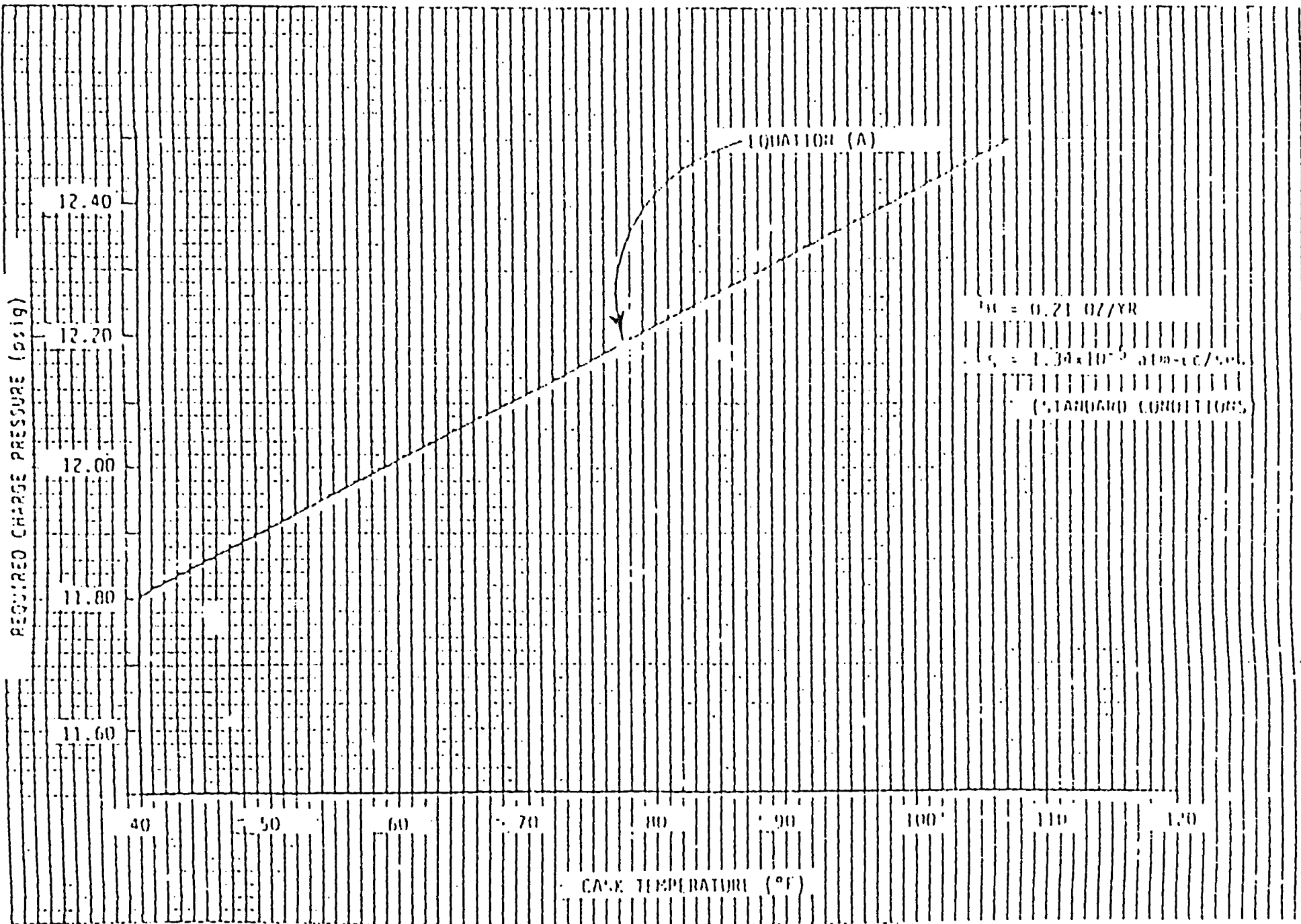
5.2 Notifications

Any problems encountered during testing which will adversely affect test results shall be forwarded to US DOE representative for resolution immediately.



5.3 Records

2-12



APPENDIX 1B  
LEAK TEST PROCEDURE

1.0 SCOPE

1.1 Purpose

This procedure will be used to perform Halogen Gas Leak Testing of the 1-13C II Transport cask.

1.2 Applicability

This procedure establishes the method for assembly verification, leak testing prior to each shipment of a loaded 1-13C II transport cask.

NOTE: THIS PROCEDURE IS NOT TO BE USED FOR FABRICATION VERIFICATION THIRD USE, ANNUAL AND SEAL REPLACEMENT LEAK TESTS.

2.0 REFERENCES

- 2.1 ANSI N14.5 - 1977, American National Standard for leak test on packages for shipment of radioactive materials.
- 2.2 General Electric Operating Instructions "The Ferret Leak Detector" Type H-25, No. 198-454OK15-001F, Dated 1/81.
- 2.3 CNSI Drawing 1-436-111, Rev. D, sheets 1 and 2.
- 2.4 1-13C II Cask Handling Procedure, TR-OP-026.

3.0 REQUIREMENTS

## 3.1 Prerequisites

- 3.1.1 Proper radiological precautions should be used during all phases of this leak test.
- 3.1.2 The cask shall be examined visually for weld integrity and condition of gasket and leak surfaces.
- 3.1.3 Cask surfaces shall be clean and free of contaminants which could affect leak test sensitivity.

## 3.2 Tools, Materials and Equipment

The following equipment is required for Halogen Gas Leak Testing:

- (1) Leak Detector - General Electric Type H-25 "The Ferret Leak Detector" or equivalent equipment.
- (2) Pressure Gauge - A gauge capable of indicating required pressure with a calibrated accuracy of  $\pm .25\%$  of gauge reading.
- (3) Temperature recording equipment capable of reading within  $\pm 2^{\circ}\text{F}$ .
- (4) Halogen Gas Source (dichlorodifluoromethane Freon R-12) shall be the halogen gas.
- (5) Test Rig Adapter

4.0 PROCEDURE

## 4.1 Leak Detector Preparation

- (1) Leak detector is to be calibrated and operated in accordance with Reference 2.2.
- (2) Temperature measuring equipment shall be attached to cask with the temperature reading recorded.
- (3) Calibration of the leak detector shall be established at .50 oz/yr for Freon R-12.

## 4.2 Discussion of allowable leak rates derived from containment Section 4.0 of 1-13C II Safety Analysis Report.

The following calculations are shown for the determination of cask charge pressure based on the ambient temperature at time of test.

NOTE: THE GRAPH, FIGURE II, DEPICTS THE RESULTS OF THESE CALCULATIONS AND WILL BE USED FOR ALL NORMAL CONDITIONS AT THE TIME OF LEAK TEST.

$$P_t^3 - P_t^2 - P_t + 1 - (4.1534 \times 10^{-7}) \frac{I_k T_k}{L_s} = 0$$

Where:

$T_k$  = Cask Temperature, °K

$P_t$  = Required Charge Pressure, Atm

$L_s$  = Permissible Standard Leak Rate

$$5.0 \times 10^{-4} \text{ Atm} - \text{cc/sec}$$

$I_n$  = Detector Sensitivity = 0.50 oz/yr

#### 4.3 Leak Testing

- (1) Verify cask has been prepared in accordance with Reference 2.4 and is ready for shipment.
- (2) Check all surfaces with detector to determine cask is free of residual halides which could affect test.
- (3) Clean any surfaces found to have halide levels above background indications.
- (4) Record temperature measurement of cask.
- (5) Remove vent plug and connect R-12 Freon source to the cask vent port.
- (6) Pressurize cask to the proper level as determined by value from Figure II. Record Pressure
- (7) Allow 10 minutes dwell time after pressurization of cask.
- (8) Using leak detector, check area around contact surface between lid and cask, bolt connection areas and test rig adapter assembly. Record Results

- (9) If results of leak check are acceptable, proceed to next step. If leakage rate in excess of acceptance criteria is detected, disassemble cask and inspect for damage to seals and cask surfaces. Record Results
- (10) Record temperature
- (11) Turn off and remove leak testing equipment from test area. (Release of R-12 directly to test equipment may cause damage.)
- (12) Remove Freon R-12 source, release pressure, and
- (13) Use appropriate means to purge Freon gas from cask.
- (14) Complete cask assembly and prepare for shipment in accordance with Reference 2.4.

5.0

RECORDS, REPORTS AND NOTIFICATIONS

5.1 Reports

Each leak test performed shall be documented by a report which shall include as a minimum:

- (a) Type of test - assembly verification
- (b) Equipment and calibration data,
- (c) Temperature of cask surface prior to and after test,
- (d) Charge pressure of Freon R-12.
- (e) Results of all leak check performed, and
- (f) Date and signature of test operator.

5.2 Notifications

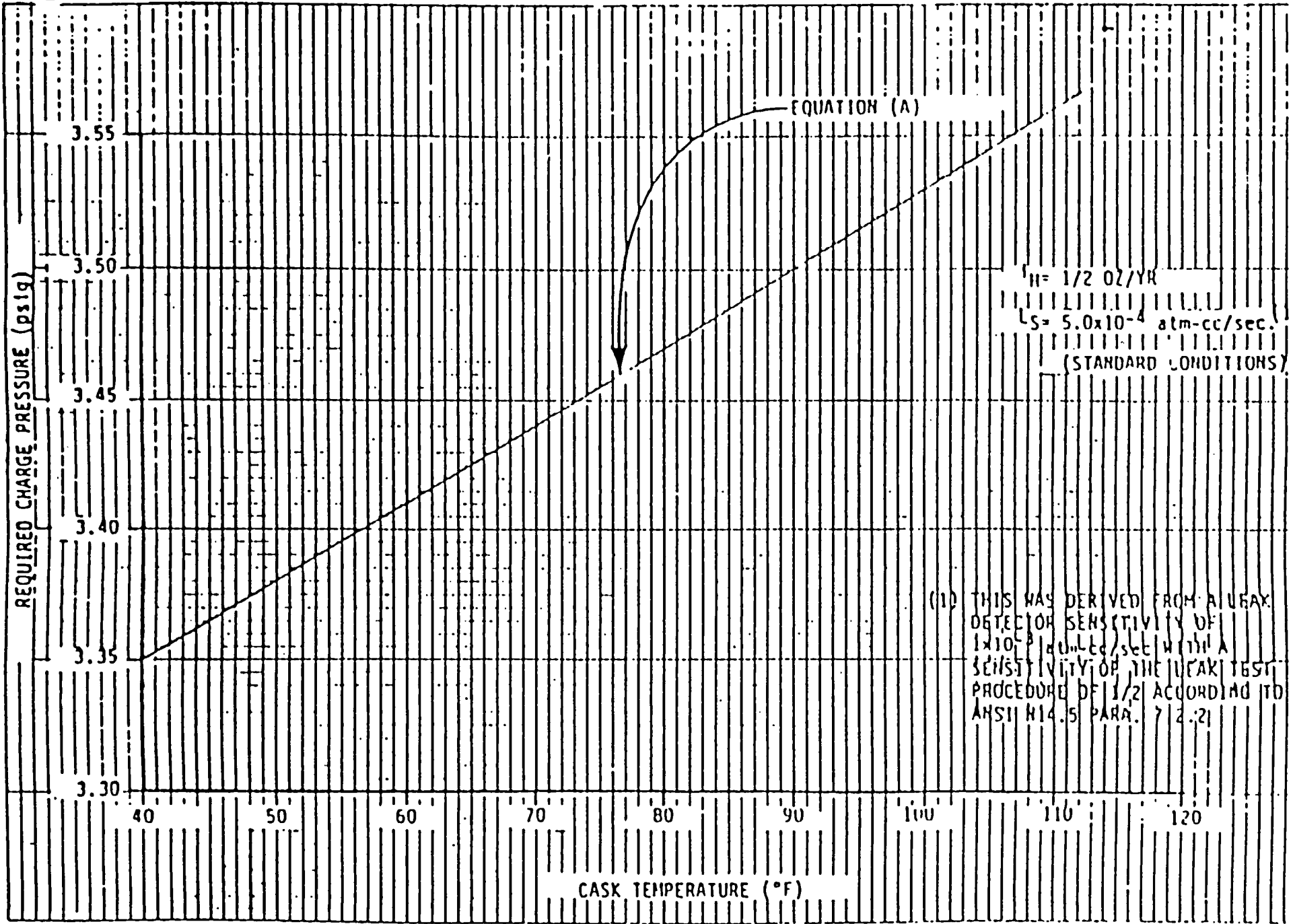
Any problems encountered during testing which will adversely affect test results shall be forwarded to DOE representative for resolution immediately.

5.3 Records

A leak check data sheet shall be forwarded to Quality Assurance department.



6T-8



$H = 1/2$  OZ/YR  
 $L_s = 5.0 \times 10^{-4}$  atm-cc/sec.  
(STANDARD CONDITIONS)

(1) THIS WAS DERIVED FROM A LEAK DETECTOR SENSITIVITY OF  $1 \times 10^{-8}$  atm-cc/sec WITH A SENSITIVITY OF THE LEAK TEST PROCEDURE OF  $1/2$  ACCORDING TO ANSI H14.5 PARA. 7.2.21